

**DEVELOPMENT AND EVALUATION OF SIMVASTATIN
BASED SNEDDS FOR TREATMENT OF
ALZHEIMER'S DISEASE**

Thesis Submitted for the award of the degree of

DOCTOR OF PHILOSOPHY

in

Pharmaceutics

By

Hardeep

Registration Number: 41900289

Supervised by

Dr. Narendra Kumar Pandey (11355)

Department of Pharmaceutics (Professor)

Lovely Professional University



**LOVELY FACULTY OF APPLIED MEDICAL SCIENCES LOVELY
PROFESSIONAL UNIVERSITY**

PUNJAB

2023

DECLARATION

I, hereby declared that the presented work in the thesis entitled “**Development and evaluation of Simvastatin based SNEDDS for treatment of Alzheimer’s disease**” in fulfilment of degree of **Doctor of Philosophy (Ph. D.)** is outcome of research work carried out by me under the supervision **Dr. Narendra Kumar Pandey** working as **Professor**, in the **School of Pharmaceutical Sciences** of Lovely Professional University, Punjab, India. In keeping with general practice of reporting scientific observations, due acknowledgements have been made whenever work described here has been based on findings of other investigator. This work has not been submitted in part or full to any other University or Institute for the award of any degree.

(Signature of Scholar)

Name of the scholar: Hardeep

Registration No.: 41900289

Department/school: School of Pharmaceutical Sciences

Lovely Professional University,

Punjab, India

CERTIFICATE

This is to certify that the work reported in the Ph. D. thesis entitled “**Development and evaluation of Simvastatin based SNEDDS for treatment of Alzheimer’s disease**” submitted in fulfillment of the requirement for the reward of degree of **Doctor of Philosophy (Ph.D.)** in the **School of Pharmaceutical Sciences** is a research work carried out by **Hardeep**, Registration No. **41900289**, is bonafide record of his/her original work carried out under my supervision and that no part of thesis has been submitted for any other degree, diploma or equivalent course.

(Signature of Supervisor)

Name of supervisor: Dr. Narendra Kumar Pandey

Designation: Professor

Department/school: School of Pharmaceutical Sciences

University: Lovely Professional University

**DEDICATED TO MY
PARENTS**

ACKNOWLEDGEMENT

We all are doing something for the betterment of our life as well as of others. But, at some point, we are not able to complete the task alone. In that case, we are seeking for someone's. No doubt, there are many peoples from whom we can get the help. But later on, after completing the task, it is our duty to acknowledge the person from whom we got the help or support. There are number of persons from whom I got the help/support during my journey of Ph.D. Listing all the names is not so easy but I tried my best to do so. First of all, I would like to express my gratitude towards my supervisor, **Dr.Narendra Kumar Pandey** for his all-time support and encouragement during the whole study period. At the same time, I would like to say thanks to **Dr. Bimlesh Kumar** for their continuous support and insightful comments during the work. I feel simply overwhelmed when I think of their extreme patience and their benevolent attitude that they've exhibited during the long hours of discussion and discourse in the course of my studies. They've always encouraged me and provided much needed motivation whenever I felt disheartened and emotionally shattered in my academic endeavours or personal pursuits. They have been and would remain the anchor of my faith and perennial source of inspiration. The example you set will make me a significantly better scholar, educator, and mentor.

I am deeply grateful to **Mr. Ashok Mittal**, Chancellor, Lovely Professional University, Punjab, Mrs. **Rashmi Mittal**, Pro-Chancellor and **Dr. Monica Gulati**, Senior Dean, Lovely Faculty of Applied Medical Sciences for providing me all the necessary infrastructural facilities as well as excellent working environment in the laboratory in order to complete my task.

I am very thankful to **Dr. Sachin Kumar Singh** who has provided his valuable words of advice during my all research work and my respected teachers, **Dr. Amit Mittal, Dr. Gurwinder Singh, Dr. Rajesh Kumar, Dr. Sheetu Wadhwa, Dr. Vijay Misra, Dr. Dileep Singh Bhagel, Mr. Sukriti Visvas, Mr. Rakesh, Mr. Shubham, Ms. Palwinder Kaur**, for their motivational support and insightful comments throughout my work.

I also acknowledge a sense of appreciation for the technical staff, **Mr. Manavar, Mr. Manoj Sharma, Mr. Madhan Rao and Mr. Ram Baran** as well as to the office staff, **Mr. Arvinder Singh, Mr. Gurdeep** and **Mrs. Reena** for their constant help.

I wish to express my special thanks to my most cherished and treasured friends **Leander Corrie, Ankit Awasthi, Shashi, Sarvi Yadav, Rehana, Pyrinka, Neha, Shivani, Shubham** for all the scientific as well as emotional support in difficult times.

I wish to express my special thanks to all the animals (Rats) those sacrificed their life for the benefits of the humans.

On personal note my sincere appreciation goes to my family, especially my **Guru ji Guru Jamna Dass ji, Guru Surinder Dass ji**, my father **S. Amarjit Singh**, my mother **Sdn. Kulwinder Kaur**, my sister **Mrs. Ramandeep Kaur**, my brother **Mr. Prince** for giving me invaluable support, opportunities and freedom to pursue my dreams and interests. A special thanks to my wife **Dr. Baljinder Kaur** for her continuous motivation and invaluable support.

This list of acknowledgements can only capture a small fraction of the people who supported my work. I send my deep thanks to all. Your contributions to this dissertation were vital, but the inevitable mistakes in it are very much my own.

Hardeep

LIST OF ABBREVIATIONS

Symbol/ Abbreviations	Full form
SNEDDS	Self-nanoemulsifying drug delivery system
SIM	Simvastatin
AD	Alzheimer's disease
GIT	Gastrointestinal tract
L-SNEDDS	Liquid self-nanoemulsifying drug delivery system
S-SNEDDS	Soild self-nanoemulsifying drug delivery system
HLB	Hydrophilic lipophilic balance
PXRD	Powder X-ray diffraction
SEM	Scanning electron microscope
HR-TEM	High Resolution- Transmission Electron Microscope (HR-TEM)
mL	Milliliter
Mg	Milligram
%	Percentage
Rpm	Rotations per minute
HCL	Hydrochloric acid
°C	Degree Centigrade
DSC	Differential scanning calorimetry
Eg	Example
H	Hour
NaoH	Sodium hydroxide
Nm	Nanometer
S.D	Standard deviation
Min	Minute
AUC	Area under curve
CAN	Acetonitrile
Cm	Centimeter
cm ²	Centimeter square
cm ⁻¹	Centimeter inverse

CPCSEA	Committee for the Purpose of Control and Supervision of Experiments on Animals
Na-CMC	Sodium carboxy methyl cellulose
et al.	And co-workers
Fig.	Figure
SEDDS	Self-emulsified drug delivery system
M.R.T	Mean retention time
RP-HPLC	Reverse Phase- High Performance Liquid Chromatography
HPMC	Hydroxypropyl Methylcellulose
IAEC	Institutional Animal Ethics Committee
ICH	International Conference on Harmonization
RT	Retention time
LQC	Lower quantification concentration
MQC	Medium quantification concentration
HQC	Higher quantification concentration
NP	Nanoparticle
PDI	Polydispersity Index
RH	Relative Humidity
RP- HPLC	Reserved Phase High Performance Liquid
μL	Microliter
% RSD	Percent Relative Standard Deviation
SIM	Simvastatin
μg	Microgram
LOD	Limits of detection
LQC	Limit of quantification
WS	Working standard
ATV	Atorvastatin
SLS	Sodium lauryl sulphate
PVP	Polyvinylpyrrolidone
BBD	Box–Behnken Design

DoE	Design of experiment
Omix	Oil mixture
S _{mix}	Surfactant mixture
SMEDDS	Self-microemulsifying drug delivery system
CMCM	Capmul MCM
L-MCS	Labrafil M 1944CS
TP	Transcutol P
T80	Tween 80
Ng	Nanogram
Conc.	Concentration
Temp.	Temperature
GS	Globule size
ZP	Zeta Potential
NFTs	Neuro fibrillary tangles
A β	Amyloid- β
APP	Amyloid β precursor protein
BDNF	Neurotrophic factors, including brain derived neurotrophic factor
AChEIs	Acetylcholinesterase inhibitors
AlCl ₃	Aluminium chloride
Al ³⁺	Aluminium

Table of Contents

	ABSTRACT	1-2
	CHAPTER-1	
1.	Introduction	3-6
	CHAPTER-2	
2.	Literature review	7
2.1	Alzheimer's Disease (AD)	7
2.2	Pathophysiology of AD	7-8
2.3	Cause of AD	8-9
2.4	Signs & Symptoms	10
2.5	Epidemiology	10-12
2.6	Challenges to the treatment of AD	12-13
2.7	Repurposing of a drug: A strategy to treat AD	14-17
2.8	SIM: A drug for AD treatment	18
2.9	Challenges of SIM (Pharmaceutical challenges)	18-19
2.10	Nanoformulations is an approach to AD	19
2.11	SNEDDS can be suitable	19-20
2.12	Preparation of SNEDDS & requirements	20
2.12.1	Preparation of liquid SNEDDS	21
2.12.2	Preparation of solid SNEDDS	21
2.12.3	Composition of SNEDDS	21
2.12.4	Excipients	21-23
2.13	Mechanism of drug transport from SNEDDS	24
2.14	SNEDDS reported for various drug molecules	24-25
2.15	Characterization of SNEDDS	25-26
2.16	Etiopathogenesis	27-28
2.17	Drug profile	29
2.17.1	Simvastatin	29
	CHAPTER-3	
3	Hypothesis of the study	30
3.1	Hypothesis	30-32
3.2	Aim	32
3.3	Objectives	32
	CHAPTER-4	
4.	Methodology	33
4.1	Materials used	33
4.2	Equipments used	34
4.3	Computer programs and software	35
4.4	Methodology	35
4.4.1	Characterization of drug	35
4.4.2	Physical description	35
4.4.3	Melting point determination	35
4.4.3.1	Capillary fusion method	35
4.4.3.2	Differential Scanning Calorimetry (DSC)	35-36
4.4.4	Determination of ultraviolet absorption maxima (λ_{max})	36
4.4.5	RP-HPLC method development for the quantification of the drug	36

4.4.5.1	Linearity and range	36
4.4.5.2	Accuracy	36
4.4.5.3	Precision	36-37
4.4.5.4	Robustness	37
4.4.5.5	LOD and LOQ estimation	37
4.4.6	Formulation development	37
4.4.6.1	Solubility study	37
4.4.6.2	Preparation of SNEDDS	38
4.4.6.3	Construction of pseudo ternary phase diagram (TPD)	38-39
4.4.6.4	Design of experiment (DOE) optimized of the Formulation	39-40
4.4.7	Evaluation of optimized SNEDDS	40
4.4.7.1	Thermodynamic, centrifugation, and cloud point Determination	40
4.4.7.2	Effect of dilution and pH	40
4.4.7.3	Drug Loading of SIM in SNEDDS	41
4.4.7.4	Determination of zeta potential (ZP) and globule size (GS) of optimized formulation	41
4.4.7.5	Differential Scanning Calorimetry (DSC) analysis	41
4.4.7.6	Scanning Electron Microscopy (SEM)	41
4.4.7.7	High Resolution-Transmission Electron Microscope (HR-TEM)	41-42
4.4.7.8	Cell line toxicity study	42
4.4.7.8.1	To determine the cell viability by MTT Assay in SH-SY5Y cell line	42
4.4.7.9	In-vitro dissolution studies	42-43
4.4.7.10	Permeation studies	43
4.4.7.11	Stability study	43
4.4.8	Animal experimentation	43
4.4.8.1	Procurement of animals	43
4.4.9	Bioanalytical method development study using RP-HPLC	44
4.4.9.1	HPLC trials	44
4.4.9.2	Blood collection and separation of plasma	44
4.4.9.3	Preparation of standard dilutions	44
4.4.9.4	Preparation of internal standard (IS)	44-45
4.4.9.5	Specificity study	45
4.4.9.6	Development of calibration curve	45
4.4.9.7	Validation of the method	45
4.4.9.8	Linearity and range	45
4.4.9.9	Accuracy	45-46
4.4.9.10	Precision	46
4.4.9.11	Validation of system suitability and determine of LOD and LOQ	46-47
4.4.9.12	Stability study	47-48
4.4.9.13	Statistical analysis	48
4.4.10	Pharmacodynamic study	48-49

4.4.11	Behaviour's analysis	49
4.4.11.1	Open field test	49
4.4.11.2	Morris Water Maze (MWM)	49-50
4.4.11.3	Novel object recognition test	50
4.4.12	Biochemical estimation	50
4.4.12.1	Acetylcholinesterase activity	50
4.4.12.2	Metal Ion Concentrations in the Hippocampus	50
4.4.12.3	Catalase (CAT) estimation	51
4.4.12.4	Reduced glutathione (GSH) assay	51
4.4.12.5	Thiobarbituric acid reactive substances (TBARS) assay	51
4.4.12.6	Superoxide dismutase (SOD) assay	51-52
4.4.12.7	TNF-alpha and IL-1 β	52
4.4.13	Pharmacokinetic study	52-53
4.4.14	Histopathological Examinations	53-54
4.4.15	Statistical Analysis	54

CHAPTER-5

5	Results and Discussion	55
5.1	API Characterization	55
5.1.1	Physical description of SIM	55
5.1.2	Melting point determination	55
5.1.2.1	Capillary fusion method	55
5.1.2.2	DSC analysis	55-56
5.1.3	Determination of ultraviolet absorption maxima (λ_{max})	56-57
5.2	Analytical method development	57
5.2.1	Selection of mobile phase of SIM	57-58
5.2.2	Linearity and Range	58
5.2.3	Accuracy	59
5.2.4	Precision	59
5.2.5	Robustness	59-62
5.2.6	LOD and LOQ	63
5.3	Solubility Study	63
5.3.1	Solubility in oils	63
5.3.2	Solubility in surfactant and co-surfactant	63-64
5.4	Construction of TPD	64-66
5.5	Thermostability study	66
5.6	Optimization of SNEDDS	66-69
5.7	Preparation & characterization of optimized SNEDDS	69
5.8	Thermodynamic and centrifugation stability	69-70
5.9	To study the dilution effect and pH change	70
5.10	Emulsion globules size and zeta potential	70-71
5.11	Field Emission Scanning Electron Microscopy (FESEM)	71-72
5.12	TEM analysis	72
5.13	DSC analysis	72-73
5.14	In vitro dissolution	73-74
5.15	Cell line toxicity study	74
5.16	Stability study	75-76

5.17	Ex-vivo permeation study	76
5.18	Bioanalytical method development	76
5.18.1	Specificity, linearity, and range	76-78
5.18.2	Accuracy	78
5.18.3	Precision	78
5.18.4	Stability study of plasma samples	78-82
5.18.5	LOD and LOQ	83
5.18.6	System suitability	83
5.19	Effect of drug treatment on Neurobehavioral parameters	83
5.19.1	Effect of drug treatment in open field test	83-86
5.19.2	Effect of drug treatment in MWM test	86-87
5.19.3	Effect of the drug treatment in novel object recognition (NOR)	88-89
5.20	Biochemical estimations	89
5.20.1	Reversal of diminished acetylcholinesterase activity by simvastatin	89-91
5.20.2	Metal Ion Concentration	91-92
5.21	Biochemical parameters	92
5.21.1	Reversal of AlCl ₃ -Induced Lipid Profile by Simvastatin	92-95
5.22	Oxidative Biomarkers	95
5.22.1	Antioxidant parameters in brain	95
5.22.1.1	Level of catalase (CAT) in brain	95
5.22.1.2	GSH level in brain	96
5.22.1.3	MDA level in brain	96-97
5.22.1.4	SOD level in brain	97-98
5.22.2	Antioxidant parameter in serum	98
5.22.2.1	GSH level in serum	98-99
5.22.2.2	MDA level in serum	99
5.22.2.3	CAT level in serum	100
5.23	Inflammatory Biomarkers	100
5.23.1	TNF- α	100-101
5.23.2	IL-1 β	101-102
5.24	Exposure of treatment to brain and plasma	101-103
5.25	Histopathological study	104-105
	Summary	106-108
	Conclusion and future perspective	109
	References	110-128
	Annexure	

List of Figures

Figure 1	Pathophysiology of AD	8
Figure 2	Clinical symptoms of AD	10
Figure 3	Global incidence rate of AD case	11
Figure 4	Structure of SIM	18
Figure 5	Composition of SNEDDS	21
Figure 6	Etiopathogenesis of AD	27
Figure 7	Schematic representation of SIM as a neuroprotective agent	31
Figure 8	Method of preparation of SIM-SNEDDS	38
Figure 9	Design of Pharmacokinetic study	53
Figure 10	Design of pharmacodynamic study	54
Figure 11	DSC thermogram of SIM	56
Figure 12	Absorption spectrum of SIM showing maximum absorbance at 238 nm	56
Figure 13	Chromatogram of SIM in ACN and formic acid (A), Chromatogram of SIM in methanol	57
Figure 14	Chromatogram of SIM in Acetonitrile – Water (90:10)	58
Figure 15	Calibration curve of SIM	58
Figure 16	Solubility of SIM using different oils	63
Figure 17	Solubility of SIM using different surfactants and co-surfactants	64
Figure 18	Ternary phase diagram	66
Figure 19	Perturbation plot for GS (A), PDI (B) and ZP(C)	68
Figure 20	3D plot for GS (A), PDI (B) and ZP (C)	68
Figure 21	Overlay plot representing optimized composition of SNEDDS	69
Figure 22	Study the dilution effect and pH change (n =3)	70
Figure 23	GS, PDI and ZP of optimized SIM-SNEDDS	71
Figure 24	SEM image of SIM-SNEDDS	71
Figure 25	TEM image of SIM-SNEDDS	72
Figure 26	DSC thermogram of TP, T-80, Pure SIM, and SIM-SNEDDS	73
Figure 27	<i>In-vitro</i> drug release profile of SIM from unprocessed SIM and SIM-SNEDDS in pH 1.2 and pH 6.8 buffer dissolution media (n=6)	74
Figure 28	<u>% Cell viability study</u>	74
Figure 29	Dissolution of fresh and old SIM-SNEDDS	75
Figure 30	<i>Ex-vivo</i> permeation study	76
Figure 31	Calibration curve of SIM	77
Figure 32	(A) Chromatogram of Blank Plasma, (B) Chromatogram of ATV (RT. 3.720) and SIM (RT. 8.331) in rat plasma	77
Figure 33	Open field test- (33a). Number of fecal balls (33b). Number of rearing (33c). Number of squares crossed (33d). Time spent immobile	84-85

Figure 34	MWM: (34a). Time taken to reach platform (34b)	87
Figure 35	NOR (35a). Discrimination Index (35b). Recognition Index	89
Figure 36	(36a). Level of AchE in cortex, (36b). Level of AchE in hippocampus	90
Figure 37	Al ³⁺ concentration in hippocampus	92
Figure 38	Lipid profile: (38a). TC in serum, (38b). TG in serum, (38c). LDL in serum, (38d). HDL in serum	93-94
Figure 39	CAT level in brain	95
Figure 40	GSH level in brain	96
Figure 41	MDA level in brain	97
Figure 42	SOD level in brain	97
Figure 43	GSH level in serum	98
Figure 44	MDA level in serum	99
Figure 45	CAT level in serum	100
Figure 46	TNF- α level in brain	100
Figure 47	Interleukin- <i>IL</i> -1 β level in brain	101
Figure 48	Bioavailability of SIM in Plasma	102
Figure 49	Bioavailability of SIM in Brain	102
Figure 50	Histopathology images for all groups	105

List of Tables

Table 1	Drugs which are used in the treatment of AD pharmacokinetic parameters	13
Table 2	Repurposing drugs used for Alzheimer's disease	15-17
Table 3	Nano formulations of treatment for AD	19
Table 4	Common oils used for preparation of SNEDDS	22
Table 5	Common surfactant and co-surfactant used for preparation of SNEDDS	23
Table 6	Different SNEDDS prepared	24-25
Table 7	Characterization methods for nanoparticles, including benefits and drawbacks	26
Table 8	Physiochemical property of SIM	29
Table 9	Materials used	33
Table 10	Equipment used	34
Table 11	Computer programs and software used	35
Table 12	Composition of SNEDDS for ternary phase study	39
Table 13	Compositions of SNEDDS using BBD	40
Table 14	Pharmacodynamic study protocol	49
Table 15	Design of pharmacokinetic study	52
Table 16	Physical description of SIM	55
Table 17	Melting point of SIM using capillary method	55
Table 18	Results of Pure DSC of SIM	55
Table 19	Results of Accuracy studies	60
Table 20	Results of precision studies for SIM	60-61
Table 21	Robustness study	62
Table 22	Formulations of SNEDDS using various oils and Smix	65
Table 23	Optimization of SNEDDS using BBD	67
Table 24	Summary of ANOVA of <i>BBD</i> batches	68
Table 25	Stability study of SIM-SNEDDS	75
Table 26	Accuracy study	78
Table 27	Precision study	79
Table 28a	Short term stability for plasma samples of SIM	80
Table 28b	Freeze thaw stability for plasma samples of SIM	81
Table 28c	Long term stability for plasma samples of SIM	82
Table 29	System suitability parameters	83
Table 30	Pharmacokinetic parameters of unprocessed SIM and SIM- SNEDDS	103

ABSTRACT

Alzheimer's disease (AD) is a global concern to the pharmaceutical and medical system due to the lack of proper treatment. Drug repurposing cannot be overruled to provide therapeutic benefits/ against AD. Hence the present work was focused on the formulation development and optimization of self-emulsifying drug delivery system (SNEDDS) of Simvastatin (SIM) against $AlCl_3$ -induced AD in rats.

In the pre-formulation study suitable oils, surfactants, and co-surfactants were identified. FTIR and DSC studies were conducted to investigate the interaction between the selected ingredients and SIM. A Box-Behnken design was utilized to optimize the effect of independent variables on the dependent variables of the formulation. Further, the optimized formulation was evaluated for various physicochemical parameters, in vitro release, ex vivo diffusion, and toxicity studies. The therapeutic efficiency of the optimized SNEDDS was investigated through cell line toxicity studies in SH-SY5Y cell lines and the final formulation in-vivo has undergone study to find out the therapeutic impact against $AlCl_3$ -challenged rats.

In the initial investigation, Capmul MCM, Tween-80, and Transcutol-P were chosen as the oil, surfactant, and co-surfactant respectively. The formulation was optimized using Box-Behnken design and had a globule size of 57.46 ± 2.65 nm, zeta potential of -13.6 ± 1.18 mv, PDI of 0.2 ± 0.11 , and drug loading was 88%. The ex-vivo permeability tests demonstrated that the SIM-SNEDDS increased SIM permeability significantly and further ex-vivo experiments confirmed the same. In-vitro toxicity studies confirmed the safety of the SIM-SNEDDS and most importantly, in vivo, administration of SIM-SNEDDS resulted in significantly increased bioavailability of SIM in the brain compared to the standard drug donepezil (DPZ) and unprocessed-SIM. The range of therapeutic efficacy was better in SIM-SNEDDS high dose followed by SIM-SNEDDS low dose, and then DPZ and further naïve SIM.

Further explorations with other models and clinical trials are required to better understand the effect of SNEDDS of SIM.

Keywords

Simvastatin, Repurposing, SNEEDS, Alzheimer's disease, Bioavailability, Solubility.

CHAPTER-1

1. Introduction

Alzheimer's disease (AD) is one of the progressive neurodegenerative disorders and is a major health problem worldwide (1, 2). It is one of the most important causes of dementia in elder individuals. An alarming information provided by AD International (ADI) is that its cases will increase to 13.8 million by 2060. Symptoms of the disease take a larger duration of time to appear and it takes about 20 years of duration to show the first degeneration to appear in the brain. These progressive alterations, particularly in the hippocampus area, cause serious deficiencies in cognitive function and, as a result, the sick person's increased dependence on third parties (3). AD can also induce brain atrophy, which is characterized by a substantial loss of brain cells and a reduction in the brain's capacity for metabolizing glucose. It is recognized by the accumulation of β - amyloid ($A\beta$)- containing plaques and tau- containing neurofibrillary tangles (NFTs) (4).

In AD the destruction of neurons takes place, which prominently affects the cortex and limbic structures of the Central Nervous System (CNS). It also causes damage, particularly in the basal forebrain, amygdala, hippocampus, and cerebral cortex. These brain regions are associated with better learning, memory, thinking, behavior, and emotional regulation (5). Hence due to damage of neuron person becomes deficient in learning, memory, cognitive, impairment, behavioral, and emotional characteristics. Disturbances in neurotransmission occurs due to oxidative stress, generation of reactive oxygen species, and genetic factors can be another contributor for sequential death of neurons.

Presenile and senile are the different types of AD. Anomia, agnosia, apraxia, aphasia these are the symptoms observed in AD patients (6). AD attacks not only on nerves and brain cells but it also causes impairment in neurotransmitters release which causes accumulation of protein to develop around plaques and bundles around the brain's cells (7). Further the condition of the individuals become worst with the aggregation of plaques (8) as it leads to progressive loss of cognitive functions (9).

Two proteins, $A\beta$ and tau, which together create extracellular neuritic plaques and intracellular NFTs, respectively, are considered to accumulate in the brain in AD (5).

According to this pathology, patients with Alzheimer's disease (AD) exhibit synaptic disruptions, neuronal death, cognitive decline, and memory problems during its development (10). The core of neuritic plaques is A β , which is a proteolytic result of the amyloid β precursor protein (APP). The hyperphosphorylated microtubule-associated protein tau is responsible for the formation of NFTs. Neuroinflammation and neuronal death caused by A β and tau lead to AD progression. (11). AD is a complicated and multifactorial disease. To describe the pathologic process of AD, several hypotheses have been suggested, including the hypothesis of cholinergic system, tau proteins, dysfunction of glutamate, amyloid cascade, inflammatory and mitochondrial cascade. Unfortunately, these ideas only target a part of the disease, and the mechanism leading AD development is still unclear. Neurotrophic factors, including brain derived neurotrophic factor (BDNF), may decrease the progression of neurodegeneration and provide as a viable alternative for AD therapy since neurodegeneration causes cognitive impairment in AD. (12).

Acetylcholinesterase inhibitors (AChEIs), an antagonist of the N-methyl-D-aspartate receptor (NMDAR), and the monoclonal IgG1 anti-A antibody are now the FDA-approved drugs for AD (aducanumab). The authorized NMDAR antagonist (memantine) and licensed AChEIs (donepezil, galantamine, and rivastigmine) are symptomatic therapies that do not deal with the fundamental pathological reasons of AD (13). As a result, aducanumab is the first and only drug authorized for treating AD (14). Donepezil is approved to treat all stages of the AD. It reversibly and selectively inhibits the enzyme known as acetylcholinesterase, which is responsible for breaking down acetylcholine, as a result of this increase the amount and duration of acetylcholine's effect in the central nervous system by preventing the enzyme acetylcholinesterase from breaking down the neurotransmitter into choline and acetate.

Drug repositioning, also referred as old drug for new purposes, is an efficient, low-cost, and risk-free method for finding new indications for existing drugs. Conventional drug research processes normally consist five stages: preclinical discovery, safety approval, clinical trials, FDA review, and FDA post-market supervision. Many drugs have been repurposed, including Raloxifene (from breast and prostate cancer to osteoporosis),

Paclitaxel (from cancer to re-stenosis), Zidovudine (from cancer to HIV/AIDS), Topiramate (from epilepsy to obesity), Minoxidil (from hypertension to hair loss), and Ropinirole (from hypertension to Parkinson disease), to name a few, to name a few (15).

SIM is also used as an example which can be repurposed for AD (hyperlipidemia to AD) of drug(16). SIM is used to prevent hypercholesterolemia. It is a reversible lactone prodrug that undergoes metabolism for lowering the level of lipid. It inhibits hydroxy-methyl-glutaryl coenzyme A (HMG CoA) reductase, which helps to convert HMG-CoA to mevalonate. Thereby it reduces low-density lipoprotein (LDL) cholesterol in plasma and causes depletion in the accumulation of intracellular cholesterol. In addition, it also increases LDL receptor expression and helps in the treatment of hypercholesterolemia (17). SIM has pleiotropic neuroprotective impacts on the brain and stimulates several paths, such as (18):

1. Suppression of inflammatory mediators and stimulation of microglia
2. Inducible nitric oxide synthase (iNOS) attenuation
3. Activation of neuroprotective factors (BDNF, NGF) synthesis
4. Apoptosis inhibition

The fascinating component of SIM's repurposing and rising clinical importance in its treatment for chronic inflammatory disorders can be ascribed to its numerous neuroprotective effects (19). Despite the various pharmacological benefits of SIM, its formulation development is difficult due to its pharmaceutical challenges which include its low water solubility, poor absorption, and rapid metabolism. Hence it exhibits low bioavailability. Some researchers developed formulations like polymeric nanoparticles, liposomes, and nano-emulsion of simvastatin (SIM) and increased bioavailability (20). When SNEDDS is taken orally, it mimics the process by forming a nano/microemulsion in the gastric fluid with the help of gastrointestinal motility (21). The nano globules have a larger surface area, which helps in the initial absorption of the drug molecule. Fisetin, curcumin, glimepiride, polypeptide-K, andrographolide, flurbiprofen, and tetrandrine have all been reported to have increased oral bioavailability by SNEDDS (22). SNEDDS have

benefits because they enhance drug solubility. It also benefits in bypassing hepatic first-pass metabolism and enhancing drug bioavailability across gastrointestinal tracts. SENDS have already demonstrated that they increase the oral bioavailability of drugs that are gastrointestinally labile and lipid soluble, such as curcumin, duloxetine, glimepiride, and polypeptide-k (23). SIM is an extremely lipophilic drug and GI labile, so it undergoes extensive first-pass metabolism and enzymatic degradation in the GIT after oral administration, and the remaining non-degraded drug is insoluble in the GIT medium. As a result, overall oral bioavailability and therapeutic efficacy are enhanced. SNEDDS are well-known for their ability to both increase drug solubility and protect the GIT from toxicity.

The current studies entail the following:

1. Development and validation of reverse-phase high-performance liquid chromatography (RP-HPLC) based bioanalytical method for estimation of SIM in rat's plasma
2. Development of SNEDDS of SIM with unique components oils, surfactants, and co-surfactants.
3. Ameliorative effects of SIM-SNEDDS against the $AlCl_3$ -provoked AD in rats.

CHAPTER-2

2. Literature review

2.1 Alzheimer's Disease (AD)

AD is the most common type of dementia among older persons. It's a devastating neurodegenerative condition that causes memory loss and cognitive decline, difficulty performing everyday tasks, and various psychological and behavior symptoms. The progression of AD is unique to each patient, but many symptoms are common. Early on, loss of short-term memory is typically seen. As the disease advances in the brain, the ability to perform higher level tasks and essential daily activities decreases. Later stages see the development of symptoms such as long-term memory loss, mood changes, confusion, aggression, and social withdrawal.

Research has found a connection between AD, neurofibrillary tangles & β -amyloid plaques found in the brain. A hallmark of the disease is the formation of neuritic plaques, which are aggregates of amyloid- β proteins. $A\beta$ is a short peptide of forty-two amino acids that is created from the abnormally cleavage of the APP by enzymes such as gamma-secretase. The buildup and deposition of $A\beta$ triggers oxidative stress, inflammation, and excessive excitotoxicity of glutamatergic neurons, resulting in neurofibrillary tangles and apoptotic cell death in the brain. Neurofibrillary tangles are composed of tau protein and are crucial for axonal growth and development in healthy cells. However, when tau protein is over phosphorylated, tangles form within nerves in the medial temporal lobe, and hippocampus, causing neural cell death. This leads to a decrease in neurotransmitter systems like norepinephrine, acetylcholine (AChE), and serotonin. Studies have shown that memory loss and neurotoxic effects in AD patients is caused by a shortage of the cholinergic system.

2.2 Pathophysiology of AD

AD is related to two significant alterations in the brain, outside neurons the formation of beta-amyloid plaques ($A\beta$), which are aggregates made of the protein fragment beta-amyloid, and inside the aggregation of abnormally abundance of the protein tau in neurons (known as neurofibrillary tangles) (24). Alzheimer's patients have a lot of plaques and

NFTs in their brains. Scientists are unsure of the actual function tangles and plaques perform in AD. The majority of scientists believe that plaques and tangles prevent nerve cell connection and interfere with vital processes for the survival of the cells (25). Cognitive loss, behavioral changes, and problems performing everyday tasks, and other signs of AD are caused on by the death and destruction of nerve cells. AD is still poorly understood by scientists. There likely is not a single cause but rather several factors that can affect each person differently.

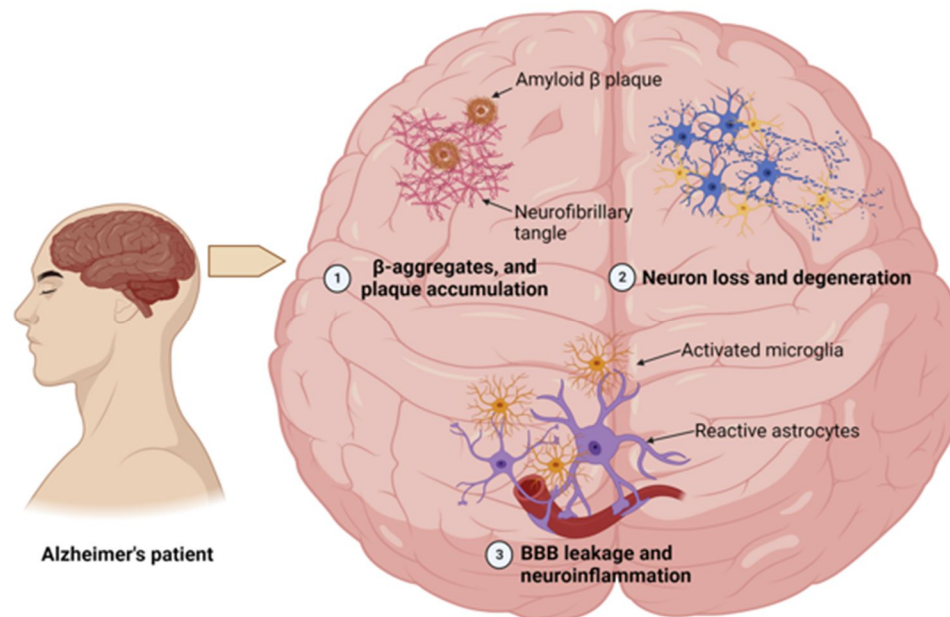


Figure 1: Pathophysiology of AD

2.3 Cause of AD

- **Age:** AD risk factors are most frequently associated with age. Growing older is the most widely understood risk factor for AD. In the age group 65 and older, one in nine individuals have AD affects around one-third of those aged 85 and over.
- **Family history:** According to researchers, genetics may cause the onset of AD. However, a healthy lifestyle may lower the risk of acquiring AD. Two

significant, Long-term studies suggest that people may benefit from getting regular exercise, eating healthily, drinking in moderation, and giving up smoking.

- **Brain injury:** Brain injury increases the future risk of dementia. To preserve your brain, wear your seatbelt and helmet when deriving, and take safety precautions when participating in sports such as wearing a sports helmet, and fall-proofing your home.
- **Heart-head connection:** The best proof indicates a relationship between heart and brain health. This relationship makes sense because the heart is responsible for circulating blood through the blood vessels of the brain, which is part of the body blood artery connection with the most diversity.
- **Cardiovascular disease:** According to the researchers, many cardiac diseases-related diseases and lifestyle variables can raise the risk of AD.

These include:

- Obesity
 - Smoking
 - Diabetes
 - Hypertension
 - Hypercholesterolemia
- **Down's syndrome:** People with suffering Down syndrome are at an enhanced risk of developing AD. This is due to the fact that the genetic abnormalities that produce Down's syndrome can cause plaques to aggregate in the brain over time, eventually leading to AD in some people.
 - **Genetics (heredity):** The cause of AD is considered to be genetic factor. Two categories of genes influence the development of AD, one is risk genes and the second is deterministic genes. In both groups, genes associated with AD have been found. AD is assumed to be caused by deterministic genes in fewer than 1% of cases.

2.4 Signs & Symptoms

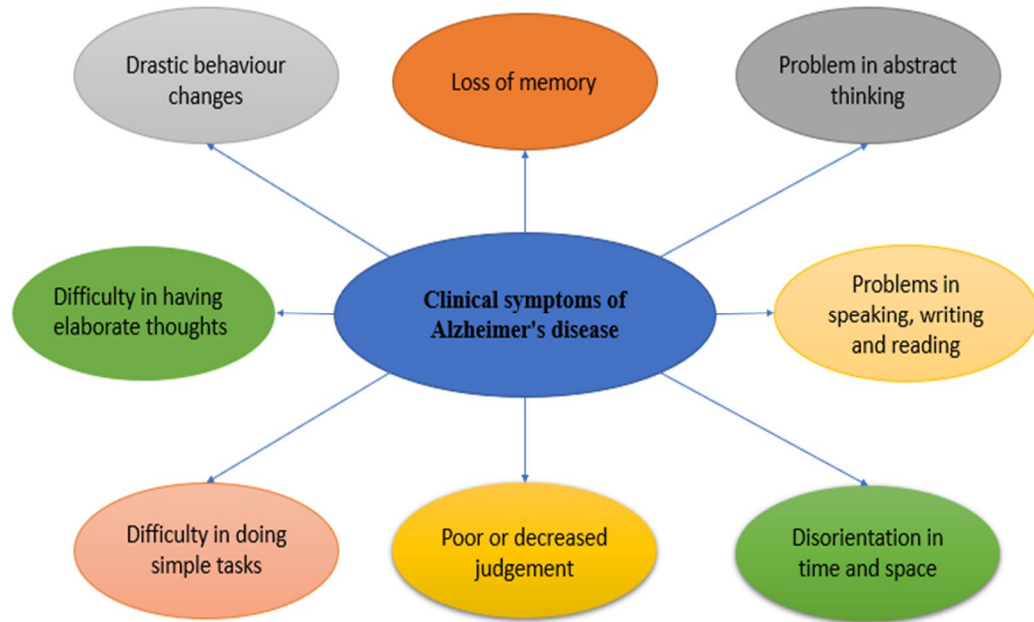


Figure 2: Clinical symptoms of AD

2.5 Epidemiology

It is estimated that the global population of individuals with AD will reach 152 million by the middle of the century. The greatest growth is predicted in low- and middle-income nations. The 2023 AD facts and figures report states that the population of individuals in the US who are 65 years of age or older and have AD is expected to increase significantly from 5.8 million to 13.8 million by the year 2050 (26). To estimate dementia prevalence in India, home to 18% (1.37 billion people) of the world's population. A trend of increased AD prevalence has also been observed in recent decades among community-dwelling populations in Japan and China. Women are 1.17 times more likely than men to have age-specific global prevalence of AD, and women have a higher age-standardized mortality rate than men, indicating that a longer lifespan is not the only factor contributing to the prevalence of AD in women (27). From 2000 to 2018, the number of AD-related mortality increased by 146.2%, and it became the fifth most common cause of death among elderly Americans.

Caretakers of AD patients often face mental stress and negative emotional influences, which will put a significant social and family burden on caring for the AD population.

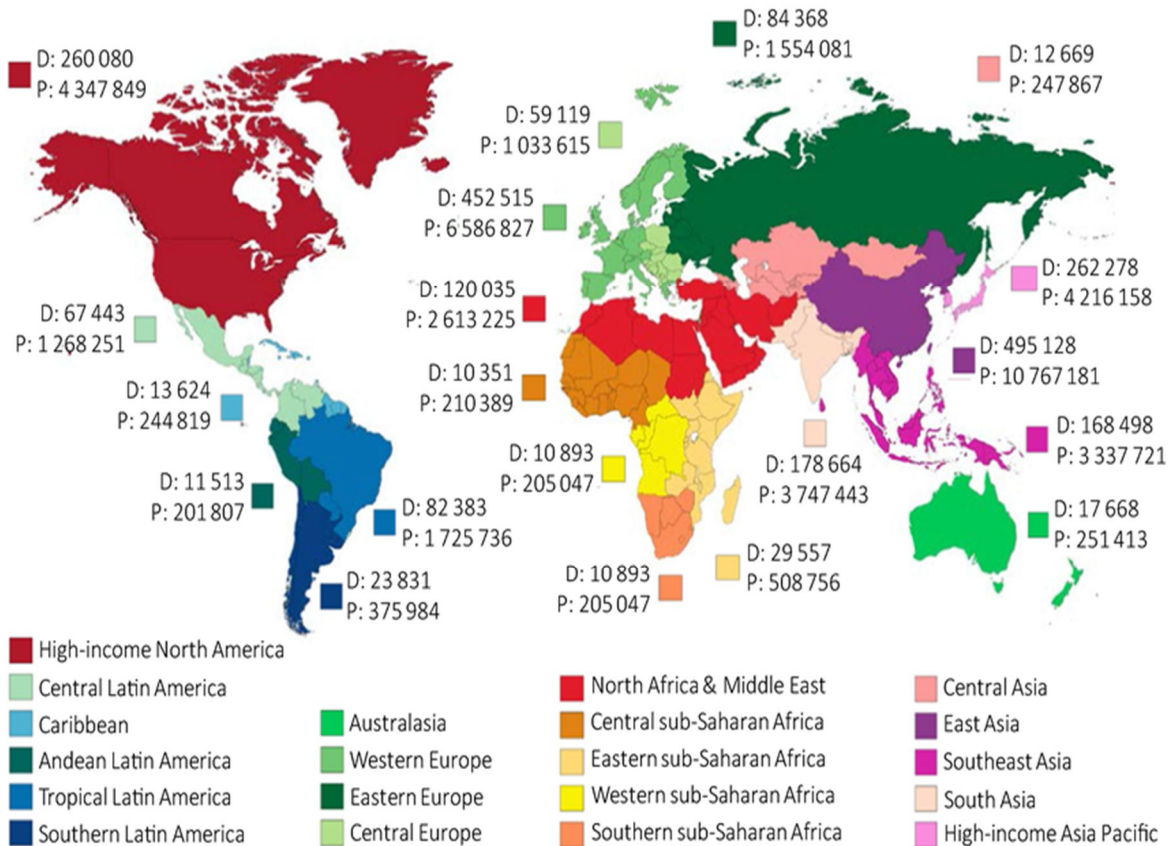


Figure 3: Global incidence rate of AD case

The aim of much AD care is to maintain wellbeing (28). AD patients experience confusing challenges and symptoms in a variety of domains, and evidence from scientific studies suggests that behavioral and environmental variables play a key role in the disease's pathogenesis and progress. Maintaining physical health, especially by reducing the risk of preexisting diseases, can help protect cognition. Several risk factors can both lead to the onset of AD and show as AD symptoms, making accurate diagnosis important for individuals suffering from cognitive dysfunction (29). While A β and tau indicators suggest AD, some individuals with these biomarkers but no cognitive impairments never develop AD, making pre-symptomatic diagnosis challenging. Future research should concentrate on developing less expensive and more sensitive indicators, as well as strategies for early

screening and diagnosis. Future studies ought to concentrate on evidence-based preventative strategies that investigate the potential relationship between risk factors that can be modified and late-onset AD. Figure 3 portrays the worldwide AD incidence rate.

2.6 Challenges to the treatment of AD

The development of drugs to treat AD. Recent efforts to develop drugs to treat AD have failed for various reasons, including the severe pre-symptomatic neuronal damage that is caused by the blocking of the amyloid β peptide and abnormalities tau protein, as well as the harmful effects of drug candidates.

The first choice to treat AD is ChEIs (Oral preparations of tacrine, galantamine, donepezil, and rivastigmine patch), which reduce the rate of acetylcholine degradation in the synaptic gap and compensate for its deficiency. Currently authorized drugs for addressing AD's underlying causes drugs for treating the basis of AD is the regulation of neurotransmitters or enzymes. AChEI (acetylcholinesterase inhibitor) drugs have reported several negative effects, such as nausea and vomiting, that cause treatment to be discontinued. For the treatment of AD at initial stage, tacrine was the first ChEI to receive approval. But it is used in rare cases due to its hepatotoxic side effects, and its short half-life (needs four times/day administrations). Rivastigmine has two hours half-life while galantamine has 5-7 hours but has 18% protein binding. In NMDA receptor antagonists, non-physiological and extended of NMDA receptors activation due to neurotransmitter glutamate, and glutamate may result in excitotoxic neuronal dysfunction. USFDA granted memantine approval in 2003, non-competitive and moderate NMDA receptor antagonist. But memantine is associated with adverse effects like dizziness, confusion, vomiting, and constipation [39] [40]. The pharmacokinetic parameters of drugs which are used in the treatment of AD are shown in Table 1.

Amyloid β ($A\beta$) build up and creation of neurofibrillary tangles (NFTs) in the brain are two possible causes of Alzheimer disease, which leads in synaptic dysfunction and neurodegeneration. Clinical studies for drugs that target $A\beta$ usually ended in failure, and clearing $A\beta$ found in the Alzheimeric brain did not give a treatment.

Table 1: Drugs which are used in the treatment of AD pharmacokinetic parameters

Summary of the pharmacokinetic parameters of the cholinesterase inhibitors and memantine Drugs	Bioavailability (%)	t_{max} (h)	Half-life (h)	Protein binding (%)	Hepatic metabolism	References
Donepezil	100	3–5	60–90	96	CYP2D6, CYP3A4	[41][42]
Tacrine	17–37	0.5–3	1.3–7.0	75	CYP1A2, CYP2D6	[41][42]
Galantamine	85–100	0.5–1.5	5–7	18	CYP2D6, CYP3A4	[41][42]
Rivastigmine	40	0.8–1.7	2	40	Non-hepatic	[42]
Memantine	100	3–7	60–80	45	--	[42]

The main histopathological markers for AD are the occurrence of tau protein (tau) hyperphosphorylation and senile plaques (A β aggregation). The exact function of these proteins in the development of AD is not clear and over time, many ideas regarding the development of AD have been suggested.

The complexity of AD pathophysiology makes it challenging to discover effective treatments for AD. In addition, BBB which helps to protect the brain against neurotoxic blood-borne ingredients and cells, is a serious barrier to the use of pharmaceuticals in the therapy of AD. Extensive research has been conducted to develop techniques for drugs with nano molecules to cross the BBB.

Effective biomolecule targeting on colloidal carriers can help drugs cross the BBB via transport/carrier proteins, transcellular lipophilic routes, adsorptive-mediated transcytosis and receptor-mediated transcytosis, as well as increase drug concentration in brain lesions. Receptor-mediated endocytosis is a recognized mechanism and an established method for targeting the brain and is capable of avoiding the multidrug efflux system.

2.7 Repurposing of a drug: A strategy to treat AD

Drug repurposing is the process of developing an agent for a different purpose than it was originally intended. This approach appeals to research universities, charities, non-profit organisations, government and research council programmes, and it benefits pharmaceutical and biotechnology industries. (30). The biopharma industry considers drug repurposing as a way to prioritize a new indication during the development process, prior to approval (31). Drug repurposing, also referred to as old drug for new uses, is a highly efficient, low-cost, and low-risk way to discover new applications for existing drugs (32). In Phase II trials evaluating repurposed agents, it is important to consider the best target population and the mechanism of action of the treatment. The conventional process of developing drugs usually involves five phases: assessment of safety, exploration and preclinical analysis, clinical trials, monitoring of safety after the drug is approved by the FDA, and review by the FDA.

Table 2: Repurposing drugs used for Alzheimer’s disease

Agents	Current use	AD-related observation	References
Paclitaxel	Anticancer	Tau protein is phosphorylated, Paclitaxel lowers phosphorylation	(33)
Fasudil	ROCK inhibitors	Reduced amyloid β and neurological improvements	(16)
Bexarotene	Oncology	Increases $A\beta$ clearance	(34)
Nilvadipine	Antihypertensive	The localized cerebral blood flow has been restored. $A\beta$ synthesis is blocked.	(35)
Liraglutide	Diabetes	Enhance neuro protection Reduction $A\beta$ oligomers Anti-inflammatory activity	(36)
Fluoxetine	SSRI	Dentate gyrus neurogenesis is increased. Antioxidant Amyloid plaques may be reduced.	(37)
Amitriptyline	Tricyclic antidepressant	Enhance hippocampal BDNF Increase neurogenesis in the dentate gyrus Neuron protective activity	(38)
Apomorphine	Parkinson disease	Reduce levels of $A\beta$ (1–42) in brain Stimulates degradation of $A\beta$	(39)
Citalopram	SSRI	Decreases plaques and $A\beta$ levels in brain	(40)
Doxycycline	Antimicrobial	Reduced $A\beta$ fibrillation Neuroprotective	(41)
Deprenyl (selegiline)	MAOI	Neuroprotective DNA fragmentation is avoided. APP α -secretase cleavage is stimulated.	(42)
Sertraline	SSRI	Increases BDNF and neurogenesis in the hippocampal region. Amyloid plaques may be reduced.	(43)
Lithium	Mood stabilizer	Reduces $A\beta$ production. Neuron protection. Reduce CSF p-tau Improves cognition.	(44)
IVIg	Autoimmune mediated illnesses	Increases clearance of cerebral $A\beta$	(45)
Metformin	Diabetes	Decrease hyperphosphorylation of tau.	(46)

Nicotine	Smoking cessation	Promotes nonamyloidogenic pathway. Neuroprotective.	(47)
Rosiglitazone	Diabetes	Anti-inflammatory. Reduced A β oligomers.	(48)
Pioglitazone	Diabetes	Lowered oxidative stress Normalizes the flow of blood in the cerebrovascular system. Anti-inflammatory.	(48)
Imatinib	Oncology	Reduction of A β production Neuroprotective	(49)
Methylene blue	Toxicities	Antioxidant. Helps in the degradation and clearance of tau. Encourages autophagy Lowers A β levels.	(50)
Valproic acid	Antiepileptic	Increase phagocyte of A β . Suppress GSK-3 β -mediated γ -secretase cleavage of APP Anti-inflammatory	(51)
Insulin	Diabetes	Reduced A β production Enhance A β clearance Neuroprotective	(52)
Valsartan	Antihypertensive	Prevents A β oligomerization	(53)
Minocycline	Antimicrobial	Neuroprotective	(54)
Paroxetine	SSRI	Decrease levels of A β Decrease level of p-tau Enhance hippocampus growth and development of nervous tissue Chances to reduce amyloid plaques	(55)
Ladostigil	MAOI	Neuroprotective DNA fragmentation is avoided APP α -secretase cleavage is stimulated Acetyl- and butyrylcholinesterase inhibition.	(56)
Rifampin	Antimicrobial	Decrease A β accumulation. Neuron protection.	(57)
Clioquinol	Antimicrobial	Metal protein-attenuating compound	(58)
Nimodipine	Antihypertensive	Neuroprotective	(59)
Nonsteroidal inflammatory Drugs	anti Analgesic	Anti-inflammatory activity Anti-oxidant Reduction of A β (1–42)	(60)

Nitrendipine	Antihypertensive	The localized cerebral circulation has been restored. Enhance the clearance of A β	(61)
Verapamil	Antihypertensive	Neuron protection activity. Decrease A β (1–40) oligomers.	(62)

2.8 SIM: A drug for AD treatment

Chemically, SIM is (1S,3R,7S,8S,8aR)-8-{2-[(2R,4R)-4-hydroxy-6-oxooan-2-yl] ethyl}-3,7-dimethyl-1,2,3,7,8,8a-hexahydronaphthalen-1-yl 2,2-dimethyl butanoate shown in Figure 4 (63). It appears as a white powder with a molecular weight of 418.566 g/mol and a log P is 4.46. SIM is a reversible lactone prodrug that goes through metabolism (64). It is a lipid-lowering drug that works by inhibiting hydroxy-methyl-glutaryl coenzyme A (HMG CoA) reductase. This helps in the conversion of HMG-CoA into mevalonate (65). Thereby it reduces plasma low-density lipoprotein (LDL) cholesterol by depleting intracellular cholesterol. In addition, it increases LDL receptor expression and helps in the treatment of hypercholesterolemia. SIM used to prevent hypercholesterolemia. It is a reversible lactone prodrug that goes under metabolism for lowering the level of lipid. It inhibiting HMG CoA reductase, which help to convert HMG-CoA to mevalonate. Thereby it reduces low-density lipoprotein (LDL) cholesterol in plasma and cause depletion in the accumulation of intracellular cholesterol (66). In addition, it also increases LDL receptor expression and helps in the treatment of hypercholesterolemia. SIM produces pleiotropic neuroprotective actions in the brain and stimulates many routes, including: Suppression of inflammatory mediators and microglial activation, Inos reduction, activation of neurotrophic factor expression (BDNF, NGF), and apoptosis inhibition (67).

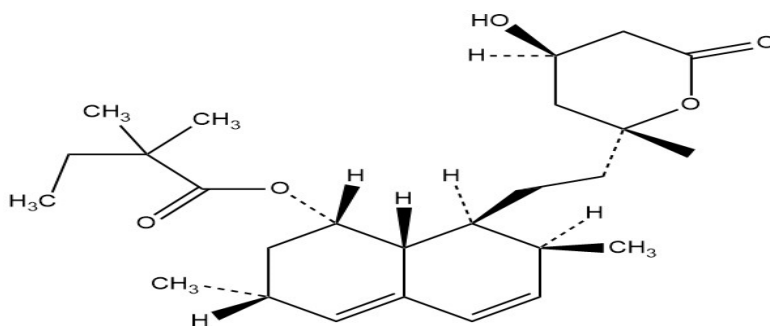


Figure 4: Structure of SIM

2.9 Challenges of SIM (Pharmaceutical challenges)

SIM is extremely lipophilic and GI labile, it undergoes extensive enzymatic breakdown and first-pass metabolism in the GIT after oral administration, and the remains non-

degradable drug is insoluble in the GIT medium (68). As a result, overall therapeutic effectiveness and oral bioavailability are reduced. SNEDDS are well-known for their ability to both increase drug solubility and protect the GIT from toxicity. SNEDDS is a thermodynamically stable that has been extensively studied for its ability to improve the bioavailability of poorly water-soluble drug molecules. The nano globules have a larger surface area, which helps in the increased bioavailability of the drug molecules.

2.10 Nanoformulations is an approach to AD

Nanoformulations are the best way to improve the bioavailability & therapeutic effect of the drug molecule. Nanoformulations have unique features like: smaller particle size, improving systemic circulation, and helping in reducing the dose (2). Due to these unique features, various researchers develop nanoformulations of different drug molecules and explored in AD in a view to improving their therapeutic effect.

Table 3: Nanoformulations of treatment for AD

Drug	Type of nanoparticles	Models	Route of administration	References
Aducanumab	Dendrimer nanoparticles	Mice	-	(69)
Curcumin	Curcumin nanoparticles	-	-	(70)
Curcumin	Pluronic F127 nanoparticles	-	IV	(71)
Curcumin	selenium nanoparticles	Mice	-	(72)
Rivastigmine	Poly (n-butylcyanoacrylate)	Rat	I.V. injection	(73)
Penicillamine	Polystyrene Nanoparticles	-	-	(74)
Clioquinol	Polymeric n-butyl-2-cyanoacrylate	AD transgenic Mice (APP/PS1)	I.V. injection	(75)
Tacrine	Chitosan nanoparticles	Rat	I.V. injection	(76)
Thioflavin T and S	Core-shell nanoparticles	APP/PS 1 Mice	Intracerebroventricular injections	(77)
Polyphenol EGCG	Nanolipidic particles	Rat	oral	(78)

2.11 SNEDDS can be suitable

Many of the drugs mainly BCS II class drugs show poor permeability and poor solubility. From last few years many traditional techniques are used to overcome this problem. Some

of these techniques are like reduction in particle size, salt form of the drug, complexation etc, but these techniques show some limitations like in case of salt formation, salt forms don't present in their original form so they may be converted into acid or base in GIT. In case of a reduction in particle size, they may cause the problems like poor wettability. So, because of certain limitations, some lipid-based techniques are used to increase the bioavailability and solubility of the drugs, one of these techniques is SNEDDS (79). Isotropic mixtures called SNEDDS consist of a combination of oil, surfactant, co-surfactant, and drug. These are clear or translucent emulsions having droplet size 100 nm and can form stable O/W type of nanoemulsions. They dissolve larger quantities of lipophilic drugs and protect drug from hydrolysis. In case of parenteral preparations, they prevent enzymatic degradation of the drug. These nanoemulsions are thermodynamically stable. It is optimized by pseudo ternary phase diagram. Now SNEDDS are applied in different aspects of drug delivery systems like in Cancer therapy, cosmetics, parenteral drug delivery, transdermal drug delivery and ophthalmic drug delivery. From last few years SNEDDS, SMEDDS and SEDDS are used to improve the hydrophilicity of poorly hydrophilic drugs. Partitioning of the drug between lipophilic as well as hydrophilic phase can be easily done by this system. SNEDDS are the type of systems which are thermodynamically stable and transparent in nature. Stability of these nanoemulsions can be increased with addition of surfactants and co-surfactants (80).

2.12 Preparation of SNEDDS & requirements

This drug is dissolved in the lipophilic part of the nanoemulsion and liquid phase is combined with co-surfactant and surfactant. Then the liquid phase has to be mixed in the oily phase slowly with continuous stirring until the suspension becomes transparent. The desired range of dispersed globules can be achieved using ultra sonicator.

SNEDDS can be prepared by two ways:

- (a) Preparation of liquid SNEDDS
- (b) Preparation of solid SNEDDS

2.12.1 Preparation of liquid SNEDDS

In this the ratio of surfactant/ co-surfactant and oil/co- solvent has to be selected via pseudo ternary phase diagram. Then, number of series of formulations has to be made by taking dissimilar concentrations of surfactant, cosurfactant and oil. All of them should be weighing accurately and then the drug has to be dissolved in the mixture. Then that mixture has to be stored or kept at room temperature.

2.12.2 Preparation of solid SNEDDS

In this type of SNEDDS preparation appropriate solvent has to be used which has to be added in mortar pestle containing drug. Then when damp mass will be formed that has to be pass through sieve and then dry at room temperature.

2.12.3 Composition of SNEDDS

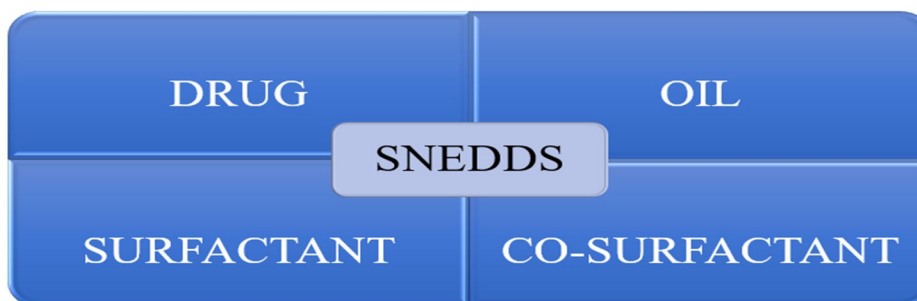


Figure 5: Composition of SNEDDS

2.12.4 Excipients

The composition of SNEDDS actually uses co-surfactants, surfactants and oils. The oils used to make SNEDDS are hydrolysable, biodegradable, and have a low HLB value. These oils improve in the solubility and transport of drugs via lymphatic pathways, hence increasing their bioavailability. Different oils used in the preparation of SNEDDS are mentioned in Table 4.

To prepare SNEDDS, a surfactant with a high HLB value and a very great safety profile is utilized. Its amphiphilic characteristic improves in the solubilization of the drug in a combination of oil and water. They enhance the oral bioavailability of lipophilic pharmaceuticals by increasing their dissolving rate.

Table 4: Common oils used for preparation of SNEDDS

Oils/Lipids	Chemical name	HLB Value	References
Capmul MCM EP	Glyceryl Caprylate/Caprates	5.5-6	(81)
Caprylic/capric Triglyceride	Caprylic/capric triglyceride	12.5-14	(82)
Capmul MCM C8	Glyceryl Monocaprylate	5-6	(83)
Castor oil	Castor oil	6.6-7.5	(84)
Cinnamon oil	Cinnamon oil	16	(85)
Cotton seed oil	Cotton seed oil	7.5	(86)
Corn oil	Corn oil	9	(87)
Crodamol GTCC	Caprylic/Capric Triglyceride	10	(88)
Cremophor EL	Macroglycerol Ricinoleate	12-14	(83)
Ethyl oleate	Ethyl oleate	10.6-11.5	(89)
Isopropyl myristate	Myristic acid isopropyl ester	11.5	(90)
Labrafac PG	Propylene glycol dicaprylocaprate EP Propylene glycol dicaprylate/dicaprate NF	14	(91)
Lauroglycol FCC	Propylene glycol mono laurate	4-5	(92)
Labrafac CC	Caprylic/Capric Triglyceride	1	(83)
Mineral oil	Higher alkanes from mineral source	4	(93)
Maisine oil	Glycerylmonolinoleate	-	(94)
Miglyol 812	Liquid lipids/C8/C10 triglycerides	15.36	(95)
Myvacet 9-45	Myvacet 9-45K NF	3.8	(96)
Methyl oleate	Oleic acid methyl ester	-	(97)
Oleic acid	Octadecenoic acid	-	(98)
Olive	Olive	8	(98)
Peanut	Peanut	-	(93)
Peceol	Glycerol monooleate	-	(99)
Sesame	Sesame	-	(93)
Sunflower	Sunflower	-	(93)
Soybean	Soybean	-	(98)

Table 5: Common surfactant and co-surfactant used for preparation of SNEDDS

Surfactants	Chemical name	HLB Value	References
Capmul MCM	mono-diglyceride of medium chain fatty acids	5.5-6.0	(100)
Labrafil M 2125	PEG-6 corn oil	9	(101)
CS			
Labrafil	PEG-6 apricot kernel oil	9	(101)
M1944CS			
Labrasol	Caprylocaprylmacrogol glycerides	13.2	(92)
Polyoxamer 407	Poly (ethylene glycol)-block-poly(propylene glycol)- block-poly(ethylene glycol)	18-23	(102)
Polyoxamer 188	Pluronic F-68 solution	29	(102)
Solutol HS 15	Macrogol (15)-hydroxystearate	15	(102)
Span 20	Sorbitanmonolaurate	8.6	(93)
Span 80	Sorbitanmonooleate	4-6	(98)
Span 85	Sorbitantrioleate	1.8	(98)
Tween20	PEG-20 sorbitanmonolaurate	16.72	(102)
Tween-80	PEG-20 sorbitanmonooleate	15	(102)
Tween-85	PEG-20 sorbitantrioleate	11	(102)
Capmul MCM- C8	Glycerylcaprylate	5-6	(87)
Lauroglycol	Propylene glycol monolaurate	4	(92)
FCC			
Lutrol F127	PolyoxamersPh Eur., Polyoxamers	-	(92)
PEG 400	Polyethylene glycol 400	11.6	(92)
PG	Propylene glycol	3	(102)
Transcutol P	Diethylene glycol mono ethyl ether	-	(102)

Several surfactants used in the preparation of SNEDDS are mentioned in Table 5. To lower the concentration of surfactant, reduce the size of the droplets, and enhance drug loading. It is suggested to utilize co-surfactants. Table 5 lists the co-surfactants used in the preparation of SNEDDS, which aid in increasing the solubility of hydrophilic surfactants in the isotropic solution.

2.13 Mechanism of drug transport from SNEDDS

When SNEDDS administered orally it undergoes three phases i.e. digestive, absorptive and circulatory phase. The SNEDDS produced a coarse emulsion during the digestion phase. The developed coarse emulsion now subjected to the enzymatic hydrolysis at oil-water interface and the interactions of fatty acid and bile created the mixed micelles. Now the developed colloidal micelles get absorbed by active and passive diffusion through the enterocyte membrane as well as lymphatic system in the form of chylomicrons. After absorption, the circulatory phase starts, and in this phase, drugs get released from the excess lipid and chylomicrons gets utilized by the body.

2.14 SNEDDS reported for various drug molecules

In recent years researchers develop various SNEDDS formulations of various synthetic drugs in order to increase bioavailability, solubility, and therapeutic activity.

Table 6: Different SNEDDS prepared

Drug	Composition of Liquid SNEDDS	References
Loratadine	Sodium lauryl sulfate, T-80, Pluronic F68.	(103)
Loratidin	Capriole, Liquid paraffin, TP, and Span 20	(104)
Carvedilol	Nikkol HCO 50 and C-MCM	(105)
Lovastatin	Capmul MCXM, Nikkol HCO- 50, Lutrol F127	(106)
Nifedipine	Imwitor 742	(107)
Vitamin A acetate	Capmul MCM-C8, Cremophore EL, and Soyabean oil	(108)
Darunavir	TP, T-80, and C-MCM	(83)
Cilostazol	T-80, Labrasol, and Peceol	(109)
Embelin	PEG 400, Capryol 90, and Acrysol EL 135	(110)
Rosuvastatin calcium	PEG 400, olive oil, Garlic oil and Tween-80	(111)
Valsartan	C-MCM, Labrasol, T-20	(112)
Loratidine	Solutol HS 15, Capmul MCM C8	(113)
Celecoxib	Propylene Glycol, Capryol 90, and Cremophor RH 40	(114)
Rosuvastatin	poloxamer 407, TP, and Capryol 90	(115)
Flurbiprofen	Labrasol, Transcutol HP, and Labrafill M 1944	(116)
Glimepiride	PEG and Mygliol 812, PEG, and Tween 80	(117)
Olmesartan medoxomil	T-80 Oelic acid, and Transcutol-HP	(118)

Repaglinide	Olive oil, Miglyol Cremophore RH 40, Capryol 90 and Labrasol	(119)
Erlotinib	Labrasol ,Transcutol HP, and Labrafil M2125CS	(120)
Docetaxel	Capryol 90, Cremophore EL and Transcutol HP	(121)
Irbesartan	Capryol 90, Cremophor RH40 and Transcutol HP	(122)
Glipizide	Solutol HS15, Imwitor 988, and Captex 355	(123)

2.15 Characterization of SNEDDS

Characterization of created nanoformulations is a critical step in formulations development and optimization. The several assessment methods used to evaluate nanoformulations, as well as their benefits and drawbacks shown in Table 7.

Table 7: Characterization methods for nanoparticles, including benefits and drawbacks

Parameters	Techniques	Benefits	Drawbacks
Droplet size, and size distribution	Laser diffraction	Wide measurement range Quick Non-invasive This technique is suitable for analyzing both liquid suspension and dry powder samples	Spherical particles are assumed
	Coulter counter PCS/DLS	More precised rapid, non-invasive	Only apply to spherical particles. Short measurements limit Only applicable for liquid suspensions
Zeta potential and surface charge of particles	Laser electrophoresis	Doppler Fast and precise	-
Droplet size and shape	FE-SEM and TEM	Consider droplets shape as well as particle size. Only a small amount of sample is required.	Difficult to obtain statistical size distribution Time-consuming
	AFM	Non-invasive Examine droplet size and shape Little amount of sample is necessary.	Usually invasive, Consuming more time Difficult to get statistical particle sizes
Crystalline phase level	DSC and XRD	Provides data on drug polymorphism, crystal stability, and crystallinity	-
Interaction between chemicals	FTIR/ IR/ FTIR/ LCMS	Selective and sensitive	-

2.16 Etiopathogenesis

SNEDDS is a thermodynamically stable system that has been extensively studied for its ability to increase the bioavailability of lipophilic drug molecules. The nano sizes have a larger surface area, which helps in the increased bioavailability of the drug molecule. The isotropic mixtures were prepared by mixing the concentration of oil, surfactant, and co-surfactant and then vortexed for 15 mi.

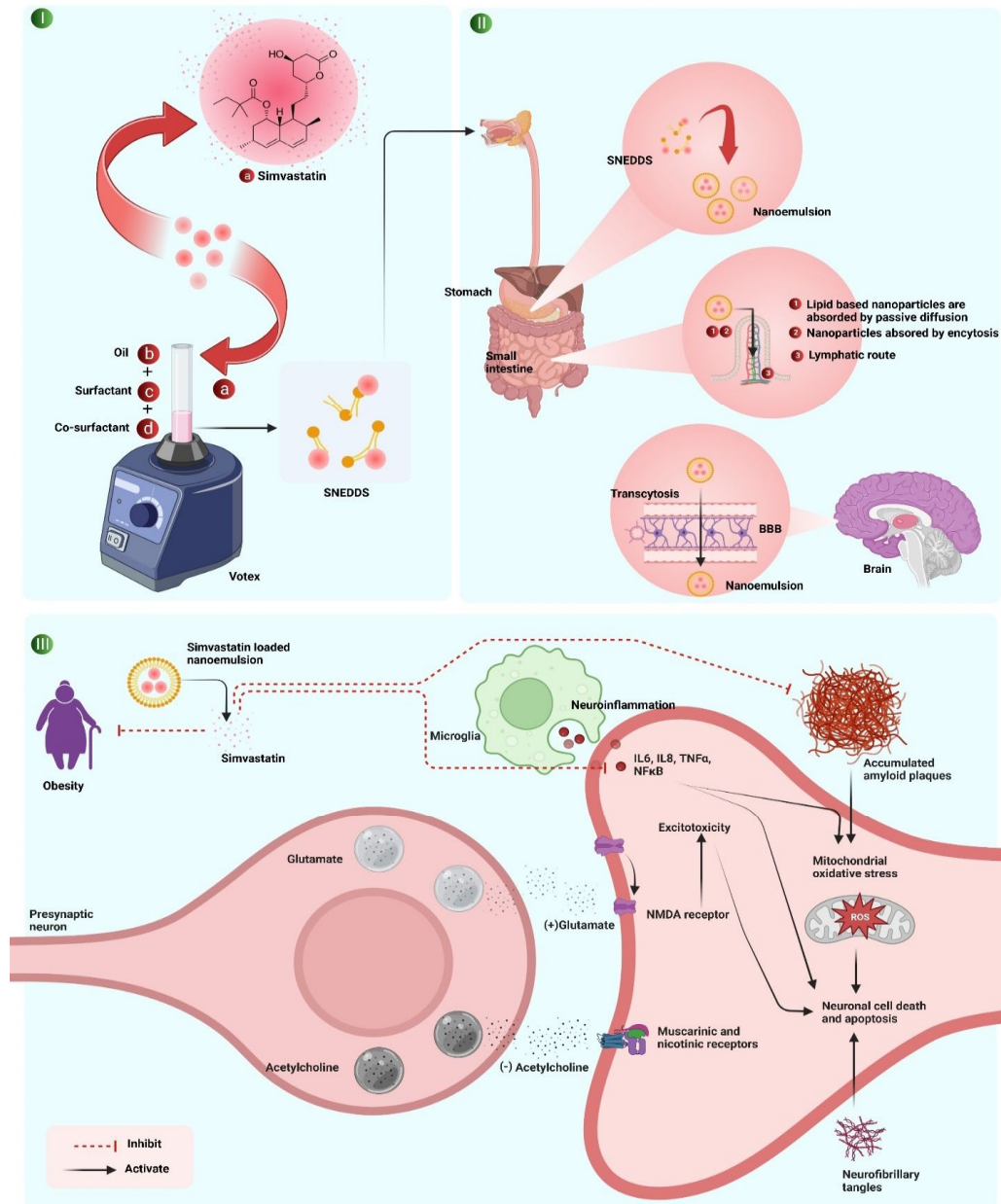


Figure 6: Etiopathogenesis of AD

When SNEDDS is administered orally it undergoes three phases i.e. digestive, absorptive, and circulatory phases. During the digestive phase, a coarse emulsion was formed by the SNEDDS. The developed coarse emulsion now undergoes enzymatic hydrolysis at the oil-water interface, resulting in mixed micelles formed by the interaction of fatty acid and bile. Colloidal micelles are now absorbed via passive or active diffusion through the enterocyte membrane, as well as lymphatic circulation in the form of chylomicrons. Following absorption, the circulatory phase begins, during which drugs are released from the excess lipid and chylomicrons is used by the body. AD is a chronic condition in which degeneration of neurons is observed in various parts of the brain. There are many factors associated with AD. Those factors led to promote pathogenetic abnormality in the brain, such as enhanced oxidative stress, neuroinflammation, mitochondrial dysfunction degeneration of cholinergic neurons, amelioration of glutaminergic neurons, and formation of amyloid β . SIM can be successfully attributed to pathogenic factors associated with AD, it can reduce oxidative, neuroinflammation, accumulated amyloid β , as well as obesity and due to this, it produces symptomatic relief in AD.

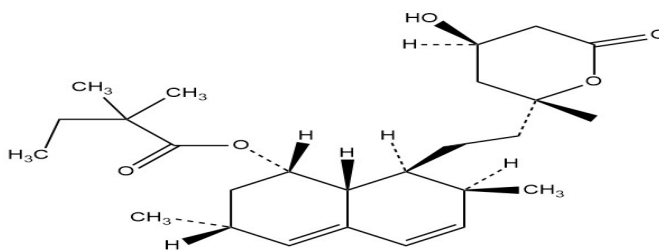
2.17 Drug profile

2.17.1 Simvastatin

Table 8: Physiochemical property of SIM

Characteristic	Description
Name of drug	Simvastatin
Pharmacological class	Antihyperlipidemic
Chemical formula	C ₂₅ H ₃₈ O ₅
Molecular weight	418.5 g/mol
Synonyms	Zocor
IUPAC name	(1S,3R,7S,8S,8aR)-8-{2-[(2R,4R)-4-hydroxy-6-oxooxan-2-yl] ethyl}-3,7-dimethyl-1,2,3,7,8,8a-hexahydronaphthalen-1-yl 2,2-dimethylbutanoate

Chemical structure



Solubility	Insoluble in water
Melting point	134-138°C
Partition coefficient (Log P)	4.68
Protein binding	95% (Approximately)
Half life	3 hrs (Approximately)

CHAPTER-3

3. Hypothesis of the study

3.1 Hypothesis

1. AD is a most challenging neurological disorder and one of the critical examples of failure of medical, pharmaceutical and health care sector. In present situation, around 55 million people are suffering, from dementia which make AD as a 7th leading reason for death (9). It is very important to note that neurological disease is 6.3% of global burden of diseases and people with this disease die before the age of 80 which indicates that death rate in AD is 30%.
2. Aluminium can enter into human body through utilization of utensils, food supplements, drinkable water, perfumes, antacids and drugs (124). Once it enters into human body it affects as neurotoxicants and reaches to hippocampus as well as frontal cortex area of brain (125) and bring etiogenesis of AD (126). Aluminium also known to induce misfolding of proteins and causes development of β -plaques (127). Since Aluminium is most abundant metal on the earth causes cognitive impairment. These all abnormal development is due to oxidative stress and cholinotoxication (128). Aluminum causes impairment of cholinergic system (cholinotoxication) as a result of this impairment of acquisition and retrieval of learning with memory skills takes place (129). Various animal studies also suggests that $AlCl_3$ causes alteration in chemicals of neurons, behavioral activities and pathology of neurons in the brain (130). $AlCl_3$ is responsible to cause hyperlipidemia and dementia (131).
3. Current treatment strategies provide partial and unsatisfactory relief from AD with multiple side effects but they are not suitable to provide stoppage of progression of diseases. Therefore, there is requirement of drug with proper delivery system capable of targeting multiple sites or target with reduction in the symptoms of AD. The drug candidate must be able to contribute in reversal of pathology of AD with fewer side effects. In another way we need to develop novel and effective medication focusing on alternative of present treatment.

- Recent studies highlight that the prevalence of dementia low among patients taking statin over a longer period of time (67) statin not only lower the level of cholesterol but also produces anti-inflammatory, antioxidant and neuroprotective effects (132).

USFDA reported on February 28,2012 that the statin provides reversal of dementia (133). FDA also recommended it as cardioprotective (134). SIM is poorly soluble in water and is known to show its action is with its hydrolysis to form β -hydroxy acid which is responsible to inhibit 3 hydroxy-3methylglutaryl co-enzyme A (HMG-CoA) reductase. This inhibits stops cholesterol biosynthesis which can protect AD indicated in figure 7

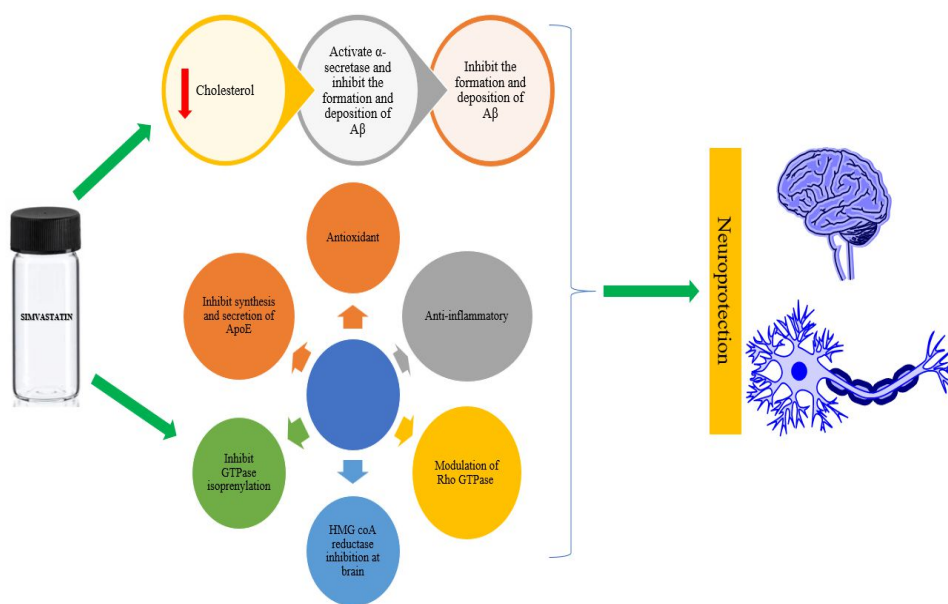


Figure 7: Schematic representation of SIM as a neuroprotective agent

- Owing to its poor solubility, several formulation approaches have been investigated, including cyclodextrin complex, solid dispersion, nanosuspension, bionanocomposites, co-solvent assisted solubilization and microparticles to improve solubility of SIM. SNEDDS is a thermodynamically stable isotropic mixture of oil, surfactant, co-surfactant and drug that form a spontaneous oil-in-water nanoemulsion with a droplet size less than 20-200nm. when introduced into an aqueous medium under gentle agitation. The free energy required for

self nanoemulsification process is low. Thus, the process will occur spontaneously. The enhanced interfacial area of micronized globules will facilitate the dissolution of drug thereby improving the bioavailability and enhance permeability through biological membranes due to presence of lipid and surfactant. Several potential advantages of SNEDDS include their ability to present drug in a solubilized form inside the gastrointestinal (GI) lumen, thus providing greater interfacial area for drug absorption, providing greater chemical and enzymatic stability, inhibiting P-glycoprotein (p-gp) mediated drug efflux, enhancing lymphatic transport.

6. Consequently, In present study SNEDDS of SIM is formulated, developed and investigated here for the evaluation of its level of protection in AlCl₃-triggered AD in animals.

3.2 Aim

Development and evaluation of Simvastatin based SNEDDS for treatment of Alzheimer's disease.

3.3 Objectives

1. Formulation development and optimization of self-emulsifying drug delivery system (SNEDDS) of Simvastatin.
2. Characterization and evaluation of developed formulations.
3. Stability study and *ex vivo* permeation study of optimized formulation.
4. *In vivo* evaluation of optimized formulation.

CHAPTER-4

4. Methodology

4.1 Materials used

Table 9: Materials used

Chemicals	Manufacturers
Simvastatin (SIM)	Micro lab, Pvt. Ltd, Mumbai, India
Acetonitrile HPLC Grade, Orthophosphoric acid, Triethylamine, Hydrochloric acid, Ammonium acetate, Hydrochloric acid, Aluminium Chloride, Formic acid, Trehalose Mannitol, Sorbitol	Lobachemie Pvt. Ltd., Mumbai, India
Aerosil 200, Potassium Dihydrogen Orthophosphate (KH ₂ PO ₄), Sodium Hydroxide pellets, Ethanol, Tween (80,20 and 60), Span (20,40,60 and 80), PEG (200,400,600 and 800) Pluronic F-68, Sesame oil, Peanut oil, Sunflower oil, Cotton seed oil, Soyabean oil, Mustard oil, Oleic acid, Olive oil, Eucalyptus oil Castor oil, Hydroxy propyl beta cyclodextrin (HPBCD), Polyviny alcohol (PVA), Sodium carboxy methyl cellulose (NA-CMC)	Central drug house Pvt. Ltd, New Delhi, India
Millipore water	Bio-Age Equipment Ltd., Mohali, India
Transcutol P, Lauroglycol FCC, Labrafac CC, Labrafil MI944CS, Labrafil M2125, Labrasol, Maisine 35-1, Capryol 90	Gattefosse Pvt. Ltd., Mumbai, India
Miglyol 812N	Cremer Ole GmbH& Co.KG, Germany
Syloid XDP3150	Grace Material Technologies, Discovery Sciences, Pune, India
Capmul MCM	M/S Abitec Corp., Ohio

4.2 Equipments used

Table 10: Equipment used

Types of equipment	Model/Manufacturer
Electronic weighing balance	CY360, Shimadzu Co. Ltd., Kyoto, Japan
Dissolution apparatus	DS 8000 (Manual) Lab India, Mumbai, India
pH meter	Phan, Lab India, Mumbai, India
RP-HPLC	HPLC LC-20AD, Shimadzu Co. Ltd., Kyoto, Japan
UV spectrophotometer	UV-1800, Shimadzu Co. Ltd., Kyoto, Japan
Spray dryer	JISL Spray Mate, Jay Instruments, Navi Mumbai, India
Ultrasonication bath	Loba Life, Lobachemie, Mumbai, India
Hot air oven	Cadmach Drying Oven, Cadmach Machinery Ltd., Ahmadabad, India
Magnetic stirrer	Remi 5MLH, Vasai, Mumbai, India
FTIR spectrophotometer	Shimadzu Co. Ltd., Kyoto, Japan
Stability chamber	Remi CHM 10S, Remi Sales & Engineering Ltd., Mumbai, India
Differential scanning calorimeter	DSC Q200 V24.4 Build 116
Scanning electron microscope	Hitachi S-3400N
Transmission electron microscope	FEI Tecnai G 2 F20 model, Netherlands
XRD analyzer	PAN analytical X'pert 3 Pro, Netherlands
Partilce size	Zetasizer, Malvern Instruments Ltd., Malvern, U. K.
Actophotometer	INCO Pvt. Ltd., India
Centrifuge	Remi Instruments, India

4.3 Computer programs and software

Table 11: Computer programs and software used

Software	Manufacturer
GraphPad Prism	GraphPad Inc., La Jolla, USA
Origin Pro (version. 8.5)	Origin Lab Corporation, Northampton, USA
BioRender	Crunchbase Pvt. Ltd. Toronto, Canada
Design Expert (version 11.0.5.0)	Stat-Ease, Inc, Minneapolis, USA
Endnote X8	Thomson Reuters, USA
Chem draw	Perkin Elmer, USA

4.4. Methodology

4.4.1 Characterization of drug

Characterization of SIM was carried out to determine its physical nature, melting point, λ_{\max} .

4.4.2 Physical description

About 1g of drug was taken and spread on a glass slide. The colour of the drug was identified through personal inspection (135).

4.4.3 Melting Point Determination

The melting point of the drug was carried out by both capillary fusion method and Differential Scanning Calorimetry (DSC) method.

4.4.3.1 Capillary fusion method

The melting point of SIM was determined using a popular India equipment. The capillary was sealed at one end by heating on a flame. The sample (SIM) was placed in a thin-walled capillary tube of 10-15cm length and a diameter of 1 mm. The capillary containing the drug and a thermometer was put in the melting point equipment and properly heated. The capillary tube was observed through a window and the temperature at which the sample melted was noted (136).

4.4.3.2 Differential Scanning Calorimetry (DSC)

The DSC of SIM was evaluated by the Perkin Elmer DSC Apparatus. Powdered

sample (2-3mg) was taken in aluminium pan, heated over the range of 30-440°C at 10°C/min using a dry-nitrogen flush at rate of 19.8mL/min (80).

4.4.4 Determination of ultraviolet absorption maxima (λ_{max})

Drug sample (SIM) (10 µg/mL) was prepared in methanol and scanned to determine absorption maxima in the range of 200-800 nm on UV spectrophotometer against methanol as blank (137).

4.4.5 RP-HPLC method development for the quantification of the drug

To separate the components in high-performance liquid chromatography, the following instruments were used, a 20-L loop [Rheodyne], a photodiode arrays detector [PDA] [SPDM20A, Shimadzu., Japan], a mobile phase delivery pump [LC 20 AD, Prominence, Shimadzu., Japan], and a C-18 reverse phase column [Nucleodur C18, 250 mm 4.6mm i.d., 5 Macherey Nagel]. LC solution software was used to operate the HPLC equipment. Acetonitrile (A) and water (B) in ration of 90:10 was used as a mobile phase. The chromatogram showed a wavelength of 238 nm with the flow rate set to 1 mL/min.

4.4.5.1 Linearity and range

Plotting the average peak area of 6 samples versus the SIM concentrations and finding out the regression equation obtained the calibration curve. (138).

4.4.5.2 Accuracy

All the quality control standard (QCS) solution i.e., LQC, MQC, and HQC were prepared and injected repeatedly (six times) and average response was reported. The % accuracy calculated by given equation 1 (139).

$$\% \text{ Accuracy} = \frac{\text{Actual concentration recovered}}{\text{Theoretical concentration}} * 100 \quad - \text{ Eq. 1}$$

4.4.5.3 Precision

This was determined based on intermediate precision and repeatability precision of the developed method. Repeatability of the standard concentration were tested by injections six times at the same day and under the same chromatographic conditions.

Same procedure repeated by different 3 analyst (inter-analyst), under the same experimental environment to determine intermediate procedure. The mean of the responses was used to determine the % relative standard deviation (%RSD). (80, 140) (141).

$$\% \text{Relative standard deviation} = \frac{\text{Standard deviation of peak area}}{\text{Average peak area}} * 100 - \text{Eq.2}$$

4.4.5.4 Robustness

To evaluate the effect of small changes chromatographic condition on the developed method such as λ max (236nm, 238nm, 240nm) of the drug, flow rate (0.8 mL/min, 1 mL/min, and 1.2 mL/min), and ratio (88:12, 90:10, and 92:08) of the mobile phase were determined by the injecting MQC samples repeatedly (six times) in the HPLC. Retention time, peak area and % recovery of the drug was recorded (142).

4.4.5.5 LOD and LOQ estimation

The LOD and LOQ were determined by utilizing the calibration curve's slope (S) and the standard deviation of the response (σ). Standard deviation was calculated using by intercept of the regression plot (141).

$$\text{LOD} = 3.3 \frac{\sigma}{S} - \text{Eq. 3}$$

$$\text{LOQ} = 10 \frac{\sigma}{S} - \text{Eq. 4}$$

4.4.6 Formulation development

4.4.6.1 Solubility study

The solubility analysis was carried out to choose the most acceptable co-surfactant, surfactant, and oil for the preparation of SIM-SNEDDS. Analysis solubility of SIM were carried out in various oils (castor oil, olive oil, eucalyptus oil, Almond oil, cotton seed oil, Lauroglycol FCC, C-MCM), surfactants (tween 20, tween 80, polyoxamer 407, polyoxamer 188, labrafil M 1944 CS) and co-surfactant (TP) respectively. SIM (10mg) was added to 1mL of each co-surfactant, surfactant, and oil in a 5 mL glass vial and vortexed for 2-3 min. with a vortex. Further, all the vials were stoppered and kept in shaking water bath for 48 hours at $37 \pm 0.2^\circ\text{C}$ at 50 R.P.M. After that methanol was used to dissolve the supernatant and concentration of the drug was calculated by injecting the samples into an RP-HPLC and response was measured at 238nm (143).

4.4.6.2 Preparation of SNEDDS

After the analysis of solubility data, CMCM, T-80, and TP were selected as an oil, surfactant and co-surfactant respectively, for the formulation of SNEDDS. By adjusting the oil and S_{mix} (surfactants and co-surfactants) concentrations, a number of (27) prototypes formulations were developed. S_{mix} by changing the ratio between 1:1,1:2, and 2:1. Composition of SNEDDS prototypes were shown in Table 1. The oil, surfactants, and co-surfactants were vortexed (Cyclo Mixer, REMI, India) for 15 minutes to develop the SNEDDS pre-concentrate (1 mL) for all batches. Further, SIM (10 mg) was added to each prepared pre-concentrate and vortexed for 15 min. All the pre-concentrate was converted into emulsion by diluting it with 500 mL of distilled water. The mixture was stirred at 500 rpm and temperature was maintained $37 \pm 0.2^\circ \text{C}$ for 5-7 min (144).

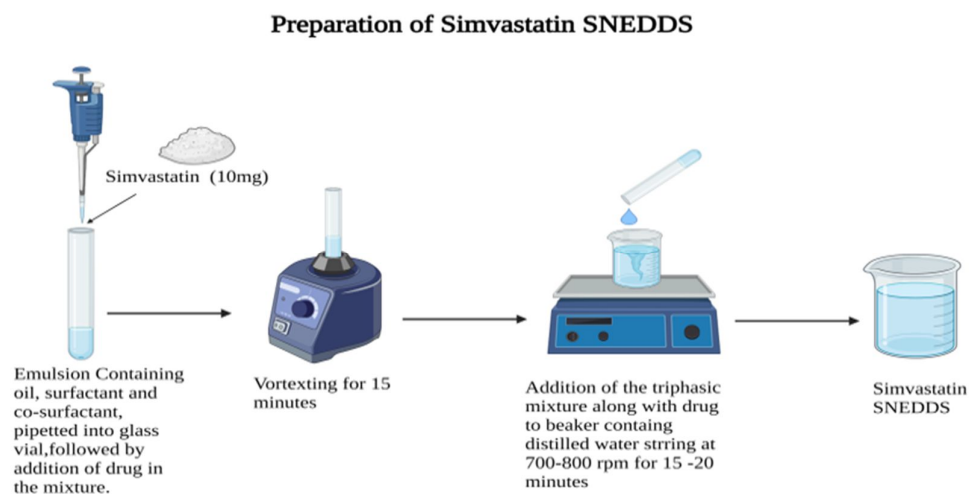


Figure 8: Method of preparation of SIM-SNEDDS

4.4.6.3 Construction of pseudo ternary phase diagram (TPD)

After the analysis of solubility data, CMCM, T-80, and TP were selected as an oil, surfactant and co-surfactant respectively, for the formulation of SNEDDS. By adjusting the oil and S_{mix} concentrations, a number (27) SNEDDS prototypes were prepared. S_{mix} composition varying between 1:1,1:2, and 2:1. Composition of SNEDDS prototypes were shown in Table 12. All the stable emulsion having clear and transparent appearance were considered as a SNEDDS while stable but translucent emulsion were

identified as a SMEDDS. Triplot software version 4.1.2 was used to construct a simulated pseudo TPD. In this diagram formulation components such as oil, surfactant and co-surfactant represent triangles apices (145).

Table 12: Composition of SNEDDS for ternary phase study

Formulation Smix (1:1)	Capmul MCM (μL)	Tween 80 (μL)	Transcutol P (μL)
F1	100	450	450
F2	200	400	400
F3	300	350	350
F4	400	300	300
F5	500	250	250
F6	600	200	200
F7	700	150	150
F8	800	100	100
F9	900	50	50
Formulation Smix (2:1)	Capmul MCM	Tween 80	Transcutol P
F10	100	600	300
F11	200	530	270
F12	300	470	230
F13	400	400	200
F14	500	330	170
F15	600	270	130
F16	700	200	100
F17	800	130	70
F18	900	70	30
Formulation Smix (1:2)	Capmul MCM	Tween 80	Transcutol P
F19	100	300	600
F20	200	270	530
F21	300	230	470
F22	400	200	400
F23	500	170	330
F24	600	130	270
F25	700	100	200
F26	800	70	130
F27	900	30	70

4.4.6.4 Design of experiment (DOE) optimized of the formulation

The SNEDDS formulation was optimized using the Box-Behnken design. Oil, surfactant, and co-surfactant concentrations were adjusted at 3 levels: high (+1), medium (0), and low (-1) were selected as independent variables. Dependent variables were checked against for GS (nm), PDI, ZP (mV). The developed model was adjusted to suit in the design model and the level of relevance was determined. The perturbation plots and 3D surface responses obtained were used to evaluate the influence of different concentrations of independent variables (Factors) on the SNEDDS formulations.

Graphical optimization was carried out the overlay plot obtained defined the fully model's optimal region. The equation of a polynomial found was also used to study the effect of independent variables on the responses (dependent variables) (145). The BBD design formulation codes and the runs are given in Table 13.

Table 13: Compositions of SNEDDS using BBD

Run	Factor 1 Oil (μL)	Factor 2 Surfactant (μL)	Factor 3 Co-Surfactant (μL)
1	150	530	300
2	100	565	270
3	200	530	285
4	200	600	285
5	150	565	285
6	200	565	270
7	100	600	285
8	150	600	270
9	100	565	300
10	150	600	300
11	200	565	300
12	100	530	285
13	150	530	270

4.4.7 Evaluation of optimized SNEDDS

4.4.7.1 Thermodynamic, centrifugation, and cloud point determination

To determine thermodynamic stability, the optimized SIM- SNEDDS were put to stress conditions through heating-cooling (4°C, and 40°C) cycles and freeze-thaw (-21°C, and +25°C) cycles. To determine the cloud point temperature, 10 mL of diluted formulations was put down over a heating water-bath while the temperature of the composition was continuously measured and the appearance of cloudiness was recorded. When the transparent SNEDDS began to turn turbid, the temperature was recorded as cloud point temperature. Phase separation during centrifugation was observed visually after centrifugation of 1 mL of diluted formulation at 10000 rpm for 20 min (146).

4.4.7.2 Effect of dilution and pH

SIM-SNEDDS were studied to evaluate how variations in dilute volume and pH influenced mean droplet size, drug precipitation and phase separation in formulations. SIM-SNEDDS were dissolved in various volumes of water (250, 500, and 900mL) and pH levels (1.2,6.8,7.4) and the influence of dilution and pH changed was noticed (147).

4.4.7.3 Drug Loading of SIM in SNEDDS

The SIM-containing SNEDDS were vortexed for 15 min with 1 mL of the optimized formulation of SNEDDS. This was mixed with 500 mL of double distilled water at 500 r.p.m using magnetic stirrer. The water bath temperature was kept constant at 37±2°C. The un-dissolved SIM was removed from the sample (5 mL) by centrifugation at 11200 g for 15 minutes and collected distilled water was used to make suitable dilutions, the area of diluted samples was measured using RP-HPLC at 238 nm (63). Equation 5 formula was used to measure the percentage of drug loading.

$$\% \text{Drug Loading} = \frac{\text{concentration of formulation}}{\text{concentration of standard}} * 100 \quad - \quad \text{Eq. 5}$$

4.4.7.4 Determination of zeta potential (ZP) and globule size (GS) of optimized formulation

The ZP and GS of SNEDDS were measured using a Malvern zeta sizer nano ZS-90 (Malvern-Instruments Ltd., UK) by passing a laser light with a potential of 50 mV through samples held in polystyrene cuvettes at a 90-degree angle. The optimized formulation mixture (0.1 mL) was diluted with distilled water (100 mL) and filtered through a 0.2µm syringe filter. One milliliter diluted sample was taken and analyzed in the sample cell. The procedure was carried out at a temperature of 25° C (63).

4.4.7.5 Differential Scanning Calorimetry (DSC) analysis

The DSC of pure SIM, C-MCM, T-80, TP, SIM-SNEDDS were evaluated by the Perkin Elmer DSC Apparatus. Powdered sample (2-3mg) was taken in Al³⁺ pan, heated over the range of 30-440°C at 10°C/min using a dry-nitrogen flush at rate of 19.8 mL/min (80).

4.4.7.6 Scanning Electron Microscopy (SEM)

SEM of optimized SNEDDS was conducted to check the morphology of the prepared SNEDDS. The material is scanned with electrons in a zig-zag pattern. It is accomplished by covering them with a very fine coating (1.5 - 3.0 nm) of gold palladium. FE-SEM is utilized to detect extremely fine topography information on the surface of whole or aliquoted materials.(144).

4.4.7.7 High Resolution-Transmission Electron Microscope (HR-TEM)

The HR-TEM was used to assess the surface structure of the optimized SNEDDS formulation. The pre-concentrate SNEDDS (1mL) was mixed in water till the nanoemulsion with the correct droplet size was formed. 1 drop of the prepared nanoemulsion was left on the metal plate, and the extra formulation was wiped away using filter paper. The plates were dyed with 0.5% phosphotungstic acid, and any excess staining was removed with filter paper. When the squares were dried the HR-TEM image was captured (21).

4.4.7.8 Cell line toxicity study

4.4.7.8.1 To determine the cell viability by MTT Assay in SH-SY5Y cell line

SH-SY5Y is a Thrice-subcloned cell line derived from the SK-N-SH neuroblastoma cell line.

On day first, cells are cultured in DMEM media till it got confluent more than 70%. The cells were trypsinized and then it transferred into 15mL falcon and then centrifuged it for 5 min at 1000 rpm. After removing the supernatant, the cell pellet was placed in fresh medium. Pipette out 10 μ L from that for the cell counting purpose. According to the counting, approx. 10,000 cells per well was seeded in triplicates (100 μ L per well) on 96 well plate and incubated it for 24 hrs at 37°C and 5% CO₂.

On day second, the media was removed from each well, and the sample was added according to the concentration to each well. Incubated it for 24hr at 37°C and 5% CO₂. On day third, 10 μ L MTT was added in each well without removing anything from the well and incubated it for 3hr. After that, each and every well were emptied and 100 μ L DMSO was added and placed it on the rocker shaker for 20min. Took the absorbance at 570nm. The percentage of cell viability was estimated by given equation 6:

$$\% \text{Cell viability} = \frac{\text{Mean OD of individual test group}}{\text{Mean OD of control group}} * 100 \quad - \quad \text{Eq. 6}$$

4.4.7.9 *In-vitro* dissolution studies

Dissolution apparatus (USP type II) was used and an amount equivalent to 10 mg of SIM was taken for investigation. During study as per standard protocol 900 mL of 6.8 phosphate buffer and 0.1N HCl (pH 1.2) were performed and temperature of dissolution medium was adjusted at at 37 \pm 0.5° C and stirring speed was set at 50 r.p.m. Further naïve and optimized batch of SIM-SNEDDS were added to this medium and subjected

for dissolution. Five milliliter aliquots were taken at an interval of 5, 10,15,20,30,45, and 60 min. & filtered through a 0.2 µm membrane filter. The filtered solution was then subjected to centrifugation for 15 min. at 9864g after that supernatant was examined using HPLC at 238 nm to estimate the release characteristics of SIM (148).

4.4.7.10 Permeation studies

Franz diffusion cells were used in skin permeation research where the square pieces of skin after, hydration using distilled water, placed between the donor and receiver compartment with the stratum corneum facing toward the donor compartment. As a diffusion medium, phosphate buffer saline pH 7.4 was utilized in the receptor chamber, which was maintained at $37 \pm 0.5^\circ \text{C}$. SIM-SNEDDS was allowed to permeate the skin from donor to receiver compartment for 24 h. 1mL of the formulation was placed in a donor compartment and samples were taken at predetermined time intervals of 0,5,10,15,30 and 60 min from the receptor compartment. The RP-HPLC technique was utilized to examine the samples and determine their permeation.

4.4.7.11 Stability study

The SIM-SNEDDS was stored in a stability chamber for 6 months at $5^\circ\text{C} \pm 3^\circ\text{C}$, $25 \pm 0.2^\circ\text{C} / 65 \pm 5\%$ relative humidity (RH) and $40 \pm 0.2^\circ / 75 \pm 5\%$ RH. Samples were analyzed at different time intervals for droplet/particles size, polydispersity index and assay and comparison with newly prepared samples. Dissolution of six months old samples (sample stored $40 \pm 0.2^\circ / 75 \pm 5\%$ relative humidity) was compared with dissolution of freshly prepared SIM-SNEDDS (63) (83).

4.4.8 Animal experimentation

4.4.8.1 Procurement of animals

The male SD (250-300 gm) 42 rats, were procured from Panjab University in Chandigarh, India. The rats were kept in husk-covered polypropylene cages. Rats were kept in a 12 hours light/dark cycle at $25 \pm 2^\circ\text{C}$ and $55 \pm 10\%$ RH. Rats were given a regular pellet diet with free access to water. The design of animal experiment was authorized with protocol no. LPU/IAEC/2022/04 by the Institutional Animal Ethics Committee (IAEC) of the Lovely Institute of technology (LIT Pharmacy), Lovely Professional University (LPU), Punjab, India.

4.4.9 Bioanalytical method development study using RP-HPLC

4.4.9.1 HPLC trials

This method was established utilizing ICH M10 standards to estimation drugs in rat plasma. ACN and water (90:10) was used as a mobile phase and chromatogram was determined at 238 nm at a flow rate of 1 mL/min. SIM was analyzed using various mobile phase compositions, such as ACN-formic acid (0.1%), methanol-water, and ACN-water, ACN and ortho-phosphoric acid, ACN and water, by adjusting the mobile phase ratio (149).

4.4.9.2 Blood collection and separation of plasma

Rat blood was taken by a retro-orbital puncture using a capillary tube and radio immuno assay (RIA) vial with EDTA crystals. The animal was initially held while having its neck scuffed and its eye made to bulge. A capillary was inserted dorsally into the retro-orbital region of the eye, and blood was permitted to enter into the EDTA vial via a capillary tube. The EDTA tube was kept for centrifugation at 5000 rpm for 15 min with the temperature set to 2-8°C. The clear supernatant was removed with a micropipette and stored for processing in a deep freezer at -20 °C (Solution C).

4.4.9.3 Preparation of standard dilutions

SIM (10 mg) was dissolved in 10 mL of acetonitrile in a 100 mL volumetric flask and then the volume was adjusted to 100 mL to obtain a solution concentration of 100 mg/mL (Solution A). A second volumetric flask was used to dilute Solution A to a concentration of 10 mg/mL using acetonitrile up to 100 mL (Solution B). A further SIM dilution was obtained by taking 10 mL aliquots of solution B and diluting them to 100 mL in acetonitrile to attain a concentration of 1.0 mg/mL (Solution C). To obtain a concentration of 200 ng/mL, 20 mL of liquid from solution C was dissolved in a 100 mL volumetric flask, and the volume was increased by 100 mL of acetonitrile (Solution D). ATV (10 mg) was dissolved in a small amount of acetonitrile in a 100 mL volumetric flask, and the volume was then adjusted to 100 mL using acetonitrile to obtain a final concentration of 100 mg/mL (Solution E).

4.4.9.4 Preparation of internal standard (IS)

To prepare the standard stock solution of IS, 10mg of atorvastatin (ATV) was weighed accurately and dissolved in 100 mL ACN solution was sonicated (10 min.) to ensure

the complete solubilization of the ATV in ACN. Further, stock solution was diluted 10 times, 10mg/mL solution was prepared and utilized as the IS.

4.4.9.5 Specificity study

SIM and blank plasma samples were injected on HPLC utilized ACN: water (90:10 v/v) as a mobile phase to validate method specificity. The possibility of drug-plasma peak interference was examined.

4.4.9.6 Development of calibration curve

One mL of solution E was added after aliquots of 1.25, 2.5, 3.75, 5, and 6.25 mL of solution D were put into separate 10 mL volumetric flasks. 0.1 mL of plasma was added to each of the above dilutions and mixed for 5 minutes. To precipitate and break down plasma protein, acetone (1 mL) was taken to each sample and thoroughly agitated using a sonicator for 15 minutes. Then, the all samples were centrifuged in an eppendorf for 30 minutes at 4 °C at 10,000 rpm. To get theoretical SIM concentrations of 50, 100, 150, 200, and 250 ng/mL and ATV concentrations of 10 mg/mL, using a micropipette, the supernatant was separated and the volume was set at 10 mL in a volumetric flask. HPLC was used to analyze SIM and ATV using the final prepared samples (150).

4.4.9.7 Validation of the method

ICM M10 standard was referred for the validation of developed method. To evaluate system performance, system suitability characteristics such as tailing factor, theoretical plate, detection limit, and quantification limit, and height equivalent to the theoretical plate were assessed. (151).

4.4.9.8 Linearity and range

The concentration was plotted on the X-axis, and the mean peak area was plotted on the Y-axis, to create the calibration curve. The slope, standard deviation of the intercept, standard deviation of response (σ), regression coefficient (r^2), y-intercept, and were calculated using the calibration data (152).

4.4.9.9 Accuracy

Absolute drug recovery from quality control samples was estimated to determine the method's accuracy. Three different concentration levels of the method were used to prepare dilutions: LQC-80%, MQC-100%, and HQC-120% with a medium

concentration of 100 ng/mL. Aliquots of solution D in the amounts of 3.0, 3.75, and 4.5 mL were added into separate 10 mL volumetric flasks to obtain these concentrations. 1 mL of solution E and 0.1 mL of plasma were then added. After adding plasma, the samples were sonicated and centrifuged in an eppendorf at 10,000 rpm at 4 °C for 30 minutes. The supernatant was placed into a 10 mL volumetric flask with a micropipette, and 3.75 mL of solution F was added. After that, 10mL of ACN were added to the volume to dilute it. As a result, the theoretical concentrations of SIM in these solutions were 120 ng/mL, 150 ng/mL, and 180 ng/m respectively, with 10 mg/mL of ATV. HPLC was used to determine these concentrations in six replicate samples (150). The formula shown in the following equation was used to estimate the absolute percentage of drug recovery 7:

$$\text{Actual \% recovery} = \frac{\text{Actual concentration recovered}}{\text{Theoretical concentration}} * 100 \quad - \quad \text{Eq. 7}$$

4.4.9.10 Precision

The repeatability and intermediate precision of the developed method were used to determine its precision. Six injections of the LQC, MQC, and HQC samples were performed into the same experimental setup on the same day to ensure repeatability (without the addition of sample solution F). By calculating LQC, MQC, and HQC samples six times under similar experimental conditions but on different days with different analysts (inter-analyst), the intermediate accuracy was determined (150). Following the collection of the mean data, the given equation 8 was utilized to find the percentage relative standard deviation:

%Relative standard deviation

$$= \frac{\text{Standard deviation of peak area}}{\text{Average peak area}} * 100 \quad - \quad \text{Eq. 8}$$

4.4.9.11 Validation of system suitability and determine of LOD and LOQ

System compatibility were evaluated using the tailing factor, peak purity index, theoretical plate, and height equivalent to theoretical plate (HETP). The standard deviation of response (sigma) and slope of the calibration curve were used to determine the LOD and LOQ (S) (153). The regression line's Y intercepts' standard deviation was

used to estimate the standard deviation. The following equations (9) and (10) were used to calculate the results.

$$\text{LOD} = 3.3 \frac{\sigma}{S} \quad - \quad \text{Eq. 9}$$

$$\text{LOQ} = 10 \frac{\sigma}{S} \quad - \quad \text{Eq. 10}$$

4.4.9.12 Stability study

Three freeze-thaw cycles were used to study the stability of plasma samples spiked with SIM, with short-term stability at room temperature for three hours and long-term stability at -20 °C for three weeks. 3 mL plasma was collected in one RIA vial for freeze-thaw stability. To this vial, 10 mg of SIM was added (to reach a 1000 mg/mL concentration), and solution was vortexed for 5 minutes. This test tube was placed in a freezer at a -20 °C temperature. The frozen sample was removed from the test tube. These sample thawed at room temperature. One mL of plasma was extracted from the thawed samples (Cycle 1), and the remaining 2 mL of plasma was kept in the deep freezer for the subsequent cycle. The drug was precipitated from the extracted plasma (1 mL), and the centrifugation of the supernatant. The transparent clear supernatant was collected by centrifugation and diluted to 100 mL with ACN to obtain a concentration of 100 mg/mL (18). Dilutions were also prepared to obtain LQC-120 ng/mL, MQC-150 ng/mL, and HQC-180 ng/mL. Similar to Cycle 1, the last sample of frozen plasma (2 mL) was carried out, allowed to thaw at room temperature, and then 1 mL was extracted (Cycle 2). The final 1 mL of thawed plasma was then placed back in the deep freezer. After frozen, it was removed and thawed (Cycle 3). In order to prepare LQC, MQC, and HQC samples for Cycles 2 and 3, the procedure was repeated. IS was introduced at a concentration of 10 mg/mL to each of these solutions. Every dilution was prepared in triplicate and then put into an HPLC, and their retention times at 238 nm were determined. For every concentration, the average, standard deviation, and percent RSD were determined (154). Similar to this, at room temperature, the short-term stability of a plasma sample injected with SIM was determined. Before extraction, the stability was tested at 1, 2, and 3 hours. In the short term, 3 mL of plasma and 10 mg of SIM were added (to obtain a 1000 mg/mL concentration), to the RIA vial and for five minutes, vortexed (155). The RIA vial was maintained at a constant temperature of room

temperature. A sample (1 mL) was collected after every interval, the drug was removed from the plasma, IS (10 mg/mL) was added after the samples for the LQC, MQC, and HQC had been prepared. The retention times of each dilution were measured at 238 nm after they had been produced in triplicate and put into the RP-HPLC. For each concentration, the mean, standard deviation, and percent RSD were estimated. The 3 RIA vials containing 1 mg of SIM each were filled with 1 mL of plasma to ensure long-term stability (to achieve a concentration of 1000 mg/mL). All three vials were put in the freezer at -20 °C after the mixture had been vortexed for 5 minutes. The 3 vials were taken out of the freezer after 1, 2, and 3 weeks. The drugs were removed from the plasma after every interval, IS (10 mg/mL) was added after the LQC, MQC, and HQC samples were prepared. In order to measure the retention times at 238 nm, each dilution was made in triplicate and then put into the RP-HPLC. For every concentration, the mean, standard deviation, and percent RSD were quantified.

4.4.9.13 Statistical analysis

All experimental results are presented as means with standard deviations (SD). The mean, SD, and % relative standard deviation were determined and used an MS Excel spreadsheet. The calibration curve was created using Graph Pad Prism version 7.0 and the results were compared using Tukey's multiple comparison test. (GraphPad Software Inc., CA, USA). A significant difference in the collected data was shown by a P value of less than 0.05.

4.4.10 Pharmacodynamic study

As shown in Table 15, all 42 male SD rats were allocated into 7 groups (n=6 each group) at random. All groups except the first (normal control) group consumed the normal pellet diets for the first 48 days, while other group of rats received groups aluminium chloride (100 mg/kg, orally) daily for the period of 0 to 8 weeks (156). Simultaneously, All the groups, of rats except first group of rats received the assigned treatment of drug from 8 to 12 weeks (48th to 84th). During this study period at 0, 56, 70 and 84 days the open filed test (OFT), novel object recognition (NOR) tests and morris water maze (MWM) test were performed record behavioral parameters. The biochemical parameters were also evaluated at the end of study after scarification of experimental animals and their tissues were also isolated to investigate determination

of acetylcholinesterase activity, catalase estimation, superoxide dismutase assay, MDA assay, glutathione assay, enzyme linked immunosorbent (ELISA) assay for TNF- α , IL, metal ion concentration and lipid level.

Table 15: Pharmacodynamic study protocol

Sr. No.	Treatment (n=6)	Dose (mg/kg), Route of administration (p.o.)
I	Normal Control	1 mL 0.5% CMC
II	Disease Control	100 mg/kg Aluminium chloride
III	SNEDDS Placebo	10g/kg
IV	Standard Control	1mg/kg (Donepezil)
V	Unprocessed SIM	0.987mg
VI	SIM SNEDDS (Low dose)	1.974 mg
VII	SIM SNEDDS (High dose)	3.948 Mg

4.4.11 Behaviors analysis

4.4.11.1 Open field test

An open-field performance monitoring test was performed on the rats to check at both locomotor and behavioural performance. A wooden apparatus with 16 (4x4) squares was used to record observations. The animal was put in a corner of the apparatus, and for 5 minutes its behaviour was recorded (157) (158). The study evaluates:

1. Rearing
2. Fecal pellets
3. Total time movements
4. Squared explored

4.4.11.2 Morris Water Maze (MWM)

Rats' retention of working (reference) and spatial memory was examined by using the Morris water maze. The equipment includes a big circular pool partitioned into 4 quadrants, with a platform in the fourth quadrant. Around the pool, there were external cues that maintained constant during the trial. Reference memory was given by these cues. The platform was set During in the acquisition phase, the water surface was 1 cm above the surface, and the rats were given five consecutive days of trials. Then one by one these rats were placed in one of the quadrants of the pool while facing the pool's wall. For each trial, the drop location was different. The animal was permitted to find the platform and was helped and guided toward it if it did not find it within 120 seconds.

The animal was then permitted to remain on the platform for 20 seconds (158). The memory test for both cognitive and spatial memory was divided into two phases. The time duration (s) needed by the rat to go to the platform after being immersed in the water was examined to test spatial memory. The rat's time (s) stayed in the targeted zone (up to 120 s) without the platforms was noted for working (reference) memories.

4.4.11.3 Novel object recognition test

Rats were used in studies to examine the hippocampus's working and spatial memories as well as its memory for novel objects. The apparatus consists of a large open container divided into arenas. The rat was located in the centre of the field during the acquisition phase, having two similar items positioned in the corners of the area. The rat was given 10 minutes to explore the area (158). The rat was removed from the area during the retrieval phase and two objects—one familiar (the similar object from the phase of acquisition) and one new placed in its place (one that the rat has not before seen). The rat was given ten minutes to roam the areas. To determine the discrimination and recognition index, the amount of time (s) spent examining both familiar and unfamiliar objects was recorded (159).

4.4.12 Biochemical estimation

4.4.12.1 Acetylcholinesterase activity

The AChE was utilized as a biomarker for the loss of cholinergic neurons in the brain. AChE activity was determined using the Ellman methods. In summary, 3 mL of 0.1 M sodium phosphate buffer and 0.05 mL of protein sample (pH 8.0) were mixed. The solution was given 0.1 mL of acetylthiocholine iodide and 0.1 mL of DTNB. A UV spectrophotometer was used to measure the difference in absorbance at 412 nm at 30-second intervals for 2 minutes. (79).

4.4.12.2 Metal Ion Concentrations in the Hippocampus

Hippocampus (25mg) added in 3 mL of 65% HNO₃ and allow to keep for 18 hrs. Further, after filtration through filter paper. A clear filtrate was analysed by the optimal 8300 ICPOES model of Inductively coupled plasma mass spectrometry(ICP-MS) is produced by Perkin Elmer Corporation (160).

4.4.12.3 Catalase (CAT) estimation

In each group, CAT activity was assessed in a brain sample. After centrifugation of the homogenized brain, the clear supernatant was collected. One mL of H₂O₂ (30mM) was added to 1.95 mL of supernatant, and the absorbance was measured for 30 seconds after 15 seconds of internal time (0,15,30 sec). The absorbance was measured with a UV spectrophotometer at lambda max 240nm (161).

$$\text{CAT} = \left\{ \left[(2.3 \times \log \frac{OD_{initial}}{OD_{final}}) / \Delta t * 100 \right] / 0.693 \right\} / \text{mg of protein} - \text{Eq.12}$$

4.4.12.4 Reduced glutathione (GSH) assay

Beutler's method was used to determine the GSH level. The cerebral cortex and hippocampus homogenate tissue was mixed with one mL of supernatant trichloroacetic acid (10% w/v in water) and centrifuged at 1000 g for 10 minutes (79). 0.5 mL of the supernatant was collected after centrifugation, 2 mL of disodium hydrogen phosphate (0.3M), and 0.25 mL of newly prepared 5,5,-dithio-bis-(2-nitrobenzoic acid (DTNB, 0.001 M in 1% w/v sodium citrate) were added. The reduced glutathione's absorbance was recorded at 412 nm, and the standard plot was used to determine the concentration of GSH (10-100 M) (162).

4.4.12.5 Thiobarbituric acid reactive substances (TBARS) assay

The TBARS test measures the concentration of malondialdehyde (MDA) to estimate the degree of lipid peroxidation. Supernatant and Tris HCl (pH 7.4) were combined in 0.2 mL, and the mixture was then kept at 37°C for two hours. 1 mL of 10% ice-cold TCA was added during incubated, and then the mixture was agitated at 1000 g for ten minutes. (79). After 10 minutes in a hot water bath, 1 mL of the supernatant and 1 mL of 0.67% TBA were added, and the samples were allowed to cool before the absorbance at 532 nm was determined. The extinction coefficient of MDA, 0.156 M⁻¹, was used in further calculations, and A nanomole of MDA per mg of protein was used to express the final concentration (163).

4.4.12.6 Superoxide dismutase (SOD) assay

0.1 mL of supernatant of brain homogenate were considered for this estimation which was added to 2 mL mixture of 0.1 mM ethylenediamine tetra acetic acid, NBT 96 mM, and sodium carbonate 50 mM at pH 10.8, followed by 0.1 mL of hydroxylamine

hydrochloride (20 mM, pH 6). The absorbance was determined at 560 nm at 60-sec intervals for 2 minutes. The activity was measured using the following formula (163).

$$\text{SOD} = \left(\frac{\Delta OD \text{ of control} - \Delta OD \text{ of sample}}{OD \text{ of control}} \right) * 100 / 50 / \text{vol. of homogenate/mg of protein}$$

Eq. 13

4.4.12.7 TNF-alpha and IL-1β

For the estimation of TNF-α and IL-1β enzyme linked immunosorbent assay (ELISA) kits Ray Bio Rat TNF-alpha and IL-1 ELISA Kit, USA) were used and the method given in the kit were followed (164).

4.4.13 Pharmacokinetic study

To evaluate SIM bioavailability in the plasma and brain, rats fasted for 16 hours before SIM administration. SIM and SIM-SNEDDS were both given orally at doses of 1.974 mg/kg mg/kg body weight shown in Table 14. At the end of study all animals of their respective groups where undergone sacrifice to collect the blood using heart puncture method at the same time brain tissue where also taken out at the specified interval of 1, 2, 3, 4, 5, 6, 8, and 24 hours. Plasma was extracted from blood samples after 5 minutes of 16,000 g centrifugation. After homogenizing the brain tissues in sodium phosphate (Na₃PO₄) buffer (pH 6.5) for ten minutes at 10,000 g, the supernatant was taken. The stabilizing agents used for SIM were ascorbic acid (AA) and tris (2-carboxyethyl) phosphine (TCEP).

Table 14: Design of pharmacokinetic study

Group	Treatment	Dose	Animals used
I	Unprocessed SIM	1.974 mg/kg	6
II	SIM SNEDDS	1.974 mg/kg	6

All samples were immediately frozen and kept at 20°C. From the samples, unconjugated SIM was calculated (158). The sample was mixed with 10 mL of K₂HPO₄ and incubated at 37°C for 45 minutes to extract the unconjugated SIM. The ethyl acetate layer was evaporated using a nitrogen evaporator, and ethyl acetate was then utilized to extract the SIM. The filtrate was reformed with 100 mL of 15% v/v aqueous ACN solution. Following that, 50 mL of the sample was added to the HPLC for further measurement using the HPLC/UV technique. (165).

$$\text{Relative bioavailability (Fr)} = \frac{(\text{AUC})_{\text{test}} \times D_{\text{std.}}}{(\text{AUC})_{\text{std}} \times D_{\text{test}}} \quad \text{Eq. 11}$$

AUC= area under the curve, and

D = dose administered.

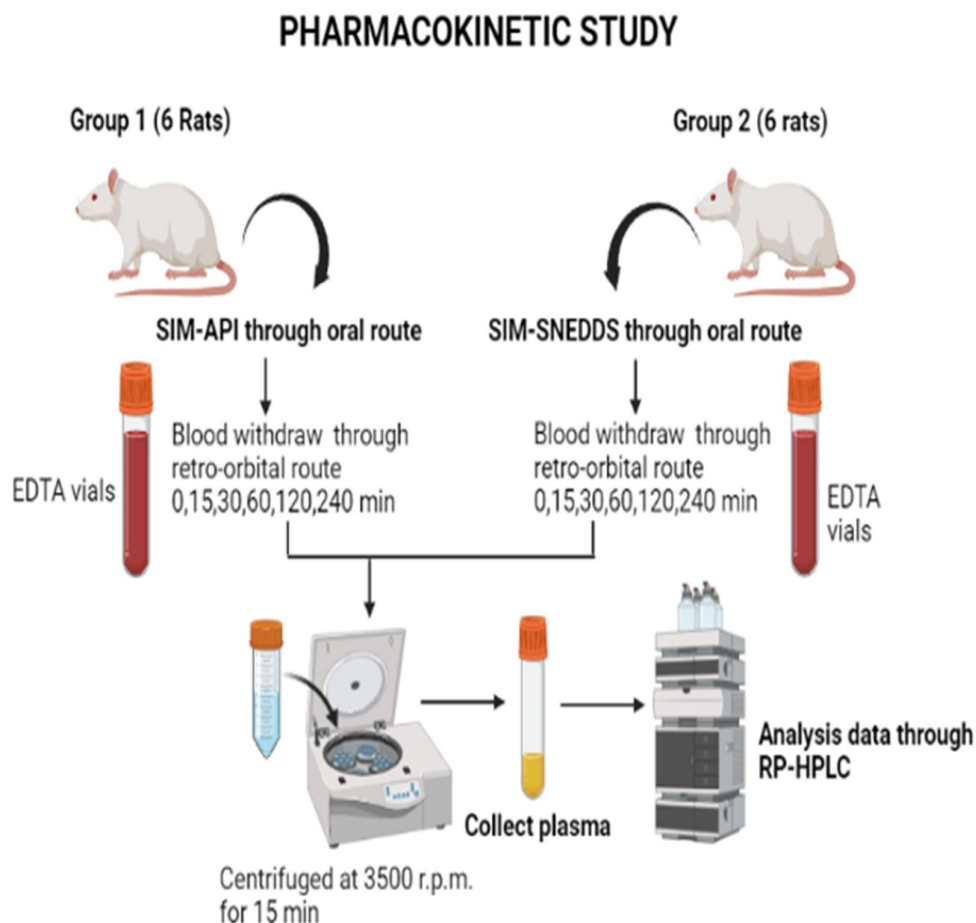


Figure 9: Design of Pharmacokinetic study

4.4.14 Histopathological Examinations

Cortex and hippocampus portions were isolated after sacrifice of animals from different groups and then fixed with 10% formalin after being cleaned with cold phosphate-buffered saline. Both tissues were ready as paraffin-embedded blocks. After cutting the paraffin sections, they were dyed using hematoxylin and eosin, and then examined using a light microscope (100x). The study was done in triplicate. Histopathological evaluation was carried out by blinded experimenters (166).

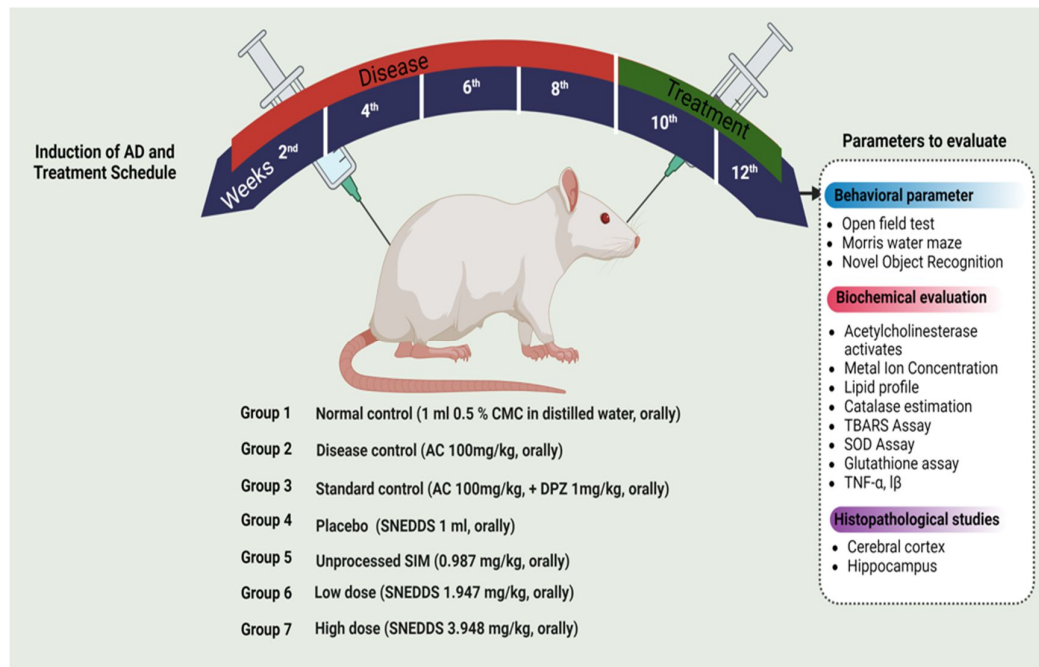


Figure 10: Design of pharmacodynamic study

4.4.15 Statistical Analysis

Statistical analysis was performed with two-way analysis of variance (ANOVA) followed by Tukey's multiple comparison test using GraphPad Prism trial version 8.0 for behavioural parameters while one-way analysis of variance (ANOVA) was considered for other parameters. The experimental data was represented as mean \pm SEM. The results were considered significant when $p < 0.001$, $p < 0.01$ and $p < 0.05$.

CHAPTER-5

5. Results and Discussion

5.1 API Characterization

5.1.1 Physical description of SIM

Table 16: Physical description of SIM

Drug	Property	Observation	Literature Report	Reference
SIM	Colour	Off-White	Off-White	(63)

5.1.2 Melting point determination

5.1.2.1 Capillary fusion method

The value obtained after performing the melting point through capillary fusion method are shown in Table 17.

Table 17: Melting point of SIM using capillary method

Drug	Observed value	Reported value	Reference
SIM	142-143°C	135- 138°C	(167)

5.1.2.2 DSC analysis

The DSC of pure SIM was evaluated by the Perkin Elmer DSC Apparatus. Powdered sample (2-3mg) was taken in aluminium pan, heated over the range of 30-440⁰C at 10⁰C/min using a dry-nitrogen flush at rate of 19.8mL/min. The thermograph of SIM showed sharp endothermic peak at 141.73⁰C and ΔH was 73.1658J/g. It was concluded that SIM was crystalline in nature. The results are given in Table 18 and Figure 11 (168).

Table 18: Results of Pure DSC of SIM

Drug	Observed Endothermic peak	Reported Endothermic peak	References
SIM	141.73 ⁰	139.54 ⁰ C	(168)

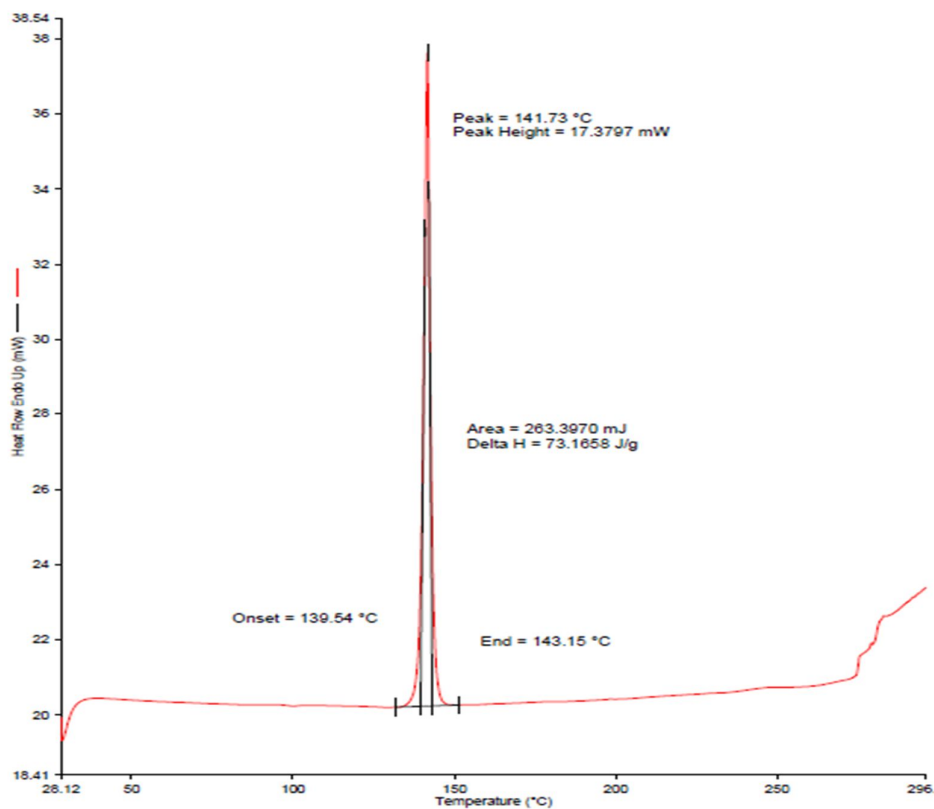


Figure 11: DSC thermogram of SIM

5.1.3 Determination of ultraviolet absorption maxima (λ_{max})

The maximum wavelength of SIM was measured by using UV-1800 Shimadzu-spectrophotometer (Kyoto JAPAN). Spectrum of SIM samples (10 μ g/mL) were prepared in methanol and scanned in the range of 400-200nm against methanol as blank.

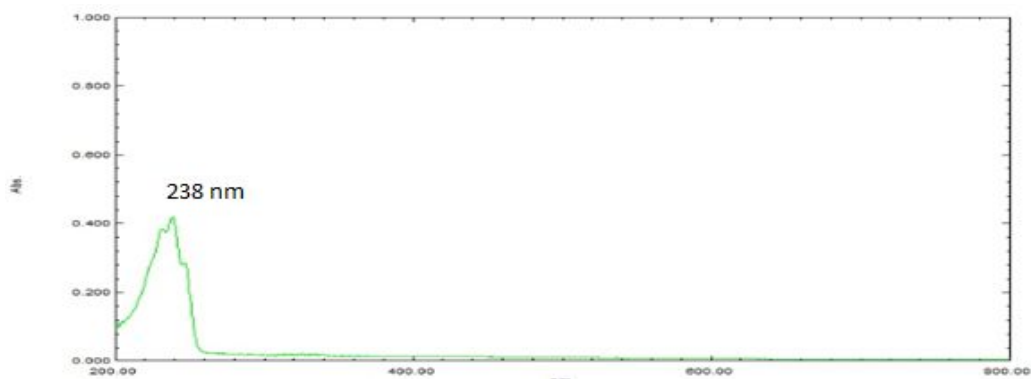


Figure 12: Absorption spectrum of SIM showing maximum absorbance at 238 nm

It was showed the maximum absorbance at 238 nm (169). The spectrum was showed in the Figure 12.

5.2 Analytical method development

5.2.1 Selection of mobile phase of SIM

Different trials with different mobile phase and compositions, such as acetonitrile-formic acid, methanol-water, and ACN-water, ACN and ortho-phosphoric acid (0.1), ACN and water was tried for SIM, by adjusting the ratio of the mobile phase as shown in Figure 13.

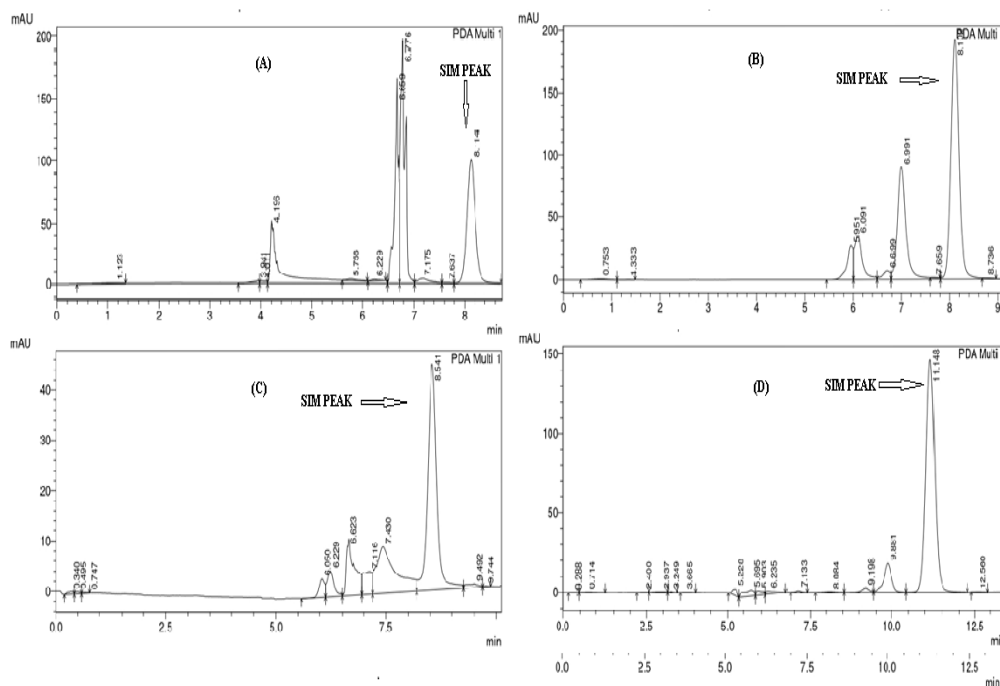


Figure 13: Chromatogram of SIM in ACN and formic acid (A), Chromatogram of SIM in methanol-water (B), Chromatogram of SIM in ACN and ortho-phosphoric acid (0.1) (C), Chromatogram of SIM in ACN and water (D)

SIM retention time was observed to be 8.114 minutes in trial 1. Nevertheless, the various peaks indicated broadening, shouldering and splitting. As a result, the method was not assessed any further for validation purposes. Trial 2 was not accepted because the SIM peak was too distinct, but two extra splitting and shouldering peaks were seen. In trial 3, this method was also rejected due to multiple broadening, shouldering and splitting peaks. SIM retention time was 11.148 minutes in trial 4, which was too long. So, this trial was also not accepted.

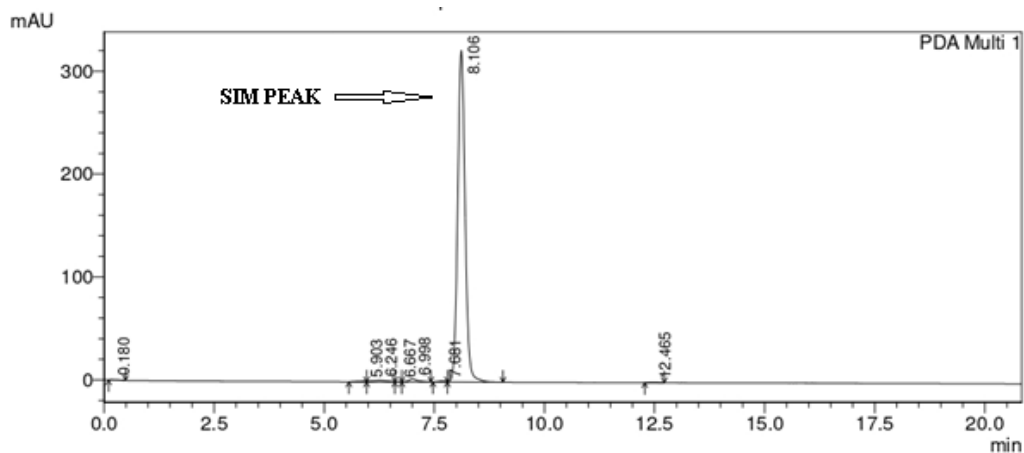


Figure 14: Chromatogram of SIM in Acetonitrile – Water (90:10)

Out of these trials 90:10 ratio of ACN: water showed better results in term of sharpness of the peak. Additionally, the value of the theoretical plate for SIM in this trial was 71579.436, which was above 2000. The tailing factor for SIM was less than 2. SIM's retention time was observed to be 8.106 minutes, 90:10 ratio is selected for validation as shown in Figure 14.

5.2.2 Linearity and Range

To check that the linearity was accurate, the obtained calibration curve that was plotted with concentration versus mean area. The calibration curve was found to be linear in the range of 2-10 $\mu\text{g/mL}$, with an R^2 value of 0.998, as depicted in Figure 15 (170).

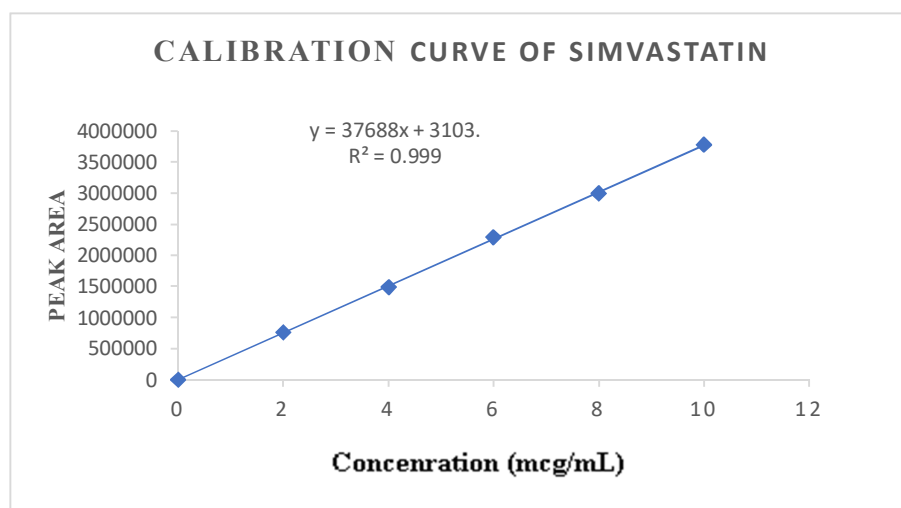


Figure 15. Calibration curve of SIM

5.2.3 Accuracy

The mean % recovery of the LOQ, MQC, and HQC solutions in mobile phase was used to assess the suggested method's accuracy. The data indicated that the % mean recovery in mobile phase was found within the specified limits of 95-105 % for all three levels (171). The developed method's accuracy was verified using a % relative standard deviation less than 2% as shown in Table 19.

5.2.4 Precision

The percentage RSD was calculated to validate the precision of developed analytical method. %RSD of all the 3 standard solutions i.e., LQC, MQC, and HQC were measured by using response area of interday, intraday and interanalyst. The % RSD of inter & intra days was found in the range of 0.21-0.53 % whereas, 0.21-0.61 % was observed in the case of interanalyst. All these calculated RSD were found within the acceptable limits of 2% RSD shown in Table 20 (172).

5.2.5 Robustness

Evaluation of robustness of any analytical method is the expression of resistance (% recovery) of the developed method by small changes in the experimental conditions such as λ_{max} , flow rate, and ratio of mobile phase. % recovery of all 3 standard solution were calculated by injecting the sample in HPLC by varying the λ_{max} , flow rate and ratio of mobile phase. % recovery was found in the range of 96-102% after small change in λ_{max} & ratio of mobile phase and it was found 96-105% by altering the flow rate of the mobile phase shown in Table 21 (173).

Table 19: Results of Accuracy studies

Level	Conc. (µg/mL)	Responses (area), injections						Mean (*N=6)	SD	%RSD	%Recovery
		1	2	3	4	5	6				
SIM											
LQC	4.8	1856251	1855622	1852242	1868541	1844622	1865655	1850488.8	9814.40	0.5303	102.28
MQC	6.0	2296514	2295685	2287568	2291562	2288450	2299112	2258149.0	4885.35	0.2163	99.72
HQC	7.2	2684565	2675685	2678562	2681562	2681258	2662552	2682364.0	7843.23	0.2924	98.61

Table 20: Results of precision studies for SIM

Parameter	Level	Concentration (µg/mL)	Analytical responses (area), injections						Mean (*N=6)	SD	%RSD
			1	2	3	4	5	6			
Repeatability (intraday precision)											
	LQC	4.8	1856251	1855622	1852242	1868541	1844622	1865655	1850488.80	9814.40	0.53
	MQC	6.0	2296514	2295685	2287568	2291562	2288450	2299112	2258149.00	4885.35	0.21
	HQC	7.2	2684565	2675685	2678562	2681562	2681258	2662552	2682364.00	7843.23	0.29
Intermediate precision (interday)											
Day 1	LQC	4.8	1856251	1855622	1852242	1868541	1844622	1865655	1850488.80	9814.40	0.53
	MQC	6.0	2296514	2295685	2287568	2291562	2288450	2299112	2258149.00	4885.35	0.21
	HQC	7.2	2684565	2675685	2678562	2681562	2681258	2662552	2682364.00	7843.23	0.29
Day 2	LQC	4.8	1859256	1852632	1866521	1864556	1845245	1856323	1852424.00	8738.49	0.47
	MQC	6.0	2289526	2282622	2265545	2286562	2266526	2275655	2261073.00	9389.89	0.41

Day 3	HQC	7.2	2696554	2685463	2666989	2678466	2688533	2669695	2670283.00	9446.25	0.35
	LQC	4.8	1856522	1868562	1865682	1846252	1855845	1856523	1864898.00	8856.77	0.47
	MQC	6.0	2296952	2288526	2266545	2289639	2288622	2296584	2261144.00	11368.70	0.50
	HQC	7.2	2686625	2696322	2685636	2696324	2676984	2676545	2656406.00	9788.90	0.36
Intermediate precision (inter analyst)											
Day 1	LQC	4.8	1865852	1882612	1873622	1877562	1896955	1874562	1856860.00	9550.43	0.51
	MQC	6.0	2286569	2293146	2279522	2279652	2286595	2298696	2270696.00	8415.50	0.37
	HQC	7.2	2685962	2696526	2698562	2686256	2683878	2686854	2689673.00	6641.32	0.24
Day 2	LQC	4.8	1875695	1859542	1886854	1899885	1889544	1896585	1863017.00	15945.13	0.85
	MQC	6.0	2286952	2279146	2299855	2293123	2288965	2296985	2257504.00	8084.82	0.35
	HQC	7.2	2696585	2665954	2695489	2687955	2689755	2699554	2685882.00	13022.60	0.48
Day 3	LQC	4.8	1889556	1889854	1896589	1869887	1898545	1885685	1866686.00	11421.30	0.61
	MQC	6.0	2296854	2279854	2289844	2295698	2295122	2295644	2272169.00	6817.78	0.30
	HQC	7.2	2694589	2688954	2695414	2685598	2689541	2671155	2698542.00	9087.83	0.33

Table 21: Robustness study

Level	Conc. (µg/mL)	Analytical responses (area), injections						Mean (*N=6)	SD	%RSD	%Recovery
		1	2	3	4	5	6				
Amax	4.8	2143791	2180685	2143931	2174387	2192771	2137993	2178926	4194.50	0.1925	96.22
	6.0	2297514	2289685	2297568	2298562	2288450	2275112	2291149	8980.89	0.3919	101.18
	7.2	2286952	2279148	2299855	2293123	2289965	2296985	2257504	8084.81	0.3581	99.69
Flow rate (mL/min)	4.8	2176389	2178137	2180872	2175791	2190343	2180938	2180412	5325.91	0.2442	96.28
	6.0	2296854	2289854	2289844	2295698	2295122	2285644	2292169	4392.35	0.1916	101.22
	7.2	2376081	2389371	2380872	2378606	2397745	2380238	2383936	8108.19	0.3401	105.28
Mobile phase ratio (A: B) v/v	4.8	2178555	2168552	2185844	2168447	2169652	2175954	2174500	6967.98	0.3204	96.02
	6.0	2278554	2289854	2279844	2295698	2295122	2285644	2287453	7388.09	0.3229	101.01
	7.2	2268966	2289641	2278672	2295915	2289454	2298555	2286867	11139.72	0.4871	100.99

5.2.6 LOD and LOQ

The value of LOQ and LOD were 0.52 μ g/mL and 0.17 μ g/mL respectively.

5.3 Solubility Study

The solubility of the SIM in various oils, surfactant and co-surfactant were determined and report in Figure 16&17. The drug was shown maximal solubility in CMCM (42.78 \pm 0.05%) oil, TP (43.96 \pm 0.15%) co-surfactant, and T-80 (42.63 \pm 0.25%) surfactant.

5.3.1 Solubility in oils

Capmul MCM (42.78 \pm 0.05%)> Lauroglycol FCC (39.04 \pm 0.15%)> Cotton Seed (19.26 \pm 0.36%)> Eucalyptus oil (18.56 \pm 0.55%)> Olive oil (17.52 \pm 0.42%)> Labrafac PG (16.35 \pm 0.36%)> Captex 300 (15.45 \pm 0.19%)> Castor oil (14.95 \pm 0.21%)> Peanut oil (12.85 \pm 0.29%)

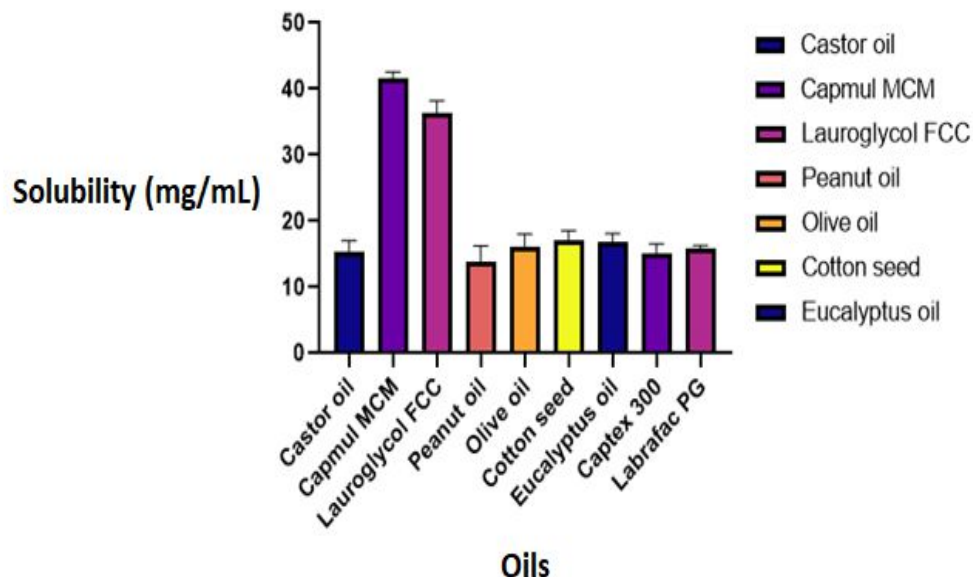


Figure 16: Solubility of SIM using different oils

5.3.2 Solubility in surfactant and co-surfactant

Transcutol P (43.96 \pm 0.15)> Tween 80 (42.63 \pm 0.25)> Labrasol (41.26 \pm 0.18)> Tween 20 (37.65 \pm 0.05)> Polyoxamer 407 (19.65 \pm 0.09)> Polyoxamer 188 (18.56 \pm 0.18)> Labrafil M 1994 (16.35 \pm 0.21)

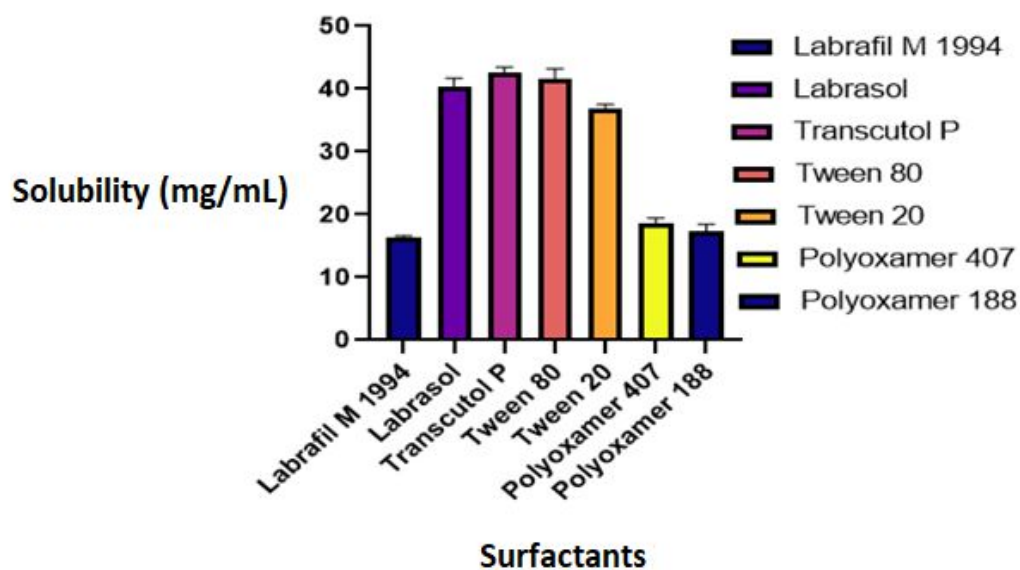


Figure 17: Solubility of SIM using different surfactants and co-surfactants

The maximum solubility of SIM was found to be in Capmul MCM (42.78%), Lauroglycol FCC (39.04%), Transcutol P (43.96%) and, Tween 80 (42.63%).

5.4 Construction of TPD

By adjusting the oil and Smix (surfactants and co-surfactants) concentrations, a number of (27) prototypes formulations were developed. S_{mix} by changing the ratio between 1:1,1:2, and 2:1. Composition of SNEDDS prototypes were shown in Table 22. Ternary phase for these formulations are shown in Figure 18. According to the TPD, increasing the oil ratio in the formulation, reduced the formulation transparency. Resulting in an increase in particle size. When increasing the oil phase, it led to an increase in the lipid concentration of the emulsion, and the surfactant concentration was insufficient to ensure a uniform mixture of nano-size particles due to an increase in interfacial tension at the o/w interface. On the other hand, when the level of oil was reduced and the level of surfactants was increased, the interfacial tension between the o/w interface was reduced, this refers to the outcome of a process where nano particles are evenly distributed and appear clear and transparent. F1, F2, F3, F10, F11, F12, F19, and F20 were noticed to be transparent and clear emulsions in results are shown in Figure (indicated as SNEDDS).

Table 22: Formulations of SNEDDS using various oils and S_{mix}

Formulation Smix (1:1)	Capmul MCM	Tween 80	Transcutol P	Appearance
F1	100 μ L	450 μ L	450 μ L	Transparent
F2	200 μ L	400 μ L	400 μ L	Transparent
F3	300 μ L	350 μ L	350 μ L	Transparent
F4	400 μ L	300 μ L	300 μ L	Turbid
F5	500 μ L	250 μ L	250 μ L	Turbid
F6	600 μ L	200 μ L	200 μ L	Turbid
F7	700 μ L	150 μ L	150 μ L	Turbid
F8	800 μ L	100 μ L	100 μ L	Turbid
F9	900 μ L	50 μ L	50 μ L	Turbid
Formulation Smix (2:1)	Capmul MCM	Tween 80	Transcutol P	Appearance
F10	100 μ L	600 μ L	300 μ L	Transparent
F11	200 μ L	530 μ L	270 μ L	Transparent
F12	300 μ L	470 μ L	230 μ L	Transparent
F13	400 μ L	400 μ L	200 μ L	Turbid
F14	500 μ L	330 μ L	170 μ L	Turbid
F15	600 μ L	270 μ L	130 μ L	Turbid
F16	700 μ L	200 μ L	100 μ L	Turbid
F17	800 μ L	130 μ L	70 μ L	Turbid
F18	900 μ L	70 μ L	30 μ L	Turbid
Formulation Smix (1:2)	Capmul MCM	Tween 80	Transcutol P	Appearance
F19	100 μ L	300 μ L	600 μ L	Transparent
F20	200 μ L	270 μ L	530 μ L	Transparent
F21	300 μ L	230 μ L	470 μ L	Transparent
F22	400 μ L	200 μ L	400 μ L	Turbid
F23	500 μ L	170 μ L	330 μ L	Turbid
F24	600 μ L	130 μ L	270 μ L	Turbid
F25	700 μ L	100 μ L	200 μ L	Turbid
F26	800 μ L	70 μ L	130 μ L	Turbid
F27	900 μ L	30 μ L	70 μ L	Turbid

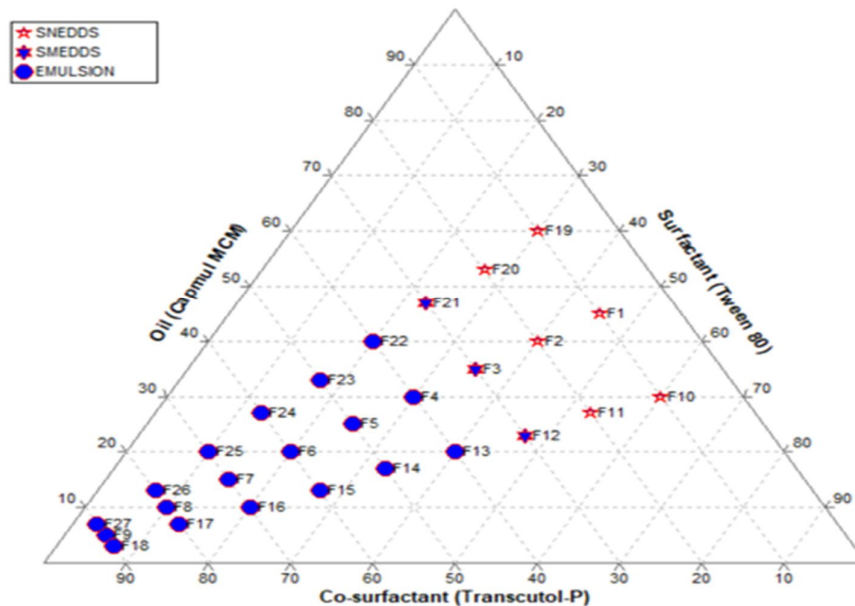


Figure 18: Ternary phase diagram

This implies that the amount of CMCM played a significant role in decreasing the GS of SNEDDS. Similarly, the higher concentration of TP among surfactant (T80) and co-surfactant (TP) played a major role in reducing GS to the nano level. These 27 SNEDDS formulations were evaluated further.

5.5 Thermostability study

SIM-SNEDDS showed good stability. The results demonstrated that there was no phase separation observed in the centrifugation, heating-cooling cycle, or freeze-thaw cycle tests. The results of SIM-SNEDDS demonstrated results in which, the particle sizes were less than 100nm, a PDI of 0.20-0.40, and a % transmittance value close to 100 percent. Formulation F11 was found to have the smallest GS and the best stability against thermodynamic and kinetic stress of the 27 SNEDDS prototypes tested (centrifugation).

5.6 Optimization of SNEDDS

Thirteen experiments were conducted to examine how the ingredients (oil, surfactant, and co-surfactant) affected the SIM-SNEDDS. The responses of all the trials of BBD are given in Table 23. Analysis of variance was used to determine the adequacy of the design (i.e., $p > 0.05$). The polynomial equation obtained for the design demonstrated

that each variable had significant effect on the GS, ZP, and PDI. Linear equation was found for GS, PDI, and quadratic equation for ZP. The equations 13, 14, and 15 below represent the ultimate mathematical model in relation to encoded factors, which has been identified by the Design-Expert software.

$$\text{Particle size} = +68.04 + 47.16 * A + 4.81 * B + 15.38 * C \quad - \quad \text{Eq. (13)}$$

$$\text{PDI} = +0.4069 + 0.0125 * A - 0.1388 * B + 0.0013 * C \quad - \quad \text{Eq. (14)}$$

$$\begin{aligned} \text{Zeta potential} = & -13.40 - 1.05 * A + 0.7625 * B - 1.79 * C + 0.6750 * AB - 1.97 * AC - 3.50 * BC - \\ & 0.3250 * A^2 - 5.10 * B^2 + 0.0500 * C^2 \quad - \quad \text{Eq. (15)} \end{aligned}$$

Table 23: Optimization of SNEDDS using BBD

	Factor 1	Factor 2	Factor 3	Response 1	Response 2	Response 3
Run	A: Oil (μL)	B: Surfactant (μL)	C: Co-Surfactant (μL)	Size (nm)	PDI	ZETA (mAU)
1	150	530	300	76.60	0.54	-17.20
2	100	565	270	14.48	0.22	-12.10
3	200	530	285	129.00	0.41	-20.90
4	200	600	285	176.50	0.24	-18.20
5	150	565	285	54.03	0.4	-13.40
6	200	565	270	78.58	0.54	-10.90
7	100	600	285	12.81	0.29	-18.10
8	150	600	270	53.09	0.26	-12.70
9	100	565	300	40.99	0.53	-12.50
10	150	600	300	72.19	0.24	-22.50
11	200	565	300	105.70	0.43	-19.20
12	100	530	285	44.26	0.48	-18.10
13	150	530	270	26.26	0.71	-21.40

In the above equation positive sign in the indication of synergistic whereas, negative sign is the indication of antagonistic effect of factors on the mentioned response. Equation 13 for GS revealed that with an increase in factors A, B, and C there was an increase in the GS of SNEDDS. Similarly, equation 14 showed that with an increase in concentration of oil (factor A) and concentration of co-surfactant (factor C) PDI of the

SNEDDS increase, whereas concentration of surfactant (factor B) showed the opposite effect. Similarly, concentration of oil and co-surfactant have antagonistic effect and concentration of surfactant had synergistic effect on ZP of SNEDDS (Eq. 15). These equations were used to generate various countour plots for various independent factors, which indicated that each factor played a critical role in the formulation of SNEDDS.

Table 24: Summary of ANOVA of *BBD* batches

Independent variables	Regression coefficient	P value
R^2		Fvalue
Globules Size	0.7502	9.01
PDI	0.5661	3.91
Zeta Potential	0.9886	28.99

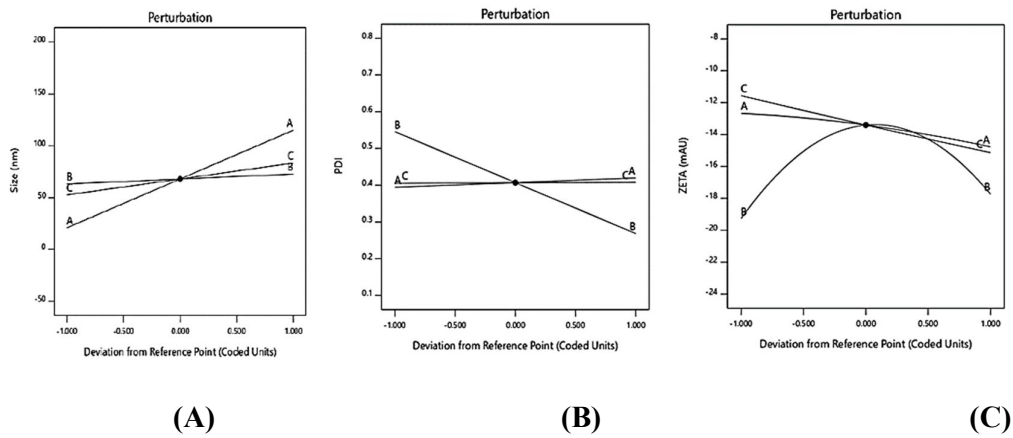


Figure 19: Perturbation plot for GS (A), PDI (B) and ZP(C)

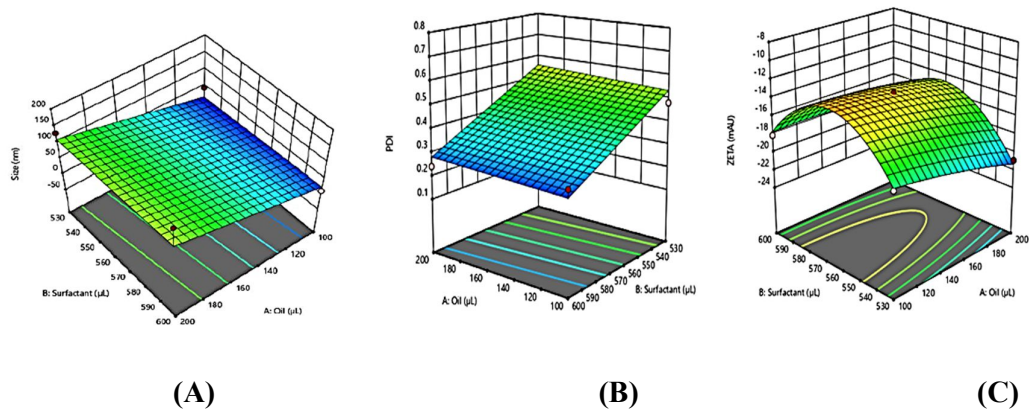


Figure 20: 3D plot for GS (A), PDI (B) and ZP (C)

Design-Expert® Software
Factor Coding: Actual

Overlay Plot

Size
PI Low
PI High
PDI
PI Low
PI High
ZETA
PI Low
PI High

● Design Points

X1 = A: Oil
X2 = B: Surfactant

Actual Factor
C: Co-Surfactant = 270

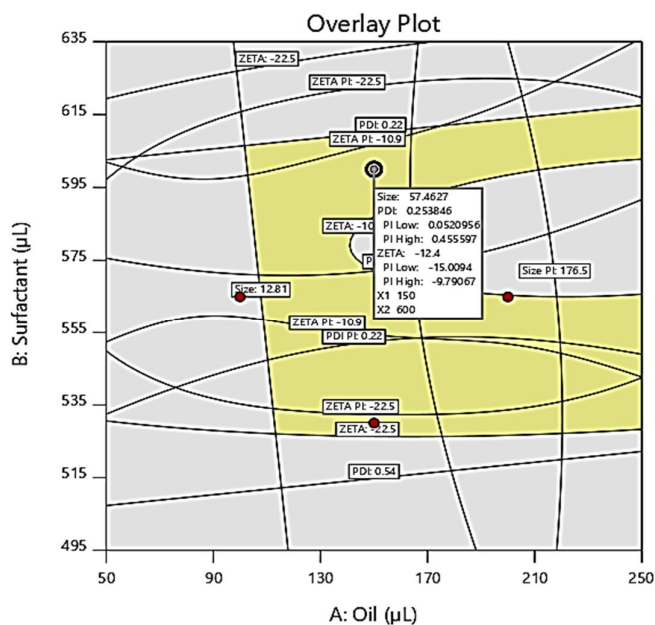


Figure 21: Overlay plot representing optimized composition of SNEDDS

The perturbation plot (Figure 19A) and 3D plot (Figure 20A) for GS indicated that factor A, B, and C had a significant effect on GS. Conversely, perturbation plot (Figure 19B) and 3D plot (Figure 20B) indicated that independent factor B had a dominant effect as compared to factor A&B. This showed that as the concentration of surfactant increased, it led to a decrease in factor D of the formulation. The perturbation plot (Figure 19C) and 3D plot (Figure 20C) for ZP indicated that factor B had a dominant effect on the ZP of the formulation. This showed that with increased surfactant concentration (factor B), ZP shifted more towards the positive side.

5.7 Preparation & characterization of optimized SNEDDS

The results of DoE study provides an optimized composition for SNEDDS which includes capmul MCM (150 μL), tween 80 (600 μL) and Transcutol P (270 μL). This composition was vortexed properly and SIM (10mg) was added to form liquid SNEDDS of SIM which was further evaluated for various parameters.

5.8 Thermodynamic and centrifugation stability

Optimized formulation was analyzed after the centrifugation and by varying the temperature during thermodynamic stability study (heating, cooling and freeze thaw cycle) no precipitation and phase separation was observed. The optimized formulation's

cloud point was determined to be $95 \pm 0.36^\circ\text{C}$. The diluted SNEDDS showed no drug precipitation, creaming, or cracking after 7 days.

5.9 To study the dilution effect and pH change

Due to the fact that, liquid SNEDDS are pre-concentrate mixtures, gentle agitation during dilution, leads to the production of an o/w type fine emulsion. When L-SNEDDS are orally administered, they undergo infinite dilution in the GI route and pass-through, a change acidic environment to basic pH condition. It is important that the GS does not change significantly when the medium volume or pH of the GIT changes. Furthermore, they should be stable in the body.

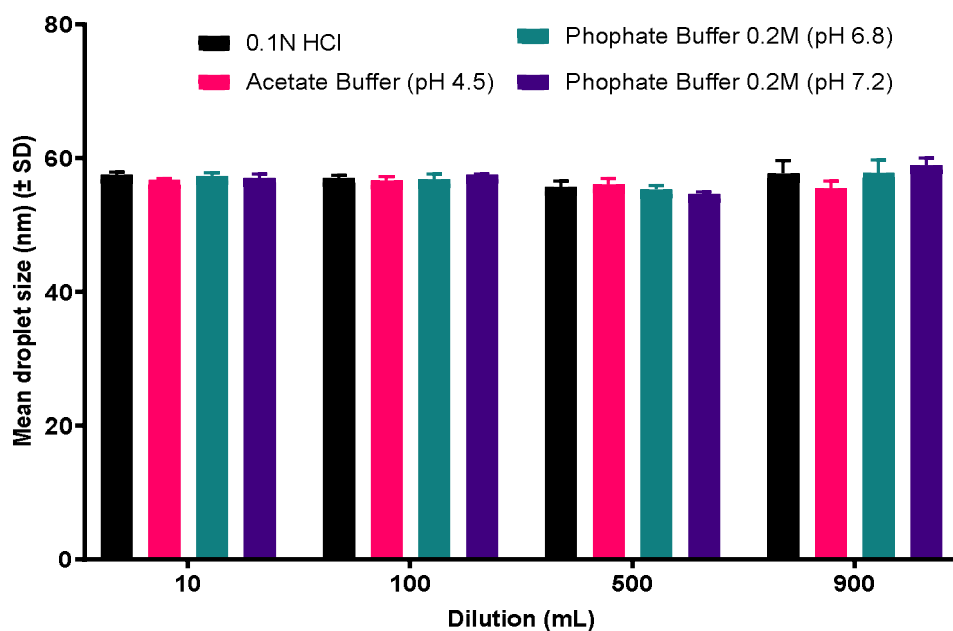


Figure 22: Study the dilution effect and pH change (n=3)

The optimized SNEDDS was diluted in different volumes of water and buffers with pH 1.2, 6.8, and 7.4 to evaluate the effect of pH and dilution. There was no phase separation or drug precipitation observed during dilution in different volumes and pH. It is important to note that droplet size (Figure 22) varied with dilution volume and pH.

5.10 Emulsion globules size and zeta potential

The mean GS, PDI and ZP of optimized formulation were found to be 57.46 ± 2.65 nm, 0.253 ± 0.005 and -13.6 ± 4.1 mV, respectively (Figure 23).

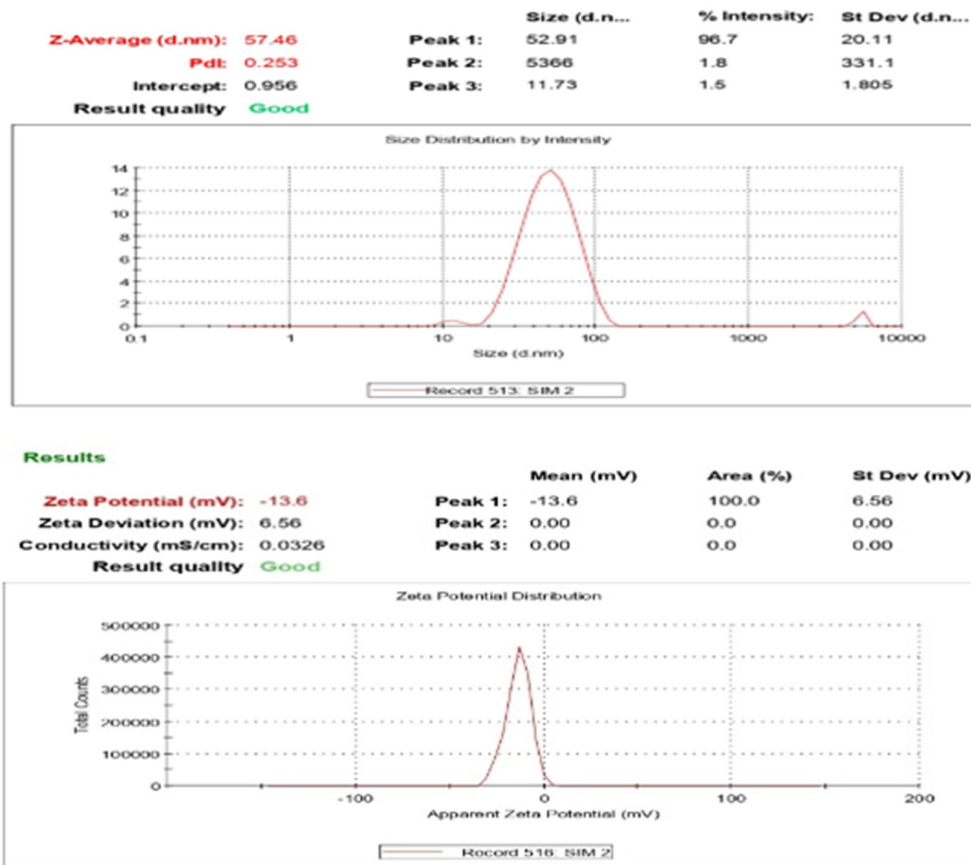


Figure 23: GS, PDI and ZP of optimized SIM-SNEDDS

5.11 Field Emission Scanning Electron Microscopy (FESEM)

The FESEM image indicated that the SIM-SNEDDS was in spherical in shape.

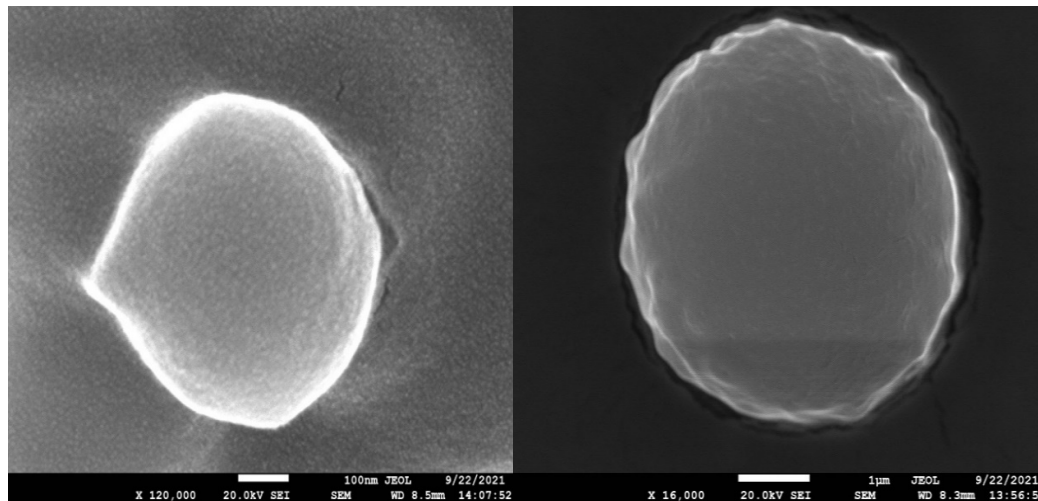


Figure 24: SEM image of SIM-SNEDDS

FESEM image of individual particles clearly revealed the shape with irregular surfaces as shown in Figure 24.

5.12 TEM analysis

The TEM image showed nanometer-sized spherical and un-agglomerated globules. This image was examined for the globule's diameter. There was no globules aggregation seen, and the globules were spherical and uniform in diameter as shown in Figure 25. Furthermore, the GS obtained by TEM showed that the GS was found to be less than 100 nm. This was in concordance with the results obtained in dynamic scattering results. Indicating that the developed SNEDDS were truly in nanometer size.

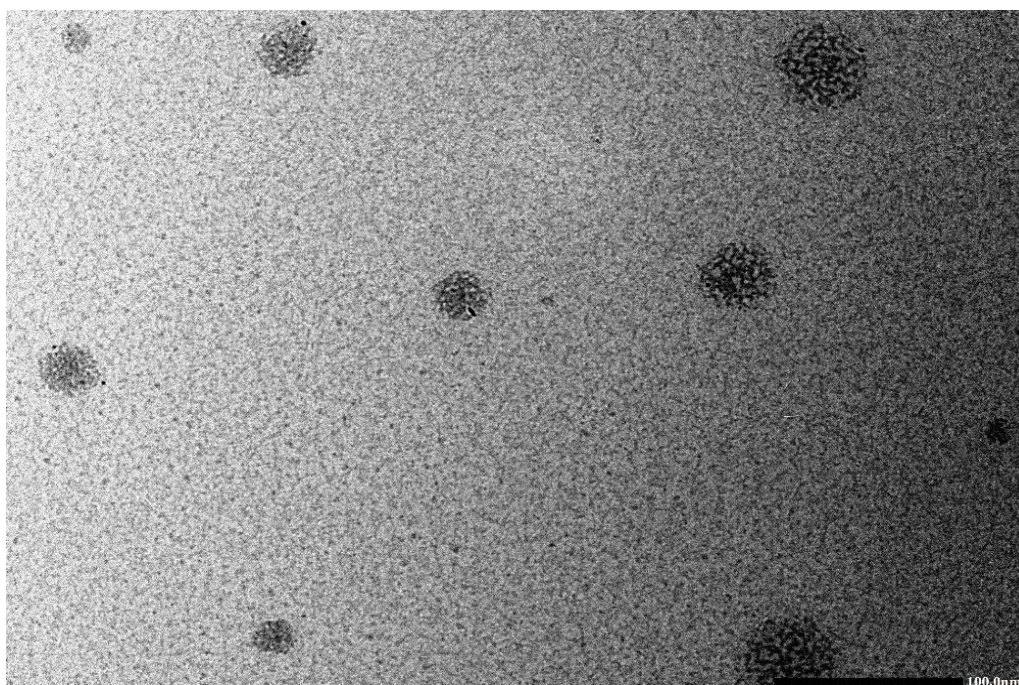


Figure 25: TEM image of SIM-SNEDDS

5.13 DSC analysis

The DSC peak of pure SIM was found to be endothermic at 138°C, indicating its crystallinity. The other excipients, namely, CMC, T-80 and TP showed the absence of any sharp crystalline peaks as depicted by their halo pattern. This shows the amorphous nature of the excipients. The final formulation also showed the absence of any sharp peaks or peaks at the melting point of the drug indicating that there was no precipitation and the drug had excellent drug loading shown in Figure 26.

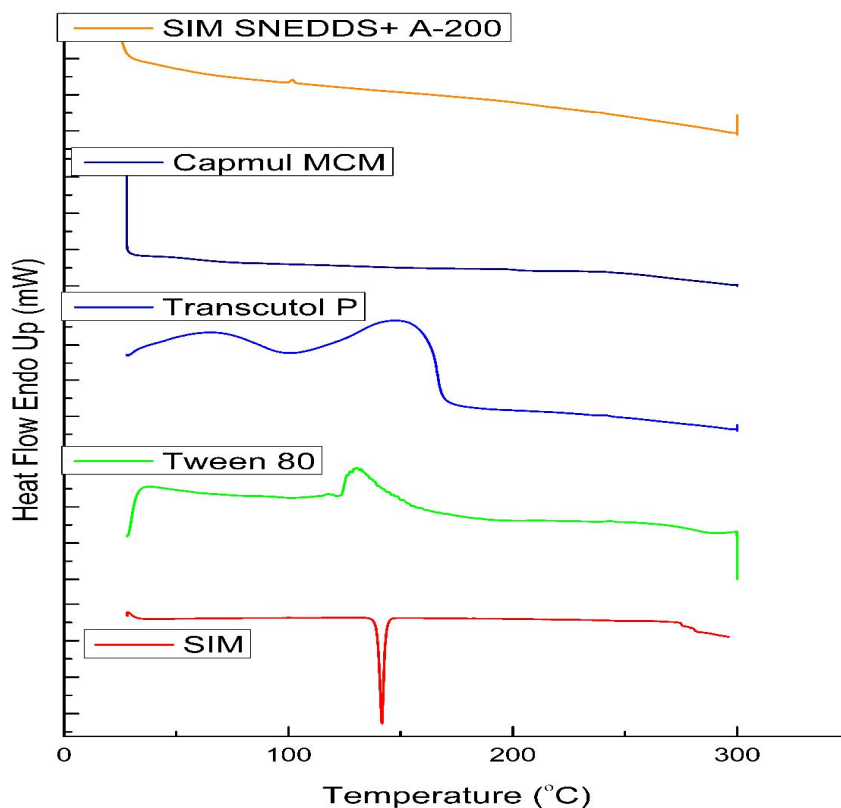


Figure 26: DSC thermogram of TP, T-80, Pure SIM, and SIM-SNEDDS

5.14 *In vitro* dissolution

An *in-vitro* dissolution study was conducted on SIM-SNEDDS and the % drug release was compared with unprocessed SIM. The results showed a significant ($p < 0.05$) increase in the dissolution rate of SIM from SIM-SNEDDS in pH 6.8 phosphate buffer and pH 1.2 buffer compared to unprocessed SIM. More than 60% of the drug was released in pH 6.8 phosphate buffer and more than 90% drug was released in pH 1.2 dissolution media within the first 5 minutes of SNEDDS formulation. However, at the end of 60 minutes, the release was only 81.25% in 6.8 phosphate buffer, while the release in pH 1.2 buffer was found to be 94.54%. The dissolution rate of SIM from SNEDDS increased by approximately 4.5 and 5.22 folds in pH 6.8 phosphate buffer and pH 1.2 buffer in the first 5 minutes, respectively, when compared to its unprocessed form. These findings suggest that the SNEDDS formulation effectively increased the dissolution rate of SIM, as demonstrated in Figure 27.

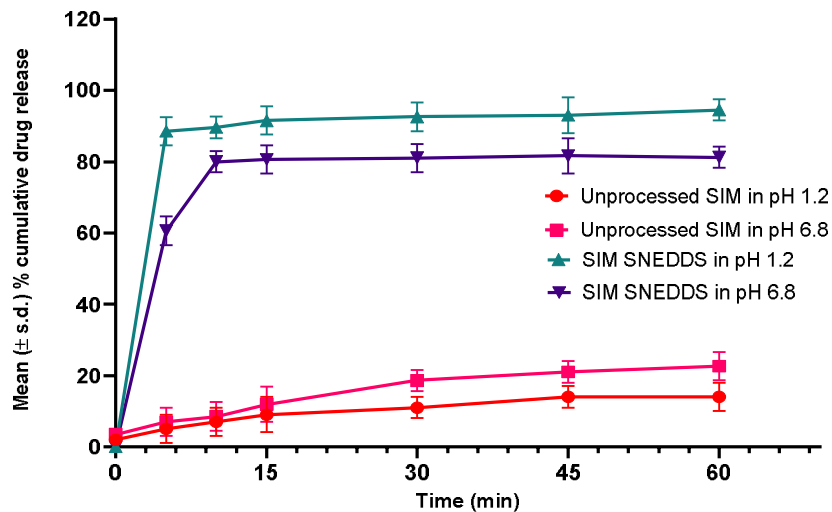


Figure 27: *In-vitro* drug release profile of SIM from unprocessed SIM and SIM-SNEDDS in pH 1.2 and pH 6.8 buffer dissolution media (n=6)

5.15 Cell line toxicity study

Control used was PBS (pH 7.4) shown 100% viability of the SH-SY5Y cells. The blank had 14% cytotoxicity. The cytotoxicity was greater for the groups A-10 and A-5. Whereas, the toxicity is reduced upon serial dilutions. An optimum of 77%–82% cell viability was observed for the formulations upon dilution. So, SNEDDS loaded with SIM when coming in contact with gastric fluid get diluted and form nano-emulsion confirming that the carrier is non-toxic.

Cell viability% = Mean Absorbance of Test sample / Mean Absorbance of Negative Control *100

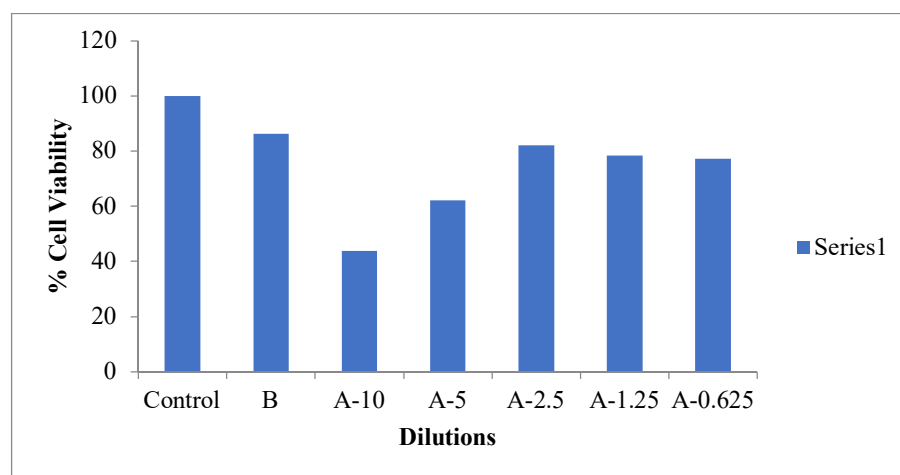


Figure 28: % Cell viability study

5.16 Stability study

Table 25 presents the results of several stability parameters. Over time, the droplet size and PDI of SIM SNEDDS increased when stored at various temperature conditions. However, the increase in droplet size and PDI was not statistically significant ($p>0.05$) when compared to the fresh SIM-SNEDDS. Additionally, after six months of storage at three different conditions, there was no significant ($p>0.05$) decrease in the assay of aged SIM-SNEDDS compared to the fresh one.

Table 25: Stability study of SIM-SNEDDS

Day	MDS	PDI	Assay
25°C±0.2°C/65 RH±5%			
0	58.86±4.51	0.258±0.05	99.54
90	60.24±3.84	0.267±0.06	98.01
180	62.15±4.66	0.271±0.04	97.65
40°C±0.2°C/75 H± 5%			
0	58.86±3.55	0.258±0.05	99.54
90	61.41±4.50	0.274±0.07	97.88
180	65.14±2.35	0.289±0.04	97.05

MDS- mean droplet size, PDI- polydispersity index

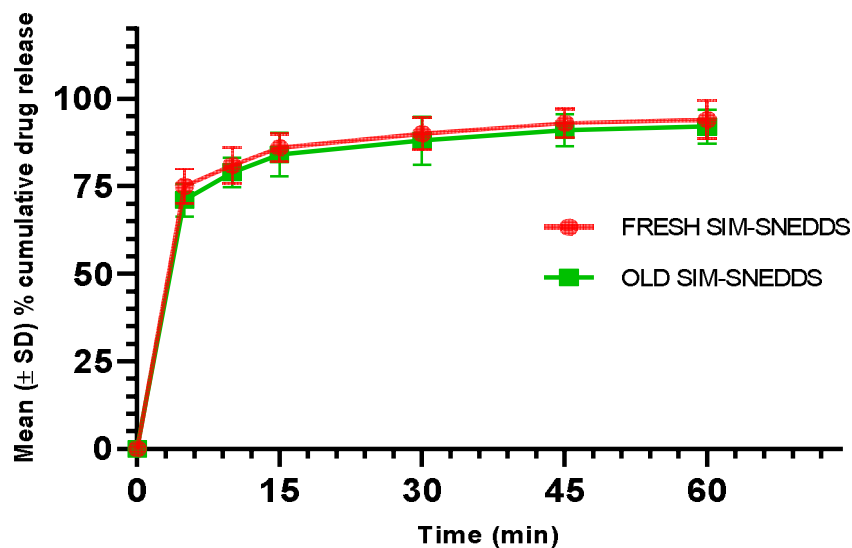


Figure 29: Dissolution of fresh and old SIM-SNEDDS

Additionally, similar results were observed in the dissolution study. There was no much difference that occurred in the release of SIM from the old SIM-SNEDDS when compared to the release of SIM from the fresh SIM-SNEDDS (Figure 29).

5.17 *Ex-vivo* permeation study

This study gives an information about permeation differences of un-processed and SNEDDS of SIM. With the increase in time permeation was found more in the developed SIM-SNEDDS while unprocessed SIM exhibited very less permeability. The value of percentage cumulative drug release of SIM-SNEDDS at 0,5,10,15,30 and 60 min was 0.00, 68.15, 75.18, 81.09, 87.56, 90.25, and 94.27 respectively while unprocessed form of SIM reached 19.23 maximum at 60 min.

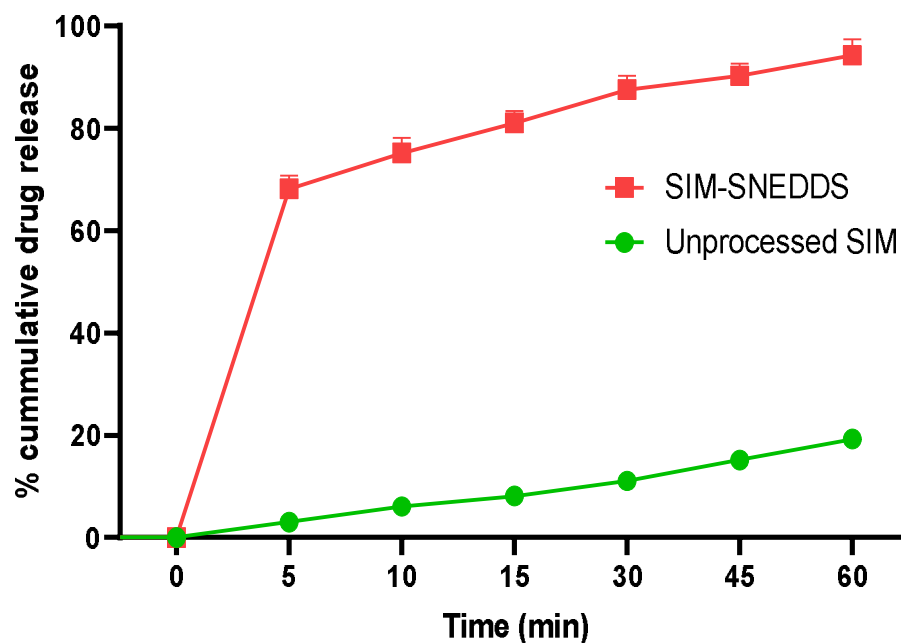


Figure 30: *Ex-vivo* permeation study

5.18 Bioanalytical method development

5.18.1 Specificity, linearity, and range

It was verified that the method developed was exclusive to the drug molecule, as there were no additional peaks observed in the chromatogram of the blank plasma sample at the drug's retention time and lambda max. This confirmed that the method chosen was specific to the drug.

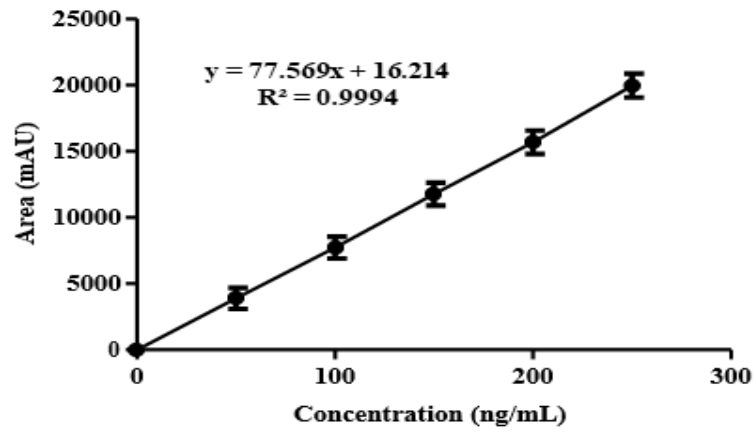


Figure 31: Calibration curve of SIM

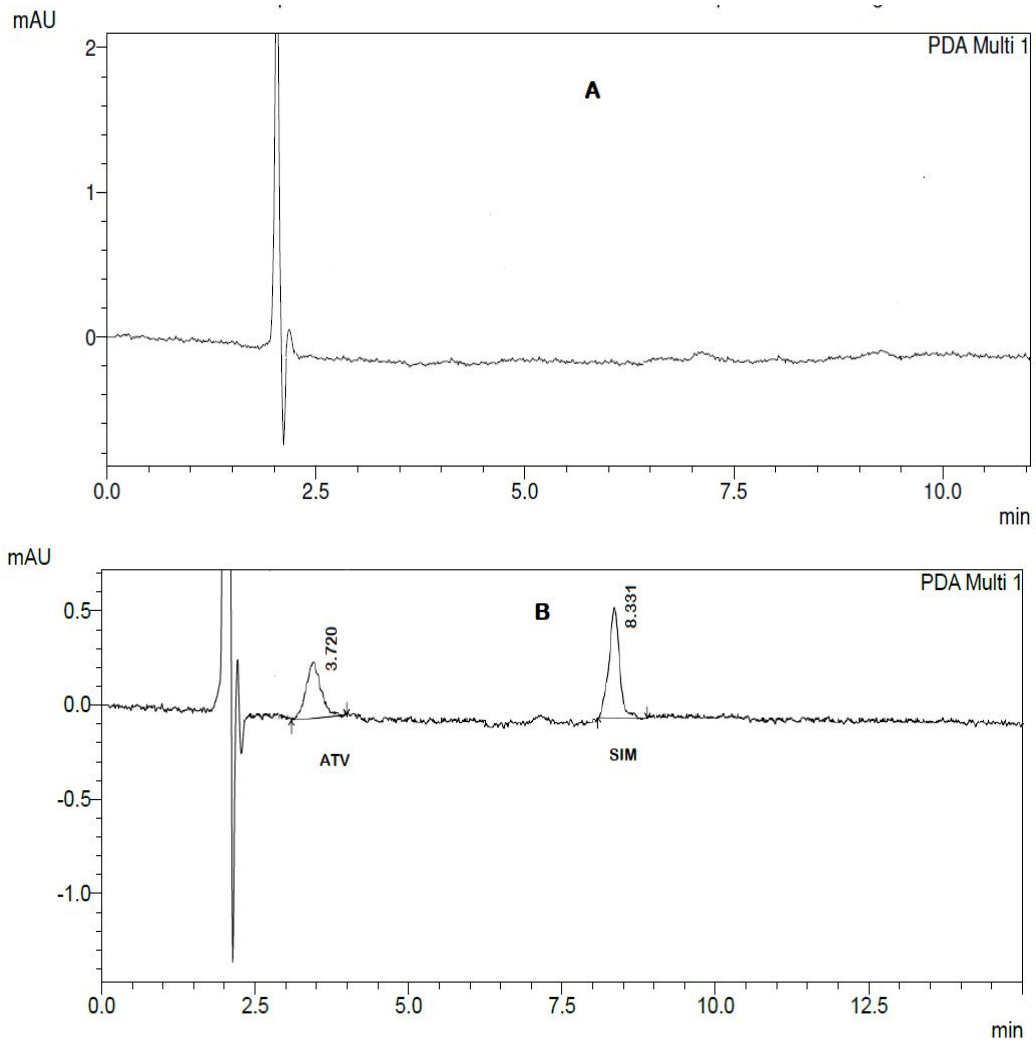


Figure 32: (A) Chromatogram of Blank Plasma, (B) Chromatogram of ATV (RT. 3.720) and SIM (RT. 8.331) in rat plasma

The calibration curve established using plasma as the base was demonstrated to be linear in the range of 50-250 ng/mL, with an r2 value of 0.9994 indicating a high level of linearity. Figure 2 illustrates the calibration curve, while Figures 32a and 32b display the chromatogram of the blank plasma and the drug in rat plasma, respectively (174).

5.18.2 Accuracy

The mean % recovery of the LOQ, MQC, and HQC solutions in mobile phase was used to assess the suggested method's accuracy. The data indicated that the % mean recovery in mobile phase was found within the specified limits of 95-105 % for all three levels (171). The developed method's accuracy was verified using a % RSD less than 2% as shown in Table 26.

Table 26: Accuracy study

Level	Concentration of sample solution (ng/mL)	Total concentration of solution, actual (ng/mL)	Concentration of drug recovered (ng/mL), (N=5)	% Recovery	Mean % recovery
LQC	50	120	118.7±0.65	98.91±0.95	
MQC	50	150	152.7±1.21	101.8±0.86	99.88±0.82
HQC	50	180	178.1±0.96	98.94±0.65	

5.18.3 Precision

The percentage RSD was calculated to validate the precision of developed analytical method. %RSD of all the 3 standard solutions i.e., LQC, MQC, and HQC were measured by using response area of interday, intraday and interanalyst. The % RSD of inter & intra days was found in the range of 0.53-1.29 % whereas, 0.51-1.27 % was observed in the case of interanalyst. All these calculated RSD were found within the acceptable limits of 2% RSD shown in Table 27 (172).

5.18.4. Stability study of plasma samples

Stability studies were done on LQC, MQC, and HQC samples spiked with SIM in plasma at 3 different levels, which included short-term stability (as shown in Table 28a), freeze-thaw stability (as shown in Table 28b), and long-term stability (as shown in Table 28c). In all cases, the results indicated that more than 95% of the drug was recovered, with an RSD of less than 2%. These studies' results showed that drugs in plasma samples were stress- and long-term storage-stable (175).

Table 27: Precision study

Parameter	Level	Concentration (ng/mL)	Area (cm ²)	1	Area 2 (cm ²)	Area 3 (cm ²)	Area 4 (cm ²)	Area 5 (cm ²)	Area 6 (cm ²)	Mean (cm ²)	S.D.	RSD (%)
Intra-day												
1 hour	LQC	120	9258.81	9196.52	9296.43	9125.23	9189.34	9279.21	9224.257	65.142	0.706206	
	MQC	150	11825.32	11956.27	11910.82	11892.83	11781.88	11835.36	11867.08	64.094	0.540099	
	HQC	180	13951.2	13767.23	13876.84	13938.89	13837.14	13638.87	13835.03	117.5674	0.849781	
2 hours	LQC	120	9263.62	9352.51	9515.45	9365.25	9264.34	9159.6	9320.128	121.086	1.299196	
	MQC	150	11756.55	11896.45	11874.26	11795.25	11668.75	11885.63	11812.82	89.778	0.760013	
	HQC	180	13841.24	13552.45	13795.48	13896.56	13696.84	13759.36	13756.99	121.259	0.881441	
3 hours	LQC	120	9256.45	9357.56	9284.45	9454.15	9354.54	9248.45	9325.933	78.499	0.841729	
	MQC	150	11854.45	11956.54	11695.21	11954.45	11768.85	11865.74	11849.21	103.0239	0.869458	
	HQC	180	13769.56	13954.42	13659.78	13759.69	13896.65	13856.87	13816.16	106.833	0.77325	
Inter-day												
Day 1	LQC	120	9258.81	9196.52	9296.43	9125.23	9189.34	9279.21	9224.257	65.142	0.706206	
	MQC	150	11825.32	11956.27	11910.82	11892.83	11781.88	11835.36	11867.08	64.094	0.540099	
	HQC	180	13951.22	13767.23	13876.84	13938.89	13837.14	13638.87	13835.03	117.571	0.849809	
Day 2	LQC	120	9364.56	9256.45	9348.85	9485.74	9394.78	9457.55	9384.655	82.166	0.875541	
	MQC	150	11958.58	11896.45	11826.54	11964.34	11863.45	11725.86	11872.54	89.571	0.754445	
	HQC	180	13894.56	13856.57	13758.25	13964.75	13899.45	13589.75	13827.22	134.667	0.97393	
Day 3	LQC	120	9353.36	9245.51	9459.59	9354.29	9265.65	9489.56	9361.327	98.774	1.055112	
	MQC	150	11796.54	11865.63	11794.56	11855.65	11795.45	11954.49	11843.72	63.036	0.532196	
	HQC	180	13769.56	13954.42	13659.78	13759.69	13896.65	13856.87	13816.16	106.833	0.77325	
Intermediate precision (inter analyst)												
Analyst 1	LQC	120	9258.81	9196.52	9296.43	9125.23	9189.34	9279.21	9224.257	65.142	0.706206	
	MQC	150	11825.32	11956.27	11910.82	11892.83	11781.88	11835.36	11867.08	64.094	0.540099	
	HQC	180	13951.22	13767.23	13876.84	13938.89	13837.14	13638.87	13835.03	117.5714	0.849809	
Analyst 2	LQC	120	9156.45	9265.12	9298.62	9156.36	9365.24	9456.75	9283.09	117.9565	1.27066	
	MQC	150	11586.55	11656.45	11825.59	11789.41	11796.85	11789.56	11740.74	95.895	0.816773	
	HQC	180	13895.54	13956.78	13756.45	13896.95	13756.36	13696.96	13826.51	103.256	0.746803	
Analyst 3	LQC	120	9355.55	9268.45	9556.63	9268.56	9355.36	9389.21	9365.627	105.934	1.131099	
	MQC	150	11759.15	11869.46	11789.78	11896.45	11815.78	11911.85	11840.41	61.418	0.518721	
	HQC	180	13694.44	13965.86	13756.12	13896.63	13737.65	13864.96	13819.28	105.634	0.764398	

Table 28a: Short term stability for plasma samples of SIM

Actual Concentration of drug (ng/mL)	Area (cm²)	1 Area (cm²)	2 Area (cm²)	3 Area (cm²)	Mean (cm²)	S.D.	RSD (%)	Amount of drug recovered in plasma sample (ng/mL)	Recovery (%)
1 hour									
120 (LQC)	9265.78	9156.45	9365.56	9262.597	104.5913	1.129179	119.21	99.34	
150 (MQC)	11486.26	11569.78	11656.48	11570.84	85.11495	0.735599	148.97	99.31	
180 (HQC)	13756.78	13886.48	13785.59	13809.62	68.10641	0.493181	177.80	98.77	
2 hours									
120 (LQC)	9159.41	9252.51	9368.79	9260.237	104.9036	1.13284	119.18	99.31	
150 (MQC)	11695.26	11656.95	11597.42	11649.88	49.30203	0.423198	149.99	99.99	
180 (HQC)	13896.42	13796.49	13965.52	13886.14	84.98231	0.611994	178.82	99.34	
3 hours									
120 (LQC)	9365.64	9258.45	9469.34	9364.477	105.4498	1.126062	120.52	100.43	
150 (MQC)	11469.42	11582.65	11695.59	11582.55	113.085	0.976339	149.12	99.41	
180 (HQC)	13965.46	13869.69	13759.54	13864.9	103.0436	0.743198	178.55	99.19	

Table 28b: Freeze thaw stability for plasma samples of SIM

Actual Concentration of drug (ng/mL)	Area (cm²)	1 Area (cm²)	2 Area (cm²)	3 Area (cm²)	Mean (cm²)	S.D.	RSD (%)	Amount of drug recovered in plasma sample (ng/mL)	Recovery (%)
Cycle 1									
120 (LQC)	9236.25	9363.68	9169.32	9256.417	98.73689	1.066686	119.13	99.27	
150 (MQC)	11469.62	11569.45	11653.56	11564.21	92.08189	0.796266	148.89	99.26	
180 (HQC)	13756.35	13896.63	13664.36	13772.45	116.9687	0.849295	177.36	98.53	
Cycle 2									
120 (LQC)	9296.36	9369.64	9595.49	9420.497	155.915	1.655061	121.25	101.04	
150 (MQC)	11394.39	11269.94	11496.29	11386.87	113.3621	0.99555	146.60	97.73	
180 (HQC)	13964.62	13869.34	13795.89	13876.62	84.60003	0.609659	178.70	99.27	
Cycle 3									
120 (LQC)	9169.56	9346.97	9267.93	9261.487	88.88034	0.959677	119.20	99.33	
150 (MQC)	11469.63	11536.96	11695.75	11567.45	116.1019	1.003695	148.93	99.28	
180 (HQC)	13569.61	13791.34	13694.47	13685.14	111.1591	0.812261	176.23	97.90	

Table 28c: Long term stability for plasma samples of SIM

Actual Concentration of drug (ng/mL)	Area 1 (cm²)	Area 2 (cm²)	Area 3 (cm²)	Mean (cm²)	S.D.	RSD (%)	Amount of drug recovered in plasma sample (ng/mL)	Recovery (%)
Week 1								
120 (LQC)	9136.45	9256.78	9315.45	9236.227	91.25283	0.987988	118.87	99.05
150 (MQC)	11369.29	11496.45	11654.15	11506.63	142.7026	1.240177	148.14	98.76
180 (HQC)	13695.15	13956.95	13865.14	13839.08	132.8313	0.959827	178.22	99.01
Week 2								
120 (LQC)	9365.95	9189.58	9268.78	9274.77	88.33745	0.952449	119.37	99.47
150 (MQC)	11269.36	11369.15	11455.75	11364.75	93.27275	0.82072	146.31	97.54
180 (HQC)	13569.36	13776.95	13645.94	13664.08	104.9776	0.768274	175.96	97.75
Week 3								
120 (LQC)	9268.96	9278.38	9136.63	9227.99	79.26015	0.85891	118.76	98.96
150 (MQC)	11363.54	11275.36	11415.45	11351.45	70.82322	0.623913	146.14	97.42
180 (HQC)	13695.63	13862.39	13865.15	13807.72	97.08548	0.703124	177.81	98.78

5.18.5. LOD and LOQ

LOD and LOQ were found in rat plasma to be 0.12 ng/mL and 0.38 ng/mL, respectively.

5.18.6. System suitability

To evaluate the suitability and effectiveness of a chromatographic system, a system suitability test is typically performed. In this case, the tailing factor for all peaks, including SIM and ATV peaks, did not exceed 2, indicating good peak symmetry (with acceptance limits < 2). In all the chromatographic runs, the theoretical plates count remained above 2000, which indicates that the column was highly efficient during the separation process as shown in Table 29 (176).

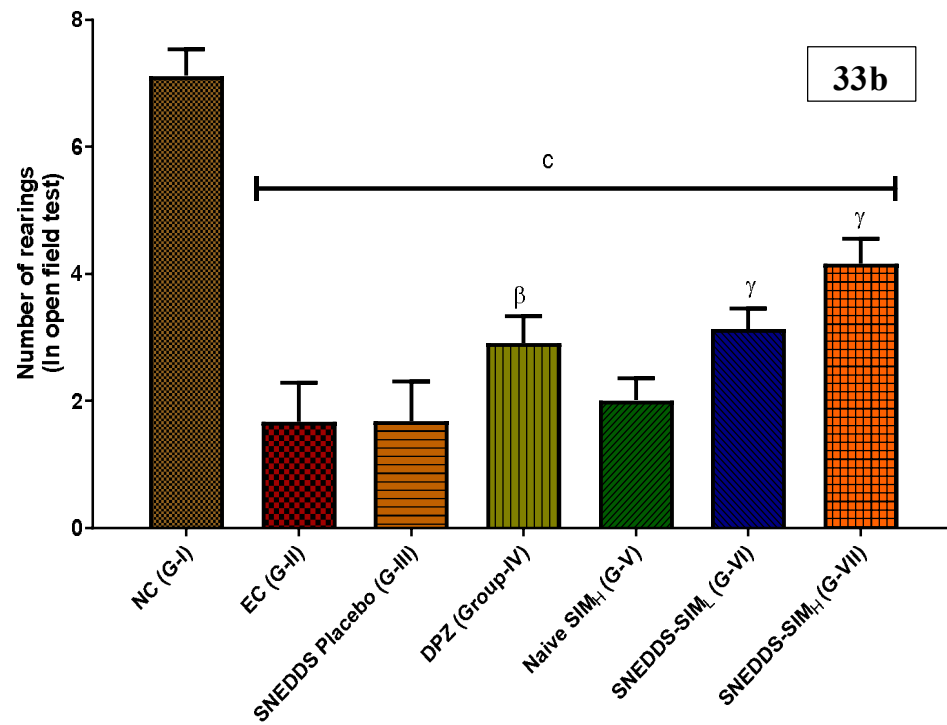
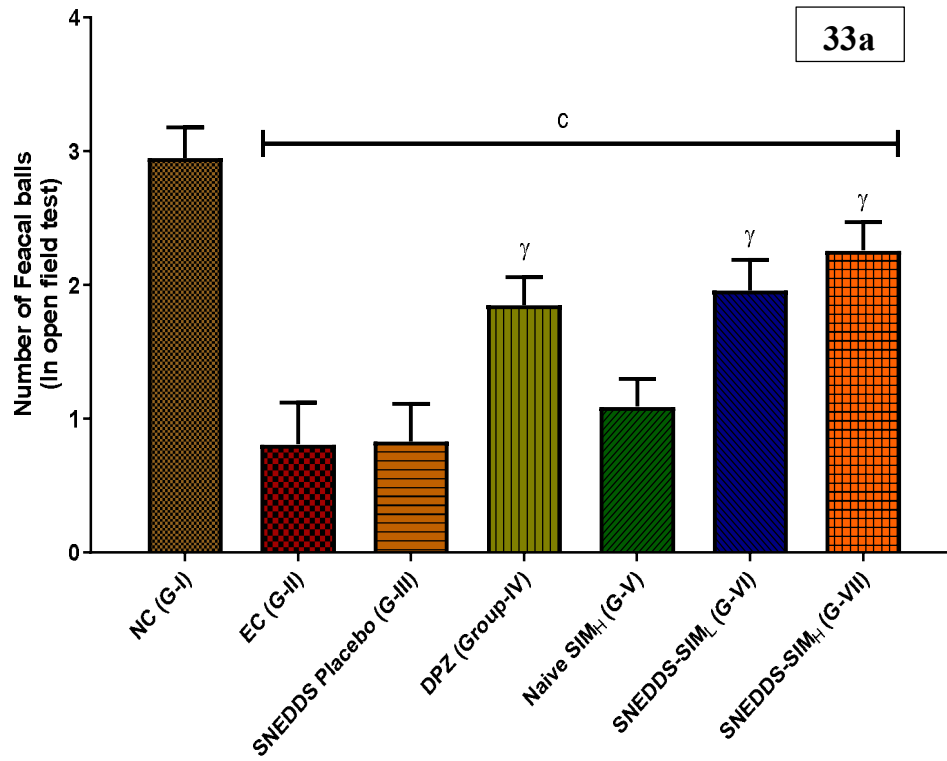
Table 29: System suitability parameters

Sr. no.	Parameter	SIM	ATV
1.	Theoretical Plates	7853.56±15.11	3869.34±11.87
2.	HETP	35.21±2.41	18.31±2.11
3.	Tailing factor	1.35±0.32	1.28±0.29

5.19 Effect of drug treatment on Neurobehavioral parameters

5.19.1. Effect of drug treatment in open field test

In groups I, II, III, IV, V, VI, and VII the number of fecal balls counts were 2.95 ± 0.23 , 0.81 ± 0.31 , 0.83 ± 0.28 , 1.85 ± 0.21 , 1.09 ± 0.21 , 1.96 ± 0.23 , and 2.26 ± 0.21 , respectively shown in Figure 33a. On the other hand, the number of rearing counts were 7.12 ± 0.42 , 1.67 ± 0.61 , 1.68 ± 0.63 , 2.91 ± 0.42 , 2.01 ± 0.35 , 3.13 ± 0.33 , and 4.16 ± 0.39 in groups, I, II, III, IV, V, VI, and VII respectively shown in Figure 33b. In this test the number of squares crossed by rats were 32.22 ± 1.09 , 4.16 ± 1.11 , 4.14 ± 1.08 , 19.12 ± 1.23 , 6.02 ± 1.12 , 27.03 ± 1.13 , and 29.18 ± 1.03 in groups, I, II, III, IV, V, VI, and VII respectively (Figure 33c). While in groups, I, II, III, IV, V, VI, and VII, time spent in immobile stage was 119.22 ± 1.10 , 254.12 ± 2.01 , 254.09 ± 2.08 , 181.18 ± 2.23 , 233.02 ± 1.12 , 153.13 ± 2.01 , and 139.18 ± 1.19 in seconds respectively as shown in Figure 33d.



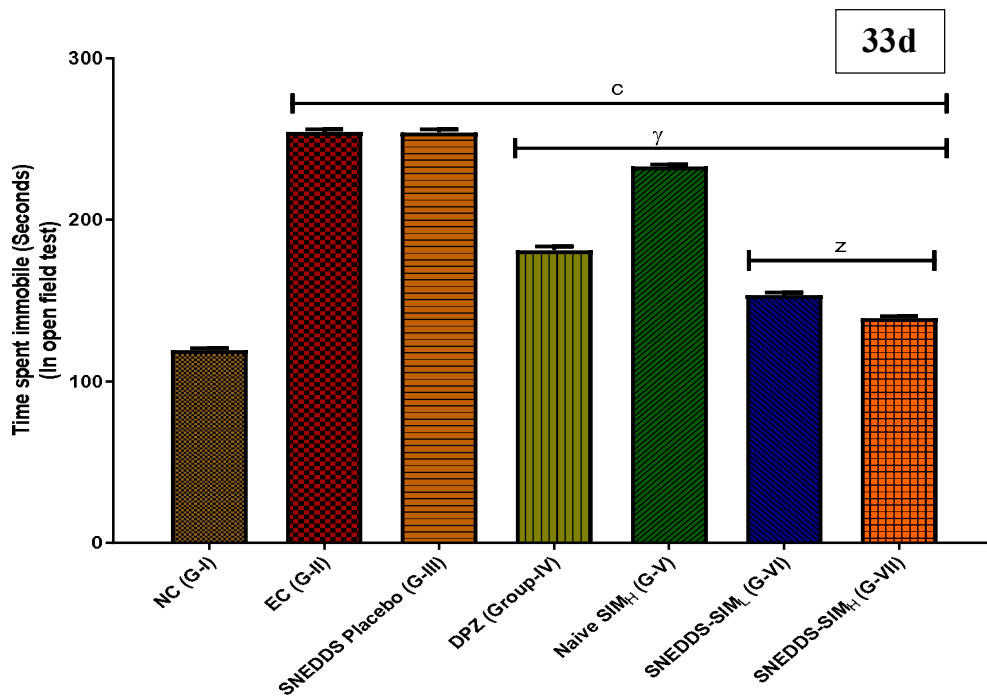
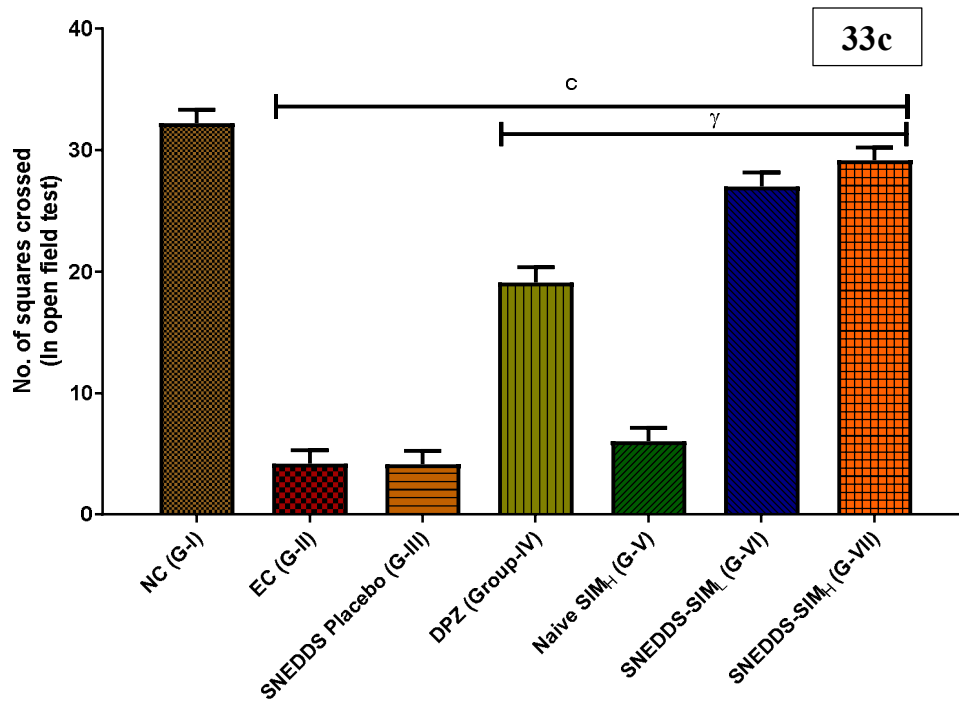


Figure 33: Open field test- (33a). Number of fecal balls (33b). Number of rearing (33c). Number of squares crossed (33d). Time spent immobile, All data are represented as Mean \pm SEM at N = 6 rats in each groups. ^ap < 0.05, ^bp < 0.01, ^cp < 0.001 when compared with normal control (NC), ^ap < 0.05, ^bp < 0.01, ^γp < 0.001 when compared with experimental control (EC), and ^xp < 0.05, ^yp < 0.01, ^zp < 0.001 when compared with Donepezil (DPZ).

By these parameters locomotor and other hand exploration behavioral pattern were investigated. AlCl_3 is a well-established neurotoxicant to evoke AD in the rats which results in significant decline in locomotion. In AlCl_3 induced rats (Alzheimeric rats). It is also very important to note that the significant increase in the time spent in immobile stage was noted as compared to control rats. Treatment with SIM-SNEDDS to these Alzheimeric rats causes significant improvement in locomotor as well as time spent immobile. However, treatment with SIM-SNEDDS causes reversal in rearing count and number of fecal balls. It is also observed that SIM-SNEDDS at their both doses exhibited better responses with respect to DPZ (G-IV) treated rats.

5.19.2. Effect of drug treatment in MWM test

Spatial memory and memory changes were most important parameter were assessed using MWM test. This test clearly showed that the group of rats received a treatment of AlCl_3 causes a significant increase in the time taken to reach platform with respect to rats of control groups. This parameter is recorded for spatial memory. Further treatment improves the parameters of spatial memory.

Time taken to reach platform were 8.92 ± 1.34 , 42.12 ± 1.29 , 41.34 ± 1.32 , 18.13 ± 1.38 , 38.11 ± 1.19 , 14.03 ± 1.28 , and 12.13 ± 1.34 seconds in groups I, II, III, IV, V, VI, and VII respectively shown in Figure 34a. It indicates that SIM-SNEDDS could reverse this spatial memory depicts in Alzheimeric rats. Time spend by rats in target quadrants were 42.65 ± 1.66 , 20.18 ± 1.78 , 20.11 ± 1.64 , 26.12 ± 1.23 , 23.19 ± 1.18 , 29.23 ± 1.20 , and 34.12 ± 1.02 seconds was observed in groups I, II, III, IV, V, VI, and VII respectively (Figure 34b) it was the case of working or referencing memory observation where the number of entries in the quadrant (where the platform) was previously placed was noted.

Significant reduction in the number of eateries were observed in group of rats receiving only AlCl_3 . When compared with normal control group of rats. SIM-SNEDDS treatments, provided substantial enhancement in the number of entries in the targeted region. This important point to note that the none of the changes were observed between Alzheimeric rats and SNEDDS placebo-treated Alzheimeric rats.

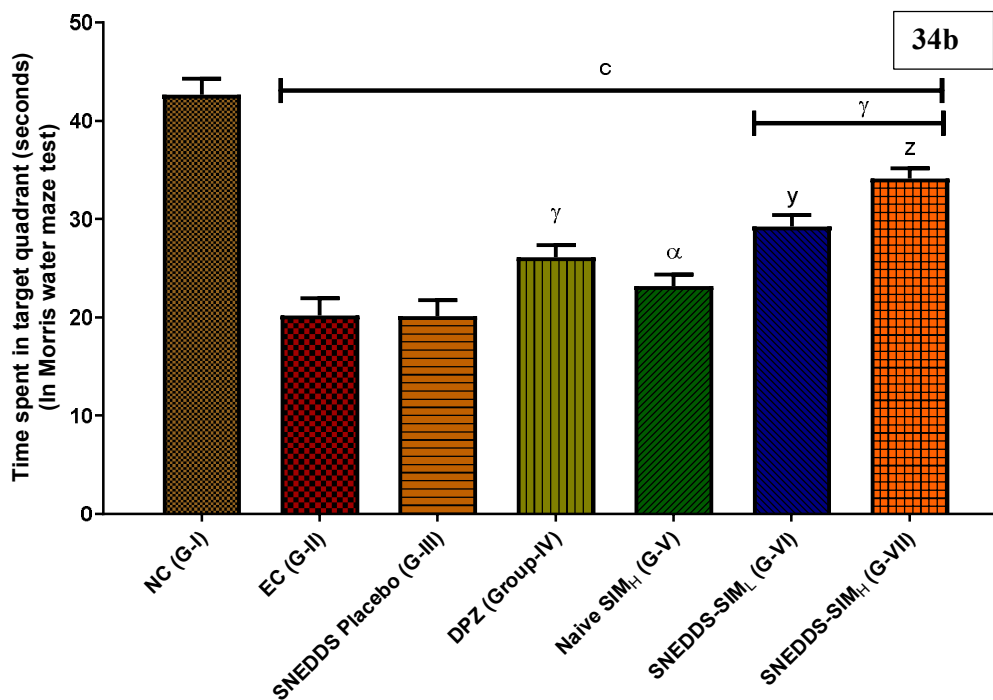
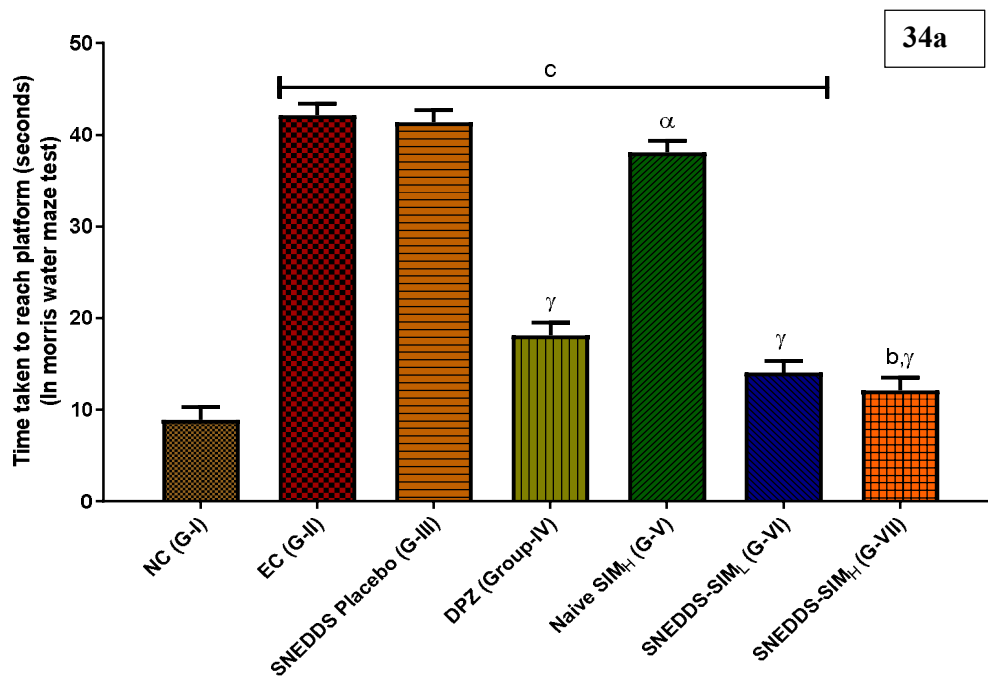


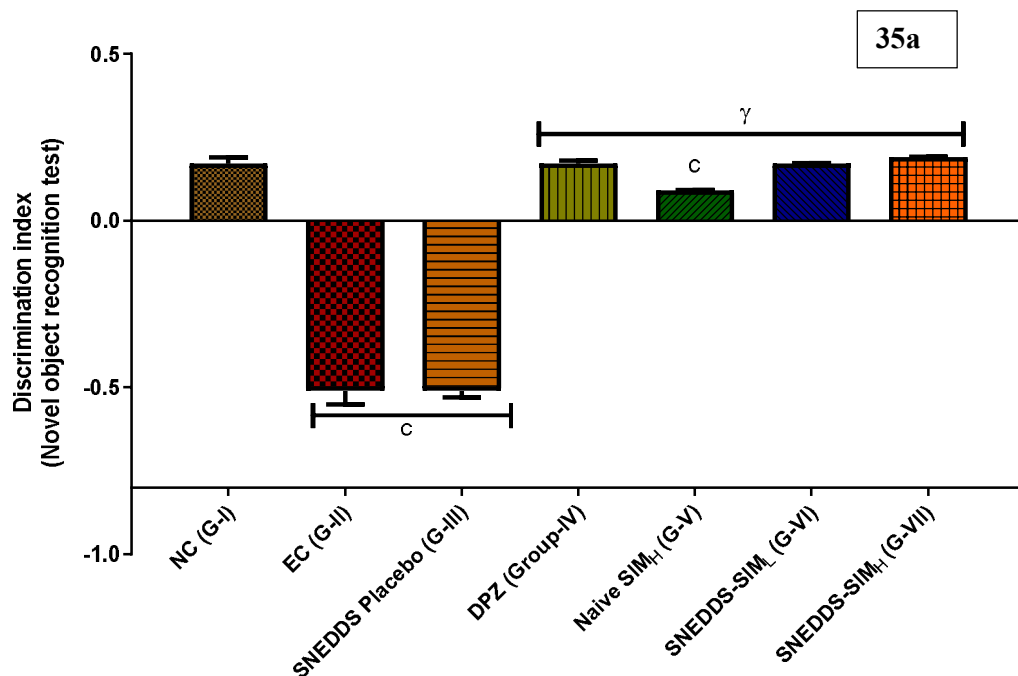
Figure 34: MWM: (34a). Time taken to reach platform (34b). Time spent in target quadrant, All data are represented as Mean \pm SEM at N = 6 rats in each groups. ^ap < 0.05, ^bp < 0.01, ^cp < 0.001 when compared with normal control (NC), ^αp < 0.05, ^βp < 0.01, ^γp < 0.001 when compared with experimental control (EC), and ^xp < 0.05, ^yp < 0.01, ^zp < 0.001 when compared with Donepezil (DPZ).

5.19.3. Effect of the drug treatment in novel object recognition (NOR)

Basically, this parameter is used to investigate hippocampus function with the recognition of the object in such a way that recognition memory can be observed. Hence, discrimination index was analyzed here.

Discrimination index were 0.17 ± 0.02 , -0.51 ± 0.04 , -0.51 ± 0.02 , 0.17 ± 0.01 , 0.09 ± 0.001 , 0.17 ± 0.002 , and 0.19 ± 0.002 in groups, I, II, III, IV, V, VI, and VII respectively shown in Figure 35a.

Here, the discrimination index was found extremely less with $AlCl_3$ induced group of rats (G-I) and similar finding was noted with placebo treated group of rats. Hence, group of rats II&III were unable to distinguished familiar and novel object with respect to control group (G-I).



However, in other group of rats when drug treatment was provided, should reversed of such impairment and they were significantly differentiating as well as recognized the object when compared with rats of group II.

Recognition index were 59.12 ± 1.60 , 17.11 ± 1.29 , 16.11 ± 1.23 , 39.19 ± 1.21 , 24.11 ± 1.13 , 41.14 ± 1.18 , and 48.29 ± 1.32 in groups, I, II, III, IV, V, VI, and VII respectively shown in Figure 35b.

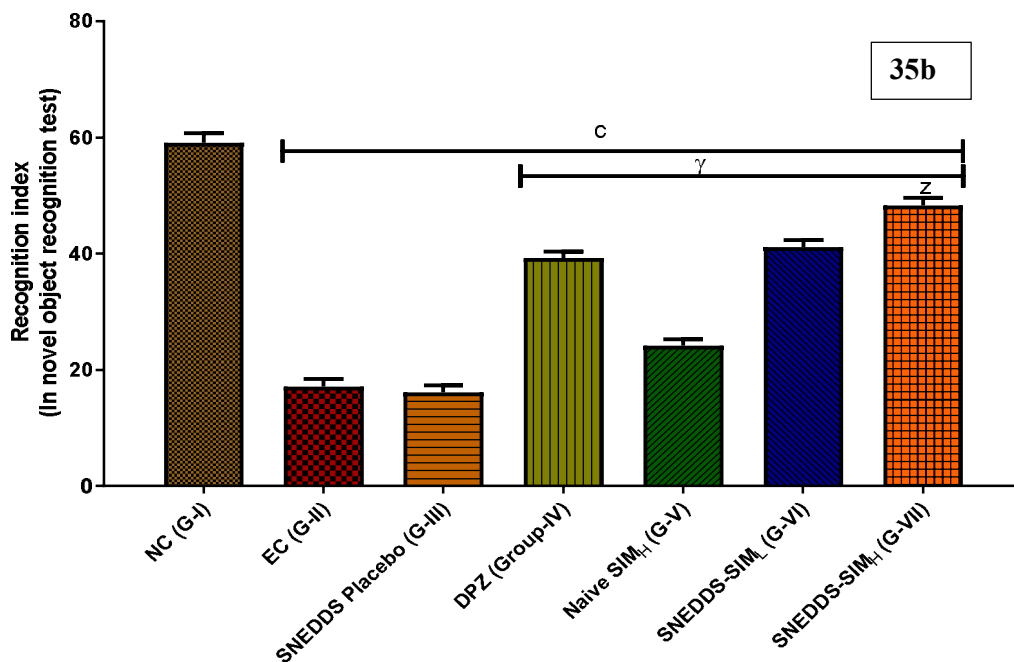


Figure 35: NOR (35a). Discrimination Index (35b). Recognition Index, All data are represented as Mean ± SEM at N = 6 rats in each groups. ^ap < 0.05, ^bp < 0.01, ^cp < 0.001 when compared with normal control (NC), ^αp < 0.05, ^βp < 0.01, ^γp < 0.001 when compared with experimental control (EC), and ^zp < 0.05, ^γp < 0.01, ^zp < 0.001 when compared with Donepezil (DPZ).

In addition to this it was also observed that rats of group were not able to recognize novel object also when compared with control group but amelioration was recorded with the drug treatment specially with SIM-SNEDDS at their both doses.

5.20 Biochemical estimations

5.20.1 Reversal of diminished acetylcholinesterase activity by SIM

AChE was utilized as a biomarker for brain cholinergic neuronal death. The Ellman technique was used to measure the AchE activity. The activity of AchE was investigated in the cortex as well as the hippocampus region of the brain after the sacrifice of animals on terminal days.

It was observed that the level of AchE activity was found more in a group of rats that received only AlCl₃ indicated in figure. It is crucial to remember that similar findings of an increased level of AchE were observed in a group of rats received a placebo in the cortex as well as the hippocampus. But amelioration in the level of AchE was observed in groups IV, V, VI, and VII. Since the groups of rats received only naïve of

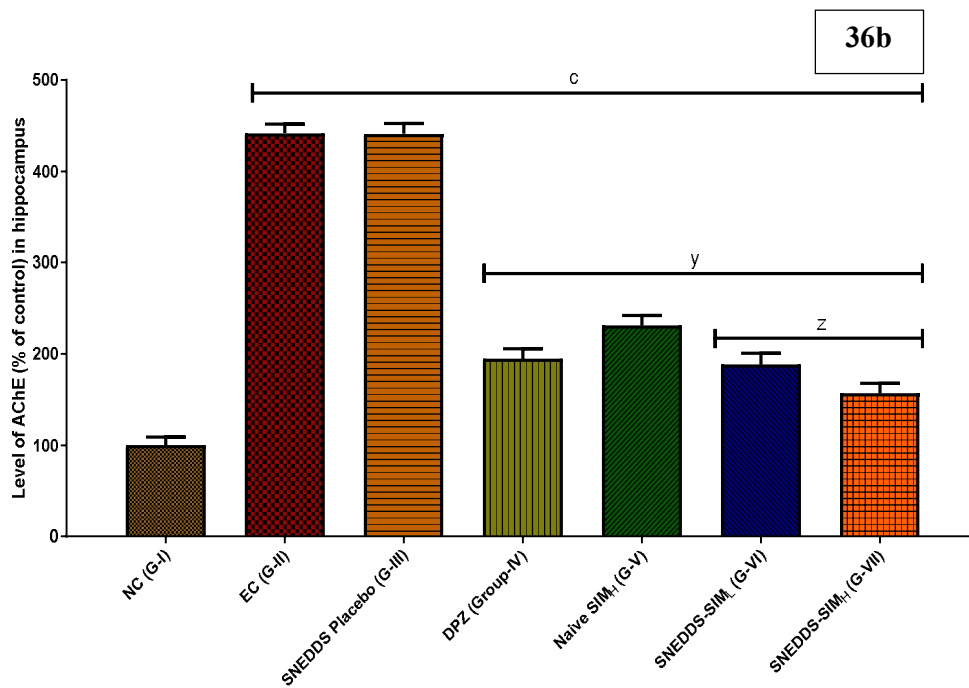
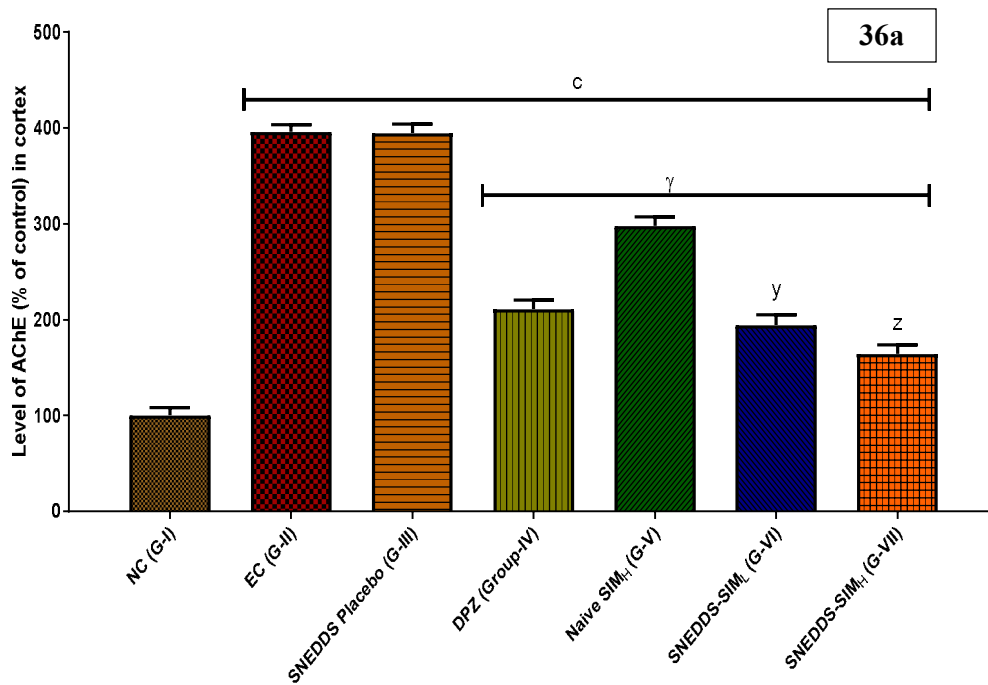


Figure 36: (36a). Level of AchE in cortex, (36b). Level of AchE in hippocampus, All data are represented as Mean \pm SEM at N = 6 rats in each groups. ^ap < 0.05, ^bp < 0.01, ^cp < 0.001 when compared with normal control (NC), ^αp < 0.05, ^βp < 0.01, ^γp < 0.001 when compared with experimental control (EC), and ^λp < 0.05, ^ϕp < 0.01, ^zp < 0.001 when compared with Donepezil (DPZ).

SIM hence the level of reduction of AchE was least with respect to groups IV, VI, and VII. A substantial decrease in AchE activity was found in groups IV, VI, and VIII. SNEDDS-treated group of rats showed better results with respect to group IV while group VII was found better than group VI.

Chronic $AlCl_3$ administration to the rats significantly reduced AchE activity in the cortex as well as the brain as compared to G-I. In the hippocampus and frontal cortex, by AchE activity was significantly reduced SIM at both doses as well as DPZ compared to G-I. $AlCl_3$ effectiveness on AchE activity was significantly reduced by G-IV, G-V, G-VI, and G-VII as 211.47 ± 9.31 , 298.08 ± 9.22 , 194.73 ± 10.28 , 164.34 ± 9.33 in the cortex, and 194.54 ± 11.29 , 231.12 ± 11.18 , 188.50 ± 12.03 , 156.63 ± 11.29 in hippocampus respectively shown in Figure 36b.

The enhancement in AchE activity caused by Al^{3+} could be attributed to interactions between Al^{3+} and AchE peripheral regions, which alter the secondary structure of AchE, enhancing its efficacy. Extensive increased activity of AchE leading to increased degradation of acetylcholine which in turns reduces the normal level of Ach in the brain. It is very clearly reported in various literature that Ach is important for learning and memory. But here $AlCl_3$ causes amplification of AchE activity. The current study was consistent with earlier research in that Alzheimeric rats had much higher AchE levels than control rats. SIM-SNEDDS therapy of these Alzheimer's rats significantly reduced AchE levels, probably because of lowering aluminum stress in the brain. As a result, SIM-SNEDDS treatment may be capable of avoiding acetylcholine neuronal loss in the brain.

5.20.2 Metal Ion Concentration

$AlCl_3$ is the used here for the development of AD in rats. Hence, it is very important to note the availability of Al^{3+} in the rat's brain. All the treatment except control group has higher amount of Al^{3+} concentration, but reduction was found remarkable by SIM-SNEDDS at their both doses. The reason for enhanced availability of Al^{3+} in hippocampus was Al^{3+} crosses blood brain barrier and its accumulation cause long time potential and inducement of apoptosis due to oxidative stress. As a result of this stress neurons becomes deficient of endogenous oxidative enzymes which was also

maximally protected due to administration of SIM-SNEDDS. In less with these finding suggest that efficacy was highest in group VII>VI>IV>V.

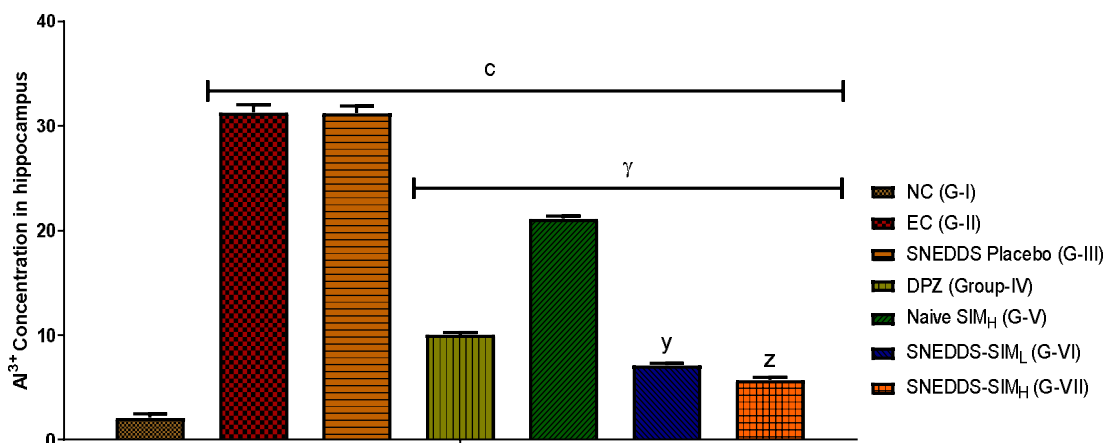


Figure 37: Al³⁺ concentration in hippocampus, All data are represented as Mean ± SEM at N = 6 rats in each groups. ^ap < 0.05, ^bp < 0.01, ^cp < 0.001 when compared with normal control (NC), ^αp < 0.05, ^βp < 0.01, ^γp < 0.001 when compared with experimental control (EC), and ^χp < 0.05, ^ψp < 0.01, ^ζp < 0.001 when compared with Donepezil (DPZ).

The observation of ICP showed that concentration of Al³⁺ ion in hippocampus were 2.12 ± 0.83, 31.29 ± 1.88, 31.22 ± 1.78, 10.03 ± 0.56, 21.14 ± 0.62, 7.11 ± 0.56, and 5.72 ± 0.61 in groups I, II, III, IV, V, VI, and VII respectively shown in Figure 37.

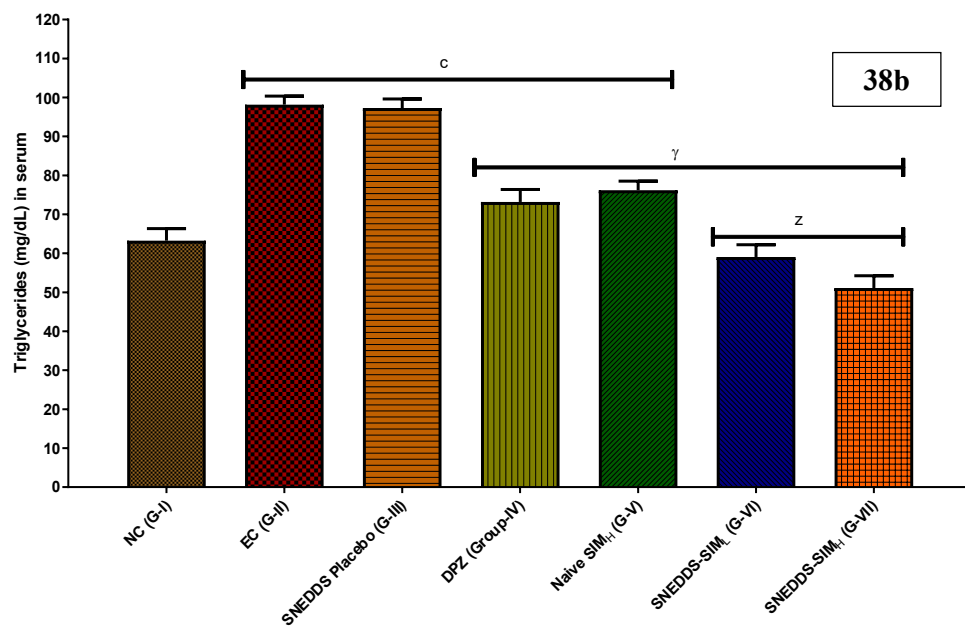
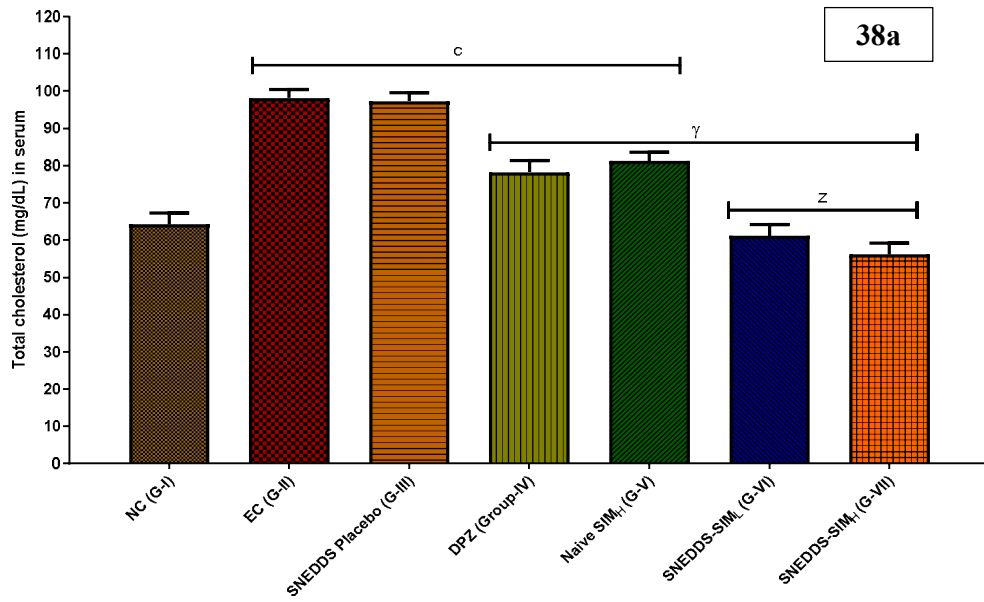
5.21 Biochemical parameters

5.21.1 Reversal of AlCl₃-Induced Lipid Profile by SIM

In our investigation, it was observed that AlCl₃ significantly produced (*P* < 0.05) upswing in total cholesterol (TC), triglycerides (TG), and low-density lipoprotein (LDL) levels and significantly decreased serum high-density lipoprotein (HDL) levels compared with G-I. Here, the level of TC was reduced to 78.19±3.18, 81.22±2.32, 61.08± 3.12, 56.13±3.13 mg/dL by the G-IV, G-V, G-VI, and G-VII respectively (Figure 38a).

Elevated TC and AD are interrelated with each other (177) and was found to be correlated the cognitive impairment. This dyslipidemia may be due to accumulation of aluminium in liver (178). It is also very interesting that cholesterol is important for protein trafficking (179) and Aβ is an apical targeted peptides in cholesterol depleted MDCK cells (180). Hence, Sim regulated the level of Aβ level and after a potential

mechanism for the treatment of AD even in long term condition. Earlier evidences suggest that lipid lowering drug reduces intracellular and secretory neuronal A β 42 & A β 40 level. So, SIM is capable of reducing A β (during normal cellular processing of amyloid precursor protein, APP level).



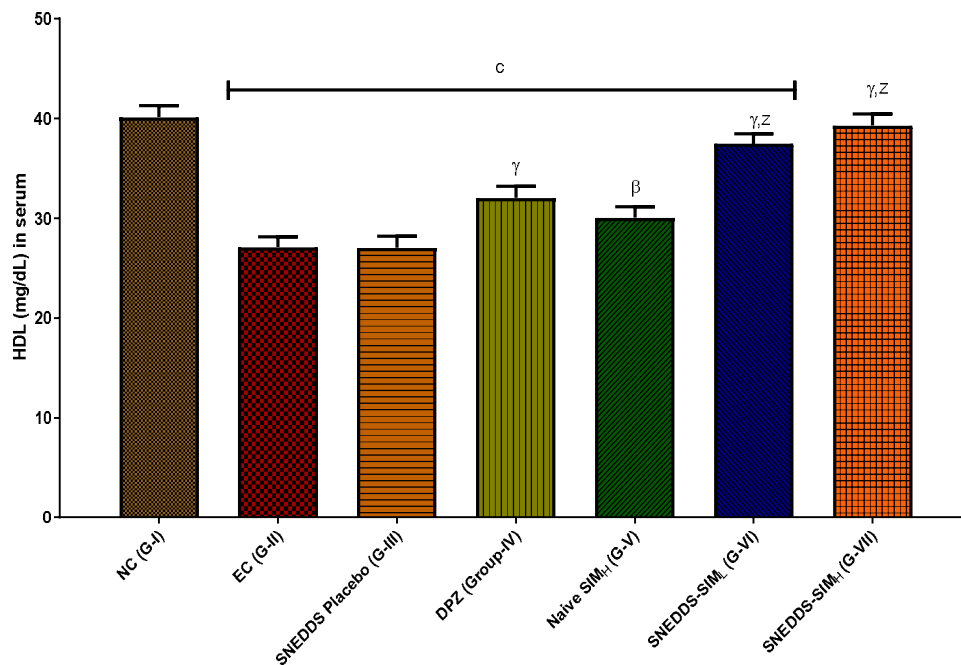
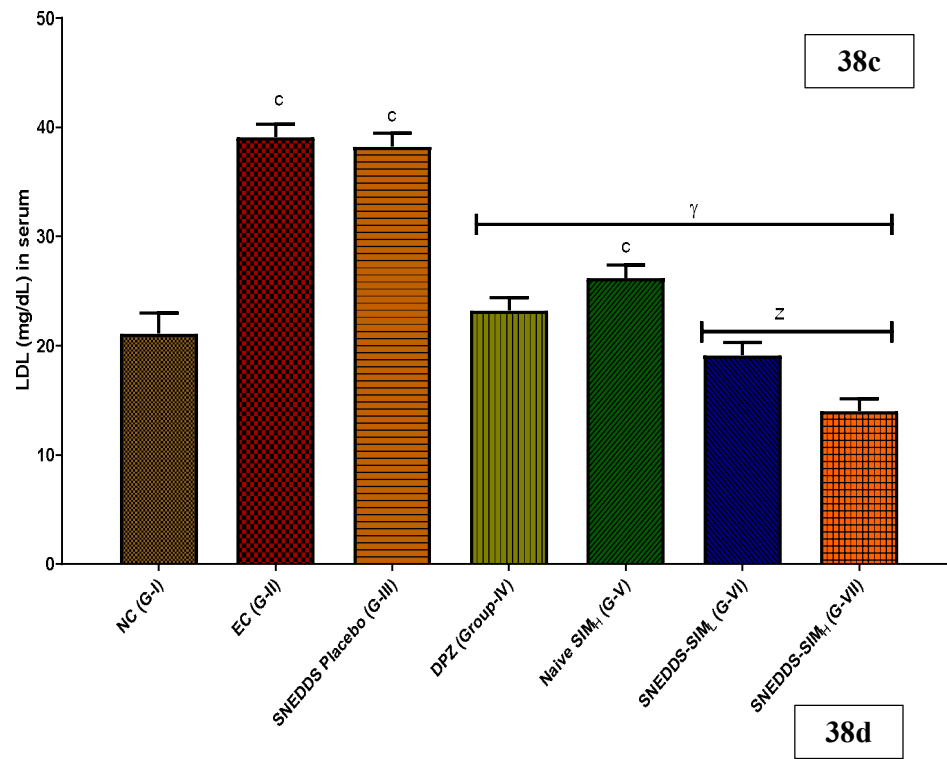


Figure 38: Lipid profile: (38a). TC in serum, (38b). TG in serum, (38c). LDL in serum, (38d). HDL in serum, All data are represented as Mean \pm SEM at N = 6 rats in each groups. ^ap < 0.05, ^bp < 0.01, ^cp < 0.001 when compared with normal control (NC), ^αp < 0.05, ^βp < 0.01, ^γp < 0.001 when compared with experimental control (EC), and ^xp < 0.05, ^yp < 0.01, ^zp < 0.001 when compared with Donepezil (DPZ).

On the other hand, amelioration in the level of TG was also obtained as to 73.19±3.18, 76.22±2.32, 59.08±3.12, and 51.13±3.13 mg/dL by the G-IV, G-V, G-VI, and G-VII respectively (Figure 38b). The impact of treatment was also noted in the abolishment of LDL where G-IV, G-V, G-VI, and G-VII produced, 23.22±1.16, 26.17±1.22, 19.12±1.18, and 14.03±1.14 mg/dL respectively (Figure 38c). The level of HDL was reduced to 32.02±1.16, 30.03±1.13, 37.46±1.04, and 39.29±1.17 mg/dL by the G-IV, G-V, G-VI, and G-VII respectively (Figure 38d). Consequently, the SIM-treated group (G-VI and VII), but not other treatment groups, reversed the increased lipid profiles induced by AlCl₃ in rats.

5.22 Oxidative Biomarkers

5.22.1 Antioxidant parameters in brain

5.22.1.1. Level of catalase (CAT) in brain

The level of CAT in brain homogenate was 3.16±0.05, 1.70±0.02, 1.70±0.03, 2.32±0.02, 2.04±0.04, 2.54±0.02, and 2.96 ± 0.02, μ/g of protein in groups I, II, III, IV, V, VI, and VII respectively (Figure 39). AlCl₃ induced neurotoxicity causes decline in the level of CAT activity in the brain which was further improve with the treatment of SIM-SNEDDS.

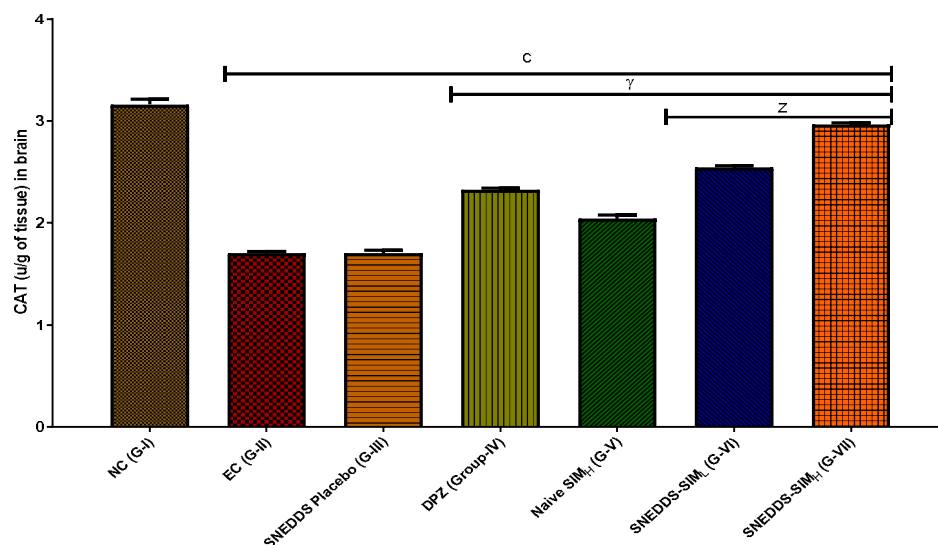


Figure 39: CAT level in brain All data are represented as Mean ± SEM at N = 6 rats in each groups. ^ap < 0.05, ^bp < 0.01, ^cp < 0.001 when compared with normal control (NC), ^αp < 0.05, ^βp < 0.01, ^γp < 0.001 when compared with experimental control (EC), and ^xp < 0.05, ^yp < 0.01, ^zp < 0.001 when compared with Donepezil (DPZ).

5.21.1.2 GSH level in brain

The concentrations of GSH in brain homogenate was noted as 0.82 ± 0.02 , 0.18 ± 0.03 , 0.17 ± 0.01 , 0.53 ± 0.04 , 0.38 ± 0.03 , 0.61 ± 0.02 , and 0.72 ± 0.03 , nmol/g of tissue in groups I, II, III, IV, V, VI, and VII respectively (Figure 40). In case of AD the level of GSH was found very less but significant impairment was recorded in group of rats received both the doses of SIM-SNEDDS (G-VI & VII), DPZ (G-IV) and naïve SIM (G-V).

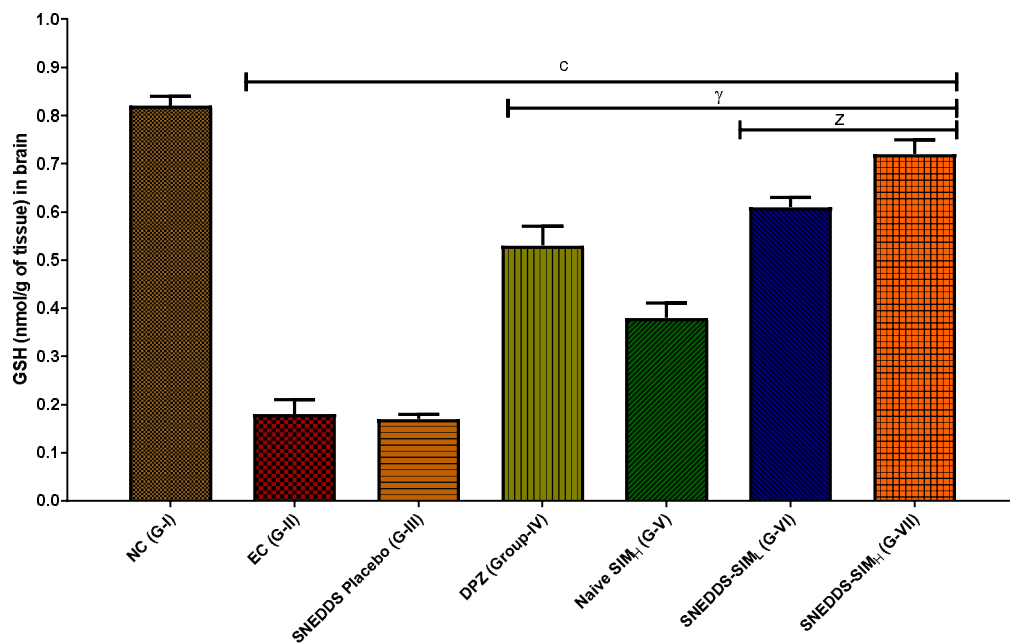


Figure 40: GSH level in brain, All data are represented as Mean \pm SEM at N = 6 rats in each groups. ^ap < 0.05, ^bp < 0.01, ^cp < 0.001 when compared with normal control (NC), ^αp < 0.05, ^βp < 0.01, ^γp < 0.001 when compared with experimental control (EC), and ^xp < 0.05, ^yp < 0.01, ^zp < 0.001 when compared with Donepezil (DPZ).

5.21.1.3 MDA level in brain

The level of MDA in brain homogenate was 0.623 ± 0.24 , 3.04 ± 0.22 , 3.02 ± 0.24 , 1.48 ± 0.26 , 2.88 ± 0.28 , 1.43 ± 0.24 , and 1.19 ± 0.22 , nmol/g of tissue in groups I, II, III, IV, V, VI, and VII respectively (Figure 41). Such significant increase in the level of MDA in brain indicates the failure of antioxidant activity brain but significant alteration was recorded in groups VII, VI, VI as well as V. Since the delivery of the SIM-

SNEDDS was fast and improved with respect to naïve form so that SIM-SNEDDS provided better and significant protection.

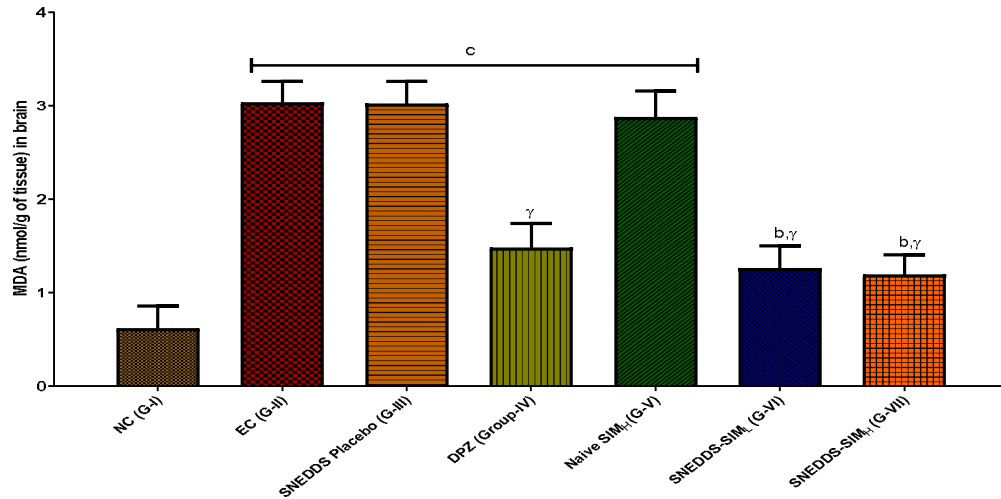


Figure 41: MDA level in brain, All data are represented as Mean ± SEM at N = 6 rats in each groups. ^ap < 0.05, ^bp < 0.01, ^cp < 0.001 when compared with normal control (NC), ^αp < 0.05, ^βp < 0.01, ^γp < 0.001 when compared with experimental control (EC), and ^xp < 0.05, ^yp < 0.01, ^zp < 0.001 when compared with Donepezil (DPZ).

5.21.1.4. SOD level in brain

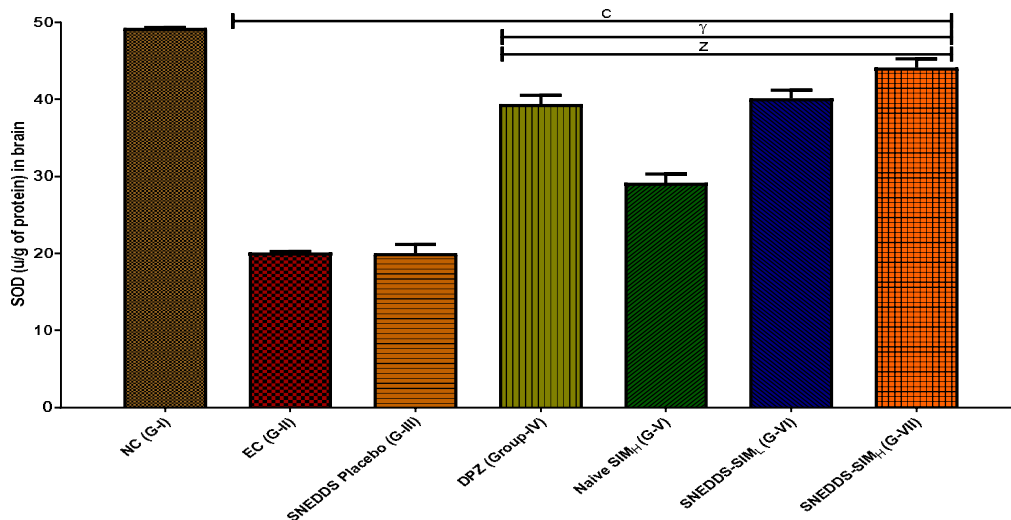


Figure 42: SOD level in brain, All data are represented as Mean ± SEM at N = 6 rats in each groups. ^ap < 0.05, ^bp < 0.01, ^cp < 0.001 when compared with normal control (NC), ^αp < 0.05, ^βp < 0.01, ^γp < 0.001 when compared with experimental control (EC), and ^xp < 0.05, ^yp < 0.01, ^zp < 0.001 when compared with Donepezil (DPZ).

The level of SOD in brain homogenate was 49.23 ± 0.13 , 20.12 ± 0.15 , 20.03 ± 1.13 , 39.34 ± 1.18 , 29.13 ± 1.19 , 40.08 ± 1.12 , and 44.13 ± 1.13 μg of protein in groups I, II, III, IV, V, VI, and VII respectively (Figure 42).

Significant alteration of SOD level was recorded in treatment groups specially SNEDDS treatment group of rats. The administration AlCl_3 reduced the levels of endogenous antioxidative enzymes including SOD, CAT, and GSH in the brain. With the increased level of MDA in brain. SIM-SNEDDS therapy restored the antioxidative system's changes, including SOD, CAT, GSH, and MDA levels. These protective values may be attributed to its antioxidant property.

5.22 Antioxidant parameters in serum

5.22.1 GSH level in serum

GSH concentrations in serum were 0.73 ± 0.06 , 0.29 ± 0.03 , 0.29 ± 0.02 , 0.53 ± 0.04 , 0.39 ± 0.03 , 0.62 ± 0.02 , and 0.66 ± 0.03 nmol/g of tissue in groups I, II, III, IV, V, VI, and VII respectively (Figure 43).

Currently Al^{3+} has been reported to induce oxidative stress leading to develop AD and its markers in rats which was observed as altered antioxidant parameter in brain and serum (181). AlCl_3 induced oxidative stress generates apoptosis in PC12 cells (182).

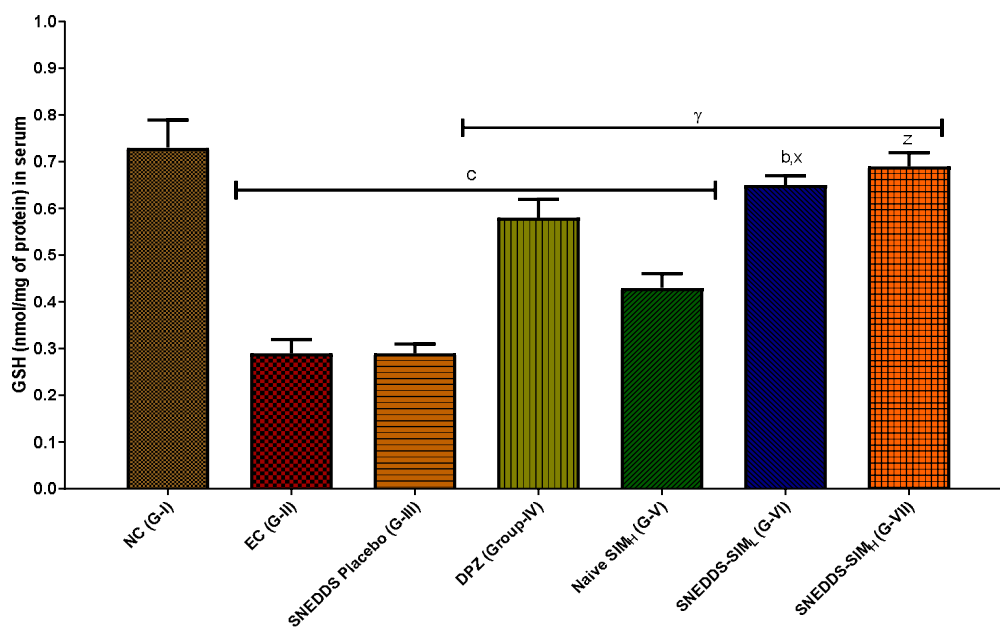


Figure 43: GSH level in serum, All data are represented as Mean \pm SEM at N = 6 rats in each groups. ^ap < 0.05, ^bp < 0.01, ^cp < 0.001 when compared with normal control (NC), ^{α} p < 0.05, ^{β} p < 0.01, ^{γ} p < 0.001 when compared with experimental control (EC), and ^xp < 0.05, ^yp < 0.01, ^zp < 0.001 when compared with Donepezil (DPZ).

In this context in neurons alteration in antioxidant enzymes which in turn produces elevation reaches oxygen species (ROS) (183). Brain cells are known to contain increased percentage of long chain polyunsaturated fatty acids which are subjected to lipid peroxidation and leading to accumulation of ROS (184). this oxidative stress and ROS generation was significantly attenuated by SIM-SNEDDS due to its antioxidant nature.

5.22.2 MDA level in serum

In groups, I, II, III, IV, V, VI, and VII the levels of MDA in serum homogenate were 0.64 \pm 0.24, 1.56 \pm 0.22, 1.54 \pm 0.24, 0.93 \pm 0.26, 1.12 \pm 0.28, 0.88 \pm 0.24, and 0.78 \pm 0.22 nmol/g of tissue, respectively (Figure 44).

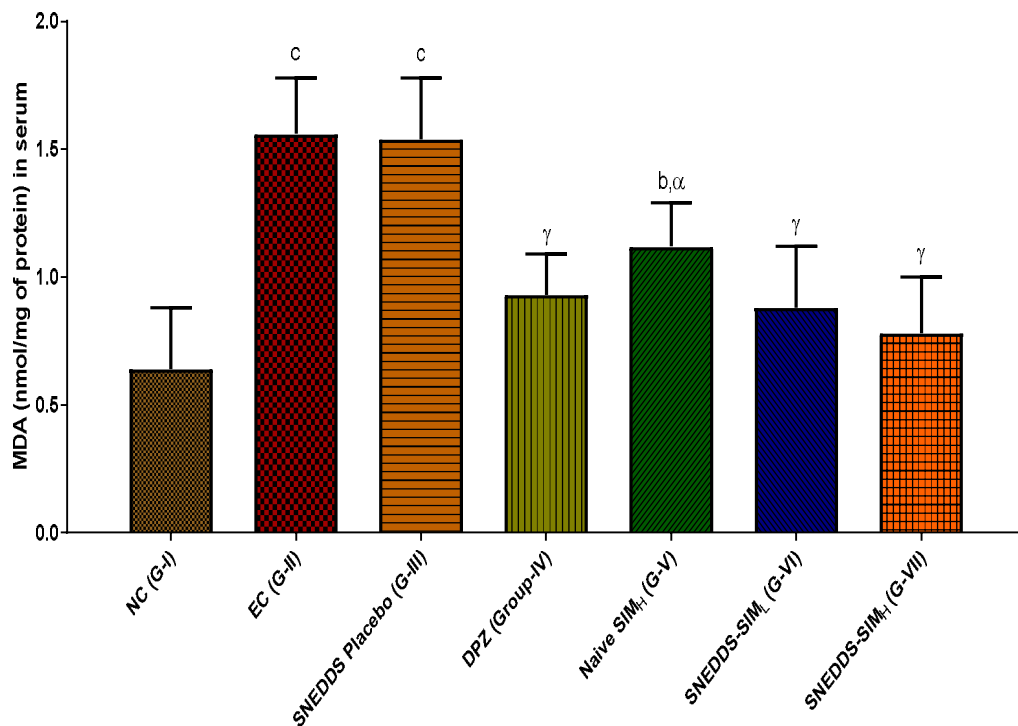


Figure 44: MDA level in serum, All data are represented as Mean \pm SEM at N = 6 rats in each groups. ^ap < 0.05, ^bp < 0.01, ^cp < 0.001 when compared with normal control (NC), ^{α} p < 0.05, ^{β} p < 0.01, ^{γ} p < 0.001 when compared with experimental control (EC), and ^xp < 0.05, ^yp < 0.01, ^zp < 0.001 when compared with Donepezil (DPZ).

5.22.3 CAT level in serum

In groups I, II, III, IV, V, VI, and VII the levels of CAT in serum homogenate were 2.58 ± 0.03 , 1.63 ± 0.03 , 1.64 ± 0.02 , 2.38 ± 0.04 , 2.04 ± 0.04 , 2.54 ± 0.02 , and 2.77 ± 0.03 μg of protein, respectively (Figure 45).

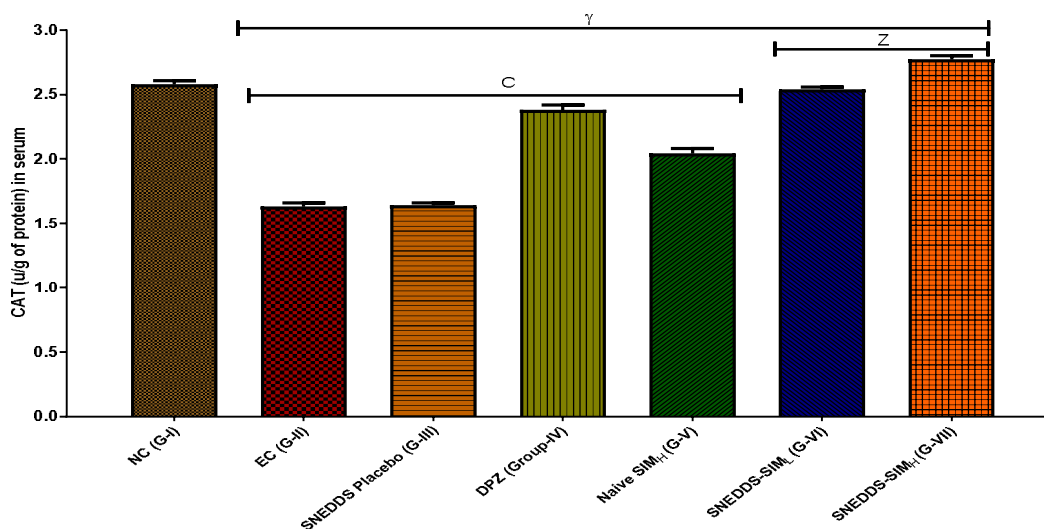


Figure 45: CAT level in serum, All data are represented as Mean \pm SEM at N = 6 rats in each groups. ^ap < 0.05, ^bp < 0.01, ^cp < 0.001 when compared with normal control (NC), ^{α} p < 0.05, ^{β} p < 0.01, ^{γ} p < 0.001 when compared with experimental control (EC), and ^{x} p < 0.05, ^{y} p < 0.01, ^{z} p < 0.001 when compared with Donepezil (DPZ).

5.23 Inflammatory Biomarkers

5.23.1 TNF- α

The level of TNF- α was investigated in the brain of rats received AlCl_3 for the induction of AD. TNF- α was found 3.03-fold excessively high in a group of rats that received AlCl_3 (i.e., G-II) only whereas the reduction of TNF- α was recorded in G-IV, V, VI, & VII i.e., 41.29 ± 0.27 , 48.12 ± 0.21 , 37.19 ± 0.23 & 29.23 ± 0.19 g/mL (Figure 46). The level of TNF- α was found less in SIM-SNEDDS treated group of rats as well as DPZ treated group rats in significant manner.

TNF- α is pathogenic factor, was found elevated due to accumulation of Al^{3+} in the brain. Excess TNF- α in the brain induces microglia to release more glutamate, which leads to neurotoxic effects. SIM-SNEDDS therapy reduced neurotoxicity, and ultimately reversing AD.

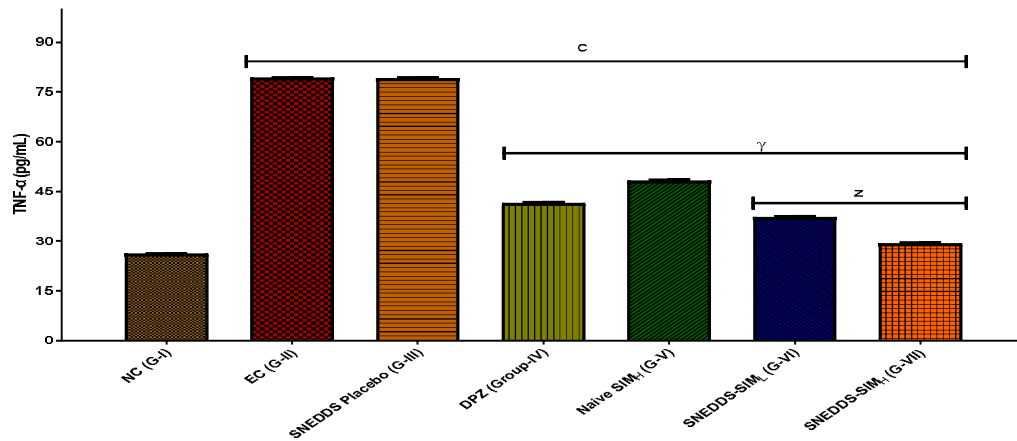


Figure 46: TNF- α level in brain, All data are represented as Mean \pm SEM at N = 6 rats in each groups. ^ap < 0.05, ^bp < 0.01, ^cp < 0.001 when compared with normal control (NC), α^a p < 0.05, β^b p < 0.01, γ^c p < 0.001 when compared with experimental control (EC), and ^xp < 0.05, ^yp < 0.01, ^zp < 0.001 when compared with Donepezil (DPZ).

5.23.2 IL-1 β

The increased concentration of IL-1 β was observed due to the administration of AlCl₃ in rats responsible to cause AD. The significant alteration of IL-1 β was observed as 41.11 \pm 0.68, 47.18 \pm 0.76, and 38.16 \pm 0.89, & 30.13 \pm 0.76 in G- IV, V, VI & VII (Figure 47).

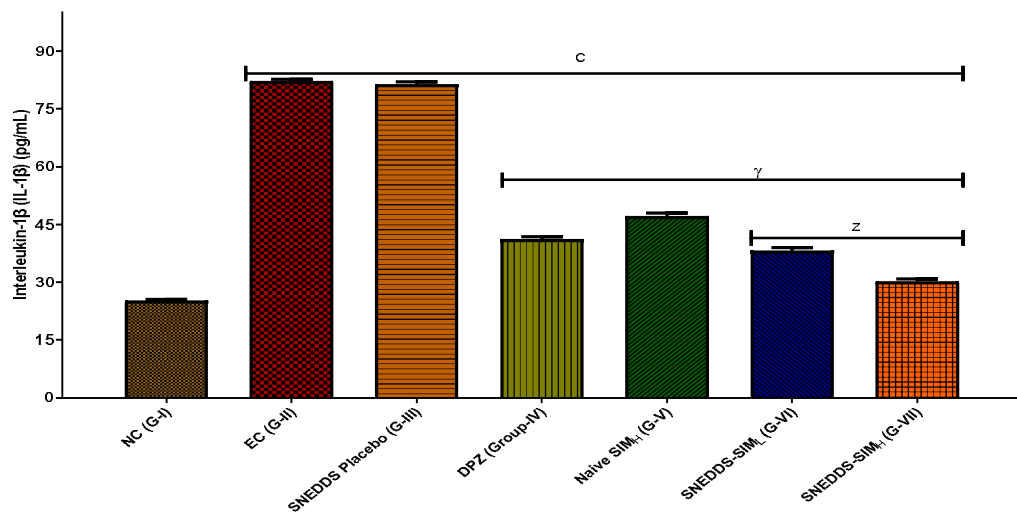


Figure 47: Interleukin- IL-1 β level in brain, All data are represented as Mean \pm SEM at N = 6 rats in each groups. ^ap < 0.05, ^bp < 0.01, ^cp < 0.001 when compared with normal control (NC), α^a p < 0.05, β^b p < 0.01, γ^c p < 0.001 when compared with experimental control (EC), and ^xp < 0.05, ^yp < 0.01, ^zp < 0.001 when compared with Donepezil (DPZ).

Similar to TNF- α of both the dose SIM-SNEDDS attenuated the increasing level of *IL-1 β* . Since SIM is antioxidant and anti-inflammatory in native hence, it reduces inflammatory cascade.

5.24 Exposure of treatment to brain and plasma

The important step of this study was to find the estimation of bioavailability of developed formulation of SNEDDS in the plasma as well as brain (Figure 48 and 49).

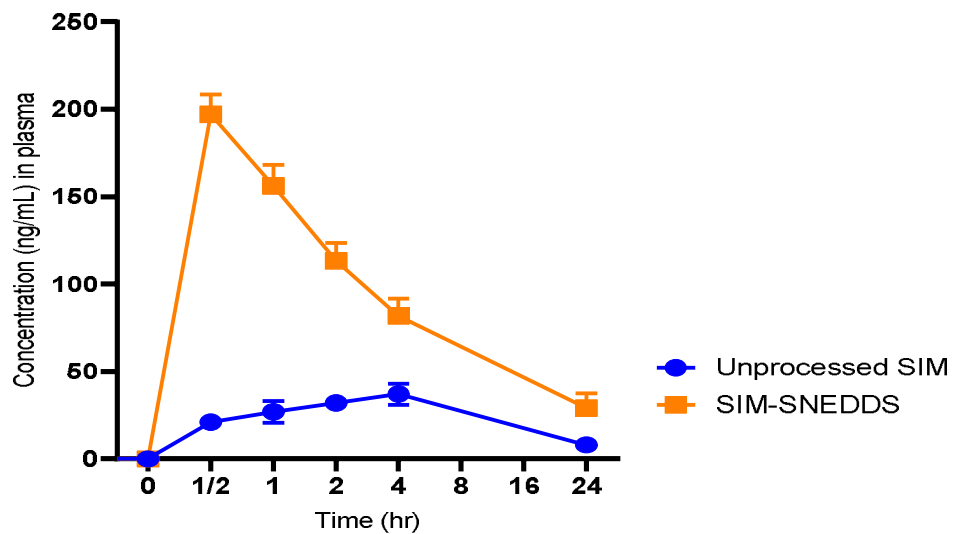


Figure 48: Bioavailability of SIM in plasma

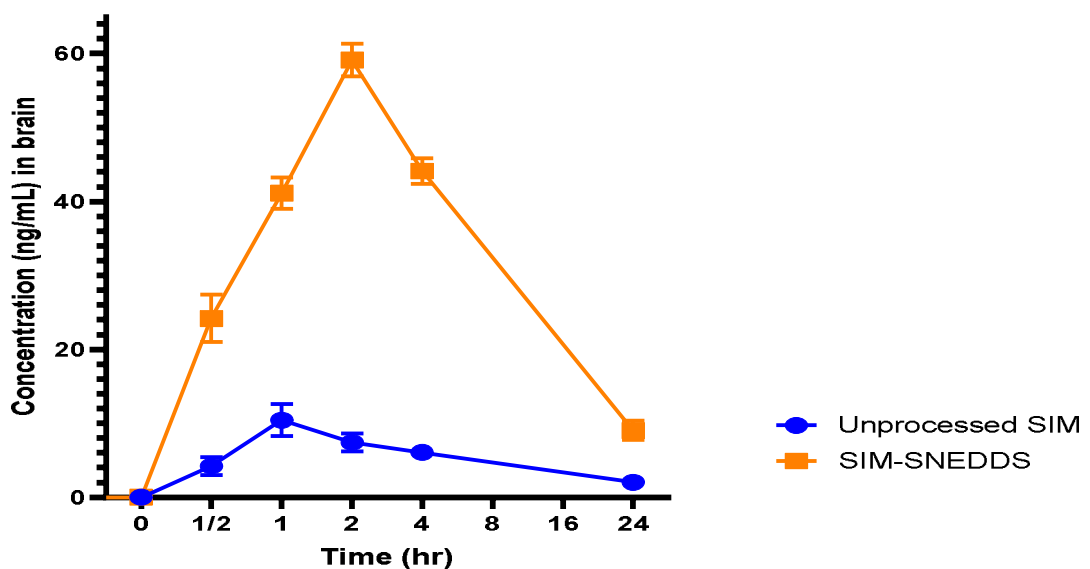


Figure 49: Bioavailability of SIM in Brain

The outcomes are shown in the table and figure. The results showed that the Tmax of unprocessed SIM was found to be 4 hrs and 1 hr in plasma and brain respectively, whereas it was 30 min and 2 hrs in the case of SIM-SNEDDS in plasma and brain respectively. It indicates the delay in the absorption of unprocessed SIM from the stomach to the systemic circulation due to its poor aqueous solubility.

The Cmax for unprocessed SIM was found to be in plasma 37.09 ng/mL and in brain 10.43 ng/mL and for SIM-SNEDDS it was 197.18 ng/mL and 59.11 ng/mL, in plasma and brain respectively, which was about 5.31 and 5.66 folds in plasma and brain respectively shown in Table 30.

The AUC_{0-t} is in plasma 486.26 ng/mL*h and in the brain 97.83486.26 ng/mL*h for unprocessed SIM and in plasma 1424.66 ng/mL*h and in brain 610.56 ng/mL*h for SIM-SNEDDS. As a result, higher Cmax and AUC for SIM-SNEDDS comparison to unprocessed SIM are evidence of improved systemic drug absorption, which increases oral bioavailability.

Table 30: Pharmacokinetic parameters of unprocessed SIM and SIM-SNEDDS

Parameters	Unit	Plasma		Brain	
		Unprocessed SIM	SIM-SNEDDS	Unprocessed SIM	SIM-SNEDDS
Tmax	H	4	0.5	1	2
Cmax	ng/mL	37.09	197.18	10.43	59.11
AUC _{0-t}	ng/mL*h	486.26	1424.66	97.83	610.56

Oral administration of SNEDDS SIM showed increased impact on the parameter of the present data also suggest that the developed SNEDDS protects the drug to degrade and increase concentration in plasma and brain. The values obtained for SIM-SNEDDS in AUC_{0-t} measurement attests its higher bioavailability with respect to conventional dosage form. These finding corroborates to previous formulation development of SNEDDS.

5.25 Histopathological study

In the line of all the observations, the group of rats received only the AlCl_3 revealed the higher extent of damage in the brain while in the control group of rats normal architecture of the neurons were recorded, Here in control group of rats the neurons are properly arranged and light-stained. AlCl_3 produces NFTs, and plaques which is clearly visible in the figure. AlCl_3 produces extensive vacuolation, necrosis in cortex, pyknosis of nuclei and degeneration in hippocampus. Administration of doses standard drugs, naïve SIM, SIM-SNEDDS (low dose), and SIM-SNEDDS (high dose) attenuated these features of neuropathological changes. Maximum protection was observed in followed by SIM-SNEDDS (low doses), SIM-SNEDDS (high dose). Hence, developed formulation clearly showed in protection against AlCl_3 induced development of AD.

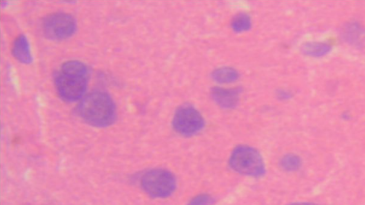
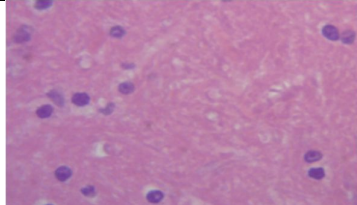
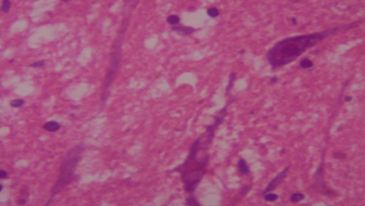
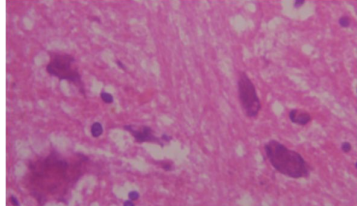
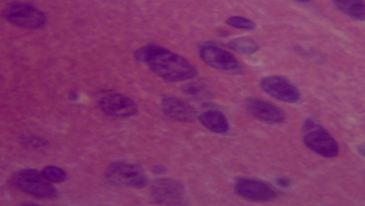
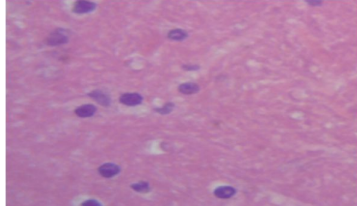
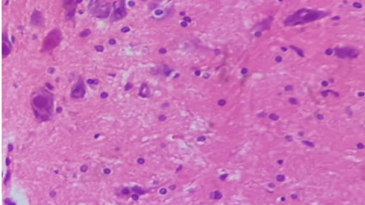
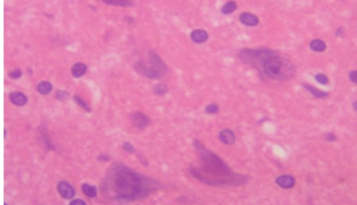
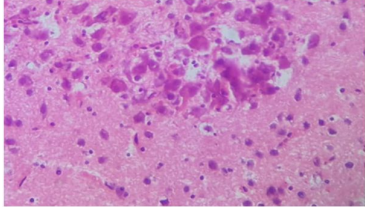
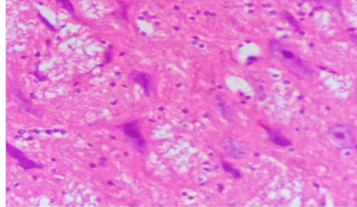
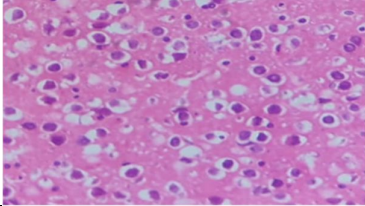
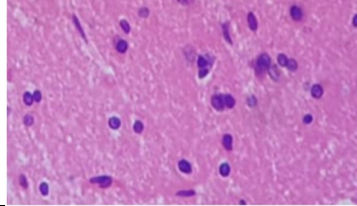
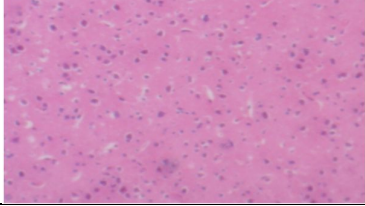
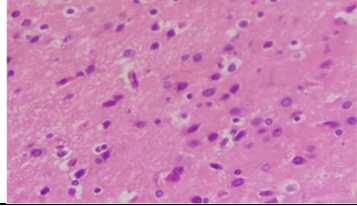
Groups	Cerebral Cortex	Hippocampus
Normal Control		
Disease Control		
SNEDDS Placebo		
Standard Control (Donepezil) (Marketed)		
Naïve SIM		
SIM-SNEDDS (Low dose)		
SIM-SNEDDS (High dose)		

Figure 50: Histopathology images for all groups

SUMMARY

Alzheimer's disease is a most challenging neurological disorder and its treatment is failure one of the critical examples of failure of medical, pharmaceutical and health care sector. In present situation, around 55 million people are suffering, from dementia which make AD as a 7th leading reason for death (3). It is very important to note that neurological disease is 6.3% of global burden of diseases and people with this disease die before the age of 80 which indicates that death rate in AD is 30%.

Drug repositioning, also referred as old drug for new purposes, is an efficient, low-cost, and risk-free method for finding new indications for existing drugs. Conventional drug research processes normally consist five stages: preclinical discovery, safety approval, clinical trials, FDA review, and FDA post-market supervision. Many drugs have been repurposed, including Raloxifene (from breast and prostate cancer to osteoporosis), Paclitaxel (from cancer to re-stenosis), Zidovudine (from cancer to HIV/AIDS), Topiramate (from epilepsy to obesity), Minoxidil (from hypertension to hair loss), and Ropinirole (from hypertension to Parkinson disease), to name a few (15), to name a few.

SIM is also used as an example which can be repurposed for AD (hyperlipidemia to AD) of drug(16). SIM is used to prevent hypercholesterolemia. It is a reversible lactone prodrug that undergoes metabolism for lowering the level of lipid. It inhibits hydroxy-methyl-glutaryl coenzyme A (HMG CoA) reductase, which helps to convert HMG-CoA to mevalonate. Thereby it reduces low-density lipoprotein (LDL) cholesterol in plasma and causes depletion in the accumulation of intracellular cholesterol. In addition, it also increases LDL receptor expression and helps in the treatment of hypercholesterolemia (17).

Although SIM's numerous pharmacological advantages, formulation development is challenging due to pharmaceutical problems such as poor water solubility, poor absorption, and fast metabolism. As a result, its bioavailability is poor. Several scientists have created formulations of SIM that enhanced bioavailability, such as polymeric nanoparticles, liposomes, and nano-emulsions (20). When SNEDDS is administered orally, it simulates the process by producing a nano/microemulsion in the stomach fluid with the support of gastrointestinal motility (21). The greater surface area

of the nano particles improves in the early absorption of the drug molecule. SNEDDS has found that fisetin, curcumin, glimepiride, polypeptide-K, andrographolide, flurbiprofen, and tetrandrine each have enhanced oral bioavailability (22). SNEDDS provide benefits by increasing drug solubilization. It also benefits in bypassing hepatic first-pass metabolism and enhancing drug permeability across gastrointestinal tracts. SNEDDS have initially demonstrated that they enhance the oral bioavailability of lipid soluble and gastrointestinal labile drugs such as curcumin, duloxetine, glimepiride, and Polypeptide-k (23). SIM is a lipid soluble and GI labile drug, hence it undergoes considerable first-pass metabolism and enzymatic degradation in the GIT following oral administration, and the residual non-degraded substance is insoluble in the GIT media. As a result, total oral bioavailability and therapeutic effectiveness are improved. The potential of SNEDDS to both enhance drug solubility and protect the GIT against toxicity is well established.

SIM-SNEDDS were designed following a quality by design method in the current research. The optimized SIM-SNEDDS formulation was composed of CMCM, T-80, and TP along with SIM. Drug loading, size of droplet, and zeta potential of the optimized SIM-SNEDDS were found to be 88%, 57.46 nm, 0.2, and -13.6 mv respectively. The SIM-SNEDDS was used to conduct other pharmacokinetic and pharmacodynamic studies. It was observed that SIM-SNEDDS show enhanced oral bioavailability than naive SIM and standard drug.

the T_{max} of unprocessed SIM was found to be 4 hrs and 1 hr in plasma and brain respectively, whereas it was 30 min and 2 hrs in the case of SIM-SNEDDS in plasma and brain respectively. The C_{max} for unprocessed SIM was found to be in plasma 37.09 ng/mL and in brain 10.43 ng/mL and for SIM-SNEDDS it was 197.18 ng/mL and 59.11 ng/mL, in plasma and brain respectively, which was about 5.31 and 5.66 folds in plasma and brain respectively. The AUC_{0-t} is in plasma 486.26 ng/mL*h and in the brain 97.83486.26 ng/mL*h for unprocessed SIM and in plasma 1424.66 ng/mL*h and in brain 610.56 ng/mL*h for SIM-SNEDDS. A pharmacodynamics study was performed using groups depending on their treatment. Aluminum chloride (AlCl₃) was administered at a dose of 100 mg/kg to induce AD. Donepezil (1 mg/kg) was used as standard drug treatment. Naïve SIM and SIM-SNEDDS were administered at two dose

levels i.e. low 1.974 mg and high 3.948 mg doses. Combination treatment was given with naïve SIM dose along with standard drugs and SIM-SNEDDS dose along with standard drugs. It was observed that with the administration of AlCl_3 body weight get reduced. Naïve SIM and SIM-SNEDDS were able to reverse the loss in body weight. Behavioral analysis revealed that AlCl_3 significantly ($p < 0.001$) reduces the open field, Morris's water maze, and novel object recognition movement. It was observed that these all effects of AlCl_3 were ameliorated with the administration of standard drug, naïve SIM and SIM-SNEDDS. SIM-SNEDDS provide better results when compared to the naïve SIM. The results of the combination treatment groups of naïve SIM dose along with standard drugs and SIM-SNEDDS dose along with standard drugs represent the synergistic effect when compared to the individual treatment groups. The results of biochemical estimation represent that with the administration of AlCl_3 , there is an elevation in the oxidative stress in the brain regions (hippocampus and cortex). Due to this oxidative stress, the level of AChE, MDA, and IL-1B increased and the activity of antioxidant enzymes like GSH, SOD, and CAT get decreased. The increased level of AChE, MDA, and IL-1B significantly ($p < 0.001$) reduced with the treatment of standard drug, naïve SIM and SIM-SNEDDS. But SIM-SNEDDS showed better results as compared to the standard drug and naïve SIM. Similarly, the decreased activity of GSH, SOD, and CAT get improved more significantly ($p < 0.001$) in the case of SIM-SNEDDS groups when compared to the naïve SIM and standard drug treatment groups. This effect of AlCl_3 gets reversed significantly ($p < 0.001$) when treatment was given with SIM-SNEDDS. The results of histopathological evaluation support the results of behavioral, biochemical, and ELISA. As with the administration of AlCl_3 tissue damage was there which was reversed when treatment was given with standard drug, naïve SIM and SIM-SNEDDS, but a more prominent result was observed in the SIM-SNEDDS group. The outcomes of this research clearly show that the SNEDDS preparation improves SIM oral bioavailability, and that enhanced bioavailability improves SIM therapeutic potential.

CONCLUSION AND FUTURE PERSPECTIVE

Based on the present investigation, the study supports that the formulation of SNEDDS reduces the level of inflammatory mediators decrease the oxidative responses i.e., protection observed by oxidative biomarkers. SIM-SNEDDS could be suitable alternative to prevent progressive damage of AD symptoms in the long-term use. This repurposing provides its use could improve learning, memory damaged caused by oxidative stress in the brain region. It also exemplifies an inhibition of acetylcholinesterase with increased responses of antioxidant enzymes. Consequently, SIM-SNEDDS is suggested to applied for the survival of neurons of regeneration of neurons to decrease hallmarks AD.

The most relevant and notable point in this investigation was SIM-SNEDDS was found better than DPZ which showed that the developed SNEDDS was providing better bioavailability and overcome the pharmaceutical challenges of SIM.

Further explorations with other models and clinical trial are required to better understand the effect of SNEDDS of SIM.

REFERENCES

1. Knopman DS, Amieva H, Petersen RC, Chetelat G, Holtzman DM, Hyman BT, et al. Alzheimer disease. *Nat Rev Dis Primers*. 2021;7(1):33.
2. Nawzat D. Enhanced oral bioavailability through nanotechnology in Saudi Arabia: A meta-analysis. *Arabian Journal of Chemistry*. 2022;15(4):103715.
3. Breijyeh Z, Karaman R. Comprehensive Review on Alzheimer's Disease: Causes and Treatment. *Molecules*. 2020;25(24).
4. Sharma B, Singh N, Singh M. Modulation of celecoxib- and streptozotocin-induced experimental dementia of Alzheimer's disease by pitavastatin and donepezil. *J Psychopharmacol*. 2008;22(2):162-71.
5. DeTure MA, Dickson DW. The neuropathological diagnosis of Alzheimer's disease. *Mol Neurodegener*. 2019;14(1):32.
6. Atri A. 360 Alzheimer's Disease and Alzheimer's Dementia. In: Dickerson B, Atri A, editors. *Dementia: Comprehensive Principles and Practices*: Oxford University Press; 2014. p. 0.
7. Danysz W, Parsons CG. Alzheimer's disease, beta-amyloid, glutamate, NMDA receptors and memantine--searching for the connections. *Br J Pharmacol*. 2012;167(2):324-52.
8. Sardar Sinha M, Ansell-Schultz A, Civitelli L, Hildesjo C, Larsson M, Lannfelt L, et al. Alzheimer's disease pathology propagation by exosomes containing toxic amyloid-beta oligomers. *Acta Neuropathol*. 2018;136(1):41-56.
9. Breijyeh Z, Karaman R. Comprehensive Review on Alzheimer's Disease: Causes and Treatment. *Molecules*. 2020;25(24):5789.
10. Chen XQ, Mobley WC. Alzheimer Disease Pathogenesis: Insights From Molecular and Cellular Biology Studies of Oligomeric Abeta and Tau Species. *Front Neurosci*. 2019;13:659.
11. d'Errico P, Meyer-Luehmann M. Mechanisms of Pathogenic Tau and Abeta Protein Spreading in Alzheimer's Disease. *Front Aging Neurosci*. 2020;12:265.
12. Gao L, Zhang Y, Sterling K, Song W. Brain-derived neurotrophic factor in Alzheimer's disease and its pharmaceutical potential. *Transl Neurodegener*. 2022;11(1):4.

13. Alhazmi HA, Albratty M. An update on the novel and approved drugs for Alzheimer disease. *Saudi Pharmaceutical Journal*. 2022;30(12):1755-64.
14. Esang M, Gupta M. Aducanumab as a Novel Treatment for Alzheimer's Disease: A Decade of Hope, Controversies, and the Future. *Cureus*. 2021;13(8):e17591.
15. Aggarwal S, Verma SS, Aggarwal S, Gupta SC. Drug repurposing for breast cancer therapy: Old weapon for new battle. *Semin Cancer Biol*. 2021;68:8-20.
16. Ballard C, Aarsland D, Cummings J, O'Brien J, Mills R, Molinuevo JL, et al. Drug repositioning and repurposing for Alzheimer disease. *Nat Rev Neurol*. 2020;16(12):661-73.
17. Martin MG, Pfrieger F, Dotti CG. Cholesterol in brain disease: sometimes determinant and frequently implicated. *EMBO Rep*. 2014;15(10):1036-52.
18. Willems S, Marschner JA, Kilu W, Faudone G, Busch R, Duensing-Kropp S, et al. Nurr1 Modulation Mediates Neuroprotective Effects of Statins. *Adv Sci (Weinh)*. 2022;9(18):e2104640.
19. Chen X, Drew J, Berney W, Lei W. Neuroprotective Natural Products for Alzheimer's Disease. *Cells*. 2021;10(6).
20. Das S, Chaudhury A. Recent advances in lipid nanoparticle formulations with solid matrix for oral drug delivery. *AAPS PharmSciTech*. 2011;12(1):62-76.
21. Nasr A, Gardouh A, Ghorab M. Novel Solid Self-Nanoemulsifying Drug Delivery System (S-SNEDDS) for Oral Delivery of Olmesartan Medoxomil: Design, Formulation, Pharmacokinetic and Bioavailability Evaluation. *Pharmaceutics*. 2016;8(3).
22. Kumar R, Khursheed R, Kumar R, Awasthi A, Sharma N, Khurana S, et al. Self-nanoemulsifying drug delivery system of fisetin: Formulation, optimization, characterization and cytotoxicity assessment. *Journal of Drug Delivery Science and Technology*. 2019;54.
23. Kumar B, Singh SK, Prakash T, Bhatia A, Gulati M, Garg V, et al. Pharmacokinetic and pharmacodynamic evaluation of Solid self-nanoemulsifying delivery system (SSNEDDS) loaded with curcumin and duloxetine in attenuation of neuropathic pain in rats. *Neurol Sci*. 2021;42(5):1785-97.
24. Kumar A, Singh A, Ekavali. A review on Alzheimer's disease pathophysiology and its management: an update. *Pharmacol Rep*. 2015;67(2):195-203.

25. Arranz AM, De Strooper B. The role of astroglia in Alzheimer's disease: pathophysiology and clinical implications. *Lancet Neurol.* 2019;18(4):406-14.
26. Tahami Monfared AA, Byrnes MJ, White LA, Zhang Q. Alzheimer's Disease: Epidemiology and Clinical Progression. *Neurol Ther.* 2022;11(2):553-69.
27. 2020 Alzheimer's disease facts and figures. *Alzheimers Dement.* 2020.
28. Livingston G, Huntley J, Sommerlad A, Ames D, Ballard C, Banerjee S, et al. Dementia prevention, intervention, and care: 2020 report of the Lancet Commission. *Lancet.* 2020;396(10248):413-46.
29. Qiu C, Kivipelto M, von Strauss E. Epidemiology of Alzheimer's disease: occurrence, determinants, and strategies toward intervention. *Dialogues Clin Neurosci.* 2009;11(2):111-28.
30. O'Brien JT, Chouliaras L, Sultana J, Taylor J-P, Ballard C, Aarsland D, et al. RENEWAL: REpurposing study to find NEW compounds with Activity for Lewy body dementia—an international Delphi consensus. *Alzheimer's Research & Therapy.* 2022;14(1):169.
31. Kirtonia A, Gala K, Fernandes SG, Pandya G, Pandey AK, Sethi G, et al. Repurposing of drugs: An attractive pharmacological strategy for cancer therapeutics. *Semin Cancer Biol.* 2021;68:258-78.
32. Desai RJ, Varma VR, Gerhard T, Segal J, Mahesri M, Chin K, et al. Targeting abnormal metabolism in Alzheimer's disease: The Drug Repurposing for Effective Alzheimer's Medicines (DREAM) study. *Alzheimers Dement (N Y).* 2020;6(1):e12095.
33. Cross DJ, Huber BR, Silverman MA, Cline MM, Gill TB, Cross CG, et al. Intranasal Paclitaxel Alters Alzheimer's Disease Phenotypic Features in 3xTg-AD Mice. *Journal of Alzheimer's Disease.* 2021;83:379-94.
34. Aicardi G. New Hope from an Old Drug: Fighting Alzheimer's Disease with the Cancer Drug Bexarotene (Targretin)? *Rejuvenation Research.* 2013;16(6):524-8.
35. Anekonda TS, Quinn JF. Calcium channel blocking as a therapeutic strategy for Alzheimer's disease: The case for isradipine. *Biochimica et Biophysica Acta (BBA) - Molecular Basis of Disease.* 2011;1812(12):1584-90.

36. McClean PL, Parthasarathy V, Faivre E, Holscher C. The diabetes drug liraglutide prevents degenerative processes in a mouse model of Alzheimer's disease. *J Neurosci*. 2011;31(17):6587-94.
37. Yamada K, Cirrito JR, Stewart FR, Jiang H, Finn MB, Holmes BB, et al. In vivo microdialysis reveals age-dependent decrease of brain interstitial fluid tau levels in P301S human tau transgenic mice. *J Neurosci*. 2011;31(37):13110-7.
38. Chadwick W, Mitchell N, Carroll J, Zhou Y, Park S-S, Wang L, et al. Amitriptyline-mediated cognitive enhancement in aged 3× Tg Alzheimer's disease mice is associated with neurogenesis and neurotrophic activity. *PloS one*. 2011;6(6):e21660.
39. Liu M, Su X, Li G, Zhao G, Zhao L. Validated UPLC-MS/MS method for simultaneous determination of simvastatin, simvastatin hydroxy acid and berberine in rat plasma: Application to the drug-drug pharmacokinetic interaction study of simvastatin combined with berberine after oral administration in rats. *J Chromatogr B Analyt Technol Biomed Life Sci*. 2015;1006:8-15.
40. Ma L, Ohyagi Y, Nakamura N, Iinuma KM, Miyoshi K, Himeno E, et al. Activation of glutathione peroxidase and inhibition of p53-related apoptosis by apomorphine. *Journal of Alzheimer's Disease*. 2011;27(1):225-37.
41. Costa R, Speretta E, Crowther DC, Cardoso I. Testing the therapeutic potential of doxycycline in a *Drosophila melanogaster* model of Alzheimer disease. *Journal of Biological Chemistry*. 2011;286(48):41647-55.
42. Bar-Am O, Amit T, Weinreb O, Youdim MB, Mandel S. Propargylamine containing Compounds as modulators of proteolytic cleavage of amyloid protein precursor: involvement of MAPK and PKC activation. *Journal of Alzheimer's Disease*. 2010;21(2):361-71.
43. Lauterbach EC, Victoroff J, Coburn KL, Shillcutt SD, Doonan SM, Mendez MF. Psychopharmacological neuroprotection in neurodegenerative disease: assessing the preclinical data. *The Journal of neuropsychiatry and clinical neurosciences*. 2010;22(1):8-18.
44. Hampel H, Ewers M, Burger K, Annas P, Mortberg A, Bogstedt A, et al. Lithium trial in Alzheimer's disease: a randomized, single-blind, placebo-controlled, multicenter 10-week study. *Journal of Clinical Psychiatry*. 2009;70(6):922.

45. Fillit H, Hess G, Hill J, Bonnet P, Toso C. IV immunoglobulin is associated with a reduced risk of Alzheimer disease and related disorders. *Neurology*. 2009;73(3):180-5.
46. Chen Y, Zhou K, Wang R, Liu Y, Kwak Y-D, Ma T, et al. Antidiabetic drug metformin (GlucophageR) increases biogenesis of Alzheimer's amyloid peptides via up-regulating BACE1 transcription. *Proceedings of the National Academy of Sciences*. 2009;106(10):3907-12.
47. Mousavi M, Hellström-Lindahl E. Nicotinic receptor agonists and antagonists increase sAPP α secretion and decrease A β levels in vitro. *Neurochemistry international*. 2009;54(3-4):237-44.
48. De Felice FG, Vieira MN, Bomfim TR, Decker H, Velasco PT, Lambert MP, et al. Protection of synapses against Alzheimer's-linked toxins: insulin signaling prevents the pathogenic binding of A β oligomers. *Proceedings of the National Academy of Sciences*. 2009;106(6):1971-6.
49. Alvarez AR, Klein A, Castro J, Cancino GI, Amigo J, Mosqueira M, et al. Imatinib therapy blocks cerebellar apoptosis and improves neurological symptoms in a mouse model of Niemann-Pick type C disease. *The FASEB Journal*. 2008;22(10):3617-27.
50. Atamna H, Nguyen A, Schultz C, Boyle K, Newberry J, Kato H, et al. Methylene blue delays cellular senescence and enhances key mitochondrial biochemical pathways. *The FASEB Journal*. 2008;22(3):703-12.
51. Qing H, He G, Ly PT, Fox CJ, Staufenbiel M, Cai F, et al. Valproic acid inhibits A β production, neuritic plaque formation, and behavioral deficits in Alzheimer's disease mouse models. *The Journal of experimental medicine*. 2008;205(12):2781-9.
52. Rosenstock J, Ahmann AJ, Colon G, Scism-Bacon J, Jiang H, Martin S. Advancing insulin therapy in type 2 diabetes previously treated with glargine plus oral agents: prandial premixed (insulin lispro protamine suspension/lispro) versus basal/bolus (glargine/lispro) therapy. *Diabetes care*. 2008;31(1):20-5.
53. Wang J, Ho L, Chen L, Zhao Z, Zhao W, Qian X, et al. Valsartan lowers brain β -amyloid protein levels and improves spatial learning in a mouse model of Alzheimer disease. *The Journal of clinical investigation*. 2007;117(11):3393-402.

54. Choi Y, Kim H-S, Shin KY, Kim E-M, Kim M, Kim H-S, et al. Minocycline attenuates neuronal cell death and improves cognitive impairment in Alzheimer's disease models. *Neuropsychopharmacology*. 2007;32(11):2393-404.
55. Chow TW, Pollock BG, Milgram NW. Potential cognitive enhancing and disease modification effects of SSRIs for Alzheimer's disease. *Neuropsychiatric disease and treatment*. 2007;3(5):627.
56. Youdim MB. The path from anti Parkinson drug selegiline and rasagiline to multifunctional neuroprotective anti Alzheimer drugs ladostigil and m30. *Current Alzheimer Research*. 2006;3(5):541-50.
57. Chan Carusone S, Smieja M, Molloy W, Goldsmith CH, Mahony J, Chernesky M, et al. Lack of association between vascular dementia and Chlamydia pneumoniae infection: a case-control study. *BMC neurology*. 2004;4(1):1-7.
58. Ritchie CW, Bush AI, Mackinnon A, Macfarlane S, Mastwyk M, MacGregor L, et al. Metal-protein attenuation with iodochlorhydroxyquin (clioquinol) targeting A β amyloid deposition and toxicity in Alzheimer disease: a pilot phase 2 clinical trial. *Archives of neurology*. 2003;60(12):1685-91.
59. López Arrieta JM. Role of meta-analysis of clinical trials for Alzheimer's disease. *Drug development research*. 2002;56(3):401-11.
60. Weggen S, Eriksen JL, Das P, Sagi SA, Wang R, Pietrzik CU, et al. A subset of NSAIDs lower amyloidogenic A β 42 independently of cyclooxygenase activity. *Nature*. 2001;414(6860):212-6.
61. Forette F, Seux M-L, Staessen JA, Thijs L, Birkenhäger WH, Babarskiene M-R, et al. Prevention of dementia in randomised double-blind placebo-controlled Systolic Hypertension in Europe (Syst-Eur) trial. *The Lancet*. 1998;352(9137):1347-51.
62. Popović M, Popović N, Jovanova-Nešć K, Bokonjić D, Dobrić S, Kostić VS, et al. Effect of physostigmine and verapamil on active avoidance in an experimental model of Alzheimer's disease. *International journal of neuroscience*. 1997;90(1-2):87-97.
63. Pandey NK, Singh SK, Gulati M, Kumar B, Kapoor B, Ghosh D, et al. Overcoming the dissolution rate, gastrointestinal permeability and oral bioavailability of glimepiride and simvastatin co-delivered in the form of nanosuspension and solid

self-nanoemulsifying drug delivery system: A comparative study. *Journal of Drug Delivery Science and Technology*. 2020;60.

64. Hardeep, Pandey NK, Singh SK, Kumar B, Corrie L, Goutam U, et al. Development and Validation of Reverse-Phase High-Performance Liquid Chromatography Based Bioanalytical Method for Estimation of Simvastatin in Rat's Plasma. *ASSAY and Drug Development Technologies*. 2022.

65. Sathasivam S, Lecky B. Statin induced myopathy. *BMJ*. 2008;337:a2286.

66. Cruz PM, Mo H, McConathy WJ, Sabnis N, Lacko AG. The role of cholesterol metabolism and cholesterol transport in carcinogenesis: a review of scientific findings, relevant to future cancer therapeutics. *Front Pharmacol*. 2013;4:119.

67. Torrandell-Haro G, Branigan GL, Vitali F, Geifman N, Zissimopoulos JM, Brinton RD. Statin therapy and risk of Alzheimer's and age-related neurodegenerative diseases. *Alzheimers Dement (N Y)*. 2020;6(1):e12108.

68. Vigneshwaran E, Alakhali K, Shaik MA. Effect of food and antacid on simvastatin bioavailability on healthy adult volunteers. *Journal of Health Research and Reviews*. 2018;5(1).

69. Zhong G, Long H, Zhou T, Liu Y, Zhao J, Han J, et al. Blood-brain barrier Permeable nanoparticles for Alzheimer's disease treatment by selective mitophagy of microglia. *Biomaterials*. 2022;288:121690.

70. Lv H, Wang Y, Yang X, Ling G, Zhang P. Application of curcumin nanoformulations in Alzheimer's disease: prevention, diagnosis and treatment. *Nutritional Neuroscience*. 2022:1-16.

71. Singh A, Kutscher HL, Bulmahn JC, Mahajan SD, He GS, Prasad PN. Laser ablation for pharmaceutical nanoformulations: Multi-drug nanoencapsulation and theranostics for HIV. *Nanomedicine: Nanotechnology, Biology and Medicine*. 2020;25:102172.

72. Huo X, Zhang Y, Jin X, Li Y, Zhang L. A novel synthesis of selenium nanoparticles encapsulated PLGA nanospheres with curcumin molecules for the inhibition of amyloid β aggregation in Alzheimer's disease. *Journal of Photochemistry and Photobiology B: Biology*. 2019;190:98-102.

73. Wilson B, Samanta MK, Santhi K, Kumar KPS, Paramakrishnan N, Suresh B. Poly (n-butylcyanoacrylate) nanoparticles coated with polysorbate 80 for the targeted

delivery of rivastigmine into the brain to treat Alzheimer's disease. *Brain research*. 2008;1200:159-68.

74. Cui Z, Lockman PR, Atwood CS, Hsu C-H, Gupte A, Allen DD, et al. Novel D-penicillamine carrying nanoparticles for metal chelation therapy in Alzheimer's and other CNS diseases. *European journal of pharmaceutics and biopharmaceutics*. 2005;59(2):263-72.

75. Kulkarni PV, Roney CA, Antich PP, Bonte FJ, Raghu AV, Aminabhavi TM. Quinoline-n-butylcyanoacrylate-based nanoparticles for brain targeting for the diagnosis of Alzheimer's disease. *Wiley Interdisciplinary Reviews: Nanomedicine and Nanobiotechnology*. 2010;2(1):35-47.

76. Wilson B, Samanta MK, Santhi K, Kumar KPS, Paramakrishnan N, Suresh B. Targeted delivery of tacrine into the brain with polysorbate 80-coated poly (n-butylcyanoacrylate) nanoparticles. *European Journal of Pharmaceutics and Biopharmaceutics*. 2008;70(1):75-84.

77. Siegemund T, Paulke B-R, Schmiedel H, Bordag N, Hoffmann A, Harkany T, et al. Thioflavins released from nanoparticles target fibrillar amyloid β in the hippocampus of APP/PS1 transgenic mice. *International journal of developmental neuroscience*. 2006;24(2-3):195-201.

78. Wang Y-J, Thomas P, Zhong J-H, Bi F-F, Kosaraju S, Pollard A, et al. Consumption of grape seed extract prevents amyloid- β deposition and attenuates inflammation in brain of an Alzheimer's disease mouse. *Neurotoxicity research*. 2009;15(1):3-14.

79. Kumar R, Kumar R, Khurana N, Singh SK, Khurana S, Verma S, et al. Enhanced oral bioavailability and neuroprotective effect of fisetin through its SNEDDS against rotenone-induced Parkinson's disease rat model. *Food Chem Toxicol*. 2020;144:111590.

80. Khurshheed R, Singh SK, Wadhwa S, Gulati M, Kapoor B, Jain SK, et al. Development of mushroom polysaccharide and probiotics based solid self-nanoemulsifying drug delivery system loaded with curcumin and quercetin to improve their dissolution rate and permeability: State of the art. *Int J Biol Macromol*. 2021;189:744-57.

81. Jain AK, Thanki K, Jain S. Solidified self-nanoemulsifying formulation for oral delivery of combinatorial therapeutic regimen: part I. Formulation development, statistical optimization, and in vitro characterization. *Pharmaceutical research*. 2014;31(4):923-45.
82. Shao A, Chen G, Jiang N, Li Y, Zhang X, Wen L, et al. Development and evaluation of self-microemulsifying liquid and granule formulations of Brucea javanica oil. *Archives of pharmacal research*. 2013;36(8):993-1003.
83. Inugala S, Eedara BB, Sunkavalli S, Dhurke R, Kandadi P, Jukanti R, et al. Solid self-nanoemulsifying drug delivery system (S-SNEDDS) of darunavir for improved dissolution and oral bioavailability: In vitro and in vivo evaluation. *Eur J Pharm Sci*. 2015;74:1-10.
84. Poorani G, Uppuluri S, Uppuluri KB. Formulation, characterization, in vitro and in vivo evaluation of castor oil based self-nano emulsifying levosulpiride delivery systems. *Journal of Microencapsulation*. 2016;33(6):535-43.
85. Zhang Y, Liu X, Wang Y, Jiang P, Quek S. Antibacterial activity and mechanism of cinnamon essential oil against *Escherichia coli* and *Staphylococcus aureus*. *Food Control*. 2016;59:282-9.
86. Alhassan Y, Kumar N, Bugaje I, Pali H, Kathkar P. Co-solvents transesterification of cotton seed oil into biodiesel: effects of reaction conditions on quality of fatty acids methyl esters. *Energy Conversion and Management*. 2014;84:640-8.
87. Kang H, Moon H-B, Choi K. Toxicological responses following short-term exposure through gavage feeding or water-borne exposure to Dechlorane Plus in zebrafish (*Danio rerio*). *Chemosphere*. 2016;146:226-32.
88. Wang S, Yang R, Yao H, Zhou G, Zhang Y, Yang B, et al. In vivo lymphatic targeting of methylene blue with microemulsion and multiple microemulsion. *Drug Delivery*. 2009;16(7):371-7.
89. Cui S, Zhao C, Chen D, He Z. Self-microemulsifying drug delivery systems (SMEDDS) for improving in vitro dissolution and oral absorption of Pueraria lobata isoflavone. *Drug development and industrial pharmacy*. 2005;31(4-5):349-56.

90. Wang L, Dong J, Chen J, Eastoe J, Li X. Design and optimization of a new self-nanoemulsifying drug delivery system. *Journal of colloid and interface science*. 2009;330(2):443-8.
91. Setthacheewakul S, Mahattanadol S, Phadoongsombut N, Pichayakorn W, Wiwattanapatapee R. Development and evaluation of self-microemulsifying liquid and pellet formulations of curcumin, and absorption studies in rats. *European Journal of Pharmaceutics and Biopharmaceutics*. 2010;76(3):475-85.
92. Rao SVR, Shao J. Self-nanoemulsifying drug delivery systems (SNEDDS) for oral delivery of protein drugs: I. Formulation development. *International journal of pharmaceutics*. 2008;362(1-2):2-9.
93. Zhao J, Yang D, Kang Z, Feng Z. A micro-CT study of changes in the internal structure of Daqing and Yan'an oil shales at high temperatures. *Oil Shale*. 2012;29(4):357.
94. Meola TR, Joyce P, Wignall A, Bremmell KE, Prestidge CA. Harnessing the potential of nanostructured formulations to mimic the food effect of lurasidone. *International Journal of Pharmaceutics*. 2021;608:121098.
95. Rayner M, Sjöo M, Timgren A, Dejmek P. Quinoa starch granules as stabilizing particles for production of Pickering emulsions. *Faraday discussions*. 2012;158(1):139-55.
96. Kommuru T, Gurley B, Khan M, Reddy I. Self-emulsifying drug delivery systems (SEDDS) of coenzyme Q10: formulation development and bioavailability assessment. *International journal of pharmaceutics*. 2001;212(2):233-46.
97. Wang W, Gowdagiri S, Oehlschlaeger MA. The high-temperature autoignition of biodiesels and biodiesel components. *Combustion and flame*. 2014;161(12):3014-21.
98. Qi X, Wang L, Zhu J, Hu Z, Zhang J. Self-double-emulsifying drug delivery system (SDED DS): A new way for oral delivery of drugs with high solubility and low permeability. *International journal of pharmaceutics*. 2011;409(1-2):245-51.
99. Kim DW, Kwon MS, Yousaf AM, Balakrishnan P, Park JH, Kim DS, et al. Comparison of a solid SMEDDS and solid dispersion for enhanced stability and bioavailability of clopidogrel napadisilate. *Carbohydrate polymers*. 2014;114:365-74.

100. Basalious EB, Shawky N, Badr-Eldin SM. SNEDDS containing bioenhancers for improvement of dissolution and oral absorption of lacidipine. I: development and optimization. *International journal of pharmaceutics*. 2010;391(1-2):203-11.
101. Inugala S, Eedara BB, Sunkavalli S, Dhurke R, Kandadi P, Jukanti R, et al. Solid self-nanoemulsifying drug delivery system (S-SNEDDS) of darunavir for improved dissolution and oral bioavailability: in vitro and in vivo evaluation. *European Journal of Pharmaceutical Sciences*. 2015;74:1-10.
102. Date AA, Nagarsenker M. Design and evaluation of self-nanoemulsifying drug delivery systems (SNEDDS) for cefpodoxime proxetil. *International journal of pharmaceutics*. 2007;329(1-2):166-72.
103. Alshweiat A, Katona G, Csóka I, Ambrus R. Design and characterization of loratadine nanosuspension prepared by ultrasonic-assisted precipitation. *European Journal of Pharmaceutical Sciences*. 2018;122:94-104.
104. Abbaspour M, Jalayer N, Makhmalzadeh BS. Development and evaluation of a solid self-nanoemulsifying drug delivery system for loratadin by extrusion-spheronization. *Advanced pharmaceutical bulletin*. 2014;4(2):113.
105. Singh B, Singh R, Bandyopadhyay S, Kapil R, Garg B. Optimized nanoemulsifying systems with enhanced bioavailability of carvedilol. *Colloids and Surfaces B: Biointerfaces*. 2013;101:465-74.
106. Beg S, Sandhu PS, Batra RS, Khurana RK, Singh B. QbD-based systematic development of novel optimized solid self-nanoemulsifying drug delivery systems (SNEDDS) of lovastatin with enhanced biopharmaceutical performance. *Drug delivery*. 2015;22(6):765-84.
107. Weerapol Y, Limmatvapirat S, Nunthanid J, Sriamornsak P. Self-nanoemulsifying drug delivery system of nifedipine: impact of hydrophilic–lipophilic balance and molecular structure of mixed surfactants. *AAPS pharmscitech*. 2014;15(2):456-64.
108. Taha EI, Al-Suwayeh SA, Anwer MK. Preparation, in vitro and in vivo evaluation of solid-state self-nanoemulsifying drug delivery system (SNEDDS) of vitamin A acetate. *Journal of drug targeting*. 2009;17(6):468-73.
109. Mostafa RE, Salama AA, Abdel-Rahman RF, Ogaly HA. Hepato- and neuro-protective influences of biopropolis on thioacetamide-induced acute hepatic

encephalopathy in rats. *Canadian journal of physiology and pharmacology*. 2017;95(5):539-47.

110. Parmar K, Patel J, Sheth N. Self nano-emulsifying drug delivery system for Embelin: Design, characterization and in-vitro studies. *asian journal of pharmaceutical sciences*. 2015;10(5):396-404.

111. Abo Enin HA, Abdel-Bar HM. Solid super saturated self-nanoemulsifying drug delivery system (sat-SNEDDS) as a promising alternative to conventional SNEDDS for improvement rosuvastatin calcium oral bioavailability. *Expert opinion on drug delivery*. 2016;13(11):1513-21.

112. Beg S, Swain S, Singh HP, Patra CN, Rao M. Development, optimization, and characterization of solid self-nanoemulsifying drug delivery systems of valsartan using porous carriers. *AAPS PharmSciTech*. 2012;13(4):1416-27.

113. Verma S, Singh SK, Verma PRP. Fabrication of lipidic nanocarriers of loratadine for facilitated intestinal permeation using multivariate design approach. *Drug Development and Industrial Pharmacy*. 2016;42(2):288-306.

114. Kaur G, Chandel P, Harikumar S. Formulation development of self nanoemulsifying drug delivery system (SNEDDS) of celecoxib for improvement of oral bioavailability. *Pharmacophore*. 2013;4(4):120-33.

115. Kamel AO, Mahmoud AA. Enhancement of human oral bioavailability and in vitro antitumor activity of rosuvastatin via spray dried self-nanoemulsifying drug delivery system. *Journal of biomedical nanotechnology*. 2013;9(1):26-39.

116. Kim DW, Kang JH, Oh DH, Yong CS, Choi H-G. Development of novel flurbiprofen-loaded solid self-microemulsifying drug delivery system using gelatin as solid carrier. *Journal of microencapsulation*. 2012;29(4):323-30.

117. Mohd AB, Sanka K, Bandi S, Diwan PV, Shastri N. Solid self-nanoemulsifying drug delivery system (S-SNEDDS) for oral delivery of glimepiride: development and antidiabetic activity in albino rabbits. *Drug delivery*. 2015;22(4):499-508.

118. Beg S, Katare O, Saini S, Garg B, Khurana RK, Singh B. Solid self-nanoemulsifying systems of olmesartan medoxomil: Formulation development, micromeritic characterization, in vitro and in vivo evaluation. *Powder technology*. 2016;294:93-104.

119. Ponnaganti H, Abbulu K. Enhanced dissolution of repaglinide: SMEDDS formulation and in-vitro evaluation. *Research Journal of Pharmacy and Technology*. 2014;7(11):4.
120. Truong DH, Tran TH, Ramasamy T, Choi JY, Lee HH, Moon C, et al. Development of solid self-emulsifying formulation for improving the oral bioavailability of erlotinib. *Aaps Pharmscitech*. 2016;17(2):466-73.
121. Quan Q, Kim D-W, Marasini N, Kim DH, Kim JK, Kim JO, et al. Physicochemical characterization and in vivo evaluation of solid self-nanoemulsifying drug delivery system for oral administration of docetaxel. *Journal of microencapsulation*. 2013;30(4):307-14.
122. Nasr A, Gardouh A, Ghonaim H, Abdelghany E, Ghorab M. Effect of oils, surfactants and cosurfactants on phase behavior and physicochemical properties of self-nanoemulsifying drug delivery system (SNEDDS) for irbesartan and olmesartan. *International Journal of Applied Pharmaceutics*. 2016;8(1):13-24.
123. Dash RN, Mohammed H, Humaira T, Ramesh D. Design, optimization and evaluation of glipizide solid self-nanoemulsifying drug delivery for enhanced solubility and dissolution. *Saudi Pharmaceutical Journal*. 2015;23(5):528-40.
124. Soni MG, White SM, Flamm WG, Burdock GA. Safety evaluation of dietary aluminum. *Regul Toxicol Pharmacol*. 2001;33(1):66-79.
125. Anand KS, Dhikav V. Hippocampus in health and disease: An overview. *Ann Indian Acad Neurol*. 2012;15(4):239-46.
126. Dash RN, Mohammed H, Humaira T, Ramesh D. Design, optimization and evaluation of glipizide solid self-nanoemulsifying drug delivery for enhanced solubility and dissolution. *Saudi Pharmaceutical Journal*. 2015;23(5):528-40.
127. Kandimalla R, Vallamkondu J, Corgiat EB, Gill KD. Understanding Aspects of Aluminum Exposure in Alzheimer's Disease Development. *Brain Pathol*. 2016;26(2):139-54.
128. Pizzino G, Irrera N, Cucinotta M, Pallio G, Mannino F, Arcoraci V, et al. Oxidative Stress: Harms and Benefits for Human Health. *Oxid Med Cell Longev*. 2017;2017:8416763.
129. Haam J, Yakel JL. Cholinergic modulation of the hippocampal region and memory function. *J Neurochem*. 2017;142 Suppl 2(Suppl 2):111-21.

130. Chen X, Zhang M, Ahmed M, Surapaneni KM, Veeraraghavan VP, Arulselvan P. Neuroprotective effects of ononin against the aluminium chloride-induced Alzheimer's disease in rats. *Saudi J Biol Sci.* 2021;28(8):4232-9.
131. Bazzari FH, Abdallah DM, El-Abhar HS. Chenodeoxycholic Acid Ameliorates AlCl₃-Induced Alzheimer's Disease Neurotoxicity and Cognitive Deterioration via Enhanced Insulin Signaling in Rats. *Molecules.* 2019;24(10).
132. Liao JK, Laufs U. Pleiotropic effects of statins. *Annu Rev Pharmacol Toxicol.* 2005;45:89-118.
133. Nampoothiri M, John J, Kumar N, Mudgal J, Nampurath GK, Chamallamudi MR. Modulatory role of simvastatin against aluminium chloride-induced behavioural and biochemical changes in rats. *Behav Neurol.* 2015;2015:210169.
134. Brown JM, Everett BM. Cardioprotective diabetes drugs: what cardiologists need to know. *Cardiovasc Endocrinol Metab.* 2019;8(4):96-105.
135. Camp D, Garavelas A, Campitelli M. Analysis of Physicochemical Properties for Drugs of Natural Origin. *J Nat Prod.* 2015;78(6):1370-82.
136. Dash RN, Mohammed H, Humaira T, Ramesh D. Design, optimization and evaluation of glipizide solid self-nanoemulsifying drug delivery for enhanced solubility and dissolution. *Saudi Pharmaceutical Journal.* 2015;23(5):528-40.
137. Patel J, Kevin G, Patel A, Raval M, Sheth N. Development of the UV spectrophotometric method of Olmesartan medoxomil in bulk drug and pharmaceutical formulation and stress degradation studies. *Pharm Methods.* 2011;2(1):36-41.
138. Ali H, Nazzal S. Development and validation of a reversed-phase HPLC method for the simultaneous analysis of simvastatin and tocotrienols in combined dosage forms. *Journal of Pharmaceutical and Biomedical Analysis.* 2009;49(4):950-6.
139. Suneetha A, Donepudi S. HPLC method development and validation for the estimation of Axitinib in rabbit plasma. *Brazilian Journal of Pharmaceutical Sciences.* 2017;53(3).
140. Khursheed R, Singh SK, Kapoor B, Gulati M, Wadhwa S, Gupta S, et al. Development and validation of RP-HPLC method for simultaneous determination of curcumin and quercetin in extracts, marketed formulations, and self-nanoemulsifying drug delivery system. *Re: GEN Open.* 2021;1(1):43-52.

141. Development and Validation of RP-HPLC Method for Simultaneous Determination of Curcumin and Quercetin in Extracts, Marketed Formulations, and Self-Nanoemulsifying Drug Delivery System. *Re:GEN Open*. 2021;1(1):43-52.
142. Nampoothiri M, John J, Kumar N, Mudgal J, Nampurath GK, Chamallamudi MR. Modulatory role of simvastatin against aluminium chloride-induced behavioural and biochemical changes in rats. *Behav Neurol*. 2015;2015:210169.
143. Shao A, Chen G, Jiang N, Li Y, Zhang X, Wen L, et al. Development and evaluation of self-microemulsifying liquid and granule formulations of Brucea javanica oil. *Archives of pharmacal research*. 2013;36(8):993-1003.
144. Khursheed R, Singh SK, Wadhwa S, Gulati M, Awasthi A, Kumar R, et al. Exploring role of probiotics and Ganoderma lucidum extract powder as solid carriers to solidify liquid self-nanoemulsifying delivery systems loaded with curcumin. *Carbohydr Polym*. 2020;250:116996.
145. Kumar B, Garg V, Singh S, Pandey NK, Bhatia A, Prakash T, et al. Impact of spray drying over conventional surface adsorption technique for improvement in micromeritic and biopharmaceutical characteristics of self-nanoemulsifying powder loaded with two lipophilic as well as gastrointestinal labile drugs. *Powder Technology*. 2018;326:425-42.
146. Jaiswal P, Aggarwal G, Harikumar SL, Singh K. Development of self-microemulsifying drug delivery system and solid-self-microemulsifying drug delivery system of telmisartan. *Int J Pharm Investig*. 2014;4(4):195-206.
147. Patel J, Patel A, Raval M, Sheth N. Formulation and development of a self-nanoemulsifying drug delivery system of irbesartan. *J Adv Pharm Technol Res*. 2011;2(1):9-16.
148. Garg V, Kaur P, Singh SK, Kumar B, Bawa P, Gulati M, et al. Solid self-nanoemulsifying drug delivery systems for oral delivery of polypeptide-k: Formulation, optimization, in-vitro and in-vivo antidiabetic evaluation. *Eur J Pharm Sci*. 2017;109:297-315.
149. <draft-ich-guideline-m10-bioanalytical-method-validation-step-2b_en.pdf>.
150. Kumar R, Kumar R, Khursheed R, Awasthi A, Khurana N, Singh SK, et al. Development and validation of RP-HPLC method for estimation of fisetin in rat plasma. *South African Journal of Botany*. 2020.

151. <AJPS_Volume 65_Issue 1_Pages 64-84.pdf>.
152. Kumar V, Singh S, Gulati M, Sood R, Anishetty R, Shunmugaperumal T. Development and Validation of a Simple and Sensitive Spectrometric Method for Estimation of Azithromycin Dihydrate in Tablet Dosage Forms: Application to Dissolution Studies. *Current Pharmaceutical Analysis*. 2013;10:310.
153. Kheirallah M, Almeshaly H. Simvastatin, dosage and delivery system for supporting bone regeneration, an update review. *Journal of Oral and Maxillofacial Surgery, Medicine, and Pathology*. 2016;28(3):205-9.
154. Reddy VK, Swamy N, Rathod R, Sengupta P. A Bioanalytical Method for Eliglustat Quantification in Rat Plasma. *J Chromatogr Sci*. 2019;57(7):600-5.
155. Challa BR, Boddu SH, Awen BZ, Chandu BR, Bannoth CK, Khagga M, et al. Development and validation of a sensitive bioanalytical method for the quantitative estimation of pantoprazole in human plasma samples by LC-MS/MS: application to bioequivalence study. *J Chromatogr B Analyt Technol Biomed Life Sci*. 2010;878(19):1499-505.
156. Kumar SP, Bairy KL, Nayak V, Reddy SK, Kiran A, Ballal A. Amelioration of aluminium chloride (AlCl₃) induced neurotoxicity by combination of rivastigmine and memantine with artesunate in Albino Wistar rats. *Biomedical and Pharmacology Journal*. 2019;12(2):703-11.
157. Rajasankar S, Manivasagam T, Surendran S. Ashwagandha leaf extract: a potential agent in treating oxidative damage and physiological abnormalities seen in a mouse model of Parkinson's disease. *Neurosci Lett*. 2009;454(1):11-5.
158. Singh NA, Bhardwaj V, Ravi C, Ramesh N, Mandal AKA, Khan ZA. EGCG Nanoparticles Attenuate Aluminum Chloride Induced Neurobehavioral Deficits, Beta Amyloid and Tau Pathology in a Rat Model of Alzheimer's Disease. *Front Aging Neurosci*. 2018;10:244.
159. Antunes M, Biala G. The novel object recognition memory: neurobiology, test procedure, and its modifications. *Cogn Process*. 2012;13(2):93-110.
160. Amanzadeh Jain E, Esmacili A, Rahgozar S, Noorbakhshnia M. Quercetin-Conjugated Superparamagnetic Iron Oxide Nanoparticles Protect AlCl₃-Induced Neurotoxicity in a Rat Model of Alzheimer's Disease via Antioxidant Genes, APP Gene, and miRNA-101. *Frontiers in Neuroscience*. 2021;14.

161. Pruell RJ, Engelhardt FR. Liver cadmium uptake, catalase inhibition and cadmium thionein production in the killifish (*Fundulus Heteroclitus*) induced by experimental cadmium exposure. *Marine Environmental Research*. 1980;3(2):101-11.
162. Uzel N, Sivas A, Uysal M, Öz H. Erythrocyte lipid peroxidation and glutathione peroxidase activities in patients with diabetes mellitus. *Hormone and metabolic research*. 1987;19(02):89-90.
163. Kumar B, Kuhad A, Chopra K. Neuropsychopharmacological effect of sesamol in unpredictable chronic mild stress model of depression: behavioral and biochemical evidences. *Psychopharmacology*. 2011;214:819-28.
164. Shata A, Elkashef W, Hamouda MA, Eissa H. Effect of Artesunate vs Memantine in Aluminum Chloride Induced Model of Neurotoxicity in Rats. *Advances in Alzheimer's Disease*. 2020;09(01):1-19.
165. Dube A, Nicolazzo Ja Fau - Larson I, Larson I. Chitosan nanoparticles enhance the plasma exposure of (-)-epigallocatechin gallate in mice through an enhancement in intestinal stability. (1879-0720 (Electronic)).
166. Khurana N, Gajbhiye A. Ameliorative effect of *Sida cordifolia* in rotenone induced oxidative stress model of Parkinson's disease. *Neurotoxicology*. 2013;39:57-64.
167. Sopyan I, Fudholi A, Muchtaridi M, Puspitasari I. A Novel of Cocrystalization to Improve Solubility and Dissolution rate of Simvastatin. *Int J PharmTech Res*. 2016;9(6):483-91.
168. Chen J, Mu L, Jiang B, Yin H, Song X, Li A. TG/DSC-FTIR and Py-GC investigation on pyrolysis characteristics of petrochemical wastewater sludge. *Bioresource technology*. 2015;192:1-10.
169. Chavhan V, Reddy K, Ahhirao K. Development of UV spectrophotometric methods and validation for estimation of simvastatin in bulk and tablet dosage form by absorbance maxima and area under the curve method. *Journal of Applied Pharmacy*. 2014;6:55-64.
170. Sen AK, Hinsu D, Sen D, Zanwar A, Maheshwari R, Chandrakar V. Analytical method development and validation for simultaneous estimation of Teneligliptin hydrobromide hydrate and Metformin hydrochloride from its pharmaceutical dosage form by three different UV spectrophotometric methods. 2016.

171. Sharma S, Goyal S, Chauhan K. A review on analytical method development and validation. *International Journal of Applied Pharmaceutics*. 2018;10(6):8-15.
172. Westgard JO, Carey RN, Wold S. Criteria for judging precision and accuracy in method development and evaluation. *Clinical chemistry*. 1974;20(7):825-33.
173. Ferreira SL, Caires AO, Borges TdS, Lima AM, Silva LO, dos Santos WN. Robustness evaluation in analytical methods optimized using experimental designs. *Microchemical Journal*. 2017;131:163-9.
174. Kapoor B, Gupta R, Gulati M, Singh SK, Khatik GL, Chawla M, et al. High-performance liquid chromatography and liquid chromatography/mass spectrometry studies on stress degradation behavior of sulfapyridine and development of a validated, specific, stability-indicating HPLC assay method. *ASSAY and Drug Development Technologies*. 2020;18(3):119-33.
175. Singh S, Bakshi M. Guidance on the conduct of stress tests to determine inherent stability of drugs. *Pharmaceutical Technology Asia*. 2000:24-.
176. Khurshed R, Wadhwa S, Kumar B, Gulati M, Gupta S, Chaitanya M, et al. Development and validation of RP-HPLC based bioanalytical method for simultaneous estimation of curcumin and quercetin in rat's plasma. *South African Journal of Botany*. 2022;149:870-7.
177. Cheng Y, Jin Y, Unverzagt FW, Su L, Yang L, Ma F, et al. The relationship between cholesterol and cognitive function is homocysteine-dependent. *Clin Interv Aging*. 2014;9:1823-9.
178. Mailloux RJ, Lemire J, Appanna VD. Hepatic response to aluminum toxicity: Dyslipidemia and liver diseases. *Experimental Cell Research*. 2011;317(16):2231-8.
179. Lippincott-Schwartz J, Phair RD. Lipids and Cholesterol as Regulators of Traffic in the Endomembrane System. *Annual Review of Biophysics*. 2010;39(1):559-78.
180. Antunes M, Biala G. The novel object recognition memory: neurobiology, test procedure, and its modifications. *Cogn Process*. 2012;13(2):93-110.
181. Flora SJS, Mehta A, Satsangi K, Kannan GM, Gupta M. Aluminum-induced oxidative stress in rat brain: response to combined administration of citric acid and HEDTA. *Comparative Biochemistry and Physiology Part C: Toxicology & Pharmacology*. 2003;134(3):319-28.

182. Lu J, Huang Q, Zhang D, Lan T, Zhang Y, Tang X, et al. The protective effect of DiDang Tang against AlCl₃-Induced oxidative stress and apoptosis in PC12 cells through the activation of SIRT1-mediated Akt/Nrf2/HO-1 pathway. *Frontiers in Pharmacology*. 2020;11:466.
183. Sies H, Jones DP. Reactive oxygen species (ROS) as pleiotropic physiological signalling agents. *Nature reviews Molecular cell biology*. 2020;21(7):363-83.
184. Forcina GC, Dixon SJ. GPX4 at the crossroads of lipid homeostasis and ferroptosis. *Proteomics*. 2019;19(18):1800311.



L OVELY
P ROFESSIONAL
U NIVERSITY

Centre for
Research Degree Programmes

LPU/CRDP/PHD/EC/20210107/000805

Dated: 17 Sep 2020

Hardeep

Registration Number: 41900289

Programme Name: Doctor of Philosophy (Pharmaceutics)

Subject: Letter of Candidacy for Ph.D.

Dear Candidate,

We are very pleased to inform you that the Department Doctoral Board has approved your candidacy for the Ph.D. Programme on 17 Sep 2020 by accepting your research proposal entitled: "Development and evaluation of simvastatin based SNEDDS for treatment of Alzheimer's disease"

As a Ph.D. candidate you are required to abide by the conditions, rules and regulations laid down for Ph.D. Programme of the University, and amendments, if any, made from time to time.

We wish you the very best!!

In case you have any query related to your programme, please contact Centre of Research Degree Programmes.

Head

Centre for Research Degree Programmes

Note:-This is a computer generated certificate and no signature is required. Please use the reference number generated on this certificate for future conversations.

CENTRAL ANIMAL HOUSE FACILITY (CAHF)
Lovely Institute of Technology (Pharmacy), Lovely Professional University
Ludhiana- Jalandhar G.T. Road, Phagwara (Punjab), 144411
Registration Number -954/PO/ReReBiBt/S/06/CPCSEA

CERTIFICATE

This is to certify that the project titled "*Development and evaluation of simvastatin based SNEDDS for treatment of Alzheimer's disease*" has been approved by the IAEC.

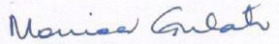
Name of Principal Investigator: Dr. Narendra Kumar Pandey

IAEC approval number: LPU/IAEC/2022/04

Date of Approval: 13th April 2022

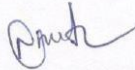
Animals approved: 42 SD/Wistar rats, Male

Remarks if any: - NA



Dr. Monica Gulati

Biological Scientist,
Chairperson IAEC



Dr. Navneet Khurana

Scientist from different
discipline



Dr. Bimlesh Kumar

Scientist In-Charge of Animal
House, Member Secretary IAEC



Extracts from the Register of Copyrights



प्रतिलिप्यधिकार कार्यालय, भारत सरकार | Copyright Office, Government Of India

दिनांक/Dated:14/06/2023

1. पंजीकरण संख्या/Registration Number

L-125559/2023

2. आवेदक का नाम, पता तथा राष्ट्रीयता
Name, address and nationality of the applicant

LOVELY PROFESSIONAL UNIVERSITY, LOVELY PROFESSIONAL UNIVERSITY, JALANDHAR, DELHI-GT ROAD, PHAGWARA PUNJAB-144411 INDIAN

3. कृति के प्रतिलिप्यधिकार में आवेदक के हित की प्रकृति
Nature of the applicant's interest in the copyright of the work

OWNER

4. कृति का वर्ग और वर्णन
Class and description of the work

LITERARY/ DRAMATIC WORK THE GRAPHICAL ABSTRACT PRESENT SELF NANO EMULSIFYING DRUG DELIVERY SYSTEM SNEDDS OF SIMVASTATIN AN ALTERNATIVE APPROACH FOR THE TREATMENT OF ALZHEIMERS DISEASE.

5. कृति का शीर्षक
Title of the work

SELF-NANO EMULSIFYING DRUG DELIVERY SYSTEM (SNEDDS) OF SIMVASTATIN: AN ALTERNATIVE APPROACH FOR THE TREATMENT OF ALZHEIMER'S DISEASE.

6. कृति की भाषा
Language of the work

ENGLISH

7. रचयिता का नाम, पता और राष्ट्रीयता तथा यदि रचयिता की मृत्यु हो गई है, तो मृत्यु की तिथि
Name, address and nationality of the author and if the author is deceased, date of his decease

HARDEEP, LOVELY PROFESSIONAL UNIVERSITY, JALANDHAR, DELHI-GT ROAD, PHAGWARA PUNJAB-144411 INDIAN

DR. NARENDRA KUMAR PANDEY, LOVELY PROFESSIONAL UNIVERSITY, JALANDHAR, DELHI-GT ROAD, PHAGWARA PUNJAB-144411 INDIAN

DR. BIMLESH KUMAR, LOVELY PROFESSIONAL UNIVERSITY, JALANDHAR, DELHI-GT ROAD, PHAGWARA PUNJAB-144411 INDIAN

DR. SACHIN KUMAR SINGH, LOVELY PROFESSIONAL UNIVERSITY, JALANDHAR, DELHI-GT ROAD, PHAGWARA PUNJAB-144411 INDIAN

SUKRITI VISHWAS, LOVELY PROFESSIONAL UNIVERSITY, JALANDHAR, DELHI-GT ROAD, PHAGWARA PUNJAB-144411 INDIAN

8. कृति प्रकाशित है या अप्रकाशित
Whether the work is published or unpublished

UNPUBLISHED

9. प्रथम प्रकाशन का वर्ष और देश तथा प्रकाशक का नाम, पता और राष्ट्रीयता
Year and country of first publication and name, address and nationality of the publisher

N.A.

10. बाद के प्रकाशनों के वर्ष और देश, यदि कोई हों, और प्रकाशकों के नाम, पते और राष्ट्रीयताएँ
Years and countries of subsequent publications, if any, and names, addresses and nationalities of the publishers

N.A.

11. कृति में प्रतिलिप्यधिकार सहित विभिन्न अधिकारों के स्वामियों के नाम, पते और राष्ट्रीयताएँ और समनुदेशन और अनुज्ञप्तियों के विवरण के साथ प्रत्येक के अधिकार का विस्तार, यदि कोई हो।
Names, addresses and nationalities of the owners of various rights comprising the copyright in the work and the extent of rights held by each, together with particulars of assignments and licences, if any

LOVELY PROFESSIONAL UNIVERSITY, LOVELY PROFESSIONAL UNIVERSITY, JALANDHAR, DELHI-GT ROAD, PHAGWARA PUNJAB-144411 INDIAN

12. अन्य व्यक्तियों के नाम, पते और राष्ट्रीयताएँ, यदि कोई हों, जो प्रतिलिप्यधिकार वाले अधिकारों को समनुदेशित करने या अनुज्ञप्ति देने के लिए अधिकृत हों
Names, addresses and nationalities of other persons, if any, authorised to assign or licence of rights comprising the copyright

N.A.

13. यदि कृति एक 'कलात्मक कृति' है, तो कृति पर अधिकार रखने वाले व्यक्ति का नाम, पता और राष्ट्रीयता सहित मूल कृति का स्थान। (एक वास्तुशिल्प कृति के मामले में कृति पूरी होने का वर्ष भी दिखाया जाना चाहिए)
If the work is an 'Artistic work', the location of the original work, including name, address and nationality of the person in possession of the work. (In the case of an architectural work, the year of completion of the work should also be shown).

N.A.

14. यदि कृति एक 'कलात्मक कृति' है जो किसी भी माल या सेवाओं के संबंध में उपयोग की जाती है या उपयोग किए जाने में सक्षम है, तो आवेदन में प्रतिलिप्यधिकार अधिनियम, 1957 की धारा 45 की उप-धारा (i) के प्रावधान के अनुसार व्यापार चिह्न रजिस्ट्रार से प्रमाणन शामिल होना चाहिए।
If the work is an 'Artistic work' which is used or capable of being used in relation to any goods or services, the application should include a certification from the Registrar of Trade Marks in the provision to Sub-Section (i) of Section 45 of the Copyright Act, 1957.

N.A.

15. यदि कृति एक 'कलात्मक कृति' है, तो क्या यह डिजाइन अधिनियम 2000 अंतर्गत पंजीकृत है? यदि हाँ, तो विवरण दें।
If the work is an 'Artistic work', whether it is registered under Designs Act 2000, if yes give details.

N.A.



Registrar of Copyrights

16. यदि कृति एक 'कलात्मक कृति' है, जो डिजाइन अधिनियम 2000 के तहत एक डिजाइन के रूप में पंजीकृत होने में सक्षम है, तो क्या यह औद्योगिक प्रक्रिया के माध्यम से किसी वस्तु पर प्रयुक्त की गई है और यदि हाँ, तो इसे कितनी बार पुनरुत्पादित किया गया है? : N.A.
If the work is an 'Artistic work', capable of being registered as a design under the Designs Act 2000, whether it has been applied to an article through an industrial process and, if yes, the number of times it is reproduced.

17. टिप्पणी, यदि कोई हो/Remarks, if any

: THE WORK IS ORIGINAL AS DONE BY THE FACULTY AND STAFF OF LOVELY PROFESSIONAL UNIVERSITY.

डायरी संख्या/Diary Number: 3601/2023-CO/L

आवेदन की तिथि/Date of Application: 10/02/2023

प्राप्ति की तिथि/Date of Receipt: 10/02/2023




Registrar of Copyrights



Office of the Controller General of Patents, Designs & Trade Marks
Department of Industrial Policy & Promotion,
Ministry of Commerce & Industry,
Government of India

(<http://ipindia.nic.in/index.htm>)



(<http://ipindia.nic.in/index.htm>)

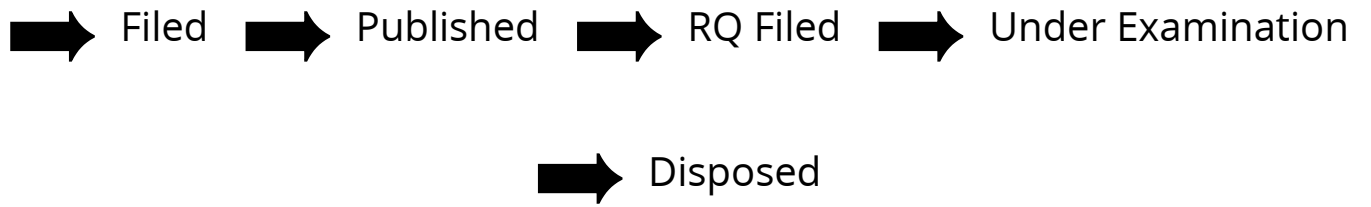
Application Details

APPLICATION NUMBER	202311029695
APPLICATION TYPE	ORDINARY APPLICATION
DATE OF FILING	25/04/2023
APPLICANT NAME	Lovely Professional University
TITLE OF INVENTION	A NOVEL SELF NANO EMULSIFYING DRUG DELIVERY SYSTEM FOR SIMVASTATIN AND PROCESS THEREOF
FIELD OF INVENTION	CHEMICAL
E-MAIL (As Per Record)	dip@lpu.co.in
ADDITIONAL-EMAIL (As Per Record)	
E-MAIL (UPDATED Online)	
PRIORITY DATE	
REQUEST FOR EXAMINATION DATE	--
PUBLICATION DATE (U/S 11A)	26/05/2023

Application Status

APPLICATION STATUS	Awaiting Request for Examination
--------------------	---

[View Documents](#)



In case of any discrepancy in status, kindly contact ipo-helpdesk@nic.in



Open camera or QR reader and scan code to access this article and other resources online.

Development and Validation of Reverse-Phase High-Performance Liquid Chromatography Based Bioanalytical Method for Estimation of Simvastatin in Rat's Plasma

Hardeep,¹ Narendra Kumar Pandey,¹ Sachin Kumar Singh,¹ Bimlesh Kumar,¹ Leander Corrie,¹ Umesh Goutam,² and Dileep Singh Baghel¹

¹School of Pharmaceutical Sciences, Lovely Professional University, Phagwara, India.

²School of Bioengineering and Biosciences, Lovely Professional University, Phagwara, India.

ABSTRACT

Simvastatin (SIM) is known to lower cholesterol levels and is speculated in the pathogenesis of Alzheimer's disease. In this study, the bioanalytical method of SIM SNEDDS was developed and validated for the estimation of SIM in the rat's plasma using reverse-phase high-performance liquid chromatography. C-18 reverse-phase octadecylsilyl column was used to validate the method. Atorvastatin (ATV) was used as an internal standard. Gradient elution was performed using acetonitrile and water in a ratio of 90:10 with a flow rate of 1 mL/min. The chromatogram of these both compounds SIM and ATV was detected at a wavelength of 238 and 244 nm. The drugs were extracted from the plasma samples using the protein precipitation method. The retention time of SIM and ATV was found to be 3.720 and 8.331 min, respectively. The developed method was found to be linear in the range between 50 and 250 ng/mL, with a regression coefficient (r^2) of 0.9994. According to ICH M10 guidelines, the method was validated. The percent of drug recovery was more than 95% and the % relative standard deviation was <2% in the replicate studies, which showed that the method was accurate

and precise. The limit of detection and limit of quantification were found in rat plasma to be 0.12 and 0.38 ng/mL, respectively. The obtained result indicated that the developed method was successful in estimating SIM in rat plasma and passed all validation test parameters.

Keywords: simvastatin, bioanalytical method, rat plasma, RP-HPLC, stability, recovery, validation

INTRODUCTION

Chemically, simvastatin (SIM) is (1S,3R,7S,8S,8aR)-8-{2-[(2R,4R)-4-hydroxy-6-oxooan-2-yl] ethyl}-3,7-dimethyl-1,2,3,7,8,8a-hexahydronaphthalen-1-yl 2,2 dimethyl Butanoate, shown in Figure 1.¹ It appears as a white powder with a molecular weight of 418.566 g/mol and log P is 4.46. SIM is a reversible lactone prodrug that goes through metabolism. It is a lipid-lowering drug that works by inhibiting hydroxy-methyl-glutaryl coenzyme A (HMG CoA) reductase.² This helps in the conversion of HMG-CoA to mevalonate. Thus, it reduces plasma low-density lipoprotein (LDL) cholesterol by depleting intracellular cholesterol. In addition, it increases LDL receptor expression and helps in the treatment of hypercholesterolemia.³

Few individual studies have reported that SIM was used to reduce the risk of dementia and Alzheimer's disease (AD),⁴ as well as AD-related neuropathological changes.⁵

SIM causes substantial toxicity in a variety of animal species when used at high doses.⁶ It has been linked to a broad range of side effects, ranging from minor gastrointestinal

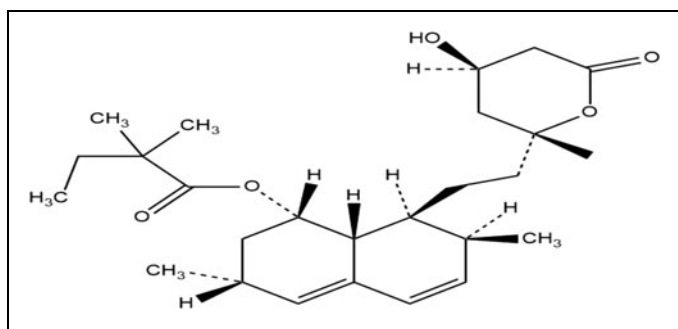


Fig. 1. Structure of SIM. SIM, simvastatin.

problems to potentially fatal disorders like rhabdomyolysis. Its high systemic dosage increases the risk of side effects such as renal damage and liver failure. Constipation, nausea, diarrhea, and myotoxicity-related side effects, which range from mild myalgia to the infrequent occurrence of rhabdomyolysis, are among the most commonly reported negative effects of statins.⁷

Hence, it becomes important to develop some suitable oral dosage forms of SIM, as well as to develop a simple, sensitive, and robust analytical method for its estimation in the dosage form as such, in biological samples such as blood, urine, feces, and saliva. It becomes crucial to have a selective and sensitive method to estimate the drug in biological fluids because, during pharmacokinetic studies, the drug concentration is very low at the nanogram level. Hence, the development of an analytical method with a very low limit of detection (LOQ) becomes the prime requirement.

Nevertheless, at some time, it becomes an important task for the analyst to look for a simple as well as an economical method for their detection.

In the past, some liquid chromatography and mass spectrometry (LC-MS) based methods have been developed and some of them are also described in this study. However, these methods are quite expensive as the operation cost and instrument cost, as well as the requirement of other accessories to run the machine make the overall method development a very expensive process. Owing to these challenges with hyphenated techniques, the search for the simple high-performance liquid chromatography (HPLC) method is always ongoing and worth exploring. Based on this objective, our work was initiated to develop a new HPLC method at our laboratory. Of course, there also exist some HPLC methods, but most of them have provided a longer run time than the run time reported in this article. Few studies are discussed below in subsequent paragraphs.

In 2015, Liu et al, described a bioanalytical method for the estimation of SIM using LC/MS with electrospray ionization.⁸

The mobile phase consisted of acetonitrile (ACN) and 10 mM ammonium acetate (pH 4.5). Its flow rate was 0.8 mL/min. The run time of SIM was found to be 3.11 min.

Similarly, in another study, Auti, in 2018, developed a bioanalytical method using reverse-phase HPLC (RP-HPLC) for the estimation of SIM, in combination with piperine in rat plasma using 0.01% formic acid and methanol as a mobile phase with a flow rate of 1.0 mL/min. The retention time of SIM was reported at 22.1 min.⁹ In 2020, Pandey et al developed an RP-HPLC bioanalytical method and validated the estimation of SIM in combination with glimepiride. The method was carried out in rat plasma using ACN and potassium dihydrogen phosphate buffer pH 5 (75:25, v/v) as a mobile phase with flow rate 1.0 mL/min. The retention time of SIM was found to be 9.59 min, % recovery was 98.96, and LOD and LOQ were 11 and 33 ng/mL, respectively.¹⁰

In both methods, the SIM was estimated after longer time duration. Longer retention time indicates toward consumption of more solvent and leads to expensive method development. Hence, it was decided to develop a faster and more affordable bioanalytical method for SIM in rat plasma.

Methods

Chromatographic conditions. A bioanalytical method was developed utilizing ICH M10 standards for drug quantification in rat plasma.¹¹ The mobile phase utilized a 90:10 v/v mixture of ACN (A) and water (B). The flow rate was set at 1 mL/min, and the chromatogram was measured at 238 nm. SIM was analyzed using various mobile phase compositions, such as ACN-0.1% formic acid, methanol-water, and ACN-water 90:10, ACN and % ortho-phosphoric acid, and ACN and water 60:40, by adjusting the mobile phase ratio.

Collection of blood and extraction of plasma. Using a capillary tube and radioimmunoassay (RIA) vials containing ethylene diamine tetra acetic acid (EDTA) crystals, a blood sample was collected from rats through the retro-orbital puncture. The rat was initially held, while having its neck scuffed and its eye made to bulge. Blood was allowed to flow into the EDTA vial through a capillary tube after a capillary was placed dorsally into the retro-orbital plexus of the eye. The EDTA tubes were centrifuged at 5,000 rpm for 15 min and the temperature was adjusted to 2°C–8°C. The clear supernatant was removed with a micropipette and stored for processing in a deep freezer at –20°C (Solution C).

Preparation of standard stock solutions. SIM (10 mg) was dissolved in 10 mL of ACN in a 100 mL volumetric flask and then the volume was adjusted to 100 mL to obtain a solution

concentration of 100 mg/mL (Solution A). A second volumetric flask was used to dilute Solution A to a concentration of 10 mg/mL using ACN up to 100 mL (Solution B). A further SIM dilution was obtained by taking 10 mL aliquots of solution B and diluting them to 100 mL in ACN to attain a concentration of 1.0 mg/mL (Solution C).

To obtain a concentration of 200 ng/mL, 20 mL of liquid from solution C was dissolved in a 100 mL volumetric flask, and the volume was increased by 100 mL of ACN (Solution D). Atorvastatin (ATV) (10 mg) was dissolved in a small amount of ACN in a 100 mL volumetric flask, and the volume was then adjusted to 100 mL using ACN to obtain a final concentration of 100 mg/mL (Solution E).

Preparation of internal standard. ATV 10 mg/mL was used as the internal standard (IS) for dilution preparation. A quantity of 10 mg was weighed and added to a volumetric flask (100 mL) containing 20 mL of ACN. The solution was sonicated for 10 min. The final volume was adjusted to 100 mL using ACN to produce a stock solution with a concentration of 100 mg/mL.

Specificity study. SIM and blank plasma samples were injected on HPLC using mobile phase ACN: water (90:10 v/v) to validate method specificity. The possibility of drug-plasma peak interference was investigated.

Development of calibration curve. One milliliter of solution E was added after aliquots of 1.25, 2.5, 3.75, 5, and 6.25 mL of solution D were transferred into separate 10 mL volumetric flasks. Around 0.1 mL of plasma was added to each of the above dilutions and mixed for 5 min. To precipitate and break down plasma protein, acetone (1 mL) was added to each sample and thoroughly agitated using a sonicator for 15 min. Then, all samples were centrifuged in an Eppendorf at 10,000 rpm for 30 min at 4°C. To get theoretical SIM concentrations of 50, 100, 150, 200, and 250 ng/mL and ATV concentrations of 10 mg/mL, the supernatant was collected using a micropipette, and the volume was adjusted to 10 mL in a volumetric flask. HPLC was used to analyze SIM and ATV using the final prepared samples.¹²

Validation of the method. According to the ICH M10 standard, the developed method was validated.¹³ System suitability parameters, including theoretical plate, height equivalent to the theoretical plate, tailing factor, detection limit, and quantification limit, were measured to assess the system performance further.

Linearity and range. The concentration was plotted on the X-axis, and the mean peak area was plotted on the Y-axis, to

create the calibration curve. The slope, the standard deviation (SD) of response (sigma), the y-intercept, the SD of the intercept, and the regression coefficient (r^2) were calculated using the calibration data.¹⁴

Accuracy. The absolute recovery of the drug from the quality control samples was estimated to determine the method's accuracy. Three different concentration levels of the method were used to prepare the samples: lower quantified concentration (LQC, 80%), medium quantified concentration (MQC, 100%), and high quantified concentration (HQC, 120%) at the midrange concentration of 100 ng/mL. Aliquots of solution D in the amounts of 3.0, 3.75, and 4.5 mL were added into separate 10 mL volumetric flasks to obtain these concentrations. One milliliter of solution E and 0.1 mL of plasma were then added. After adding plasma, the samples were sonicated and centrifuged in an Eppendorf at 10,000 rpm for 30 min at 4°C.

The supernatant was transferred using a micropipette into a 10 mL volumetric flask, and 3.75 mL of solution F was then added. The volume was then diluted to 10 mL with ACN. As a result, the theoretical concentrations of SIM in these solutions were 120, 150, and 180 ng/mL, respectively, with 10 mg/mL of ATV. These concentrations were determined using HPLC in six replicate tests.¹² The formula shown in the following Eq. (1) was used to estimate the absolute percentage of drug recovery:

$$\text{Actual \% recovery} = \frac{\text{Actual concentraion recovered}}{\text{Theoretical concentration}} * 100 \quad (1)$$

Precision. The repeatability and intermediate precision of the developed method were used to determine its precision. Six injections of the LQC, MQC, and HQC samples were performed into the same experimental setup on the same day to ensure repeatability (without the addition of sample solution F). By calculating LQC, MQC, and HQC samples six times under similar experimental conditions, but on different days with different analysts (interanalyst), the intermediate accuracy was determined.¹⁵ Following the collection of mean data, the percentage relative standard deviation (RSD) was calculated using the formula shown in the following Eq. 2:

$$\begin{aligned} &\% \text{Relative standard deviation} \\ &= \frac{\text{Standard deviation of peak area}}{\text{Average peak area}} * 100 \end{aligned} \quad (2)$$

System suitability and estimation of LOD and LOQ. System compatibility was evaluated using the peak purity index, height equivalent to theoretical plate (HETP), theoretical plate, and

tailing factor. The SD of response (sigma) and slope of the calibration curve were used to determine the LOD and LOQ (S).¹⁶ The SD was calculated using the SD of the Y intercepts of the regression line. The following Eqs. (4) and (5) were used to calculate the results¹⁷:

$$\text{LOD} = 3.3 \frac{\sigma}{S} \quad (4)$$

$$\text{LOQ} = 10 \frac{\sigma}{S} \quad (5)$$

Stability study. Three freeze-thaw cycles were used to study the stability of plasma samples spiked with SIM, with short-term stability at room temperature for 3 h and long-term stability at -20°C for 3 weeks. Three milliliters of plasma was collected in one RIA vial for freeze-thaw stability. To this vial, 10 mg of SIM was added (to achieve a concentration of 1,000 mg/mL), and the solution was vortexed for 5 min. This test tube was placed in a freezer at a -20°C temperature. The test tube was taken out and thawed at room temperature after the sample had frozen. From the thawed samples, 1 mL of plasma was removed (Cycle 1), and the remaining 2 mL of plasma was stored in the deep freezer for the following cycle.

The drug was precipitated from the extracted plasma (1 mL), and the supernatant was centrifuged. After centrifugation, the clear translucent supernatant was obtained and diluted to 100 mL with ACN to obtain a concentration of 100 mg/mL.¹⁸ Dilutions were also prepared to obtain 120 ng/mL (LQC), 150 ng/mL (MQC), and 180 ng/mL (HQC). Similar to Cycle 1, the final frozen plasma sample (2 mL) was taken out, allowed to thaw at room temperature, and then 1 mL was extracted (Cycle 2). The final 1 mL of thawed plasma was then placed back in the deep freezer. It was taken out and thawed after it had frozen (Cycle 3). As in Cycle 1, the method was repeated in Cycles 2 and 3 to prepare LQC, MQC, and HQC samples. IS was added to all these solutions at a concentration of 10 mg/mL.

All dilutions were produced in triplicate, and injected into HPLC, and their retention times at 238 nm were determined. The mean, SD, and % RSD were calculated for each concentration.^{19,20} Similar to this, at room temperature, the short-term stability of a plasma sample injected with SIM was determined. Before extraction, the stability was tested at 1, 2, and 3 h. In the short term, 3 mL of plasma and 10 mg of SIM were added (to achieve a concentration of 1,000 mg/mL) to the RIA vial and vortexed for 5 min. The RIA vial was maintained at a constant temperature (room temperature).

After each interval, a sample (1 mL) was collected, the drug was withdrawn from the plasma, processed to create the LQC,

MQC, and HQC samples, and IS (10 mg/mL) was added. The retention times of each dilution were measured at 238 nm after they had been prepared in triplicate and injected into the HPLC. The mean, SD, and % RSD were estimated for each concentration.²¹ Three RIA vials containing 1 mg of SIM each were filled with 1 mL of plasma to ensure long-term stability (to achieve a concentration of 1,000 mg/mL). All three vials were put in the freezer at -20°C after the mixture had been vortexed for 5 min.

After 1, 2, and 3 weeks, the three vials were removed from the freezer. Following each interval, the drugs were taken out of the plasma, prepared for LQC, MQC, and HQC samples, and then IS (10 mg/mL) was added. To measure the retention times at 238 nm, each dilution was made in triplicate and then injected into the HPLC. The mean, SD, and % RSD were calculated for each concentration.²²

Statistical analysis. The experimental values are all reported as mean SD. The mean, SD, and percent RSD were calculated using an MS Excel worksheet. In GraphPad Prism version 7.0, the calibration curve was developed and the results were compared using Tukey's multiple comparison test. (GraphPad Software, Inc., CA). A significant difference in the collected data was shown by a *p*-value of <0.05 .

RESULTS AND DISCUSSION

Specificity, Linearity, and Range

Since no other peak was found in the chromatogram of the blank plasma sample at the drug's retention time and lambda max, the developed method was verified to be drug molecule specific. As a result, it was determined that the chosen method

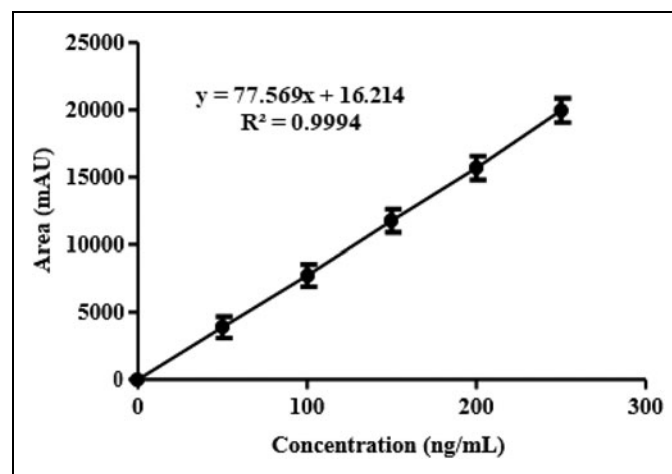


Fig. 2. Calibration curve of SIM.

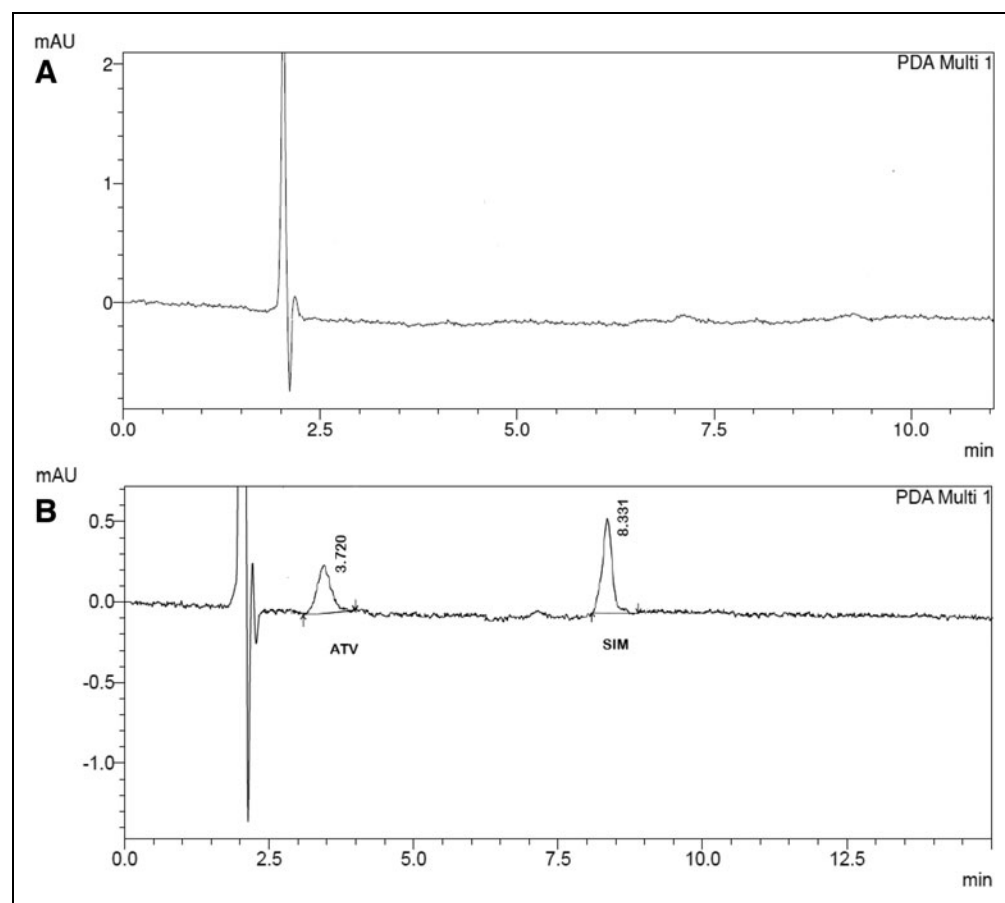


Fig. 3. (A) Chromatogram of blank plasma, (B) chromatogram of ATV (RT. 3.720) and SIM (RT. 8.331) in rat plasma. RT, retention time.

was drug specific.²³ The plasma-based calibration curve was shown to be linear in the 50–250 ng/mL range. The regression coefficient (r^2) was determined to be 0.9994, indicating linearity. The calibration curve shown in *Figure 2*, and the chromatogram of blank plasma and SIM in rat plasma are given in *Figure 3*:

Table 1. Results of Accuracy Study

Level	Concentration of sample solution (ng/mL)	Total concentration of solution, actual (ng/mL)	Concentration of drug recovered (ng/mL), (n = 5)	% Recovery	Mean % recovery
LQC	50	120	118.7 ± 0.65	98.91 ± 0.95	99.88 ± 0.82
MQC	50	150	152.7 ± 1.21	101.8 ± 0.86	
HQC	50	180	178.1 ± 0.96	98.94 ± 0.65	

HQC, high quantified concentration; LQC, lower quantified concentration; MQC, medium quantified concentration.

Accuracy

The result showed that the mean percentage recovery for all three levels was within the standard ranges, that is, 95%–105%. This shows that the developed method was accurate under the study’s test conditions, as shown in *Table 1*:

Precision

The precision of developed techniques was determined by calculating the % RSD for the six LQC, MQC, and HQC solution determinations at the intraday, interday, and interanalyst levels under the same experimental studies. The percentage relative deviation was <2%, indicating that the developed technique was precise under the specified test conditions, as shown in *Table 2*:

Stability Study of Plasma Samples

For the LQC, MQC, and HQC samples, the stability study was conducted for spiking samples of SIM in plasma at three different levels, including short term (*Table 3*), freeze-thaw cycles (*Table 4*), and long term (*Table 5*). In all cases, the results indicated that more than 95% of the drug was recovered, with an RSD <2%. These studies’ results showed that drugs in plasma samples were stress stable and long-term storage stable.²⁴

Table 2. Results of Precision Study											
Parameter	Level	Concentration (ng/mL)	Area 1 (cm ²)	Area 2 (cm ²)	Area 3 (cm ²)	Area 4 (cm ²)	Area 5 (cm ²)	Area 6 (cm ²)	Mean (cm ²)	SD	RSD (%)
Intra-day											
1 h	LQC	120	9,258.81	9,196.52	9,296.43	9,125.23	9,189.34	9,279.21	9,224.257	65.14226	0.706206
	MQC	150	11,825.32	11,956.27	11,910.82	11,892.83	11,781.88	11,835.36	11,867.08	64.094	0.540099
	HQC	180	13,951.2	13,767.23	13,876.84	13,938.89	13,837.14	13,638.87	13,835.03	117.5674	0.849781
2 h	LQC	120	9,263.62	9,352.51	9,515.45	9,365.25	9,264.34	9,159.6	9,320.128	121.0867	1.299196
	MQC	150	11,756.55	11,896.45	11,874.26	11,795.25	11,668.75	11,885.63	11,812.82	89.77898	0.760013
	HQC	180	13,841.24	13,552.45	13,795.48	13,896.56	13,696.84	13,759.36	13,756.99	121.2597	0.881441
3 h	LQC	120	9,256.45	9,357.56	9,284.45	9,454.15	9,354.54	9,248.45	9,325.933	78.49913	0.841729
	MQC	150	11,854.45	11,956.54	11,695.21	11,954.45	11,768.85	11,865.74	11,849.21	103.0239	0.869458
	HQC	180	13,769.56	13,954.42	13,659.78	13,759.69	13,896.65	13,856.87	13,816.16	106.8334	0.77325
Interday											
Day 1	LQC	120	9,258.81	9,196.52	9,296.43	9,125.23	9,189.34	9,279.21	9,224.257	65.14226	0.706206
	MQC	150	11,825.32	11,956.27	11,910.82	11,892.83	11,781.88	11,835.36	11,867.08	64.094	0.540099
	HQC	180	13,951.22	13,767.23	13,876.84	13,938.89	13,837.14	13,638.87	13,835.03	117.5714	0.849809
Day 2	LQC	120	9,364.56	9,256.45	9,348.85	9,485.74	9,394.78	9,457.55	9,384.655	82.16654	0.875541
	MQC	150	11,958.58	11,896.45	11,826.54	11,964.34	11,863.45	11,725.86	11,872.54	89.57171	0.754445
	HQC	180	13,894.56	13,856.57	13,758.25	13,964.75	13,899.45	13,589.75	13,827.22	134.6675	0.97393
Day 3	LQC	120	9,353.36	9,245.51	9,459.59	9,354.29	9,265.65	9,489.56	9,361.327	98.77244	1.055112
	MQC	150	11,796.54	11,865.63	11,794.56	11,855.65	11,795.45	11,954.49	11,843.72	63.03176	0.532196
	HQC	180	13,769.56	13,954.42	13,659.78	13,759.69	13,896.65	13,856.87	13,816.16	106.8334	0.77325
Intermediate precision (interanalyst)											
Analyst 1	LQC	120	9,258.81	9,196.52	9,296.43	9,125.23	9,189.34	9,279.21	9,224.257	65.14226	0.706206
	MQC	150	11,825.32	11,956.27	11,910.82	11,892.83	11,781.88	11,835.36	11,867.08	64.094	0.540099
	HQC	180	13,951.22	13,767.23	13,876.84	13,938.89	13,837.14	13,638.87	13,835.03	117.5714	0.849809
Analyst 2	LQC	120	9,156.45	9,265.12	9,298.62	9,156.36	9,365.24	9,456.75	9,283.09	117.9565	1.27066
	MQC	150	11,586.55	11,656.45	11,825.59	11,789.41	11,796.85	11,789.56	11,740.74	95.89513	0.816773
	HQC	180	13,895.54	13,956.78	13,756.45	13,896.95	13,756.36	13,696.96	13,826.51	103.2568	0.746803
Analyst 3	LQC	120	9,355.55	9,268.45	9,556.63	9,268.56	9,355.36	9,389.21	9,365.627	105.9345	1.131099
	MQC	150	11,759.15	11,869.46	11,789.78	11,896.45	11,815.78	11,911.85	11,840.41	61.41869	0.518721
	HQC	180	13,694.44	13,965.86	13,756.12	13,896.63	13,737.65	13,864.96	13,819.28	105.6343	0.764398

RSD, relative standard deviation; SD, standard deviation.

Table 3. Short-Term Stability for Plasma Samples of Simvastatin

Actual concentration of drug (ng/mL)	Area 1 (cm ²)	Area 2 (cm ²)	Area 3 (cm ²)	Mean (cm ²)	SD	RSD (%)	Amount of drug recovered in plasma sample (ng/mL)	Recovery (%)
1 h								
120 (LQC)	9,265.78	9,156.45	9,365.56	9,262.597	104.5913	1.129179	119.21	99.34
150 (MQC)	11,486.26	11,569.78	11,656.48	11,570.84	85.11495	0.735599	148.97	99.31
180 (HQC)	13,756.78	13,886.48	13,785.59	13,809.62	68.10641	0.493181	177.80	98.77
2 h								
120 (LQC)	9,159.41	9,252.51	9,368.79	9,260.237	104.9036	1.13284	119.18	99.31
150 (MQC)	11,695.26	11,656.95	11,597.42	11,649.88	49.30203	0.423198	149.99	99.99
180 (HQC)	13,896.42	13,796.49	13,965.52	13,886.14	84.98231	0.611994	178.82	99.34
3 h								
120 (LQC)	9,365.64	9,258.45	9,469.34	9,364.477	105.4498	1.126062	120.52	100.43
150 (MQC)	11,469.42	11,582.65	11,695.59	11,582.55	113.085	0.976339	149.12	99.41
180 (HQC)	13,965.46	13,869.69	13,759.54	13,864.9	103.0436	0.743198	178.55	99.19

Table 4. Freeze-Thaw Stability for Plasma Samples of Simvastatin

Actual concentration of drug (ng/mL)	Area 1 (cm ²)	Area 2 (cm ²)	Area 3 (cm ²)	Mean (cm ²)	SD	RSD (%)	Amount of drug recovered in plasma sample (ng/mL)	Recovery (%)
Cycle 1								
120 (LQC)	9,236.25	9,363.68	9,169.32	9,256.417	98.73689	1.066686	119.13	99.27
150 (MQC)	11,469.62	11,569.45	11,653.56	11,564.21	92.08189	0.796266	148.89	99.26
180 (HQC)	13,756.35	13,896.63	13,664.36	13,772.45	116.9687	0.849295	177.36	98.53
Cycle 2								
120 (LQC)	9,296.36	9,369.64	9,595.49	9,420.497	155.915	1.655061	121.25	101.04
150 (MQC)	11,394.39	11,269.94	11,496.29	11,386.87	113.3621	0.99555	146.60	97.73
180 (HQC)	13,964.62	13,869.34	13,795.89	13,876.62	84.60003	0.609659	178.70	99.27
Cycle 3								
120 (LQC)	9,169.56	9,346.97	9,267.93	9,261.487	88.88034	0.959677	119.20	99.33
150 (MQC)	11,469.63	11,536.96	11,695.75	11,567.45	116.1019	1.003695	148.93	99.28
180 (HQC)	13,569.61	13,791.34	13,694.47	13,685.14	111.1591	0.812261	176.23	97.90

Table 5. Long-Term Stability for Plasma Samples of Simvastatin

Actual concentration of drug (ng/mL)	Area 1 (cm ²)	Area 2 (cm ²)	Area 3 (cm ²)	Mean (cm ²)	SD	RSD (%)	Amount of drug recovered in plasma sample (ng/mL)	Recovery (%)
Week 1								
120 (LOQ)	9,136.45	9,256.78	9,315.45	9,236.227	91.25283	0.987988	118.87	99.05
150 (MQC)	11,369.29	11,496.45	11,654.15	11,506.63	142.7026	1.240177	148.14	98.76
180 (HQC)	13,695.15	13,956.95	13,865.14	13,839.08	132.8313	0.959827	178.22	99.01
Week 2								
120 (LOQ)	9,365.95	9,189.58	9,268.78	9,274.77	88.33745	0.952449	119.37	99.47
150 (MQC)	11,269.36	11,369.15	11,455.75	11,364.75	93.27275	0.82072	146.31	97.54
180 (HQC)	13,569.36	13,776.95	13,645.94	13,664.08	104.9776	0.768274	175.96	97.75
Week 3								
120 (LOQ)	9,268.96	9,278.38	9,136.63	9,227.99	79.26015	0.85891	118.76	98.96
150 (MQC)	11,363.54	11,275.36	11,415.45	11,351.45	70.82322	0.623913	146.14	97.42
180 (HQC)	13,695.63	13,862.39	13,865.15	13,807.72	97.08548	0.703124	177.81	98.78

LOD and LOQ

LOD and LOQ were found in rat plasma to be 0.12 and 0.38 ng/mL, respectively. These showed that the method was sensitive for the detection of the drug at lower concentrations.

System Suitability

According to usage, a chromatographic system's suitability and effectiveness are examined using a system suitability test. The tailing factor for all peaks, including SIM and ATV peaks, did not exceed two to show good peak regularity (acceptance limits <2) and the number of theoretical plates were always >2,000 in all chromatographic runs to ensure good column efficiency throughout the developed separation process shown in Table 6.¹⁵

Table 6. Results of System Suitability Parameters

Sr. no.	Parameter	SIM	ATV
1.	Theoretical plates	7,853.56 ± 15.11	3,869.34 ± 11.87
2.	HETP	35.21 ± 2.41	18.31 ± 2.11
3.	Tailing factor	1.35 ± 0.32	1.28 ± 0.29

ATV, atorvastatin; HETP, height equivalent to theoretical plate; SIM, simvastatin.

CONCLUSION

The work was carried out to develop a cost-effective, easy, sensitive, accurate, and precise bioanalytical method for quantifying SIM in rat plasma. The percentage recovery of SIM from plasma samples was 95%–105%, indicating excellent recovery. The percentage RSD of samples with various concentrations used for intraday and intermediate precision studies was determined to be <2%, and system suitability studies revealed that the method was repeatable and robust. When compared to other methods for determining SIM in biological samples, the method also significantly improves drug recovery from plasma samples, has lower linearity and range, and lowers LOQ and LOD values. The developed method can be used to study the pharmacokinetics and biodistribution of the drug in SIM or bulk form in different pharmaceutical formulations.

ACKNOWLEDGMENT

Authors are thankful to Central Instrumentation facility of Lovely Professional University for providing analytical support.

AUTHORS' CONTRIBUTIONS

Conception: constructing an idea or hypothesis for research and/or article (Hardeep, N.K.P.). Design: planning

the methods to generate hypothesis, or to reach the conclusion (N.K.P. and S.K.S.). Supervision: organizing and supervising the course of the project or the article and taking the responsibility (N.K.P. and S.K.S.). Resources: providing personnel, environmental and financial support, and equipment and instruments that are vital for the project (Hardeep, B.K., and D.S.B.). Materials: biological materials, reagents, and referred patients (Hardeep, N.K.P., L.C., U.G., and D.S.B.). Data collection and/or processing: taking responsibility in the execution of experiments, patient follow-up, and data management and reporting (Hardeep, N.K.P., L.C., and B.K.).

Analysis and/or interpretation: taking responsibility in logical interpretation and presentation of the results (N.K.P., S.K.S., B.K., and U.G.). Literature search: taking responsibility for conducting literature search (Hardeep, L.C., U.G., and D.S.B.). Writing article: taking responsibility in the construction of the entire or a substantial part of the article (Hardeep, N.K.P., and L.C.). Critical review: reviewing the article before submission not only for spelling and grammar but also for its intellectual content. (N.K.P., S.K.S., B.K., and U.G.).

ETHICAL APPROVAL

The study procedure was conducted at Lovely Professional University, School of Pharmaceutical Sciences and approved by Institutional Animal Ethics Committee (protocol no: LPU/IAEC/2022/04).

DISCLOSURE STATEMENT

No competing financial interests exist.

FUNDING INFORMATION

No funding was received for this article.

REFERENCES

- Pandey NK, Singh SK, Ghosh D, et al. Method development and validation for simultaneous estimation of glimepiride and simvastatin by using reversed phase high-performance liquid chromatography. *Res J Pharm Technol* 2020; 13(4):1655–1659.
- Vladutiu GD. Genetic predisposition to statin myopathy. *Curr Opin Rheumatol* 2008;20(6):648–655.
- Sathasivam S, Lecky B. Statin induced myopathy. *BMJ* 2008;337(7679):1159–1162.
- 2020 Alzheimer's disease facts and figures. *Alzheimers Dement* 2020;16(3): 391–460.
- Deture MA, Dickson DW. The neuropathological diagnosis of Alzheimer's disease. *Mol Neurodegener* 2019;14(1):1–18.

- Phillips PS, Haas RH. Statin myopathy as a metabolic muscle disease. *Expert Rev Cardiovasc Ther* 2008;6(7):971–978.
- Kheirallah M, Almshaly H. Simvastatin, dosage and delivery system for supporting bone regeneration, an update review. *J Oral Maxillofac Surg Med Pathol [Internet]* 2016;28(3):205–209; doi: 10.1016/j.ajoms.2015.10.005
- Liu M, Su X, Li G, et al. Validated UPLC-MS/MS method for simultaneous determination of simvastatin, simvastatin hydroxy acid and berberine in rat plasma: Application to the drug-drug pharmacokinetic interaction study of simvastatin combined with berberine after oral administration. *J Chromatogr B Analyt Technol Biomed Life Sci [Internet]* 2015;1006:8–15; doi: 10.1016/j.jchromb.2015.09.033
- Auti P. Bioanalytical method development, validation and its application in bioanalytical method development, validation and its application in pharmacokinetic studies of simvastatin in the presence of piperine in rats *Drug Dev Ind Pharm* 2019; doi: 10.1080/03639045.2019.1569034
- Pandey NK, Singh SK, Gulati M, et al. Overcoming the dissolution rate, gastrointestinal permeability and oral bioavailability of glimepiride and simvastatin co-delivered in the form of nanosuspension and solid self-nanoemulsifying drug delivery system: A comparative study. *J Drug Deliv Sci Technol [Internet]* 2020;60(May):102083; doi: 10.1016/j.jddst.2020.102083
- European Medicines Agency. ICH guideline M10 on bioanalytical method validation. *Sci Med Health* 2019;44(March):57.
- Kumar R, Kumar R, Khursheed R, et al. Development and validation of RP-HPLC method for estimation of fisetin in rat plasma. *South Afr J Botany* 2021;140: 284–289.
- Guy RC. International Conference on Harmonisation. In: *Encyclopedia of Toxicology: Third Edition* 2014;2(November 1994); pp. 1070–1072. Available from: <https://www.elsevier.com/books/encyclopedia-of-toxicology/wexler/978-0-12-386454-3> [Last accessed: October 20, 2022].
- Kumar V, Singh SK, Gulati M, et al. Development and validation of a simple and sensitive spectrometric method for estimation of azithromycin dihydrate in tablet dosage forms: Application to dissolution studies. *Curr Pharm Anal* 2013; 9(3):310–317.
- Khursheed R, Wadhwa S, Kumar B, et al. Development and validation of RP-HPLC based bioanalytical method for simultaneous estimation of curcumin and quercetin in rat's plasma. *South Afr J Botany [Internet]* 2021;000; doi: 10.1016/j.sajb.2021.12.009
- Awasthi A, Kumar A, Kumar R, et al. RP-HPLC method development and validation for simultaneous estimation of mesalamine and curcumin in bulk form as well as nanostructured lipid carriers. *South Afr J Botany [Internet]* 2022;000; doi: 10.1016/j.sajb.2022.05.044
- Bhaskaran NA, Kumar L, Reddy MS, et al. An analytical "quality by design" approach in RP-HPLC method development and validation for reliable and rapid estimation of irinotecan in an injectable formulation. *Acta Pharm* 2021;71(1): 57–79.
- ICH Q1A(R2). International Conference on Harmonization (ICH). Guidance for industry: Q1A(R2) Stability testing of new drug substances and products. *ICH Harmonised Tripartite Guideline* 2003;4(February); p. 24. Available from: <https://database.ich.org/sites/default/files/Q1A%28R2%29%20Guideline.pdf> [Last accessed: August 11, 2022].
- Reddy VK, Swamy N, Rathod R, et al. A bioanalytical method for eliglustat quantification in rat plasma. *J Chromatogr Sci* 2019;57(7):600–605.
- Challa BR, Boddu SHS, Awen BZ, et al. Development and validation of a Sensitive bioanalytical method for the quantitative estimation of Pantoprazole in human plasma samples by LC-MS/MS: Application to bioequivalence study. *J Chromatogr B Analyt Technol Biomed Life Sci [Internet]* 2010;878(19):1499–1505; doi: 10.1016/j.jchromb.2010.03.049
- Barfield M, Wheller R. Use of dried plasma spots in the determination of pharmacokinetics in clinical studies: Validation of a quantitative bioanalytical method. *Anal Chem* 2011;83(1):118–124.
- Nowatzke W, Woolf E. Best practices during bioanalytical method validation for the characterization of assay reagents and the evaluation of analyte stability in assay standards, quality controls, and study samples. *AAPS J* 2007;9(2):117–122.

23. Kapoor B, Gupta R, Gulati M, et al. High-performance liquid chromatography and liquid chromatography/mass spectrometry studies on stress degradation behavior of sulfapyridine and development of a validated, specific, stability-indicating HPLC assay method. *Assay Drug Dev Technol* 2020;18(3):119-133.
24. Blessy M, Patel RD, Prajapati PN, et al. Development of forced degradation and stability indicating studies of drugs—A review. *J Pharm Anal [Internet]* 2014; 4(3):159-165; doi: 10.1016/j.jppha.2013.09.003

Address correspondence to:
Narendra Kumar Pandey, PhD
School of Pharmaceutical Sciences
Lovely Professional University
Phagwara 144411
India

E-mail: herenarendra4u@gmail.com

Abbreviations Used

ACN = acetonitrile
AD = Alzheimer's disease
ATV = atorvastatin
EDTA = ethylene diamine tetra acetic acid
HETP = height equivalent to theoretical plate
HQC = high quantified concentration
IS = internal standard
LC-MS = liquid chromatography and mass spectrometry
LDL = low-density lipoprotein
LOD = limit of detection
LOQ = limit of quantification
LQC = lower quantified concentration
MQC = medium quantified concentration
RIA = radioimmunoassay
RP-HPLC = reverse-phase high-performance liquid chromatography
RSD = relative standard deviation
RT = retention time
SD = standard deviation
SIM = simvastatin

Development and evaluation of Simvastatin based SNEDDS for treatment of Alzheimer's disease

Hardeep | Narendra Kumar Pandey

Lovely Professional University, Phagwara,
India

Correspondence

Hardeep, Lovely Professional University,
Phagwara, India.
Email: hardeep3983@gmail.com

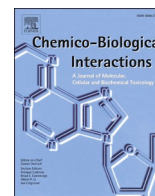
Abstract

Background: The purpose of this research work to improve solubility and bioavailability of Simvastatin using self nano-emulsifying drug delivery system (SNEDDS) for treatment the Alzheimer's disease.

Method: Self emulsifying property of various oils including essential oils was evaluated with suitable surfactants and co-surfactants. Validation of method for accuracy, repeatability, Interday and intraday precision, ruggedness, and robustness were within the acceptable limits. The liquid SNEDDS was prepared and optimized using ternary phase diagram, thermodynamic, centrifugation and cloud point studies.

Result: The globule size of optimized formulations was less than 200 nm which could be acceptable nanoemulsion size range. The mean droplet size, drug loading, PDI and zeta potential were found to be 141.0 nm, 92.22%, 0.23 and -10.13 mV and 153.5nm, 93.89%,0.41 and -11.7 mV and 164.26 nm, 95.26%, 0.41 and -10.66mV respectively. The best formulations were subjected to FESEM for surface morphology.

Conclusion: Formulation development, and evaluation of simvastatin loaded self nano-emulsifying drug delivery system (SNEDDS) for treatment the Alzheimer's disease were carried out.



Review Article

Harnessing the dual role of polysaccharides in treating gastrointestinal diseases: As therapeutics and polymers for drug delivery



Leander Corrie^a, Monica Gulati^{a,b}, Ankit Awasthi^a, Sukriti Vishwas^a, Jaskiran Kaur^a, Rubiya Khursheed^a, Omji Porwal^c, Aftab Alam^d, Shaik Rahana Parveen^a, Hardeep Singh^a, Dinesh Kumar Chellappan^e, Gaurav Gupta^{f,g,h}, Papat Kumbharⁱ, John Disouzaⁱ, Vandana Patravale^j, Jon Adams^b, Kamal Dua^{b,k}, Sachin Kumar Singh^{a,b,*}

^a School of Pharmaceutical Sciences, Lovely Professional University, Phagwara, 144411, Punjab, India

^b Faculty of Health, Australian Research Centre in Complementary and Integrative Medicine, University of Technology Sydney, Ultimo, NSW 2007, Australia

^c Department of Pharmacognosy, Faculty of Pharmacy, Tishk International University, Erbil, 44001, KRG, Iraq

^d Department of Pharmacognosy, College of Pharmacy, Prince Sattam Bin Abdulaziz University, Al Kharj, 11942, Saudi Arabia

^e Department of Life Sciences, School of Pharmacy, International Medical University, Bukit Jalil, 57000, Kuala Lumpur, Malaysia

^f School of Pharmacy, Suresh Gyan Vihar University, Mahal Road, Jagatpura, Jaipur, India

^g Department of Pharmacology, Saveetha Dental College, Saveetha Institute of Medical and Technical Sciences, Saveetha University, Chennai, India

^h Uttaranchal Institute of Pharmaceutical Sciences, Uttaranchal University, Dehradun, India

ⁱ Tatyasaheb Kore College of Pharmacy, Warananagar, Tal: Panhala, Kolhapur, Maharashtra, 416113, India

^j Department of Pharmaceutical Sciences and Technology, Institute of Chemical Technology, Matunga, Mumbai, Maharashtra, 400019, India

^k Discipline of Pharmacy, Graduate School of Health, University of Technology Sydney, Ultimo NSW, 2007, Australia

ARTICLE INFO

Keywords:

Colorectal diseases
Colon targeted delivery
Nanoparticles
Microspheres

ABSTRACT

Polysaccharides (PS) represent a broad class of polymer-based compounds that have been extensively researched as therapeutics and excipients for drug delivery. As pharmaceutical carriers, PS have mostly found their use as adsorbents, suspending agents, as well as cross-linking agents for various formulations such as liposomes, nanoparticles, nanoemulsions, nano lipid carriers, microspheres etc. This is due to inherent properties of PS such as porosity, steric stability and swellability, insolubility in pH. There have been emerging reports on the use of PS as therapeutic agent due to its anti-inflammatory and anti-oxidative properties for various diseases. In particular, for Crohn's disease, ulcerative colitis and inflammatory bowel disease. However, determining the dosage, treatment duration and effective technology transfer of these therapeutic moieties have not occurred. This is due to the fact that PS are still at a nascent stage of development to a full proof therapy for a particular disease. Recently, a combination of polysaccharide which act as a prebiotic and a probiotic have been used as a combination to treat various intestinal and colorectal (CRC) related diseases. This has proven to be beneficial, has shown good *in vivo* correlation and is well reported. The present review entails a detailed description on the role of PS used as a therapeutic agent and as a formulation pertaining to gastrointestinal diseases.

1. Introduction

A broad category of polymeric substances with natural (animal, plant, and algal) origins called polysaccharides (PS) are produced by the glycosidic interaction of monosaccharides. The monosaccharide units are mainly composed of D-galactose, L-galactose, D-fructose, D-glucose, D-xylose, D-mannose, and L-arabinose subunits [1]. PS may have a linear or branching architecture, depending on the type of monosaccharide unit. PS contain a variety of reactive groups, such as hydroxyl, amino, and

carboxylic acid groups, which further suggests the potential for chemical modification [2]. The diversity of PS is further increased by the fact that their molecular weight can range from hundreds to thousands of daltons. Moreover, PS possess many other properties such as biocompatibility, biodegradability, easy alteration in their solubility and modification of their branch chain [3]. Furthermore, PS have been extensively researched upon for drug delivery due to their ability to get triggered by change in pH, alteration in gut microflora, aid in pressure and time dependent release of the drug, which could help in the development of pulsatile release drug delivery systems [4]. Among all the PS, the most

* Corresponding author. School of Pharmaceutical Sciences, Lovely Professional University, Phagwara, 144411, Punjab, India.

E-mail address: singhsachin23@gmail.com (S.K. Singh).

<https://doi.org/10.1016/j.cbi.2022.110238>

Received 16 August 2022; Received in revised form 27 September 2022; Accepted 21 October 2022

Available online 25 October 2022

0009-2797/© 2022 Elsevier B.V. All rights reserved.

Abbreviations

5-ASA	5-Aminosalicylic Acid
Caco-2	Colon carcinoma
CD 80, 86	Cluster differentiation 80, 86
FCP	fecal calprotectin
HCT	Colorectal Carcinoma
IL-	Interleukin
iNOS	Inducible nitric oxide synthase
MAPK	Mitogen-activated protein kinase
MCF-7	Michigan Cancer foundation-7
NFκβ	Nuclear factor-κB
PGE2	Prostaglandin E ₂
PI3K	phosphatidylinositol-3 kinase
PLGA	Poly(lactic-co-glycolic acid)
TNF	Tumor Necrosis Factor
XG-PNVP	Xanthan gum polyvinyl pyrrolidone

widely studied PS include chitosan, pectin, hydroxypropyl methyl cellulose, guar gum and xanthan gum [5].

Owing to their versatility, PS have been extensively studied in the development of various drug delivery systems. Such as, PS have found their usage in parenteral drug delivery [6], ocular drug delivery [7] and topical drug delivery [8]. These have found their uses in conventional drug delivery systems such as tablets and capsules as well as novel drug delivery systems such as liposomes, micelles, nanoemulsions [9]. Most of the drug delivery systems developed, are majorly used for the treatment of colorectal diseases such as inflammatory bowel syndrome, Crohn's disease, amoebiasis, and CRC. The techniques used in the preparation of these drug delivery systems ranges from melt granulation technique and direct compression for conventional dosage forms to covalent cross-linking, metal polymer cross-linking, electrostatic cross-linking and hydrophobic cross-linking for novel drug delivery systems [10]. Due to their surface modification, PS such as dextran and heparin have been recognized as stealth coating material [11]. Additionally, numerous studies show that PS including chitosan, hyaluronic acid, and chondroitin sulphate have ligand binding properties [12]. PS are also considered to be reducing sugars and showed their versatility to form cross-links. Alginate is a best example of PS that is able to form ionic cross-links [13]. Moreover, PS also exhibit the ability of being swellable in aqueous environment facilitating them to be actively involved in the formulation of oral colon targeting agents. An example of this includes gum-based PS such as guar gum and xanthan gum that are known for their swellability [14]. Owing to aforementioned properties, PS have been used as a pharmaceutical carrier in drug delivery, some examples wherein PS have been used in formulations include metallic nanoparticles [15,16], mini tablets [17–19], microspheres [20], liposomes [21] and implantable devices [22].

It is crucial to design functional drug delivery system that react to the inherent disease state in order to provide active targeting or self-degradation activities. Enabling for preferential uptake of the transport by the reticuloendothelial system reduces the carrier's absorption and limits the therapeutic efficacy of the medicine because PS-based transporters can be non-specifically identified and adsorbed by plasma proteins [23]. In order to obtain particular identification and adherence to a particular disease state, it is important to change the structural formulation of PS at molecular level. The technique, therefore involves, functionalization of these drug delivery system to incorporate a functionalizing agent as well as the PS which possess a challenge to formulation scientists.

To overcome such challenges, researchers have actively been involved in the development of PS as therapeutic moieties. This has also enabled to decrease the load on the drug delivery system that would

otherwise incorporate the PS and functionalized polymer which would have led to improper synthesis, stability related aspects and difficulty in scale up. A wide range of properties of PS have particularly enabled them to be developed as therapeutic agents owing to their properties of anti-inflammatory [24], antidiabetic [25], anticarcinogenic [26] and antioxidative properties [27]. PS are known to act via the PI3K/AKT signaling pathway, MAPK pathway, and endocytosis pathway which are majorly linked to various metabolic diseases [28]. It is also understood that PS have a role in short chain fatty acid synthesis that could alter the gut microbiota and act via the gut brain axis, highlighting the role of PS to treat metabolic diseases apart from colorectal diseases [29]. Numerous PS have antimicrobial properties as well. For instance, it is thought that the cidal properties of chitosan are caused by a potent contact between the protonated amines and the negatively charged bacterial cell wall [30]. It is known that some PS can lessen inflammation. As an example, heparin (formed by disaccharides of β-D-glucopyranosiduronic acid or -L-idopyranosiduronic acid connected to N-acetyl or N-sulfo-D glucosamine) has the highest opposite charge as compared to any PS, that enables its interaction with a variety of proteins [31].

The present review comprehensively entails the role of PS as therapeutics as well as carrier in developing formulations to treat colonic diseases. The mechanism of PS to treat different types of colonic diseases with or without probiotics (synbiotics) has been discussed in detail in the subsequent reactions. Diving deep into the review, the role of PS in the development of various drug delivery system to treat colonic disease are also extensively described with some case studies. The article also covers some of the patents filed in this area in order to highlight the commercial importance of this research for industries and benefitting the society.

2. PS used for various colorectal and intestinal diseases

2.1. Ulcerative colitis (UC)

UC is a long-term immune-mediated inflammatory disease of the large intestine that is most commonly linked with rectal inflammation, but can also affect other parts of the colon. Rectal involvement is present in about 95% of adult patients with UC during its diagnosis [32]. PS have shown their role as anti-inflammatory agent and reported to regulate intestinal barrier function through *in vitro* and *in vivo* methods that are discussed below.

2.1.1. Cell line studies

The literature on the usage of PS for UC is limited. However, there are some studies that highlight PS role in UC. Wang and coworkers studied the role of a PS cultured mycelium of *Hericium erinaceus* using Caco-2 cell lines as models. The study confirmed that the PS was successful in increasing the activity of SOD and reactive oxygen species and oxygen damaged. As a result, this improved the mitochondrial function [33]. In another study, *Tremella fuciformis* PS (TFP) effect on Caco-2 cell lines was studied. It was found out that, TFP reduced the levels of pro-inflammatory cytokines and increased the expression of genes and proteins of the mucus and intestinal barrier respectively [34].

2.1.2. Animal studies

The important animal models used to study UC include acetic acid induced UC, dextran sulphate induced UC and carrageenan-induced colitis. In one study that was carried out to understand the degree of esterification of pectin and its effect on UC induced by dextran sulphate sodium (DSS) proved that UC mainly causes dysfunction of the mucosal barrier which leads to increase in microbial toxins entering to the intestinal layer leading to oxidative stress and activation of pro inflammatory pathways. Further, research demonstrated that plant derived pectic oligosaccharides were capable of limiting lipid peroxidation and scavenging the free radicals, which could aid in the treatment of various

immune related and metabolic disorders. Specifically, the degrees of esterification of pectin plays a role in UC. Low esterified pectin was fermented by the microbiota in the lumen while high esterified pectin was fermented by the microbiota in the proximal colon [35]. This study pointed out the early use of low esterified pectin for UC at high doses was beneficial by significantly reducing occludin and myeloperoxidase levels, IL-6 and IL-7 [36]. Using Western blotting, Horii and coworkers studied that partially hydrolyzed guar gum improves wound healing of colonic epithelial cells and boosts intestinal mucosa recovery by increasing extracellular signal regulated kinases 1 and 2 and mitogen-activated protein kinase activation. Thus, proving that guar gum could be used as a therapeutic moiety in colitis [37]. Chitosan has also been demonstrated to work as a therapeutic directly on ulcerative colitis. The upper human gastrointestinal tract (GIT) does not breakdown chitosan, therefore it can reach the colon following oral ingestion and produce a local colonic action. The effect and mechanism of chitosan on DSS-induced mice were investigated by Wang et al. It was reported that chitosan reduces disease activity index, alleviates histopathological alterations, increases tight junction protein expression, reduces TNF-expression, and regulates *Lactobacillus* and *Blautia*, spp according to the researchers [38]. Similar to chitosan, Sodium alginate, which is abundant in seaweed and mostly offers its medicinal utility of wound hemostasis was studied for its role in UC. Sodium alginate, that is made up of -D-mannuronic and -L-guluronic acids, is a by-product of extracting iodine and mannitol from kelp or sargassum. It is frequently used in medicine for its stability, solubility, tolerability, biocompatibility, and safety properties. Sodium alginate has been shown to prevent and ameliorate DSS- and 2,4,6-TNBS-induced colitis by lengthening the colon and encouraging goblet cell repair. Sodium alginate guards the upper digestive tract's injured area and prevents mucus from dissolving. It is reported that sodium alginate promotes epithelial cell migration and increases the number of goblet cells, which increases mucin production and thickens the mucus layer facilitating faster relief from colitis [39].

2.1.3. Clinical trials

In a randomized clinical trial involving 105 patients, the effect of *Plantago ovata* seeds versus mesalamine was compared to understand the maintenance of remission for UC. The study was carried out for a period of 12 months. It was concluded from the study that *Plantago ovata* was able to maintain 40% of remission and it had same efficacy as of mesalamine in the treatment of UC. Further, a significant increase in fecal butyrate levels was observed in the *Plantago ovata* group as compared to the mesalamine group [40]. Similarly, another randomized, single-blind, and positive drug parallel-controlled study was carried out on 126 UC patients to assess the efficacy of sophora colon soluble capsules versus mesalamine. The study also confirmed that membrane lesions were lesser compared to the mesalamine group and sophora was effective at higher doses respectively [41]. Seaweeds are used to produce the sulfated PS known as carrageenan. It is utilised in the food industry for its emulsifying, thickening, and stabilizing qualities and has been given the "generally regarded as safe" designation by the US Food and Drug Administration. In order to determine the impact of the ubiquitous food ingredient carrageenan on clinical recurrence rates, Bhattacharyya et al. undertook a small, randomized, double-blind, placebo-controlled, multicenter clinical trial on UC subjects. The researchers selected UC patients who were older than 18 and in clinical remission. The carrageenan-containing capsules (200 mg/day) were given to the patients randomly assigned to the carrageenan group (n = 5). Similar-looking dextrose-containing capsules were given to patients randomly assigned to the placebo group (n = 7). Participants were required to adhere to a carrageenan-free diet for the whole 12-month trial period. In contrast to patients who were on a comparable diet plus two oral capsules of carrageenan each day, they reported that UC patients who were on a carrageenan-free diet with placebo had a lower recurrence rate. Additionally, they noted that ingestion of carrageenan

increased levels of FCP and interleukin-6 (IL-6), two markers of disease activity. In terms of changes in quality-of-life scores, there was no statistically significant difference between the two groups [42].

2.2. Inflammatory bowel disease (IBD)

IBD is a chronic inflammatory disease of the GIT that includes Crohn's disease, ulcerative colitis, and other disease conditions. IBD is characterized by bouts of stomach discomfort, diarrhea, bloody stools, weight loss, and the invasion of neutrophils and macrophages that generate cytokines, proteolytic enzymes, and free radicals that cause inflammation and ulceration of the intestinal mucosa [43]. PS reduce oxidative stress by lowering the formation of oxygen free radicals such as myeloperoxidase (MPO), nitric oxide (NO), and malondialdehyde (MDA), which helps with IBD symptoms [44]. Various *in vitro* cell line, animal and clinical studies pertaining to the role of PS in treating IBD are discussed below.

2.2.1. Cell line studies

The role of PS of adlay bran (TPA) on TNF- α induced epithelial barrier dysfunction in Caco-2 cells was evaluated. To assess the intestinal epithelial barrier function, Caco-2 cells were treated with or without TPA in the absence or presence of TNF- α , and transepithelial electrical resistance (TEER) was recorded. TPA inhibited the release of pro-inflammatory factors induced by TNF- α . It also alleviated the increase in paracellular permeability, reduction in TNF- α induced upregulation of IL-8 and IL-6 expression, as well as downregulation of occludin and ZO-3 expression. It was also noticed that a significant decrease activation and protein expression of NF- κ B p65 occurred [45]. In another study involving total PS of the Sijunzi decoction (TPSJ) on the measurement of transepithelial electrical resistance (TEER) was carried out. Through Western blotting analysis, the levels of myosin light chain (MLC), phosphorylated MLC (pMLC), MLC kinase (MLCK), and nuclear factor (NF)- κ B p65 were analysed. It was understood that TPSJ significantly reduced TNF- α mediated elevation of p-MLC and MLCK expression, dysregulated the expression of claudin 1, claudin 2, ZO-3, and occludin, and mitigated TNF-induced membrane damage. Finally, TPSJ prevented NF- κ B p65 from being activated and expressed. The study highlighted the role of TPSJ improves intestinal barrier function by downregulating NF- κ B p65 pathway [46].

2.2.2. Animal studies

Diling and coworkers demonstrated that PS from *Hericium erinaceus* administered to irritable bowel syndrome (IBS) induced rats through trinitro-benzene-sulfonic acid (TNBS) enema (150 mg/kg) improved the colonic mucosa, damage activity, common morphous, and tissue damage index scores ($p < 0.05$). The activities of myeloperoxidase (MPO) were reduced. Inflammatory factors, such as serum cytokines, Foxp3 and interleukin (IL)-10, were differentially expressed in the colonic mucosa of IBD rats, with NF- κ B p65 and tumour necrosis factor (TNF)- being lowered ($p < 0.05$) and T cells being activated ($p < 0.05$) [47].

PS and their anti-inflammatory activities are closely linked to their chemical structures, particularly their monosaccharide compositions, molecular weights, chain conformations, glycosidic connections types and positions, as well as sulphate concentrations. One study indicated that PS with 9.42% of PS exhibited higher nitric oxide (NO) inflammatory activity in mice [48]. Another key aspect responsible for PS anti-inflammatory action is chain conformation. In general, polymers can take on a variety of chain conformations in solution, including random coil, duplex or triplex, rod-like, and sphere-like geometries. PS are said to be more active in the triple-helix configuration [49]. For example, β -glucans with higher immunomodulatory activity are frequently found in a triple-helix configuration. According to additional studies, the triple-helix conformation of β -glucans may be better identified by immune cell receptors due to their increased stiffness, thereby providing better therapeutic activity [50]. Similarly, the presence of

specific types of monosaccharides may have a significant impact on PS anti-inflammatory effects. Glucans, for example, are homopolymers of D glucose that have shown to have anti-inflammatory properties [51].

2.2.3. Clinical trials

In a clinical investigation including 116 children, 57 of them received the special diet made up of comminuted chicken and partially hydrolyzed guar gum (PHGG) and 59 of whom received the control diet, the effects of the special diet on humans were examined. It was reported that the stool consistency, abdominal pain and IBS was alleviated by PHGG administration respectively [52]. In another study, the influence of chaga mushroom extract on the lymphocytes of 20 patients having IBS was studied. The extract was successful in reducing DNA damage within the patient group ($p < 0.001$) and prevented oxidative stress in the lymphocytes from IBS patients respectively [53]. All these properties of PS therefore, warrant it to have versatility in treatment of various inflammatory diseases pertaining to colon.

2.3. Colorectal cancer (CRC)

With economic development, changes in modern lifestyle, particularly dietary changes, and the increasing age of populations, colorectal cancer (CRC) has become one of the malignant tumors whose incidence is increasing most rapidly, CRC also possess a threat to human life and health [54]. According to the World Health Organization, CRC is the third most prevalent cancer worldwide, with a high mortality rate and a growing incidence among people under the age of 50. The effect of PS as an anti-proliferative agent on colon cancer cells are also becoming more popular. However, very little attention is given to the use of PS for this condition [55]. There is a relationship between the chemical composition and configuration of PS with their anti-colon cancer effect of the PS [56]. Previous studies have demonstrated that PS's structural properties, such as β -(1 \rightarrow 6) links in the main chain, are crucial for their anti-colon cancer activities because they can improve the activities of immunocompetent cells or, promote tumour cell apoptosis [57].

2.3.1. Cell line studies

Sun et al. demonstrated that a PS derived from whole grass *Scutellaria barbata* (SPS2p) decreased the p-AKT/AKT ratio in HT-29 cells, implying that SPS2p suppresses the PI3K/AKT signaling pathway activation in HT-29 cells. It is well known that the PI3K/AKT signaling pathway is active in most tumour cells, and it plays a crucial role in cell proliferation and apoptosis [58]. Similarly, mitogen-activated protein kinases (MAPKs) have an effect on tumour cells, promoting cell proliferation and death [59]. One study revealed that *Ganoderma lucidum* PS (GLP) induces apoptosis in HCT-116 cells by upregulating JNK expression via the MAPK pathway. The activation of both the mitochondrial and mitogen-activated protein kinase (MAPK) pathways is linked to the apoptosis induced by GLP in human CRC cells [59]. The interaction of mitochondrial dysfunction associated with intracellular reactive oxygen species (ROS) with proteins cause induction of apoptosis [60]. The decrease of mitochondrial membrane potential has been linked to GLP-mediated apoptosis in HCT-116 cells. GLP changed the mitochondrial transmembrane potential, resulting in the release of cytochrome C and increased production of BAX/BCL-2, caspase 3, and poly (ADP-ribose), all of which led to cell death [61]. In eukaryotic cells, any disruption of the cell cycle (G1-S-G2-M) causes hindrance of the entire replication process [62]. In one study, it was found out that in colon cancer cells, a new PS known as wolfberry (*Lycium barbarum*) PS (LBP) displayed anticancer actions by inducing G0/G1 phase arrest. Changes in cell-cycle-associated proteins, cyclins, and cyclin-dependent kinases (CDKs), were understood to correspond to changes in cell-cycle distribution [63].

2.3.2. Animal studies

It is difficult to select proper animal models to induce CRC due to

variation apoptotic pathways at cellular level in animals. There are some studies wherein, PS have been reported for the treatment of CRC. In one study, 1,2 dimethyl hydrazine (DMH) was used to induce CRC in rats for 5 weeks, the effect of extracts from *Pleurotus sajor-caju* (PS1) and *Lactuca sativa* (PS2) was studied. PS were successful in downregulation of Alkaline phosphatase (ALP) and alanine aminotransferase (ALT) respectively [64]. A PS extract (PE) from cooked common beans (*P. vulgaris* L., var. Negro 8025) shown to have chemoprotective benefits in a prior investigation on azoxymethane-induced colon cancer in rats. The maximal butyrate concentration was found in the cecum due to the PE-induced short-chain fatty acid synthesis, which also enhanced the number of aberrant crypt foci (ACF), the transcriptional expression of BAX and caspase 3, and the rate of cell apoptosis. These findings suggested that PE decreased ACF and affected the expression of the colon cancer-related apoptogenic genes [65]. In another study, Luo et al. demonstrated that *Ganoderma lucidum* was effective in azoxymethane induced colorectal mice cancer by preventing colon shortening, reducing the mortality rate. According to the findings, the alleviation of CRC was caused by both the decrease of particular bacteria and the control of cancer-related genes by *Ganoderma lucidum* [66].

2.3.3. Clinical studies

Most of the clinical studies involving CRC treatment uses PS K which is a mushroom PS. It is mostly used as an adjuvant therapy after the course of the antineoplastic agent. In one prospective randomized clinical trial involving 207 stage II or stage III CRC patients, PS K was given at 3.0 g for 2 years. They found the 3-year survival rate to be 87.3% in the protein bound PS K group and recommended it as an adjuvant therapy in the management of CRC [67]. In another study using PS K as adjuvant therapy after 5-fluorouracil (5-FU) treatment, involving 446 patients. It was found that PS K increased the survival rate for cancer. Moreover, the PS group showed better response in various adverse effects such as loss of appetite, diarrhea, oral cavity disorders respectively [68]. It is therefore, promising that PS can be used for CRC.

2.4. Crohn's disease

Crohn's disease is a chronic inflammatory bowel illness that affects the intestinal part of the gastrointestinal system. It has a progressive and debilitating course and its incidence is reported worldwide. Several variables have been suggested in the aetiology of Crohn's disease, including a dysregulated immune system, altered microbiota, genetic predisposition, and environmental factors, but the cause of the disease remains unclear. The illness develops at a young age and always needs urgent but long-term therapy to avoid flare-ups and disease progression with intestinal consequences [69].

2.4.1. Cell line studies

PS have been mostly used as a carrier in the treatment for Crohn's disease. However, one study showed the effect of maltodextrin (MDX) on Crohn's disease. It pointed out that MDX was responsible for type 1 pilli expression and facilitated bacterial adhesion to human epithelial cell monolayers conducted on Caco-2 cell lines. These findings showed that the common dietary component MDX promotes *E. coli* adherence and reported to a mechanism through which western diets high in particular PS increase gut microbiota dysbiosis and disease vulnerability [70].

2.4.2. Animal studies

Reingold and coworkers entailed the role of peptidoglycan-PS (PGPS) on different type of mice models. NOD2 knockout mice, RICK/RIP2 knockout mice, and genetically inbred strains sensitive to inflammation were among the mice strains examined. Results revealed that CBA/J mice had the best response to PGPS, with consistently higher abdomen scores than other strains. The PGPS-injected CBA/J mice were tested 26 days after laparotomy and found to exhibit strongest

inflammation and resembled the PGPS rat model and human Crohn's disease the best [71]. All these studies suggest that PS can have a negative impact on Crohn's disease. However, the use of specific PS for this condition warrants further study. In another study by Yue et al. Crohn's disease was induced in SD rats using 2,4,6-trinitrobenzene sulfonic acid (TNBS). Wild jujube PS were administered orally at 80 mg/kg dose respectively for 14 days. Results demonstrated that wild jujube PS were successful in ameliorating disease activity index, and showed improvement in mucosal damage. The PS suppressed the inflammatory markers such as TNF- α , IL-1 β , IL-6 and MPO activity rats [72]. There has not been any specific trial using PS for the treatment of Crohn's disease using clinical based studies. This might be due to the fact that, Crohn's disease is an alternative progressive form of Inflammatory bowel disease.

2.5. Miscellaneous diseases

2.5.1. Amoebiasis

Amoebic colitis and amoebic liver abscesses are the most common clinical symptoms of *Entamoeba histolytica* infection. Ulceration and inflammation of the colon are symptoms of amoebic colitis. Amoebic colitis might be mistaken for inflammatory bowel disease due to the severity of the gut inflammation and therefore, proper diagnosis is required [73]. Amoebae bind to host cells via a galactose-binding lectin on the surface of *Entamoeba histolytica*, according to *in vitro* studies [74]. Amoebae can lyse the target cell after they make contact, employing pore-forming chemicals such as amoeba pores and phospholipases. Amoebic phagocytosis of the dead cell may occur after cell lysis. The molecular basis for these events is still a hot topic in amoebiasis research [75]. *Entamoeba histolytica* has a range of glycosidases, including sialidase, N-acetylgalactosamidase, and N-acetylglucosaminidase, which can eliminate branched PS from mucin or host cells or formulations containing PS. *Entamoeba histolytica* activates the mechanism for scavenging PS due to a lack of free carbohydrates in the colon and competition with the commensal bacteria [76]. This forms the rationale of using PS as a carrier or therapeutic in the treatment of amoebiasis and authorizes its use for this condition.

2.5.2. Constipation

Constipation is a condition that affects the intestinal tract and may cause painful, stiff, and infrequent feces. Severe constipation may compel the bowel to close, necessitating surgery in some cases [77]. There have been various studies highlighting the role of PS in the treatment of constipation with various viewpoints on the treatment using soy PS [78]. In one study involving diphenoxylate-induced constipation in mice, *Spirulina platensis* PS was used for treatment of constipation. The treatment was done for a period of 7 days. The beneficial effect of the PS resulted in improved defecation, increase of acetylcholine activity, reduction in nitric oxide concentration. The study entailed the successful development of *Spirulina platensis* PS for the treatment of constipation [79]. In another animal model, loperamide hydrochloride was induced to SD rats. The treatment using *Malus halliana* Koehne PS (MHKP) was conducted for a period of 7 days in loperamide hydrochloride induced rats. Results revealed that there was significant upregulation in the levels of gastrin, motilin, and substance P significantly ($p < 0.01$) respectively. It indicated that MHKP was effective in the treatment of functional constipation [80]. Furthermore, another PS from *Anemarrhena asphodeloides* demonstrated upregulation of gastrin, motilin and substance P in loperamide hydrochloride induced constipated rat model. The results indicated that the PS increased intestinal motility, improved water metabolism and showed excellent laxative action [81]. These preclinical studies are indicative that PS show excellent laxative effect and offer benefits by increasing intestinal motility and showing their action on the intestinal colorectal region. However, further studies are warranted. Various preclinical and clinical studies on the use of PS for the treatment of colorectal diseases are given in Table 1. Various

registered clinical trials in which PS has been used as therapeutics are reported in Table 2.

3. Impact of PS and probiotic combination in treatment of colorectal diseases

PS have alone been used as pharmacotherapeutic agent. However, in certain colorectal and metabolic related diseases, the gut microbiota gets altered. This leads to a condition called gut dysbiosis. During this stage, it is difficult for the PS to act on a disease state, particularly at the colonic site as there is improper balance of microorganisms to feed on the PS and show its mechanism of action [22]. Therefore, the therapeutic activity of the PS gets reduced. To overcome this, a symbiotic based approach involving the co administration and interplay of probiotics as well as prebiotics (PS) have been extensively studied. It is understood that at particular pH conditions, the microorganisms present in the formulation would be able to act on the PS and improve its therapeutic activity. This would, serve the dual purpose of replenishing the gut microbiota as well as increasing the therapeutic activity of the PS. Among all the PS, the use of inulin as prebiotic and *Lactobacillus* spp as probiotic has been extensively studied by researchers in various disease states. Table 3 Enlists various preclinical interventions where combination of PS and probiotics as symbiotic to treat colorectal diseases have been studied.

4. PS for drug delivery applications

The use of PS as a therapeutic has recently attracted much focus. However, the development of PS as mainstream for treating colorectal diseases is still speculative [146]. This is due to the understanding that PS act as special carriers for treating colorectal diseases and not treat them. Numerous studies have shown that choosing the right nano-systems or carriers and altering their physicochemical features can improve drug uptake. Carrier-based drug delivery systems can improve drug's transport through the GI barrier, protect them from enzymatic and acidic breakdown in the GI tract, and boost intraluminal drug absorption [147]. Therefore, the role of PS has been majorly focused on delivering the drug moiety to the colon rather than acting as an aid in the treatment. Previously, it was postulated that permeability through the GI tract was an inherent asset of bioactive compounds and that drug delivery systems had no or little impact on overall drug permeability [148]. Nevertheless, alternative strategies using PS have been used to improve the GI drug availability of drug in GIT have been explored over the last few decades. In addition, PS have also been used to formulate microparticles, nanoparticles based on their complexation reduction and conjugation properties. Various strategies include permeation enhancers, drug conjugation and modification, ion-pairing, micro-and nanoparticulate systems, cross-linking mechanisms, electrostatic interaction, and hydrophobic interactions [149]. Understanding these mechanisms has formed the basis for synthesizing various carrier-based drug delivery systems containing PS that has been highlighted in the subsequent section. The mechanism of drug release from PS coat is depicted in Fig. 1.

4.1. Colon targeted delivery system formulated by intra and intermolecular forces

4.1.1. Covalent cross-linking

Chemical cross-linking is commonly done to preserve the network of PS nanoparticles and reduce or inhibit dissolution of the hydrophilic polymer chains/segments into the aqueous phase while retaining the materials' biodegradability and improving bioavailability. Covalent bonds are organized between functional groups of polymeric chains in chemically cross-linked nanoparticles and gels, or they are mediated by covalent cross-linking molecules having some active moieties [150]. Under particular endogenous and external circumstances, the chemical

Table 1
Various preclinical and clinical studies on the use of PS for the treatment of colorectal diseases.

PS	Cell line model	Animal model	Human study	Treatment duration	Disease	Result	Reference
Rhamnogalacturonan	Caco-2 cells	DSS	NA	7 days	UC	Protection from macroscopic damage ↓ Cellular permeability after exposure to IL-1 β ↑ Wound healing activity	[82]
<i>Angelica Sinensis</i>	Caco-2 cells	DSS	NA	21 days	UC	↓ IL-6, IL-1 β , and TNF α Improvement in occludens 1, occludin, and claudin-1	[83]
<i>Ganoderma atrum</i>	Caco-2/DCs co-culture	DSS	NA	4 days for cell culture, 14 days for animal study	UC	↑ Co-stimulators (CD80 and CD86) Enhancement of T cell proliferation Regulation of DCs in the intestine Restoration of the expression of Atg5, Atg7 and beclin-1	[84] [85]
Aloe PS	NA	DSS	NA	7 days	Colitis	Alleviation in colonic lesion ↑ SCFA synthesis	[86]
<i>Dictyophora indusiata</i>	NA	DSS	NA	8 days	Colitis	↓ Disease activity score Relief from intestinal oxidative stress Inhibition inflammatory cytokine	[87]
Microalgae aqueous extracts	Caco-2	DSS	NA	8 days	Colitis	Alleviation from rectal bleeding, colon shortening and diarrhea ↑ Hsp-27 ↓ IL-1 β and COX-2	[88]
<i>Ziziphus jujuba</i> seed	Caco-2	TNBS	NA	28 days	Colitis	Regulation in the expression of tight junction proteins and efflux transporters ↓ <i>Bacteroidetes</i> , ↑ <i>Firmicutes</i>	[89]
β -glucan	NA	DSS	NA	7 days	Colitis	↓ Myeloperoxidase, eosinophil peroxidase and N-acetyl-b-D-glucosaminidase levels ↑ Occludin and Diamine oxidase	[90]
<i>Crataegus pinnatifida</i>	NA	DSS	NA	42 days	Colitis	↓ IL-1 β , IL-6 and TNF- α expression ↓ NF- κ B, p-I κ B α and p-IKK α / β	[91]
<i>Lonicera japonica</i> Thunb	NA	DSS	NA	9 days	Colitis	↑ Weight of immune organs ↑ IL-2, TNF- α , and IFN- γ	[92]
<i>Malva sylvestris</i>	NA	AA	NA	5 days	UC	↓ Inflammatory response	[93]
<i>Glycyrrhiza</i>	NA	DSS	NA	8 days	UC	↓ IL-1, IL-6, and TNF- α levels, intestinal permeability	[94]
<i>Angelica sinensis</i>	NA	DNBS	NA	5 days	UC	↓ MDA concentration, oxidative stress ↑ GSH levels	[95]
<i>Arctium lappa</i>	NA	DSS	NA	7 days	Colitis	↓ IL-1 β , IL-6 and TNF- α ↓ <i>Bacteroides</i> and <i>Staphylococcus</i>	[96]
Gum arabic	NA	NA	RD, CT	180 days	UC	↓ Arachidonic acid ↑ EPA and DHA and β -carotene levels	[97]
Oat Bran	NA	NA	RD, CT	168 days	UC	↑ Butyrate concentration ↓ Serum LDL levels	[98]
Pectin	NA	NA	SC, RD	5 days	UC	Mayo score lower than FMT group Delayed bacterial diversity ↑ <i>Bacteroidetes</i>	[99]
<i>Hericium erinaceus</i>	Caco-2	TNBS	NA	14 days	IBS	Improvement in tissue damaged index scores Improvement in MPO activity ↑ NF- κ B, ROS and TNF- α	[47]
<i>Lycium barbarum</i>	Caco-2	NA	NA	14 days	IBS	↑ Paracellular permeability, ↓ Transepithelial electrical resistance Prevention in the secretion of IL-8, IL-6, ICAM-1 and MCP-1	[100]
<i>Rheum tanguticum</i>	HIEC cell line	NA	NA	1 day	IBS	↑ Cell survival, SOD activity ↓ MDA, LDH activity and cell apoptosis	[101]
<i>Angelica sinensis</i>	NA	TNBS	NA	21 days	IBS	Amelioration of TNF- α TGF- β and IL-2, SOD activity	[102]
<i>Rheum tanguticum</i>	NA	TNBS	NA	5 days	IBS	↑ IFN- γ , ↓ IL-4 ↓ Th1-polarized immune response	[103]
<i>Morinda citrifolia</i>	NA	AA	NA	1 day	IBS	↓ GSH, MDA, NO $_3$ /NO $_2$, pro-inflammatory cytokines, and COX-2	[104]
<i>Digenea simplex</i>	NA	TNBS	NA	3 days	IBS	↓ MPO, proinflammatory cytokines, malondialdehyde, and nitrate/nitrite levels	[105]
<i>Poria cocos</i>	NA	TNBS	NA	7 days	IBS	↓ Pro-inflammatory cytokines ↑ Anti-inflammatory cytokines ↓ MPO activity	[106]
Fish cartilage PS	NA	NA	OP, PI	120 days	IBS	↑ Serum iron, serum ferritin Aided in the treatment of iron deficiency in patients with IBS	[107]
<i>Scutellaria barbata</i>	HT29 Cells	NA	NA	1 day	CRC	Improvement in proliferation inhibition rate Elevation in apoptosis rate ↓ Bcl-2 and FN levels	[58]
<i>Ganoderma lucidum</i>	HCT-116 cell	NA	NA	1 day	CRC	Reduction in cell viability ↑ Cell apoptosis	[108]

(continued on next page)

Table 1 (continued)

PS	Cell line model	Animal model	Human study	Treatment duration	Disease	Result	Reference
<i>Lentinus edodes</i>	HCT-116 cell, HT-29 cell	NA	NA	1 day	CRC	↑ Bax/Bcl-2, caspase-3 and poly (ADP-ribose) polymerase (PARP) Inhibition in tumor growth cells Elevation in antitumor and immunomodulatory activity	[109]
<i>Eisenia bicyclis</i>	DLD-1 colon cancer cells	NA	NA	3 days	CRC	Inhibition to the colony formation of SK-MEL-28 human melanoma cells by 32%	[57]
<i>Ganoderma atrum</i>	CT 26 cell tumor-bearing mice	NA	NA	0.6 day	CRC	↑ Immune organ index ↑ TNF- α , IL-1 β and nitric oxide	[110]
<i>Hordeum vulgare</i>	HT-29 cells	NA	NA	0.6 day	CRC	Enhancement of phosphorylation of c-Jun N-terminal kinase (JNK) Activation of caspase-8 and caspase-9	[111]
<i>Stachys floridana</i>	HT-29 cell	NA	NA	3 days	CRC	↑ Accumulation in G2/M phase ↓ Bcl-2 mRNA level ↑ Bax and p53, caspase-3	[112]
<i>Sargassum horneri</i>	Human colon cancer DLD cells	NA	NA	2 days	CRC	Inhibition to the proliferation of human colon cancer cells (DLD) in a concentration-dependent manner ↑ Accumulation of cells in G2/M phase	[113]
<i>Asterina pectinifera</i>	HT-29 cell	NA	NA	1 day	CRC	↓ MMP-1 and -2 activity ↓ Cell apoptosis	[114]
<i>Ziziphus jujuba</i>	NA	AOM/DSS	NA	91 days	CRC	Amelioration of gut dysbiosis ↓ Firmicutes/Bacteroidetes diversity	[115]
<i>Rhizopus nigricans</i>	NA	AOM/DSS	NA	70 days	CRC	↓ COX-2, β -catenin, CyclinD1 and C-Myc ↓ Ki-67, PCNA, TNF- α and IL-6	[116]
Modified apple PS	NA	DMH/DSS	NA	140 days	CRC	↓ 5% remission rate ↑ Apoptosis Inhibition of the binding of galectin 3 to its ligand	[117]
Safflower PS	HCT116	AOM/DSS	NA	102 days	CRC	↑ NF- κ B, TNF- α , NO Triggered M1 macrophage transformation ↓ Cell colony formation	[118]
<i>Dendrobium officinale</i>	NA	AOM/DSS	NA	Till induction of CRC	CRC	↓ Expression of PD-1 on CTL Infiltration of CD8 ⁺ cytotoxic T lymphocytes	[119]
PS K	NA	NA	RD, CD	365 days	CRC	Better 5-year disease free survival rate Activation in lymphokine activated killer cells	[120]
Poria PS	NA	NA	RD	15 days	Cancer related fatigue of CRC	↓ IL-6 and TNF- α Improvement in the quality of life	[121]

AA- Acetic acid; AOM- Azoxymethane; ATG-5- Autophagy related 5; ATG-7- Autophagy related 7; Bax- Apoptosis regulator; Bcl2- B cell lymphoma 2; CD8⁺ cluster of differentiation 8; CD80⁺ Cluster of differentiation 80; CD86⁺ Cluster of differentiation 86; COX-2- Cyclooxygenase-2; CRC- Colorectal cancer; CT- Controlled; CT-26- murine colorectal carcinoma cell line; Caco-2- Human colorectal adenocarcinoma cells; Caco-2/DC- Human colorectal adenocarcinoma cells/dendritic cells; DHA- docosahexaenoic acid; DLD- 1 truncated adenomatous polyposis coli protein; DMH- 1,2-dimethylhydrazine; DSS- Dextran Sulphate Sodium; EPA- Eicosapentaenoic acid; FMT- Fecal microbiota therapy; GSH- Glutathione tripeptide; HIEC- human intestinal epithelial cell line; Hsp-27- Heat shock protein 27; Ht-29- Human Colorectal Adenocarcinoma cell Line; IBS- irritable bowel syndrome; ICAM-1- Intercellular adhesion molecule-1; IFN- γ - Interferon-gamma; IL-1 β - Interleukin 1 beta; IL-6- Interleukin 6; Ki-67- cellular marker for proliferation; LDH- Lactate dehydrogenase; LDL- Low density lipoprotein; MCP-1 Monocyte chemoattractant protein; MDA- malondialdehyde; MMP-1- Matrix metalloproteinase-1; MPO- myeloperoxidase; NF- κ B- Nuclear factor kappa B; NO3- Nitrate; NO2- Nitrite; OP- Open label; P- IKK α / β - Phospho IKK α ; P53- Tumor suppressor gene; PD1- Programmed cell death protein; PI- Pilot; RD- Randomized; ROS- Reactive oxygen species; SC- Single center; SCFA- Short chain fatty acid; SK-MEL-28- melanoma cell lines established from patient-derived tumor samples; SOD- Superoxide dismutase; TNBS- 2,4,6-trinitrobenzene sulfonic acid; TNF α - Tumor necrosis factor alpha; Th1- Type 1 T helper; UC- Ulcerative colitis; p-I κ B α - kappa light polypeptide gene enhancer in B-cells inhibitor, alpha

connections in the matrix structure are generally intended to be biodegradable or stimuli-responsive to special conditions present in the gastrointestinal environment [151]. Curcio and coworkers loaded an antioxidant molecule on chitosan using a free radical grafting procedure. The resultant PS showed better antioxidant properties [152]. Similarly, Flores et al. extracted ferulated arabinoxylans (AX) from dried distillers' grains (DDG) to investigate their capability to form covalently cross-linked nanoparticles. At 1% (w/v) concentration, AX produced lactase-induced covalent gels with an elastic modulus of 224 Pa and an FA dimer concentration of 1.5 μ g/mg. Images of AX gels taken with scanning electron microscopy (SEM) revealed a microstructure showcasing a rough honeycomb [153]. Finally, it was revealed that AX formed covalently cross-linked nanoparticles (NAX) by coaxial electro-spray. Although covalent cross-linkages are the primary driving force, other noncovalent forces (such as hydrogen bonding and hydrophobic interactions) may also be present in the formulation, depending on the type of PS and chemical modifications used. Ding et al. formulated oral colon-targeted berberine loaded Konjac Glucomannan (KGM) hydrogel formulated through noncovalent cross-linking by Cucurbit [8]uril (CB

[8]) for the treatment of UC. Due to the robust homoternary complexation between CB[8] and the phenolic group under acidic circumstances, the new supramolecular hydrogel (KGM-Phe@CB[8] hydrogel) maintained good stability in acidic conditions of the stomach. Furthermore, colon-specific enzymes such as β -mannanase or, β -glucosidase broke down KGM, resulting in the regulated release of loaded berberine in the colon [154].

4.1.2. Metal polymer cross-linking

The formation of coordinate-covalent linkages (chelation) between metal cations (e.g., calcium, copper, iron, zinc) and negatively charged ligand moieties of PS, metal-polymer coordination produces more vital bridges between PS chains than covalent cross-linking [155]. This is facilitated by forming the flexible, reversible formation of metal-PS nanocomposites such as hydrogels that possess variable physicochemical activities that are interdependent on the valency of the metal ions and the concentration of the PS [156]. The use of alginate for metal-polymer cross-linking is the most popular. However, in one study, guar gum was oxidized and complexed with iron (II) complex. This

Table 2
Various registered clinical trials in which PS has been used as therapeutic.

PS	Condition	NCT number	Status	Design	Participants	Expected PS Outcome	Start date	End date/ Expected end date	Reference
Pectin	Ulcerative Colitis	NCT03444311	TMD	R PL	12	Improvement in Gut Microbiota of patients	8-Mar-18	2-Jul-20	[122]
Pectin	IBS	NCT02016469	UNK	R PL	30	Improvement in fecal calcium protein, Crohn's disease activity index	Dec-13	Feb-16	[123]
Pectin	Crohn's disease	NCT02164877	TMD	R PL	3	Improvement in clinical response, Change in fecal SCFA	Jun-14	Jun-17	[124]
Pectin and Maltodextrin	IBS	NCT02270268	CD	R PL	114	Efficacy of gut microbiota and cytokine ratio	Nov-11	Oct-13	[125]
Pectin	<i>H. pylori</i> infection	NCT04660123	ERL	SG	1000	Eradication of <i>Helicobacter pylori</i> infection	20-Dec-20	NA	[126]
Alginate	Triacylglycerol Digestion	NCT03860337	CD	R CR DB	15	Improvement in circulation of glucose in the blood	13-May-19	19-Jun-19	[127]
Alginate	GERD	NCT01338077	CD	R PL	195	Improvement in heartburn after treatment	Oct-10	Jan-12	[128]
Alginate	Anal fistula	NCT04740086	CD	CO PRO	20	Improvement in incidence after treatment	1-Jan-16	30-Nov-19	[129]
Guar gum	Constipation	NCT05037565	REC	R PL	52	Change and Improvement in Fecal Characteristics	Jan-22	Jul-22	[130]
Guar gum	Rectal Cancer	NCT04678349	NYR	R PL	30	Decrease in hospital stay	31-Dec-21	31-Dec-21	[131]
Guar Gum	IBS	NCT01779765	UNK	R PL	130	Improvement in deiteary intake	Jan-13	Jun-14	[132]
Inulin	Inflammatory Bowel Disease	NCT03653481	REC	R PL	200	Improvement and alteration of gut microbiota	29-Oct-18	Jan-23	[133]
Inulin	Constipation	NCT02548247	CD	R CR	54	Improvement in stool frequency	Mar-11	May-12	[134]
Inulin	CRC	NCT00335504	CD	R PL	85	Improvement from rectal aberrant cryptic foci	Mar-06	Apr-09	[135]
<i>Ganoderma lucidum</i>	Ulcerative Colitis	NCT04029649	UNK	R PL	204	Improvement of C-Reactive Protein	Aug-19	Dec-20	[136]
<i>Ganoderma</i> spores	Gastrointestinal neoplasm	NCT02785523	UNK	R PL	60	Improvement in the quality of life	May-16	May-17	[137]
Acacia Gum	Constipation	NCT04382456	CD	SG	12	Improvement in gut microbiota and stool frequency	1-Jun-20	7-Sep-20	[138]
Agar	Constipation	NCT02012543	CD	SG	100	Reduction in the number and amount of defecation	Nov-13	Oct-14	[139]
Locust Bean	Regurgitation	NCT04042454	REC	R PL	100	Decrease in average stool consistency	10-Dec-19	Jun-23	[140]

CD- Completed; CO- Cohort; CR- Crossover; DB- Double blind; ERL- Enrolling by invitation; GERD- Gastroesophageal reflux disorder; IBS- Irritable bowel syndrome; NYR- Not yet recruiting; PL- Parallel; PRO- Prospective; R- Randomized; REC- Currently recruiting; SG- Single group; TMD- Terminated; UNK- Unknown

cross-linking polymer was used for achieving prolonged release for tablets. The total iron content of the tablets was compared to that of ferrous fumarate produced under identical circumstances. The pH-sensitive behaviour of the guar gum-based delivery system towards regulation of iron release was demonstrated in the *in vitro* release study. However, the toxic nature of these complexes is not usually evaluated, thereby limiting their usage [157]. Another study that reported the toxicity of the cross-linking of succinyl-chitosan (CH-Su) with various polyvalent metal ions (Fe_3^+ , Al_3^+ , and Ca_2^+) found that CH-Su-metal ion complex showed higher young's modulus. While CH-Su/ Al_3^+ and CH-Su/ Ca_2^+ hydrogels were not substantially harmful in cell viability experiments, CH-Su/ Fe_3^+ hydrogels demonstrated considerably more significant cytotoxicity than controls, probably owing to Fe_3^+ release and pH reductions [158].

4.1.3. Electrostatic interactions

Polyelectrolyte complexes (PECs) can be formed via electrostatic interactions between oppositely charged PS and polyelectrolytes in solution. For the immobilisation of therapeutic payloads, PECs provide a reversible and non-covalent physical interaction without the need for reactive agents or catalysts. PECs include nucleic acids (e.g., pDNA, siRNA), proteins (e.g., albumin, collagen, gelatin), PS (e.g., chitosan, hyaluronic acid, alginate). The intrinsic characteristics of PECs (e.g., ionic strength, charge density, molecular weight, flexibility) and the physicochemical environment such as temperature, type of solvent, and

pH of the solution all influence the complexation, stability, and physical properties (e.g., permeability, swelling) of PECs [159]. Among all the polymers, chitosan showed excellent potential for its use in formation of polyelectrolyte complexes. In one study, chitosan alginate complex containing interleukin-1 receptor antagonist (IL-1Ra) was formulated in the form of microcapsules. The results revealed that the IL-1Ra complex successfully evaded the harsh acidic environment. Upon reaching to the colonic pH, the release of IL-1Ra from the microcapsules took place. This impact was caused by the reaction of microcapsule pH-change, which allowed for the targeted release of IL-1Ra in the colon [160]. In another study that involved formulation of microspheres containing polyelectrolyte complex of xanthan gum and omega-3 polyunsaturated fatty acids (PUFAs) using soaking technique, initially, 60% of the drug was released followed by 40% after burst release. This impact should not be seen as a negative factor in cancer therapy since it has been demonstrated that a rapid release rate of antineoplastic medicines may generate beneficial benefits during tumor treatment. Furthermore, PUFA was successful in its antioxidant property by protecting the biological membranes from lipid peroxidation for up to 2 h [161].

4.1.4. Hydrophobic interactions

Amphiphilic copolymers are formed due to the addition of hydrophobic segments to hydrophilic PS chains. By spontaneous hydrogen bonding between the hydrophilic backbone of the PS and water molecules, these copolymers attempt to self-assemble into stable

Table 3
Preclinical studies using PS as prebiotics.

PS	Probiotic	Animal study (model)	Treatment duration	Disease	Result	Reference
<i>Durio zibethinus</i> rind	<i>Lachnospiraceae NK4A136</i>	Loperamide hydrochloride	8 days	Constipation	↑ In the intestinal transit rate, motilin, gastrin, substance P levels and concentration of SCFAs	[141]
Inulin	<i>Lactobacillus acidophilus La-5</i> and <i>Bifidobacterium lactis Bb-12</i>	Transgenic rats	8 weeks	Colitis	After 4 months the inflammation was diminished Stimulated the diversity of <i>Bifidobacterium animalis</i>	[142]
Resistant starch	<i>Lactobacillus acidophilus</i> or <i>Bifidobacterium lactis</i>	Azoxymethane	2 days	CRC	↓ pH levels and total coliforms ↑ Proapoptotic action	[143]
Corn bran	<i>Clostridium butyricum</i>	Piglets after weaning	28 days	Intestinal impairment with metabolic disorder	↑ The growth of acetate-produced bacteria and the production of acetate and isovalerate ↓ Pathogen abundances	[144]
Guar gum and xanthan gum	<i>Lactobacillus acidophilus</i> , <i>Lactobacillus rhamnosus</i> , <i>Bifidobacterium longum</i> and <i>Saccharomyces boulardi</i>	Dilute acetic acid	17 days	UC	↑ In weight gain No change in strip colour, which indicates absence of blood in the caecal content	[20]
Guar gum-Eudragit S100	Biomix I from Unique Biotech	Dilute acetic acid	14 days	UC	Improvement in SOD, GSH, MPO activity	[18]
Guar gum	Biomix I from Unique Biotech	Dilute acetic acid	14 days	UC	Improvement in MPO Less DAI scores	[145]

CRP – C reactive protein; DAI- disease assessment index; FRAP – Ferric reducing ability of plasma; GPx – Glutathione peroxidase; HDL-C – High density lipoprotein; HFD – High fat diet; IFN – interferon; IL – Interleukin; LDL-C – Low density lipoprotein; MPO – Myeloperoxidase; NA – Not applicable; NAFLD – Non alcoholic fatty liver disease; SCFA- Short chain fatty acid; SD- Sprague dawley; SOD – Superoxide dismutase; TC – Total cholesterol; TG – Triglyceride; TNFα – Tumor necrosis factor alpha; UC- Ulcerative colitis

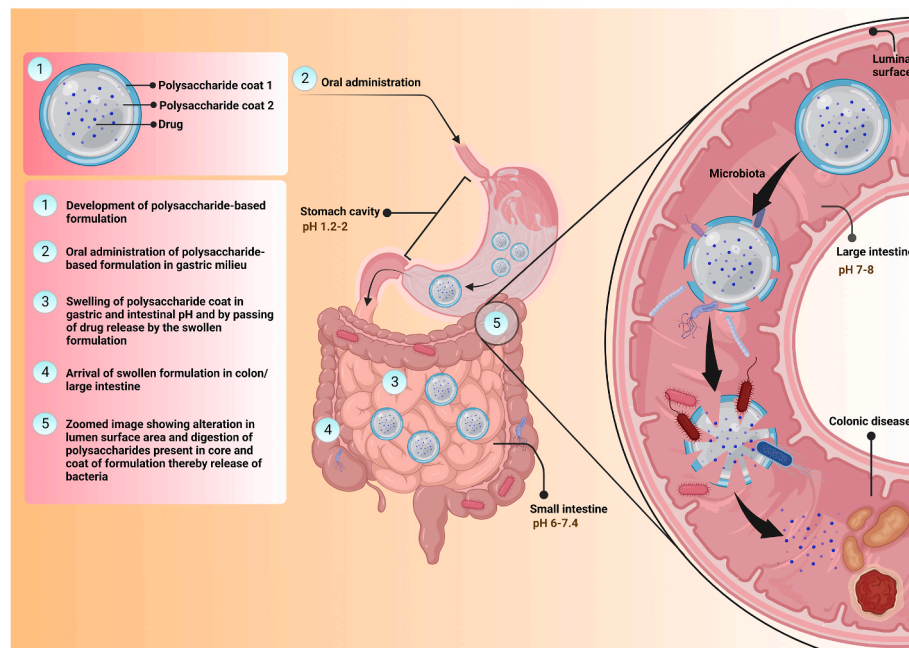


Fig. 1. Mechanism of drug release from PS coat in gastro intestinal and colonic milieu

conformations leading to the reduced free energy of the thermodynamic system [162]. Due to the unfavourable interaction with water, hydrophobic blocks self-associate to create a hydrophobic domain. The most commonly used functional pendant groups for conjugating a variety of hydrophobic segments include amino, carboxyl, and hydroxyl groups found on the PS backbone, which interact with cholesterol, fatty acids, bile acids, polyesters, pluronic polymers, poly (alkyl cyanoacrylate), and hydrophobic drugs forming these hydrophobic interactions [163]. Among all copolymers, the amphiphilic copolymer has gained popularity in pharmaceutical formulations for encapsulating hydrophobic drug moieties in their hydrophobic cavity. Xg-PNVP grafted microbeads of levofloxacin were prepared using free radical polymer method. This

was prepared to further load the levofloxacin drug. Release study revealed that the release of levofloxacin from microbeads was retarded in the gastric pH, and 80% of the drug was released in 36 h at the colonic pH [164]. Similarly, zein, sodium caseinate and pectin matrix were used to formulate a colloidal complex to generate small, homogenous, and stable complex nanoparticles. A heat and pH-induced complexation process was modified using polymer concentrations, eugenol loading percentages, and changes in pH conditions. Eugenol-loaded spherical complex nanoparticles with a size of 140 nm, were produced under optimal preparation conditions [165]. The various synthesis mechanisms of PS are depicted in Fig. 2.

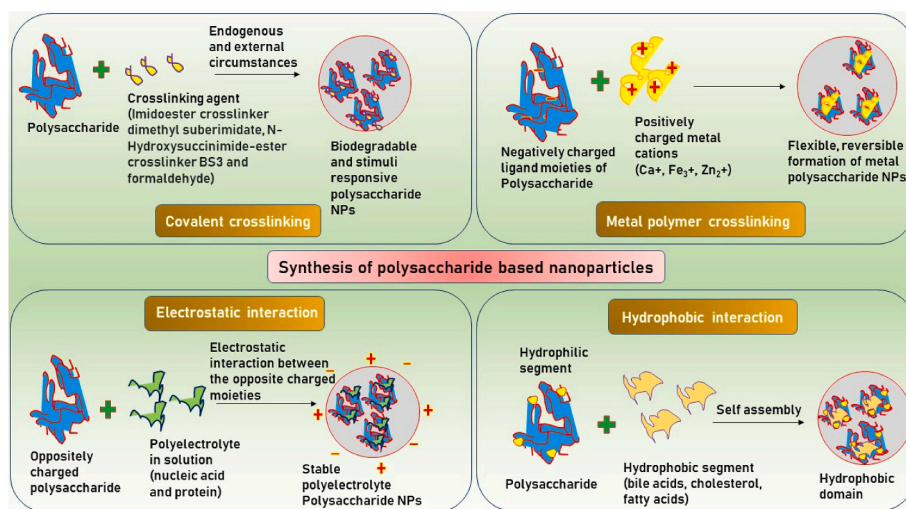


Fig. 2. Various mechanisms of synthesis of PS based nanoparticles.

4.2. Lipid vesicular carriers

4.2.1. Liposomes

Chitosan and pectin are the two widely used polymers for developing liposomes for colon targeted delivery. Their mechanism of action is by mucoadhesion for cellular uptake and drug release. In particular, chitosan-based liposomal formulations have shown increased stability in gastric pH and better drug release compared to naïve liposomes [166]. In one study involving Cyclosporine A, a liposomal matrix was fabricated using lecithin, cholesterol, N-octyl-N-arginine, and chitosan complex by thin-film evaporation-sonication extrusion method. The size of liposomes was 69 nm with an entrapment efficiency of 99%, indicating the prepared liposomes' better surface area and bioavailability. Moreover, permeability studies were also carried out for the formulation, which showed a 2-fold increase in the permeability of the drug from the intestinal barrier [167]. Similarly, in another study using chitosan liposomal complex for a BCS class IV drug, furosemide, were prepared by thin-film hydration sonication method using lecithin, cholesterol, and chitosan. The particle size was found to be 115 nm, entrapment efficiency of 71%, with an 8-fold increase in permeability from the naïve drug [168].

In one study involving alendronate, a BCS class III drug with a Log P of -4.3 , liposomes were prepared using lecithin, cholesterol, and Eudragit L 100 using the thin-film hydration method. The size of the liposomal complex was found to be 110 nm and had a zeta potential of $+5$ mV. The entrapment of drug was 44%. However, the bioavailability of the drug increased by 12.1-fold with a 4-fold increase in T_{max} and C_{max} of the drug. This indicated better solubility and bioavailability of the drug-using liposomal-PS complex [169].

Curcumin is considered a wonder drug for its versatility. However, the drug suffers from poor bioavailability and solubility. To overcome this, hyaluronan loaded multicomponent liposomes were prepared using a thin-film hydration method and freeze-dried to enhance its stability. The prepared liposomes had an entrapment efficiency of 80%. *In vivo* study was carried out to ascertain the difference between the release of the coated liposomal and standard curcumin solution. The amount of curcumin in the jejunum was found to be at 5% of the normal solution, and then coated liposomes were 20% of the total dose of curcumin. Furthermore, the intestines of rats were yellow, indicating a higher accumulation of curcumin. The amount of curcumin in the colon for a normal solution was negligible, whereas it was 3% for the liposomal product [170].

Another plant flavonoid, quercetin, that suffers from the same limitations of solubility and bioavailability. To overcome this challenge,

chitosan-based liposomes were formulated. The size of chitosan-loaded liposomes was 180 nm and had a zeta potential of $+2$ mV which suggested that the formed chitosan liposomal complex with a cross-linked shell layer was able to protect quercetin in upper GIT or, acidic pH. The entrapment efficiency was found to increase by 1.6 folds higher as compared to normal liposomal formulation, suggesting that quercetin was entrapped in the cross-linked liposomal matrix of chitosan. Furthermore, the release of quercetin in the *in vitro* studies showed two folds increased drug release in intestinal pH than a pH of 1.2 [171]. Using specific colon-targeted PS, vesicular carriers have been found successful in drug release and their mucoadhesion. However, their specificity for targeted action on a diseased colonic tissue vs a healthy colonic tissue warrants further study [172]. To overcome this, the coupling of liposomes with specific ligands has been explored, particularly with monoclonal antibodies. Iron uptake is facilitated by a carrier protein such as transferrin receptor (TfR) from the plasma glycoprotein transferrin through endocytosis [173]. The use of immunoliposomes for treating colonic diseases has been reported, wherein, the liposomal formulation containing anti TfR antibodies was developed. It has been found that the level of TfR gets elevated in human and animals during mucosal damage as in case of UC. The immunoliposomes containing AntiTfR antibodies were formulated and administered through parenteral route in DNBS induced UC rats. At the end of the study, the inflamed mucosa of rats was isolated and checked for accumulation of antiTfR immunoliposomes. The results indicated significantly higher accumulation of antiTfR antibodies in the mucosa of rats as compared to rats treated with unbound liposomes [173]. In another study, layer by layer liposomes of pectin with trimethylated chitosan coating loaded with celastrol to check its anti-UC effect using thin film hydration method was prepared. In the simulative gastrointestinal tract media, the liposomes demonstrated surface charge reversal, a modest increase in particle size, and a prolonged drug release profile. It was also noticed that 20% of the drug was released in simulated colonic fluid which was attributed to the flexibility of the PS. Due to the increased polymer coat it was noticed that the layer-by-layer liposome formulated showed even more retarded release. Further, the developed liposomes also alleviated the colonic injury indicating the antiulcerative effects of the developed formulation [174].

4.2.2. Niosomes

Niosomes are non-ionic-based lamellar vesicles. They are formulated using sorbitan fatty acid esters and polysorbates. Sometimes, cholesterol is added to give rigidity to the formulation. To date, niosomes coated with PS have not been extensively studied and developed for colorectal

diseases. However, Niosomes prepared along with chitosan have been studied recently where the preparation of niosomes by reverse-phase evaporation technique was carried out. In this study, trimethyl chitosan (TMC) was coated on the niosome by incubating the drug-niosomal suspension with TMC solution. The *in vitro* studies revealed that the drug release of the drug happened in a sustained manner compared to the uncoated niosomal formulation [175]. Similarly, chitosan-coated niosomes were studied for their delayed-release action for famotidine, which has low oral bioavailability. The coated niosomes showed an increased vesicular size. In addition, the coated niosomes showed limited drug release compared to the uncoated niosomes. However, the coated niosomes showed lower drug loading. This was attributed to the interaction between negatively charged lipid and positively charged chitosan that left no binding sites for the drug. The coated niosome also showed improved tackiness and mucoadhesion, thereby increasing the residence time and improving oral bioavailability [176]. Nateglinide, a BCS class II drug, suffers from low solubility. Niosomes loaded with nateglinide were prepared using Span 60, cholesterol, and maltodextrin. The size of the niosomes, polydispersity index, and zeta potential were found to be 262 nm, 0.26, and -45 mV, respectively. Intestinal permeability studies were also carried out that showed an increased permeation by 1.4-fold as compared to the naïve form [177].

Various mechanisms have been postulated to understand PS based niosomes as potential carriers and PS for treating colorectal diseases. Cell membrane fluidizing effects of niosomes was due to the presence of surfactants [178]. Various studies highlight the role of P-gp and/or CYP inhibition activities of surfactants that may aid in oral drug delivery of niosomes [179]. Moreover, it was understood that niosomes as a carrier facilitated improved drug localization into the mucosal layers [180]. This mechanism and controlled release properties could aid in drug transport to treat colorectal disease which warrants further studies [181].

4.2.3. Ethosomes and invasomes

Ethosomes are vesicular drug delivery systems composed of phospholipids, water, and a high quantity of ethanol. Whereas, invasomes contain turpene in their structure. The main advantage of such drug delivery systems is their ability to permeate the drug. These drug delivery systems are primarily used for transdermal application and rarely for oral colon targeting. However, their use is worth mentioning and warrants future study for colorectal diseases [182]. Ethosomes for treating UC using eugenol (EUG) and cinnamaldehyde has been developed in conjugation with hyaluronic acid (HA). When compared to the model control group, the colon lesions of the rats receiving EUG/CAH therapy were improved, demonstrating an improvement in the drug's effects on UC. Highlighting the role of the carrier [183]. The formulated ethosomes are depicted in Fig. 3. This study highlights the fact that ethosomes, in combination with PS, improve permeability and can be used as a carrier in the treatment of colorectal diseases.

To our knowledge, there is no reported literature on the *in vivo* PS based use of invasomes and PS for treating colorectal diseases. However, one study highlighted the photodynamic use of invasomes loaded with temoporfin upon topical administration showed its effect on human colorectal tumour cell line (HT29). Results revealed that the niosomal formulation could inhibit the survival of HT29 cells. The drug was mainly localized in the cytoplasm and endoplasmic reticulum of the HT29 cells and to a lesser extent in the mitochondria and lysosomes [184]. This indicated that invasomes could also be considered as a potential carrier for drug delivery to the colon.

4.3. Micelles

Micelles are core-shell nanostructured carriers that have recently gained prominence. Additionally, they possess high loading capacity, improved drug stability, improved solubility and permeability through the GI barriers, controlled drug release, and protection of the drug in the GI fluids. Mixed micelles are usually chosen over single component

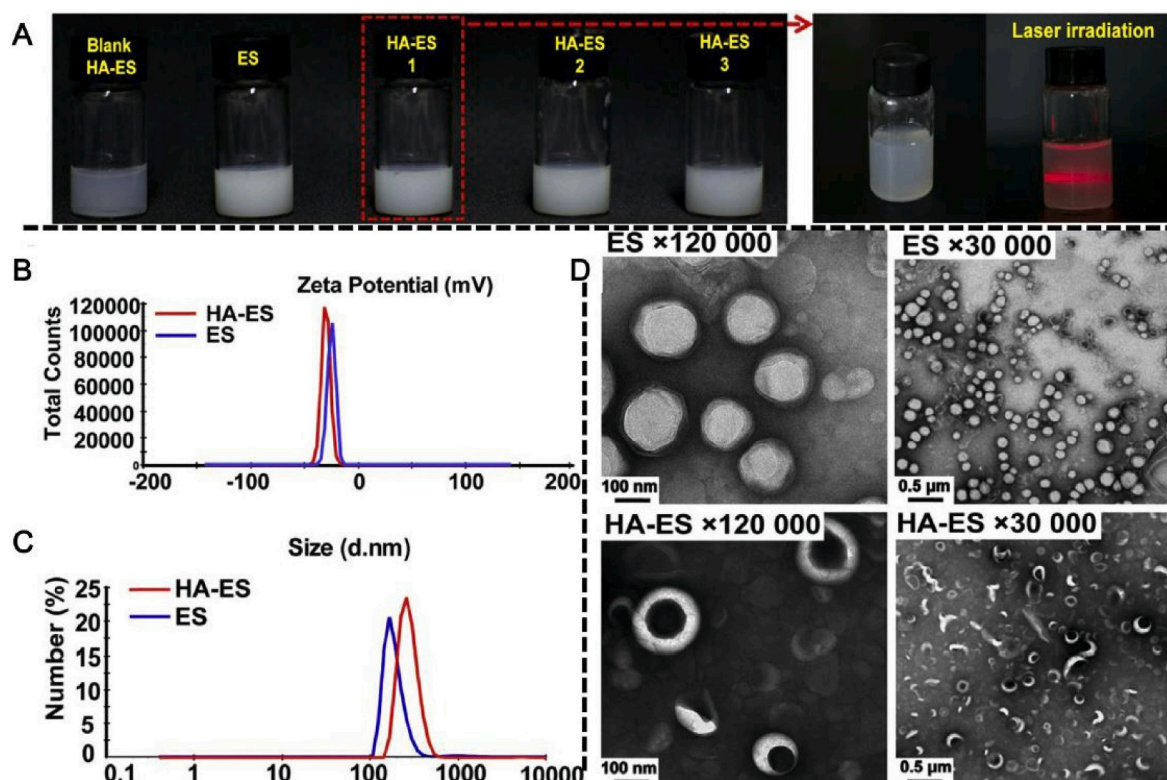


Fig. 3. A, Appearance of prepared ethosomes, B: zeta potential, C: size distribution, D: TEM images, formulations HA-ES1,2,3 with different concentrations of HA-conjugated dioleoyl phosphoethanolamine, ES- Formulation without HA dope. Copyright Elsevier, 2021.

micelles because of increased stability and drug loading efficiency [185]. In one study, micelles were formulated by a top-down approach containing stearic acid and chitosan with different amino substitutes. Results revealed that the micelles had a size in the range of 33–131 nm and zeta potential in the range of 23–48 mV. To understand the permeability and mechanisms of the transport through the GI tract, Caco-2 cell lines were used. Through caveolar and fluid-phase endocytosis and micropinocytosis, the micelles showed an energy-dependent transcytosis process. Furthermore, the micelles with amino substituents showed more permeability [186]. For oral insulin delivery, goblet cells targeting micelles were formulated and characterized. Micelles containing dodecyl amine-graft-g-polyglutamic acid were prepared and coated with trimethyl chitosan and goblet cell targeting peptide-loaded insulin for oral delivery. Cellular uptake and transport were studied in Caco-2, HT29-MTX-E-12 cell cultures to mimic the intestinal epithelium. The permeability coefficient of insulin incorporated into the micelles, chitosan micelles, and targeted chitosan micelles were found to be at 5.1, 5.4 and 6 cm/s. In diabetic rats, the targeted micelles showed higher relative bioavailability and a prolonged hypoglycemic response indicating favorable use for this condition [187].

Carboxymethyl chitosan-based micelles were prepared by dialysis sonication method for the co-delivery of paclitaxel and quercetin. The obtained micelles were found to be in a size of 186 nm, PDI of 0.13, and zeta potential of -21 mV, along with an entrapment efficiency of 86%. Drug release at the end of 10 h was 10%, and the permeability in the duodenum and jejunum showed a 22.3- and 32.8-fold increase as compared to the naïve form, respectively. Moreover, the oral bioavailability of micelles was found to be 7.2-fold higher compared to the naïve form [188]. Similarly, paclitaxel alone was formulated as micelles using N-octyl-N'-pthalyl-O-phosphoryl chitosan. The micelles showed a size of 137 nm and a zeta potential of -28 mV. Cellular uptake revealed about 6.4-fold increased uptake of paclitaxel from micelles. The bioavailability study showed a 5.5-fold increase in case of drug loaded in micelles as that of naïve paclitaxel [189]. In another study, doxorubicin loaded stearic acid-chitosan based micelles were prepared and evaluated for their efficacy against CRC. The size, PDI, zeta potential, and entrapment efficiency were found to be 28 nm, 0.60, $+46$ mV, and 76%. The drug release at the end of 10 h was found to be at 45%. The permeability was assessed through Caco-2 cell lines, and it increased 18-fold times higher as that of unprocessed doxorubicin. Furthermore, the bioavailability also increased by 4.2 folds in case of Dox micelles as compared to the unprocessed drug [190]. Micelles of curcumin were prepared for the treatment of UC, wherein alginate was used to increase the solubility and esterified to prepare Alg-Cur micelles. The micelles were kept for lyophilization followed by refrigeration. Mice were administered DSS to induce UC. Among all the groups that were studied on the UC model, TLR4 protein activity in colonic tissues revealed that only Alg-Cur inhibited TLR4 expression strongly. This was attributed to the fact that alginate facilitates the solubilization of Cur, and improving the integrity of colonic mucosa, diminishing the secretion of pre-inflammatory cytokines such as IL-1 β , IL-6 and TNF- α . It was further found out that after oral administration, 92.32% of Alg-Cur reached the colon indicating its colonic release due to the presence of PS [191].

Many mechanisms of micelles have been proposed for its improved drug dissolution, permeability, and bioavailability for colorectal diseases, such as vesicle uptake via micropinocytosis, caveolin- and clathrin-dependent, fluid-phase endocytosis pathways, increasing paracellular pathways, inhibition efflux pumps, small size, larger surface area, enhanced lymphatic transport, and deep penetration into the intestine villi [192-194]. They all highlight the possibility of using micelles and PS for colorectal disease.

4.4. Nanocrystals

Nanocrystals are considered nanosuspensions that are carrier-free submicron colloidal dispersions of drug particles (less than 500 nm)

along with surfactants or hydrophilic polymers, which are considered to stabilize the formulation [195]. These stabilizers provide steric and electrostatic repulsions. Nanocrystals are usually formulated using top-down, and bottom-up approaches and are extensively used to improve oral bioavailability by increasing the surface area, dissolution rate, and saturation solubility [196]. Currently, three USFDA-approved nanocrystals contain PS for various diseases, namely; Avinza, Cesamet, and Emend, respectively [197]. Nanocrystals containing candesartan and cilexetil were prepared by an antisolvent precipitation method using HPMC and Pluronic F127. The permeability of which was evaluated in Caco-2 cell lines. The obtained nanocrystals showed a size of 159 nm and zeta potential of -24 mV, thereby improving their bioavailability by 3.8 folds [198]. Similarly, nanocrystals of diacerein were prepared by the sonoprecipitation method using PVP-K 25 and chitosan. The prepared nanocrystals were evaluated through a rat gut sac. About 80% of drug releases occurred after 2 h, and there was no change in C_{max} [199]. Similarly, nanocrystals of nimodipine were formulated using the microprecipitation high-pressure homogenization method using pluronic F127, HPMC, and Na deoxycholate. The results revealed comparable permeability with the marketed tablet [200]. Moreover, nanocrystals were uptaken by energy-dependent processes and detected in mesenteric lymphatic fluids. In another study, Nanocrystals of cellulose were prepared by acid hydrolysis method having a viscosity of 10, 000 mPa. This led to an interconnected dense structure of polysaccharide. Further, the cellulose nanocrystals were well distributed in the polysaccharide solution (made of algae solution) due to absence of phase separation. Indicating that functional groups of cellulose nanocrystals and polysaccharide matrix chains were interconnected with one another. This led to the formation of water-soluble capsules that consisted of nanocrystals of cellulose [201]. Nanocrystals have been identified as nanostructures that enhance the drug's dissolution rate and saturation solubility [202]. The mechanism of these carriers is not well understood. It is hypothesized that nanocrystals with particle size of less than 1 μ m (100 nm) penetrate easily into the mucus layer, and smaller particles have higher uptake due to absorptive enterocytes. Nanocrystals might diffuse through the small intestine peyer's patches and be directly absorbed bypassing the first-pass metabolism [202].

4.5. Nanoemulsions

Nanoemulsions are kinetically stable colloidal particulate systems whose size is in the submicron range. The size varies from 10 to 1000 nm. Nanoemulsions are efficient carriers in delivering lipophilic drugs [203]. The preparation of nanoemulsion uses two immiscible liquids and an emulsifier. The oil phase in nanoemulsions comprises triacylglycerols, diacylglycerols, monoacylglycerols, and free fatty acids [204]. Nanoemulsions offer several advantages, such as an easy scale-up process, protection from GI conditions, enzyme degradation, enhanced drug transport across intestinal barriers, high solubilization capacity, and rapid onset of action [205].

Bai et al. formulated oil-in-water nanoemulsion by dual-channel microfluidization technique, using natural emulsifiers and PS. Gum arabic was used as a PS in this formulation. Gum Arabic demonstrated C_{min} and d_{min} that can be attributed to the slow adsorption of large gum arabic molecules, lower surface activity, and higher interfacial tension. Moreover, gum arabic successfully lowered the interfacial tension between the oil and water interface. The droplet diameter decreased with increasing homogenization pressure [206].

Bioactive PS extracted from brown seaweed has been known to have antioxidant, antibacterial and antiviral activities. In one study, nanoemulsion was prepared by an ultra-sonication method. ExoPS from brown seed weed was loaded into the orange oil nanoemulsion. The prepared nanoemulsion had an encapsulation efficiency of 67.29%, a particle size of 178 nm, and a zeta potential of -43.9 mV. The *in vitro* results showed slow drug release, indicating sustained release pattern and increased bioavailability of the exopolysaccharides. Colon cancer

cell lines (HCT 116) were used to analyze the cytotoxic effect of the PS. However, the nano lipid carrier showed better entrapment efficiency with reliable particle size and zeta potential than the orange oil nanoemulsion [207].

Another study involving the preparation of nanoemulsion using different PS such as levan, fucoidan, alginate, guar gum, and κ -carrageenan were used as emulsifiers and evaluated for their potential to entrap curcumin. Better physical properties were observed for nanoemulsion prepared from κ -carrageenan compared to other PS. The formulated nanoemulsions using κ -carrageenan behaved as Newtonian fluids. The release kinetics of PS nanoemulsions are directly related to the encapsulation efficiency. The addition of PS further enhanced the antioxidant effects of curcumin. This study highlighted the use of PS as a better emulsifier when compared to synthetic emulsifiers [208]. The use of fecal microbiota to treat colorectal diseases has gained prominence in the last decade [209]. In this regard, polysaccharide (using 1%w/w of guar gum and pectin) based solid-self nanoemulsifying drug system incorporating fecal microbiota were prepared using lyophilization technique for colon targeted action. The developed S-SNEDDS was found to have a droplet size of 78.46 ± 0.87 nm, respectively. The developed formulation demonstrated less than 10% of drug release in the initial 5 h, followed by burst release between 5 h and 10 h. Further, it was found that 2.34 folds increase in permeability of S-SNEDDS was seen as compared to naïve drug. This indicated that PS were helpful in penetration after the S-SNEDDS got released and reconstituted into colonic conditions [210].

Table 4
Recent advancements using PS nanoparticles and their key findings.

Type of Nanoparticle	PS	Drug	Size	Key findings	Reference
Nanocomposites	Triple helical β -glucan	Antisense Oligodeoxyribonucleotides	0.8 nm	↑ Drug release in pH 6.8	[213]
Nanostructured Lipid Carriers	Chitosan	Albendazole	188 nm	Enhancement in the efficacy of the drug	[214]
Silica Nanoparticles	Chitosan and sodium alginate	Insulin	256.6 nm	Followed first order type of release ↓ Cell viability	[215]
Nanoparticle	Pectin	S-adenosyl-L-methionine	301.5 nm	Improvement in oral bioavailability	[216]
Nanoparticle	Dextran	Doxorubicin	80 nm	Targeted colonic drug delivery due to negatively charged particle size ↑ Passive accumulation efficacy	[217]
Nanoparticle	<i>Ulva lactuca</i> PS	Selenium	130 nm	↑ COX-2 and iNOS Inhibition of inflammation that may aid in colitis	[218]
Gold nanocomposites	Chitosan	5-FU	5 nm	50% cell viability of MCF-7 cells Followed zero-order release	[219]
Solid lipid nanoparticles	Dextran	Doxorubicin	132 nm	Effective inhibition of primary colon tumors Slower drug release	[220]
Polyester based nanoparticles	Chitosan	Camptothecin	480 nm	↑ Cell internalization efficiency ↑ Therapeutic activity	[221]
Polymeric nanoparticle	PLGA and chitosan/alginate hydrogel	Camptothecin and CD98	270 nm	Internalization of NPs was achieved	[222]
Polymeric nanoparticle	PLGA	Camptothecin and curcumin	289 nm	Greater cellular uptake Improved Controlled drug release	[223]
Nanoparticle	Pectin/Eudragit S100	5-FU	174.65 nm	Reduction in systemic absorption Demonstrated colonic lumen specific release	[224]
Inorganic Nanoparticle	Galactosylated chitosan	5-FU	250 nm	Zero-order release ↑ Loading capacity	[225]
Silver nanoparticles	Modified apple PS	Mesalamine	101 nm	Better therapeutic efficacy 54% of drug release of 5 h	[16]
Nanoparticles	Sodium Alginate	Mesalamine	217 nm	76% drug got release after 24 h in rat caecal media Mixed order kinetics	[226]
Nanoparticles	Cyclodextrin/chitosan	Mesalamine	90 nm	NPs inhibited the production of NO, PGE2, and IL-8	[227]
Nanoparticles	Chitosan-carboxymethyl starch	Bovine serum albumin	900 nm	Displayed pH-responsive properties and ionic strength sensitive properties	[228]
Nanoparticles	Galactosylated trimethyl chitosan-cysteine	Mitogen-activated protein kinase kinase kinase 4 (Map4k4)	160 nm	A sustained release profile was observed	[229]

Improved bioavailability of drugs fabricated by nanoemulsion using PS may be attributed to various mechanisms and theories, including adhesion and uptake of nanometric droplets by enterocytes, improvement in permeability due to the use of surfactants using the paracellular and transcellular pathways, bypassing hepatic first-pass metabolism using lymphatic transport, and formation of mixed micelles with bile salts [211].

4.6. Nanoparticles

PS-coated nanoparticles for colorectal diseases offer the advantage of improved bioavailability of drugs by oral administration, increased intracellular penetration, increased retention time, and restriction of the release of encapsulated drugs providing targeted delivery in specific parts of the GIT in the treatment of various colorectal diseases [212]. Various properties of these nanoparticles play a role in cellular uptake and have efficacy in nanoparticle drug delivery systems. Usually, nanoparticles within the size range of below 200 nm have better targeting properties for colorectal diseases [23]. This facilitates the accumulation of nanoparticles in the colon tissue due to enhanced epithelial permeability and retention effect. Various nanoparticles coated with PS and their key findings are given in Table 4.

4.7. Nanogels

Nanogels are three-dimensional hydrogel materials in the nanoscale

size range formed by a swellable polymer network that can hold water. Nanogels possess various physical and chemical properties, including high water retaining capability, low surface tension, and three-dimensional structural arrangement [230]. These nanogels are designed to be mucoadhesive, so they can attach to the mucosal lining of the intestine. Feng et al. formulated chitosan-based nanogels that were cross-linked with carboxymethyl chitosan. Using various ionic cross-linkers, doxorubicin nanogels were obtained. Nanogels were taken up to a greater extent by (Caco-2) cell lines. The results demonstrated an increased contact time of formulation with the intestinal mucosa and improved local drug concentration at colon [231]. In another study involving antineoplastic agents, alginate-cyclodextrin nanogels were prepared. The drug 5-fluorouracil suffers from limited cellular uptake. Cytotoxic studies revealed high cell viability on HT-29 cells [232]. In another study, a new bidimensional composite hydrogel made of oxidized dextrin incorporating dextrin nanogels (oDex-nanogel) was prepared. Continuous protein delivery was performed by eliminating cyclic variations of proteins in the blood that offer maximum pharmacological activity with minimum drug dose [233]. Similarly, using dextran, nanogels were obtained using UV polymerization of dextran hydroxymethyl methacrylate. However, the encapsulation efficiency was low at 50% [234]. Improved bioavailability of the drugs in the colon through nanogel may be attributed to intracellular release and high-water retention capacity [147].

4.8. Microbeads

Beads are solid substrates on which the drug is coated or present within its core. The release of drugs happens in a sustained manner. Hence, increases the bioavailability of the drug. Many PS have been used in the formulation of microbeads, including guar gum and xanthan gum [235]. In one of the study, Microbeads of resveratrol were prepared using 3% sodium alginate and carboxymethyl chitosan as the PS agent. The microbeads showed a negative charge which was attributed to the carboxyl group of the chitosan. Further, the zeta potential was found to be higher which was attributed to higher charge. Drug release studies revealed that the drug release was inhibited in simulated gastric environment and sustained in the simulated intestinal fluid which indicated better bioaccessibility. It was also noted that the encapsulation of the drug was increased due to the lecithin-polysaccharide complex that was formed. The developed microbeads showed elevated antioxidant properties [236].

In another studies, a pectin-based colon-specific delivery system using 5-fluorouracil was developed to deliver the drug to the colon effectively. Microbeads were prepared using the ionotropic gelation method. The study revealed that Eudragit S 100 successfully delivered most of the drug to the colon after 9 h [237]. Microbeads of Tinidazole were prepared using sodium alginate, pectin, and Eudragit S 100 to treat amoebic colitis. The drug release happened the most in pH 6 buffer [238]. Moreover, the use of calcium alginate carboxymethyl cellulose beads in colon-targeted drug delivery systems has not been fully explored. In context to the previous study, beads were prepared by the ionic gelation method. Different concentrations of sodium alginate were formulated and evaluated as a carrier system against HT-29 adenocarcinoma cell lines. Results depicted that the cell viability decreased after 48 h [239].

4.9. Microcapsules

Microcapsules are formulated using a thin polymer coating on small solid particles or liquid droplets. They are also prepared for dispersions of solids or liquids. Many methods are used to formulate microcapsules, including ionic cross-linking or spraying sodium alginate in calcium

chloride and barium chloride solution [240]. Many colon targeting drugs have been developed using microcapsules. One of which is albendazole. Microcapsules of albendazole were prepared using various concentrations of hydroxypropyl methylcellulose, chitosan, and sodium alginate. FTIR results revealed that albendazole was encapsulated in the polymer matrix, and there was no chemical interaction. The drug release was found retarded with increasing concentration of chitosan [241]. A colon-targeted microcapsules of budesonide were formulated for UC using dextran as polymer. PS microcapsule was able to retard the drug release in the gastric environment and small intestine. After the addition of rat caecal contents, a rapid increase in drug release was observed. In conclusion, the therapeutic efficacy of the drug was enhanced [242].

Similarly, for a localized effect, tinidazole microcapsules were formulated using guar gum, and design of experiment was carried out. The microcapsules were 32.5 μm in size and had an entrapment efficiency of 95%. The drug release was the most in the 7.2 pH buffer. The release pattern followed the Korsmeyer Peppas model with super case II transport [243].

4.10. Conventional dosage forms

4.10.1. Tablets

Tablet dosages are the most widely used drug delivery system for the colonic site. Tablets offer ease of manufacture and can be produced in bulk. Various tablet dosage forms have been evaluated for colonic drug delivery [244]. Otman et al. developed colon-specific tablets containing 5-FU microsponges for colon cancer targeting of 5-FU. 5-FU has unpredictable bioavailability due to first-pass metabolism. To overcome this, tablets were prepared using hydroxypropyl methylcellulose (HPMC) and pectin-based colon targeted polymers by cross-linking. *In vivo* study on a human volunteer was also performed, revealing that the tablet reached the colon without any disturbance in the GI system [245]. Similarly, mini-tablets of 5-FU were prepared using pectin, guar gum, and Eudragit S100 by Kumar et al. The mini-tablets showed burst release after 5 h in the *in vitro* study. The *in vivo* study showed delayed levels of the drug in the plasma. The C_{max} in plasma for coated mini-tablets with and without probiotics was 104.55 ± 14.98 ng/mL (0.104 $\mu\text{g}/\text{mL}$) and 119.56 ± 14.22 ng/mL (0.119 $\mu\text{g}/\text{mL}$) respectively [246]. The similar research group prepared modified apple PS and probiotics in guar gum-Eudragit S100-based mesalamine mini-tablets to treat UC. The tablets showed a thickness of 2.0 mm and hardness of 3.7 kg/cm². The assay of the tablet was performed and found to be 97%. The dissolution data showed a delayed drug release (after 5 h) from the coated formulation endorsing the hypothesis of increased drug exposure to the targeted site [18]. Similarly, the double compression method based minitables using various concentrations of Eudragit S100 and HPMC K100 M for ketorolac tromethamine. The hardness was found to be 2.7 kg/cm², and the thickness of 1.7 mm. *In vitro* studies revealed that HPMCK100 M and Eudragit S 100 successfully based compression coated tablets provided colon targeted drug release [247].

Metronidazole (MTZ) tablets were prepared using *Abelmoschus moschatus* PS for its colonic delivery. The prepared tablets showed pH-dependent drug release. During the first few hours, negligible amounts of the drug were released due to the impermeable coating layer. It was also inferred that lesser drug release was observed when a higher PS concentration was used. This was due to the tablet's higher water uptake and holding capacity. Cell toxicity studies confirmed that it was safe. Further, gamma scintigraphy studies confirmed drug transit in the small intestine between 300 and 480 min and arrival in the colon between 360 and 480 min [248].

The similar research group carried out gamma scintigraphy studies on *Trigonella foenum-graecum* (Fenugreek) PS-based colon tablet and found the intestinal transit time between 3 and 5 h and confirmed that

the tablet reached the colon within 6–8 h. The drug showed pH-dependent release. There was a significant correlation between coating levels and lag time release of the drug. MTT assay indicated its safety profile with biological tissues [249]. Another study evaluated guar gum and pectin using gamma scintigraphy and revealed that transit of tablets in the entire colon had an average time of 5.75 h. The total drug release from the matrix at the end of 24 h was 80%, suggesting the extended-release of the formulation. Compression-coated tablets for colonic drug delivery using xanthan gum and guar gum were carried out. The total drug release after 24 h of dissolution study was 53%. When it was introduced into caecal contents, the drug release increased to 78.34%. Furthermore, gamma scintigraphy studies revealed that the tablet remained intact in the upper part of the GIT. The disintegration site of the tablet was found to be at the ascending colon flexure [250]. Gamma scintigraphy studies were carried out for colon-targeted tablets prepared using HPMC and pectin as polymers. The study revealed that the drug from tablet got released in ascending colon and found to have higher residence at the ileocecal junction [251].

4.10.2. Capsules

Compared to tablets, capsules as drug delivery vehicles have not been extensively used for the development of colon drug delivery systems. This is due to the fact that capsules offer limited dosage weight compared to tablets. However, some studies highlight the use of capsules as pulsatile drug delivery systems for colonic drug delivery [149]. The konjac glucomannan-based pulsatile capsule was prepared and evaluated through *in vitro* and *in vivo* studies. The drug release of 5-aminosalicylic acid showed a typical pulsatile drug release with a lag time followed by a rapid release rate. However, adding β -glucanase and rat caecal contents into the release medium significantly shortened their lag time. Further, *in vivo* studies revealed that the plasma drug concentration was detected after 5 h post oral administration [252]. The similar research group prepared and evaluated colon-specific sustained-release capsules of curcumin SMEDDS containing alginate beads. The capsules showed a pulsatile release with a prolonged lag time and a sustained release phase. Further the presence of rat caecal contents were able to modify the lag time. Thereby releasing 90% of the drug after 6 h,

Table 5
Conventional dosage forms using polysaccharides and their outcomes in their chronological order.

Year	Drug	PS	Conventional Dosage form	Outcome	Reference
1998	5-ASA	Eudragit L100 and Eudragit S100	Tablets	Release of tablets was based on pH dependent medium	[257]
2002	Metronidazole	Guar gum	Tablets	Solubilization of both polymers at colonic pH Release of 67% of the drug after 24 h	[258]
2002	5-FU	Guar gum	Tablets	Release of drug was limited to 5 h Drug release got increased after addition of (4% w/v) rat caecal contents indicating colonic release	[259]
2002	Mebendazole	Guar gum	Tablets	A delayed tmax and absorption time as well as decreased Cmax and absorption rate constant was noticed	[260]
2002	5-FU	Guar gum	Tablets	A delayed absorption time and decreased Cmax was observed	[261]
2003	Indomethacin	Eudragit S, ethyl cellulose	Tablets	Drug release was retarded 3–4 h in simulated intestinal fluid	[262]
2003	5-FU	Xanthan Gum and Guar gum	Tablets	Studies in colonic environment showed faster drug release as compared to normal media	[263]
2004	5-ASA	Ethylcellulose	Spheroids	The release of 5-ASA was faster in the faecal fermentation system than in the enzyme system	[264]
2006	Ketoprofen	Pectin	Capsule	Resistance of drug release in upper gastro intestinal tract	[265]
2007	Indomethacin	Guar gum and Eudragit FS30D	Pellets	The Tmax and Tlag in beagle dogs were 2.5 and 1 h which was retarded	[266]
2007	Nisin	Pectin	Tablets	At the end of 6 h, 40% of pectin got degraded Polymer hydration on pectin degradation was found to be crucial for the enzyme activity	[267]
2009	5-ASA	Nutriose	Pellets	Site specific delivery of drug to the colon ↑Release rate when exposed to patient feces	[268]
2009	Indomethacin	Xanthan Gum	Tablet	Drug release followed super case II indicating erosion type release	[269]
2009	Theophylline	Chitosan	Tablets	Drug release showed anomalous release Drug release was controlled due to polymer relaxation	[270]
2009	5-ASA	Pectin	Tablets	↑Rate of swelling was due to erosion of the polymer matrix in the colonic medium	[271]
2012	Curcumin	Pectin	Capsule	A shortened erosion time of PS in rat caecal content media was noticed	[272]
2012	5-ASA	Pectin, Ethyl cellulose	Capsule	A shortened lag time after addition of rat caecal contents indicating enzyme selectivity of pectin was noticed	[254]
2013	5-ASA	HPMC	Tablet in capsule	Roentgenographic studies revealed drug was intact after reaching colon	[273]
2014	Aceclofenac	Inulin	Tablet in capsule	Release of drug after a lag time of 2 h	[274]
2015	Sulfasalazine	Guar gum, Eudragit	Spheroids	↑Drug release in colonic conditions ↓In DAI scores	[145]
2015	Losartan Potassium	Guar gum	Tabs in cap	The formulation showed immediate release followed by delayed release with a lag time of 6 h.	[256]
2015	Ketorolac	Guar gum	Tablets	A negligible drug release in the stomach and small intestine and showed more release in the colon was noticed	[275]
2015	Tromethamine Zein	Pectin	Capsule	The ratio of 1:3 of zein and pectin showed no release in simulated gastric fluid	[276]
2015	5-FU	HPMC and Eudragit	Capsule	The capsule showed a lag time of 6 h and Cmax of 25 h	[277]
2016	Theophylline	Guar gum	Tablets	For the first 12 h, 27–54% drug release occurred and 82–104% at 24 h	[278]
2016	Recombinant human insulin	Pectin, Eudragit S100	Capsule	Release of 3.2% and 81.6% of peptide, up to 24 h in SIF Improved cellular uptake	[279]
2018	Curcumin	Guar gum and Eudragit L-100	Tablets	Restricted drug release of hydrophobic drug in stomach and small intestine	[280]
2020	Sulfasalazine	Eudragit S100	Capsule	The formulation displayed non fickian type of drug release	[281]
2020	5-FU	Chitosan, Sodium Alginate	Capsule	The capsule reduced cell viability ↑Mucoadhesion	[282]
2022	Metoprolol	Pectin	Pellets	Release mechanism was according to Higuchi model and described by diffusion control mechanism	[283]

indicating the protection of impermeable bodies [253]. Further, in another study, capsules of 5-aminosalicylic acid with gelatin capsules that were made impermeable by placing them in a mixture containing ethyl cellulose and ethyl acetate dichloromethane and ethanol. Through pharmacokinetic studies, it was analysed that the enteric capsule did not dissolve in the gastric fluid until it reached the small intestine.

Furthermore, the release of 5-aminosalicylic acid took place due to the microbial enzymes produced by the gut microflora [254]. Similarly, Yehia and coworkers prepared Eudragit S100 spray-coated capsules as pulsatile release systems for targeting the drug in the colon by incorporating tablet plugs of pectin. However, the difference between high methoxy pectin and low methoxy pectin was not considered [255]. Earlier, a time-dependent pulsatile capsular drug delivery system was prepared. The pulsatile release system consisted of an insoluble capsule body filled with drugs and an erodible plug tablet placed in the opening of the capsule body. The plug consisted mainly of pectin and pectinase in varying ratios. The lag times were dependent on pectin/pectinase ratios [254]. Another study aimed to achieve biphasic pulsatile drug release of losartan potassium by formulating a “tabs in cap” system employing guar gum. The system consisted of a non-biodegradable body capped with a water-soluble cap. A lag time of 6 h was noticed because of the optimal ratio of spray-dried lactose and guar gum. In the *ex vivo* study, it was inferred that two successive pulses for dissolution indicated a delay in absorption of the drug [256]. Various studies wherein PS based conventional drug delivery formulations to treat colonic diseases along with their outcomes are listed in Table 5.

5. Patents related to PS for the treatment of gastrointestinal diseases

There are many patents filed and granted all over the world highlighting the role of PS as therapeutics as well as polymer for drug delivery. The filing of numerous patents highlights the utility of PS to

incorporate drugs of various pharmacological classes as well as provide functionality as an excipient in the formulation. Upon analyzing the claims of various filed patents, it was observed that PS were used as part of a hydrophobic segment or pH-responsive polymer or for colon targeted action. Considering the swellability of PS, it was also noticed during the patent analysis that in the composition of formulation, PS played an important role in release of drugs incorporated in the formulation. It is pertinent to mention that PS has wide commercial scope and economical advantage as indicative with the number of patents filed for various gastrointestinal or colonic diseases. A list of patents wherein PS was used as part of the formulation for the treatment of various colon related diseases are highlighted in the present Table 6.

6. Conclusion

The global disease burden of gastrointestinal diseases is continuously expanding, and conventional drug delivery system treatment options appear to be limited due to specific problems connected with biopharmaceutical properties of traditional dosage forms and therapies. Poor dissolution rate, oral bioavailability, and lack of site specificity of conventional drug delivery systems limit the efficacy of active therapeutic. As a result, adjustments to conventional treatment procedures are being investigated in order to overcome these obstacles. Nanotechnology has made numerous advances in the realm of therapeutics employing nanomedicine methods. Over the last few years, PS-based drug delivery and therapeutics have gained prominence due to their stable, economical, biocompatible and therapeutic properties. In particular, various molecular parameters such as degree of polymerization, molecular weight, better onset of action has played an important role in the usage of PS-based drug delivery and therapeutic based options. The formulation process variables have an effect on overall PS drug delivery system as well as its physicochemical properties. Due to these bottlenecks, the use of PS as a therapeutic for colonic disease has not been extensively

Table 6

Patents on PS as therapeutic agent and as polymer for the treatment of colorectal diseases in chronological order.

Patent Number	Granting Agency	Application Year	Formulation	Disease used for	Key Claims	References
CN114668730A	CPO	2022	Enema	UC	Cross-linking agent along with PS	[284]
CN114057904A	CPO	2021	Colon targeted microcapsule	NA	PS composed of thiol codonopsis	[285]
CN113616619A	CPO	2021	Oral colon targeted formulation	UC	PS obtained from rhubarb and PS coating is from baihe polysaccharide	[286]
CN113372460A	CPO	2021	Powder	IBD	PS composed of Astragalus	[287]
CN111097921A	CPO	2020	Silver nanoparticles	CRC	PS from coltsfoot	[288]
CN110200948A	CPO	2019	Gastric controlled release capsule	NA	PS composed of tamarind	[289]
CN111867583A	CPO	2019	Capsule	UC	Mixture of PS containing modified starch and alginic acid	[290]
CN101982168A	CPO	2018	Colon specific micelle	NA	PS solution composed of Tremella and okra pectin	[291]
CN108853478A	CPO	2018	Colon targeted tablet	CRC	PS which is non starch in nature	[292]
JP2019019059A	JPO	2017	pH responsive liposome	NA	PS composed of a carboxyl group	[293]
CN106265510A	CPO	2016	pH responsive micelle	NA	Self-assembled hydrophobic PS	[294]
CN106727681A	CPO	2016	Oral Solid Dosage	CN	PS composed of isomaltose product	[295]
CN104382925A	CPO	2014	Colon targeted pellets	NA	Weight composition of PS is 10–50% w/w	[296]
CN104069204A	CPO	2014	Decoction granules	UC	PS obtained from Scutellaria baicalensis	[297]
US2015320694A1	USPO	2013	Mucoadhesive nanoparticle	NA	Hydrophilic portion is composed of PS PS composed of thiol functional group	[298]
CN104224848A	CPO	2013	Gastric floating tablet	NA	PS composed of alginate	[299]
CN102871983A	CPO	2012	Colon targeted tablet	NA	Composed of 15–18% of PS Coating layer of PS	[300]
CN103445044A	CPO	2012	Soft Capsule	IBD	PS composed of aloe polysaccharide	[301]
WO2012035561A2	PCT	2011	Microsphere	Colonic diseases	PS composed of guar gum or xanthan gum	[302]
CN101999645A	CPO	2009	Tablet	CRC	PS composed of Astragalus	[303]
CN101336950A	CPO	2008	Colon targeted tablet	NA	PS composed of Zanzhizhu extract	[304]
FR2830446A1	FPTO	2001	Colon targeted capsule	NA	PS used for coating is pectic acid or alginic acid	[305]
US5444054A	USPO	1994	Liquid Product	UC	PS part of the formulation	[306]

CPO- Chinese Patent Office; CRC- Colorectal cancer; FPTO- French Patent and Trademark Office; IBD- Irritable bowel disease; JPO- Japan Patent Office; NA- Not Applicable; PCT- Patent Cooperation Treaty; PS- Polysaccharide; UC- Ulcerative Colitis; USPO - United States Patent Office

researched upon. Moreover, the understanding of various physico-chemical parameters as well as underlying mechanisms will allow researchers to tailor the therapeutic for various PS-based therapies. This will lead to better commercialization and clinical utility of the PS.

The physical and chemical properties of PS, specifically their stereoselectivity, length, and structural activity, can have a significant impact on their various properties and their therapeutic effect [307]. Furthermore, the average size of PS has a direct impact on their catalytic and its colonic activity [308]. From a regulatory perspective, these natural products possess inherent heterogeneity in their synthesis [308]. Moreover, in the case of brown algal lineage, PS are not amendable to straightforward sequencing. PS are also considered to be hydrophobic and therefore require non aqueous solvents for their synthesis which has adverse effects on human health [309]. PS are known to be swellable in nature which limits their usage in large quantities. It is disadvantageous when scale up of the product has to be carried out. From a chemical point of view, mannose and rhamnose are ‘double-faced’ monosaccharides present in the PS, the β -linkages present in their structure are still considered a major challenge in carbohydrate chemistry, especially when cross-linking of PS is to be carried out [1]. Moreover, in case of glucan-based PS, the synthesis of the β (1–3) bond poses an inherent challenge as compared to β (1–6) bonds [310]. The synthetic PS such as polymannosides possess challenges of purification and characterization [311]. Due to the structural complexity of some PS (such as heparin), the formulation of these PS possesses an obstacle [312]. It was suggested in a recent study, that controlled hydrolysis of heparin can help overcome the challenge [313]. The glycosyl donor group present in hyaluronic acid is less reactive which can be overcome by adding a more reactive donor group [314]. Stereoselectivity and yield of PS are considered as prerequisite factors for its therapeutic activity. These factors are interdependent on acceptor conformation, and nucleophilicity thereby hindering the therapeutic activity [313]. These limitations associated with PS can be overcome by enzymatic, polymerization, and chemical synthesis.

Declaration of competing interest

The authors declare that they have no known competing financial interests or personal relationships that could have appeared to influence the work reported in this paper.

Data availability

Data will be made available on request.

References

- [1] A. Lovegrove, C.H. Edwards, I. de Noni, H. Patel, S.N. El, T. Grassby, C. Zielke, M. Ulmius, L. Nilsson, P.J. Butterworth, P.R. Ellis, P.R. Shewry, Role of polysaccharides in food, digestion, and health, *Crit. Rev. Food Sci. Nutr.* 57 (2017) 237–253, <https://doi.org/10.1080/10408398.2014.939263>.
- [2] A.S.A. Mohammed, M. Naveed, N. Jost, Polysaccharides; classification, chemical properties, and future perspective applications in fields of pharmacology and biological medicine (A review of current applications and upcoming potentialities), *J. Polym. Environ.* 29 (2021) 2359–2371, <https://doi.org/10.1007/s10924-021-02052-2>.
- [3] S.-R. Tsai, G.S.K. Sweatt, B.A. C, A.Y. L, L.Y. Li, Review of polysaccharide particle-based functional drug delivery, *Physiol. Behav.* 176 (2016) 139–148, <https://doi.org/10.1016/j.carbpol.2019.05.067>.
- [4] A.H. Teruel, I. Gonzalez-Alvarez, M. Bermejo, V. Merino, M.D. Marcos, F. Sancanon, M. Gonzalez-Alvarez, R. Martinez-Mañez, New insights of oral colonic drug delivery systems for inflammatory bowel disease therapy, *Int. J. Mol. Sci.* 21 (2020) 1–30, <https://doi.org/10.3390/ijms21186502>.
- [5] A. Kocira, K. Kozłowicz, K. Panasiewicz, M. Staniak, E. Szpunar-Krok, P. Horthyńska, Polysaccharides as Edible Films and Coatings: Characteristics and Influence on Fruit and Vegetable Quality—A Review, 2021, <https://doi.org/10.3390/agronomy11050813>.
- [6] A. Rampino, Polysaccharide-based Nanoparticles for Drug Delivery, 2011.
- [7] N. Dubashynskaya, D. Poshina, S. Raik, A. Urtili, Y.A. Skorik, Polysaccharides in ocular drug delivery, *Pharmaceuticals* 12 (2020) 1–30, <https://doi.org/10.3390/pharmaceuticals12010022>.
- [8] F. Damiri, N. Komminen, S.O. Ehbodaghe, R. Bulusu, V.G.S.S. Jyothi, A.A. Sayed, A.A. Awaji, M.O. Germoush, H.S. Al-Malky, M.Z. Nasrullah, M.H. Rahman, M. M. Abdel-Daim, M. Berrada, Microneedle-based natural polysaccharide for drug delivery systems (DDS): progress and challenges, *Pharmaceuticals* 15 (2022) 1–26, <https://doi.org/10.3390/ph15020190>.
- [9] G. Tiwari, R. Tiwari, S. Banerjee, L. Bhati, S. Pandey, P. Pandey, B. Sriwastawa, Drug delivery systems: an updated review, *Int J Pharm Investig* 2 (2012) 2, <https://doi.org/10.4103/2230-973x.96920>.
- [10] M.F. Bayan, R.F. Bayan, Recent advances in mesalamine colonic delivery systems, *Futur J Pharm Sci* 6 (2020), <https://doi.org/10.1186/s43094-020-00057-7>.
- [11] S. Salmaso, P. Caliceti, Stealth properties to improve therapeutic efficacy of drug nanocarriers, *J Drug Deliv* (2013) 1–19, <https://doi.org/10.1155/2013/374252>, 2013.
- [12] Y.Y. Kyung-Oh Doh, Appl. Polysaccharides. Surf. Modif. Nanomed. 3 (2013) 1447–1456, <https://doi.org/10.4155/tde.12.105.Application>.
- [13] S. Patil, Crosslinking of polysaccharides : methods and applications, *Pharm. Rev.* 6 (2016).
- [14] Y. Zhang, M. Li, X. You, F. Fang, B. Li, Impacts of guar and xanthan gums on pasting and gel properties of high-amylose corn starches, *Int. J. Biol. Macromol.* 146 (2020) 1060–1068, <https://doi.org/10.1016/j.ijbiomac.2019.09.231>.
- [15] Y. Kumari, S.K. Singh, R. Kumar, B. Kumar, G. Kaur, M. Gulati, D. Tewari, K. Gowthamarajan, V.V.S.N.R. Karri, C. Ayinkamiye, R. Khursheed, A. Awasthi, N.K. Pandey, S. Mohanta, S. Gupta, L. Corrie, P. Patni, R. Kumar, R. Kumar, Modified apple polysaccharide capped gold nanoparticles for oral delivery of insulin, *Int. J. Biol. Macromol.* 149 (2020) 976–988, <https://doi.org/10.1016/j.ijbiomac.2020.01.302>.
- [16] G. Kaur, S.K. Singh, R. Kumar, B. Kumar, Y. Kumari, M. Gulati, N.K. Pandey, K. Gowthamarajan, D. Ghosh, A. Clarisse, S. Wadhwa, M. Mehta, S. Satija, K. Dua, H. Dureja, S. Gupta, P.K. Singh, B. Kapoor, N. Chitranshi, A. Kumar, O. Porwal, Development of modified apple polysaccharide capped silver nanoparticles loaded with mesalamine for effective treatment of ulcerative colitis, *J. Drug Deliv. Sci. Technol.* 60 (2020), 101980, <https://doi.org/10.1016/j.jddst.2020.101980>.
- [17] A. Kumar, M. Gulati, S.K. Singh, K. Gowthamarajan, R. Prashar, D. Mankotia, J. P. Gupta, M. Banerjee, S. Sinha, A. Awasthi, L. Corrie, R. Kumar, P. Patni, B. Kumar, N.K. Pandey, M. Sadotra, P. Kumar, R. Kumar, S. Wadhwa, R. Khursheed, Effect of co-administration of probiotics with guar gum, pectin and eudragit S100 based colon targeted mini tablets containing 5-Fluorouracil for site specific release, *J. Drug Deliv. Sci. Technol.* 60 (2020), 102004, <https://doi.org/10.1016/j.jddst.2020.102004>.
- [18] S. Mohanta, S.K. Singh, B. Kumar, M. Gulati, R. Kumar, A.K. Yadav, S. Wadhwa, J. Jyoti, S. Som, K. Dua, N.K. Pandey, Efficacy of Co-administration of Modified Apple Polysaccharide and Probiotics in Guar Gum-Eudragit S100 Based Mesalamine Mini Tablets: A Novel Approach in Treating Ulcerative Colitis, Elsevier B.V., 2019, <https://doi.org/10.1016/j.ijbiomac.2018.12.154>.
- [19] S. Mohanta, S.K. Singh, B. Kumar, M. Gulati, J. Jyoti, S. Som, S. Panchal, I. Melkani, M. Banerjee, S.K. Sinha, R. Khursheed, A.K. Yadav, V. Verma, R. Kumar, D.S. Sharma, A.H. Malik, N.K. Pandey, S. Wadhwa, Solidification of liquid Modified Apple Polysaccharide by its adsorption on solid porous carriers through spray drying and evaluation of its potential as binding agent for tablets, *Int. J. Biol. Macromol.* 120 (2018), <https://doi.org/10.1016/j.ijbiomac.2018.09.181>, 1975–1998.
- [20] R. Kaur, M. Gulati, S.K. Singh, Role of Synbiotics in Polysaccharide Assisted Colon Targeted Microspheres of Mesalamine for the Treatment of Ulcerative Colitis, Elsevier B.V., 2017, <https://doi.org/10.1016/j.ijbiomac.2016.11.066>.
- [21] A.S. Gupta, S.J. Kshirsagar, M.R. Bhalekar, T. Saldanha, Design and development of liposomes for colon targeted drug delivery, *J. Drug Target.* 21 (2013) 146–160, <https://doi.org/10.3109/1061186X.2012.734311>.
- [22] S. Salave, D. Rana, A. Sharma, K. Bharathi, R. Gupta, S. Khode, D. Benival, N. Komminen, Polysaccharide based implantable drug delivery : development strategies, *Regul. Requir. Future. Perspect.* (2022) 625–654.
- [23] D. Chenthamara, S. Subramanian, S.G. Ramakrishnan, S. Krishnaswamy, M. M. Essa, F.H. Lin, M.W. Qoronfleh, Therapeutic efficacy of nanoparticles and routes of administration, *Biomater. Res.* 23 (2019) 1–29, <https://doi.org/10.1186/s40824-019-0166-x>.
- [24] C. Hou, L. Chen, L. Yang, X. Ji, An insight into anti-inflammatory effects of natural polysaccharides, *Int. J. Biol. Macromol.* 153 (2020) 248–255, <https://doi.org/10.1016/j.ijbiomac.2020.02.315>.
- [25] K. Ganesan, B. Xu, Anti-diabetic effects and mechanisms of dietary polysaccharides, *Molecules* 24 (2019), <https://doi.org/10.3390/molecules24142556>.
- [26] T. Khan, A. Date, H. Chawda, K. Patel, Polysaccharides as potential anticancer agents—a review of their progress, *Carbohydr. Polym.* 210 (2019) 412–428, <https://doi.org/10.1016/j.carbpol.2019.01.064>.
- [27] Q. Zhong, B. Wei, S. Wang, S. Ke, J. Chen, H. Zhang, H. Wang, The Antioxidant Activity of Polysaccharides Derived from Marine Organisms: an Overview, 2019, <https://doi.org/10.3390/md17120674>.
- [28] Q.X. Gan, J. Wang, J. Hu, G.H. Lou, H.J. Xiong, C.Y. Peng, Q.W. Huang, Modulation of apoptosis by plant polysaccharides for exerting anti-cancer effects: a review, *Front. Pharmacol.* 11 (2020), <https://doi.org/10.3389/fphar.2020.00792>.
- [29] Y.P. Silva, A. Bernardi, R.L. Frozza, The role of short-chain fatty acids from gut microbiota in gut-brain communication, *Front. Endocrinol.* 11 (2020) 1–14, <https://doi.org/10.3389/fendo.2020.00025>.
- [30] H.Y. Atay, Antibacterial Activity of Chitosan-Based Systems, 2020.

- [31] X. Yang, A. Li, D. Li, Y. Guo, L. Sun, Applications of mixed polysaccharide-protein systems in fabricating multi-structures of binary food gels—a review, *Trends Food Sci. Technol.* 109 (2021) 197–210, <https://doi.org/10.1016/j.tifs.2021.01.002>.
- [32] J.M. Cha, S.H. Park, K.H. Rhee, S.N. Hong, Y.H. Kim, S.I. Seo, K.H. Kim, S. K. Jeong, J.H. Lee, S.Y. Park, H. Park, J.S. Kim, J.P. Im, H. Yoon, S.H. Kim, J. Jang, J.H. Kim, S.O. Suh, Y.K. Kim, B.D. Ye, S.K. Yang, Long-term prognosis of ulcerative colitis and its temporal changes between 1986 and 2015 in a population-based cohort in the Songpa-Kangdong district of Seoul, Korea, *Gut* 69 (2020) 1432–1440, <https://doi.org/10.1136/gutjnl-2019-319699>.
- [33] D. Wang, Y. Zhang, S. Yang, D. Zhao, M. Wang, A polysaccharide from cultured mycelium of *Hericium erinaceus* relieves ulcerative colitis by counteracting oxidative stress and improving mitochondrial function, *Int. J. Biol. Macromol.* 125 (2019) 572–579, <https://doi.org/10.1016/j.ijbiomac.2018.12.092>.
- [34] X.H. Hongyu Xiao, Hailun Li, Yifan Wen, Dongxu Jiang, Shumin Zhu, J. Qingping Xiong, Jie Gao, Shaoshen Hou, Song Huang, He Lian, *Tremella fuciformis* polysaccharides ameliorated ulcerative colitis via inhibiting inflammation and enhancing intestinal epithelial barrier function, *Int. J. Biol. Macromol.* 180 (2021) 633–642.
- [35] L. Tian, G. Bruggeman, M. van den Berg, K. Borewicz, A.J.W. Scheurink, E. Bruininx, P. de Vos, H. Smidt, H.A. Schols, H. Gruppen, Effects of pectin on fermentation characteristics, carbohydrate utilization, and microbial community composition in the gastrointestinal tract of weaning pigs, *Mol. Nutr. Food Res.* 61 (2017) 1–10, <https://doi.org/10.1002/mnfr.201600186>.
- [36] L. Fan, S. Zuo, H. Tan, J. Hu, J. Cheng, Q. Wu, S. Nie, Preventive effects of pectin with various degrees of esterification on ulcerative colitis in mice, *Food Funct.* 11 (2020) 2886–2897, <https://doi.org/10.1039/c9fo03068a>.
- [37] Y. Horii, K. Uchiyama, Y. Toyokawa, Y. Hotta, M. Tanaka, Z. Yasukawa, M. Tokunaga, T. Okubo, K. Mizushima, Y. Higashimura, O. Dohi, T. Okayama, N. Yoshida, K. Katada, K. Kamada, O. Handa, T. Ishikawa, T. Takagi, H. Konishi, Y. Naito, Y. Itoh, Partially hydrolyzed guar gum enhances colonic epithelial wound healing: via activation of RhoA and ERK1/2, *Food Funct.* 7 (2016) 3176–3183, <https://doi.org/10.1039/c6fo00177g>.
- [38] X. Wang, X. Wang, H. Jiang, C. Cai, G. Li, J. Hao, G. Yu, Marine polysaccharides attenuate metabolic syndrome by fermentation products and altering gut microbiota: an overview, *Carbohydr. Polym.* 195 (2018) 601–612, <https://doi.org/10.1016/j.carbpol.2018.05.003>.
- [39] A. Yamamoto, T. Itoh, R. Nasu, R. Nishida, Effect of sodium alginate on dextran sulfate sodium- and 2,4,6-trinitrobenzene sulfonic acid-induced experimental colitis in mice, *Pharmacology* 92 (2013) 108–116, <https://doi.org/10.1159/000353192>.
- [40] F. Fernández-Bañares, J. Hinojosa, J.L. Sánchez-Lombraña, E. Navarro, J. F. Martínez-Salmerón, A. García-Pugés, F. González-Huix, J. Riera, V. González-Lara, F. Domínguez-Abascal, J.J. Giné, J. Moles, F. Gomollon, M.A. Gassull, Randomized clinical trial of Plantago ovata seeds (Dietary fiber) as compared with mesalazine in maintaining remission in ulcerative colitis, *Am. J. Gastroenterol.* 94 (1999) 427–433, [https://doi.org/10.1016/S0002-9270\(98\)00753-9](https://doi.org/10.1016/S0002-9270(98)00753-9).
- [41] Z.Q. Tong, B. Yang, B.Y. Chen, M.L. Zhao, A multi-center, randomized, single-blind, controlled clinical study on the efficacy of composite sophora colon-soluble capsules in treating ulcerative colitis, *Chin. J. Integr. Med.* 16 (2010) 486–492, <https://doi.org/10.1007/s11655-010-0562-5>.
- [42] S. Bhattacharyya, T. Shumard, H. Xie, A. Dodda, K.A. Varady, L. Fefferman, A. G. Halline, J.L. Goldstein, S.B. Hanauer, J.K. Tobacman, A randomized trial of the effects of the no-carrageenan diet on ulcerative colitis disease activity, *Nutr. Healthy Aging* 4 (2017) 181–192, <https://doi.org/10.3233/NHA-170023>.
- [43] P.C.F. Stokkers, D.W. Hommes, New cytokine therapeutics for inflammatory bowel disease, *Cytokine* 28 (2004) 167–173, <https://doi.org/10.1016/j.cyto.2004.07.012>.
- [44] Y. Wang, H. Zhu, X. Wang, Y. Jie, X. Xie, Natural Food Polysaccharides Ameliorate Inflammatory Bowel Disease and Its Mechanisms (2021) 1–19.
- [45] Y. Li, X. Tian, S. Li, P.S. LijunChang, Y. Lu1, X. Yu, S. Chen, Z. Wu, Z. Xu, W. Kang, Total polysaccharide of adlay bran (*Coix lachryma-jobi* L.) improves TNF-α induced epithelial barrier dysfunction in caco-2 cells via inhibition of inflammatory response, *Food Nutr.* (2019) 21, <https://doi.org/10.1039/C9FO00590K.Food>.
- [46] Y. Lu, L. Li, J. wei Zhang, X. qin Zhong, J.A. Wei, L. Han, Total polysaccharides of the Sijunzi decoction attenuate tumor necrosis factor-α-induced damage to the barrier function of a Caco-2 cell monolayer via the nuclear factor-κB-myosin light chain kinase-myosin light chain pathway, *World J. Gastroenterol.* 24 (2018) 2867–2877, <https://doi.org/10.3748/wjg.v24.i26.2867>.
- [47] C. Diling, Y. Xin, Z. Chaoqun, Y. Jjian, T. Xiaocui, C. Jun, S. Ou, X. Yizhen, Extracts from *Hericium erinaceus* relieve inflammatory bowel disease by regulating immunity and gut microbiota, *Oncotarget* 8 (2017) 85838–85857, <https://doi.org/10.18632/oncotarget.20689>.
- [48] G. Wu, S. Shiu, M. Hsieh, G. T. Tsai, Anti-inflammatory activity of a sulfated polysaccharide from the brown alga *Sargassum cristaeifolium*, *Food Hydrocolloids* (2015) 1–8, <https://doi.org/10.1016/j.foodhyd.2015.01.019>.
- [49] Y. Meng, F. Lyu, X. Xu, L. Zhang, Recent advances in chain conformation and bioactivities of triple-helix polysaccharides, *Biomacromolecules* 21 (2020) 1653–1677, <https://doi.org/10.1021/acs.biomac.9b01644>.
- [50] H.A. el Enshasy, R. Hatti-Kaul, Mushroom immunomodulators: unique molecules with unlimited applications, *Trends Biotechnol.* 31 (2013) 668–677, <https://doi.org/10.1016/j.tbiotech.2013.09.003>.
- [51] B.S. Park, J.O. Lee, Recognition of lipopolysaccharide pattern by TLR4 complexes, *Exp. Mol. Med.* 45 (2013) e66–e69, <https://doi.org/10.1038/emm.2013.97>.
- [52] M. Baldassarre, M. Fanelli, L. Corvaglia, N. Laforgia, Longitudinal evaluation of human β-defensins and tumor necrosis factor-α in stools of preterm and term newborns, *J. Pediatr. Gastroenterol. Nutr.* 53 (2011) 582, <https://doi.org/10.1097/MPG.0b013e31822c92f0>.
- [53] M. Najafzadeh, P.D. Reynolds, A. Baumgartner, D. Jerwood, D. Anderson, Chaga mushroom extract inhibits oxidative DNA damage in lymphocytes of patients with inflammatory bowel disease, *Biofactors* 31 (2007) 191–200, <https://doi.org/10.1002/biof.5520310306>.
- [54] F.A. Haggag, R.P. Boushey, Colorectal cancer epidemiology: incidence, mortality, survival, and risk factors, *Clin. Colon Rectal Surg.* 22 (2009) 191–197, <https://doi.org/10.1055/s-0029-1242458>.
- [55] X. Ji, Q. Peng, Y. Yuan, J. Shen, X. Xie, M. Wang, Isolation, structures and bioactivities of the polysaccharides from jujube fruit (*Ziziphus jujuba* Mill.): a review, *Food Chem.* 227 (2017) 349–357, <https://doi.org/10.1016/j.foodchem.2017.01.074>.
- [56] S. Wasser, Medicinal mushrooms as a source of antitumor and immunomodulating polysaccharides, *Appl. Microbiol. Biotechnol.* 60 (2002) 258–274, <https://doi.org/10.1007/s00253-002-1076-7>.
- [57] S. Ermakova, R. Men'shova, O. Vishchuk, S.M. Kim, B.H. Um, V. Isakov, T. Zvyagintseva, Water-soluble polysaccharides from the brown alga *Eisenia bicyclis*: structural characteristics and antitumor activity, *Algal Res.* 2 (2013) 51–58, <https://doi.org/10.1016/j.algal.2012.10.002>.
- [58] P. Sun, D. Sun, X. Wang, Effects of *Scutellaria barbata* polysaccharide on the proliferation, apoptosis and EMT of human colon cancer HT29 Cells, *Carbohydr. Polym.* 167 (2017) 90–96, <https://doi.org/10.1016/j.carbpol.2017.03.022>.
- [59] Q.H. Gao, X. Fu, R. Zhang, Z. Wang, M. Guo, Neuroprotective effects of plant polysaccharides: a review of the mechanisms, *Int. J. Biol. Macromol.* 106 (2018) 749–754, <https://doi.org/10.1016/j.ijbiomac.2017.08.075>.
- [60] M. Han, M.T. Ling, J. Chen, The key role of mitochondrial apoptotic pathway in the cytotoxic effect of mushroom extracts on cancer cells, *Crit. Rev. Eukaryot. Gene Expr.* 25 (2015) 253–258, <https://doi.org/10.1615/CritRevEukaryotGeneExpr.2015014019>.
- [61] I. Chau, D. Cunningham, Adjuvant therapy in colon cancer - what, when and how? *Ann. Oncol.* 17 (2006) 1347–1359, <https://doi.org/10.1093/annonc/mdl029>.
- [62] W. Hu, J.J. Kavanagh, Anticancer therapy targeting the apoptotic pathway, *Lancet Oncol.* 4 (2003) 721–729, [https://doi.org/10.1016/S1470-2045\(03\)01277-4](https://doi.org/10.1016/S1470-2045(03)01277-4).
- [63] F. Mao, B. Xiao, Z. Jiang, J. Zhao, X. Huang, J. Guo, Anticancer effect of *Lycium barbarum* polysaccharides on colon cancer cells involves G0/G1 phase arrest, *Med. Oncol.* 28 (2011) 121–126, <https://doi.org/10.1007/s12032-009-9415-5>.
- [64] S.A. Moharib, N.A. el Maksoud, H.M. Ragab, M.M. Shehata, Anticancer activities of mushroom polysaccharides on chemically induced colorectal cancer in rats, *J. Appl. Pharmaceut. Sci.* 4 (2014) 54–63, <https://doi.org/10.7324/JAPS.2014.40710>.
- [65] A.A. Feregrino-Pérez, L.C. Berumen, G. García-Alcocer, R.G. Guevara-Gonzalez, M. Ramos-Gomez, R. Reynoso-Camacho, J.A. Acosta-Gallegos, G. Loarca-Piña, Composition and chemopreventive effect of polysaccharides from common beans (*Phaseolus vulgaris* L.) on azoxymethane-induced colon cancer, *J. Agric. Food Chem.* 56 (2008) 8737–8744, <https://doi.org/10.1021/jf8007162>.
- [66] J. Luo, C. Zhang, R. Liu, L. Gao, S. Ou, L. Liu, X. Peng, Ganoderma lucidum polysaccharide alleviating colorectal cancer by alteration of special gut bacteria and regulation of gene expression of colonic epithelial cells, *J. Funct. Foods* 47 (2018) 127–135, <https://doi.org/10.1016/j.jff.2018.05.041>.
- [67] S. Ohwada, S. Kawate, T. Ikeya, T. Yokomori, T. Kusaba, T. Roppongi, T. Takahashi, S. Nakamura, Y. Kawashima, T. Nakajima, Y. Morishita, Adjuvant therapy with protein-bound polysaccharide K and tegafur uracil in patients with stage II or III colorectal cancer: randomized, controlled trial, *Dis. Colon Rectum* 46 (2003) 1060–1068, <https://doi.org/10.1007/s10350-004-7281-y>.
- [68] K. Ito, H. Nakazato, A. Koike, H. Takagi, S. Saji, S. Baba, M. Mai, J.I. Sakamoto, Y. Ohashi, Long-term effect of 5-fluorouracil enhanced by intermittent administration of polysaccharide K after curative resection of colon cancer. A randomized controlled trial for 7-year follow-up, *Int. J. Colorectal Dis.* 19 (2004) 157–164, <https://doi.org/10.1007/s00384-003-0532-x>.
- [69] F. Ho, H. Khalil, Crohn's disease: a clinical update, *Therap Adv Gastroenterol* 8 (2015) 352–359, <https://doi.org/10.1177/1756283X15592585>.
- [70] K.P. Nickerson, C. McDonald, Crohn's disease-associated adherent-invasive *Escherichia coli* adhesion is enhanced by exposure to the ubiquitous dietary polysaccharide maltodextrin, *PLoS One* 7 (2012) 1–13, <https://doi.org/10.1371/journal.pone.0052132>.
- [71] L. Reingold, K. Rahal, P. Schmiedlin-Ren, A.C. Rittershaus, D. Bender, S. R. Owens, J. Adler, E.M. Zimmermann, Development of a peptidoglycan-polysaccharide murine model of Crohn's disease: effect of genetic background, *Inflamm. Bowel Dis.* 19 (2013) 1238–1244, <https://doi.org/10.1097/MIB.0b013e31828132b4>.
- [72] Y. Yue, S. Wu, Z. Li, J. Li, X. Li, J. Xiang, H. Ding, Function Wild Jujube Polysaccharides Protect against Experimental in Inflammatory Bowel Disease by Enabling Enhanced Intestinal Barrier Function, 2015, <https://doi.org/10.1039/c5fo00378d>.
- [73] Y. Den, J. Kinoshita, G.A. Deshpande, E. Hiraoka, Amoebiasis masquerading as inflammatory bowel disease, *BMJ Case Rep.* (2015) 1–2, <https://doi.org/10.1136/bcr-2015-212102>, 2015.
- [74] A. Vaithilingam, J.E. Teixeira, P.J. Miller, B.T. Heron, C.D. Huston, Entamoeba histolytica cell surface calreticulin binds human C1q and functions in amebic phagocytosis of host cells, *Infect. Immun.* 80 (2012), <https://doi.org/10.1128/IAI.06287-11>, 2008–2018.

- [75] S.L. Stanley, Pathophysiology of amoebiasis, *Trends Parasitol.* 17 (2001) 280–285, [https://doi.org/10.1016/S1471-4922\(01\)01903-1](https://doi.org/10.1016/S1471-4922(01)01903-1).
- [76] J.R. Frederick, W.A. Petri, Roles for the galactose-*N*-acetylgalactosamine-binding lectin of *Entamoeba* in parasite virulence and differentiation, *Glycobiology* 15 (2005), <https://doi.org/10.1093/glycob/cwj007>.
- [77] D.M. Brenner, M. Shah, Chronic constipation, *Gastroenterol. Clin. N. Am.* 45 (2016) 205–216, <https://doi.org/10.1016/j.gtc.2016.02.013>.
- [78] H.V.L. Maffei, Chronic functional constipation. Which supplementary fiber to choose? *J. Pediatr.* 80 (2004) 167–168, <https://doi.org/10.2223/1177>.
- [79] H. Ma, H. Xiong, X. Zhu, C. Ji, J. Xue, R. Li, B. Ge, H. Cui, Polysaccharide from *Spirulina platensis* ameliorates diphenoxylate-induced constipation symptoms in mice, *Int. J. Biol. Macromol.* 133 (2019) 1090–1101, <https://doi.org/10.1016/j.ijbiomac.2019.04.209>.
- [80] O. Chem, C. Att, H. Pro, H. Un, *Effect of Malus Halliana Koehne Polysaccharides on Functional Constipation*, 2018, pp. 956–962.
- [81] X. Li, Y. Liu, W. Guan, Y. Xia, Y. Zhou, B. Yang, H. Kuang, Physicochemical properties and laxative effects of polysaccharides from *Anemarrhena asphodeloides* Bge. in loperamide-induced rats, *J. Ethnopharmacol.* 240 (2019), 111961, <https://doi.org/10.1016/j.jep.2019.111961>.
- [82] D. Maria-Ferreira, A.M. Nascimento, T.R. Cipriani, A.P. Santana-Filho, P. da S. Watanabe, D. de M.G. Sant'Ana, F.B. Luciano, K.C.P. Bocate, R.M. van den Wijngaard, M.F. de P. Werner, C.H. Baggio, Rhamnogalacturonan, a chemically-defined polysaccharide, improves intestinal barrier function in DSS-induced colitis in mice and human Caco-2 cells, *Sci. Rep.* 8 (2018) 1–14, <https://doi.org/10.1038/s41598-018-30526-2>.
- [83] F. Cheng, Y. Zhang, Q. Li, F. Zeng, K. Wang, Inhibition of dextran sodium sulfate-induced experimental colitis in mice by angelica sinensis polysaccharide, *J. Med. Food* 23 (2020) 584–592, <https://doi.org/10.1089/jmf.2019.4607>.
- [84] X. Ding, Q. Yu, K. Hou, X. Hu, Y. Wang, Y. Chen, J. Xie, S. Nie, M. Xie, Indirect stimulation of DCs by Ganoderma atrum polysaccharide in intestinal-like Caco-2/DCs co-culture model based on RNA-seq, *J. Funct. Foods* 67 (2020), 103850, <https://doi.org/10.1016/j.jff.2020.103850>.
- [85] B. Zheng, M. Ying, J. Xie, Y. Chen, Y. Wang, X. Ding, J. Hong, W. Liao, Q. Yu, Ganoderma atrum polysaccharide alleviated DSS-induced ulcerative colitis by protecting the apoptosis/autophagy-regulated physical barrier and the DC-related immune barrier, *Food Funct.* 11 (2020) 10690–10699, <https://doi.org/10.1039/d0fo02260h>.
- [86] C. Liu, H. Hua, H.K. Zhu, Y. Cheng, Y. Guo, W. Yao, H. Qian, Aloe polysaccharides ameliorate acute colitis in mice via Nrf2/HO-1 signaling pathway and short-chain fatty acids metabolism, *Int. J. Biol. Macromol.* 185 (2021) 804–812, <https://doi.org/10.1016/j.ijbiomac.2021.07.007>.
- [87] Y. Wang, X. Ji, M. Yan, X. Chen, M. Kang, L. Teng, X. Wu, J. Chen, C. Deng, Protective effect and mechanism of polysaccharide from *Diclyophora indusiata* on dextran sodium sulfate-induced colitis in C57BL/6 mice, *Int. J. Biol. Macromol.* 140 (2019) 973–984, <https://doi.org/10.1016/j.ijbiomac.2019.08.198>.
- [88] W. Guo, S. Zhu, G. Feng, L. Wu, Y. Feng, T. Guo, Y. Yang, H. Wu, M. Zeng, Microalgae aqueous extracts exert intestinal protective effects in Caco-2 cells and dextran sodium sulphate-induced mouse colitis, *Food Funct.* 11 (2020) 1098–1109, <https://doi.org/10.1039/c9fo01028a>.
- [89] Y. Liu, X. Zhao, T. Lin, Q. Wang, Y. Zhang, J. Xie, Molecular mechanisms of polysaccharides from *Ziziphos jujuba* Mill var. *spinosa* seeds regulating the bioavailability of spinosin and preventing colitis, *Int. J. Biol. Macromol.* 163 (2020) 1393–1402, <https://doi.org/10.1016/j.ijbiomac.2020.07.229>.
- [90] F. Han, H. Fan, M. Yao, S. Yang, J. Han, Oral administration of yeast β -glucan ameliorates inflammation and intestinal barrier in dextran sodium sulfate-induced acute colitis, *J. Funct. Foods* 35 (2017) 115–126, <https://doi.org/10.1016/j.jff.2017.05.036>.
- [91] C. Guo, Y. Wang, S. Zhang, X. Zhang, Z. Du, M. Li, K. Ding, *Crataegus pinnatifida* polysaccharide alleviates colitis via modulation of gut microbiota and SCFAs metabolism, *Int. J. Biol. Macromol.* 181 (2021) 357–368, <https://doi.org/10.1016/j.ijbiomac.2021.03.137>.
- [92] X. Zhou, Q. Lu, X. Kang, G. Tian, D. Ming, J. Yang, Protective role of a new polysaccharide extracted from *Lonicera japonica* thunb in mice with ulcerative colitis induced by dextran sulphate sodium, *BioMed Res. Int.* 2021 (2021), <https://doi.org/10.1155/2021/8878633>.
- [93] A. Hamed, H. Rezaei, N. Azarpira, M. Jafarpour, F. Ahmadi, Effects of malva sylvestris and its isolated polysaccharide on experimental ulcerative colitis in rats, *J Evid Based Complementary Altern Med* 21 (2016) 14–22, <https://doi.org/10.1177/2156587215589184>.
- [94] C. Huang, X. Luo, L. Li, N. Xue, Y. Dang, H. Zhang, J. Liu, J. Li, C. Li, F. Li, Glycyrrhiza Polysaccharide Alleviates Dextran Sulfate Sodium-Induced Ulcerative Colitis in Mice, Evidence-Based Complementary and Alternative Medicine, 2022, p. 2022, <https://doi.org/10.1155/2022/1345852>.
- [95] V.K.C. Wong, L. Yu, C.H. Cho, Protective effect of polysaccharides from *Angelica sinensis* on ulcerative colitis in rats, *Inflammopharmacology* 16 (2008) 162–167, <https://doi.org/10.1007/s10787-007-0026-5>.
- [96] Y. Wang, N. Zhang, J. Kan, X. Zhang, X. Wu, R. Sun, S. Tang, J. Liu, C. Qian, C. Jin, Structural characterization of water-soluble polysaccharide from *Arctium lappa* and its effects on colitis mice, *Carbohydr. Polym.* 213 (2019) 89–99, <https://doi.org/10.1016/j.carbpol.2019.02.090>.
- [97] D.L. Seidner, B.A. Lashner, A. Brzezinski, P.L.C. Banks, J. Goldblum, C. Fiocchi, J. Katz, G.R. Lichtenstein, P.A. Anton, L.Y. Kam, K.A. Garleb, S.J. Demichele, An oral supplement enriched with fish oil, soluble fiber, and antioxidants for corticosteroid sparing in ulcerative colitis: a randomized, controlled trial, *Clin. Gastroenterol. Hepatol.* 3 (2005) 358–369, [https://doi.org/10.1016/S1542-3565\(04\)00672-X](https://doi.org/10.1016/S1542-3565(04)00672-X).
- [98] M. Nyman, T.D. Nguyen, O. Wikman, H. Hjortswang, C. Hallert, Oat bran increased fecal butyrate and prevented gastrointestinal symptoms in patients with quiescent ulcerative colitis-randomized controlled trial, *Crohns Colitis* 360 (2020) 1–13, <https://doi.org/10.1093/crocol/otaa005>, 2.
- [99] Y. Wei, J. Gong, W. Zhu, H. Tian, C. Ding, L. Gu, N. Li, J. Li, Pectin enhances the effect of fecal microbiota transplantation in ulcerative colitis by delaying the loss of diversity of gut flora, *BMC Microbiol.* 16 (2016) 1–9, <https://doi.org/10.1186/s12866-016-0869-2>.
- [100] W. Li, M. Gao, T. Han, Lycium barbarum polysaccharides ameliorate intestinal barrier dysfunction and inflammation through the MLCK-MLC signaling pathway in Caco-2 cells, *Food Funct.* 11 (2020) 3741–3748, <https://doi.org/10.1039/d0fo00030b>.
- [101] L.N. Liu, Q.B. Mei, L. Liu, F. Zhang, Z.G. Liu, Z.P. Wang, R.T. Wang, Protective effects of Rheum tanguticum polysaccharide against hydrogen peroxide-induced intestinal epithelial cell injury, *World J. Gastroenterol.* 11 (2005) 1503–1507, <https://doi.org/10.3748/wjg.v11.i10.1503>.
- [102] S.P. Liu, W.G. Dong, D.F. Wu, H.S. Luo, J.P. Yu, Protective effect of angelica sinensis polysaccharide on experimental immunological colon injury in rats, *World J. Gastroenterol.* 9 (2003) 2786–2790, <https://doi.org/10.3748/wjg.v9.i12.2786>.
- [103] L. Liu, Z. Guo, Z. Lv, Y. Sun, W. Cao, R. Zhang, Z. Liu, C. Li, S. Cao, Q. Mei, The beneficial effect of Rheum tanguticum polysaccharide on protecting against diarrhea, colonic inflammation and ulceration in rats with TNBS-induced colitis: the role of macrophage mannose receptor in inflammation and immune response, *Int. Immunopharm.* 8 (2008) 1481–1492, <https://doi.org/10.1016/j.intimp.2008.04.013>.
- [104] J.A. Batista, D. de A. Magalhães, S.G. Sousa, J. dos S. Ferreira, C.M.C. Pereira, J.V. do N. Lima, I.F. de Albuquerque, N.L.S.D. Bezerra, T.V. de Brito, C.E. da S. Monteiro, A.X. Franco, D. di Lenardo, L.A. Oliveira, J.P. de A. Feitosa, R.C. M. de Paula, F.C.N. Barros, A.L.P. Freitas, J.S. de Oliveira, D.F.P. Vasconcelos, P. M.G. Soares, A.L. dos R. Barbosa, Polysaccharides derived from *Morinda citrifolia* Linn reduce inflammatory markers during experimental colitis, *J. Ethnopharmacol.* 248 (2020), 112303, <https://doi.org/10.1016/j.jep.2019.112303>.
- [105] H.P.H.R. Monturil, T.V. de Brito, J.S. da Cruz Júnior, G.J.D. Júnior, D. de Aguiar Magalhães, S.G. Sousa, J.A. Batista, R.O.S. Damasceno, J.G. Pereira, J. X. Mesquita, D.F.P. Vasconcelos, J.S. de Oliveira, R.D.S. Bezerra, P.M.G. Soares, M.H.L.P. Souza, A.L.P. Freitas, A.L. dos R. Barbosa, Sulfated polysaccharide from *Digenaea simplex* decreases intestinal inflammation in rats, *Revista Brasileira de Farmacognosia* 30 (2020) 388–396, <https://doi.org/10.1007/s43450-020-00073-x>.
- [106] X. Liu, X. Yu, X. Xu, X. Zheng, X. Zhang, The protective effects of Poria cocos-derived polysaccharide CMP33 against IBD in mice and its molecular mechanism, *Food Funct.* 9 (2018) 5936–5949, <https://doi.org/10.1039/c8fo01604f>.
- [107] A. Belluzi, G. Roda, F. Tonon, A. Soletti, A. Caponi, A. Tuci, A. Roda, E. Roda, A new iron free treatment with oral fish cartilage polysaccharide for iron deficiency chronic anemia in inflammatory bowel disease: a pilot study, *World J. Gastroenterol.* 13 (2007) 1575–1578, <https://doi.org/10.3748/wjg.v13.i10.1575>.
- [108] Z. Liang, Y. Yi, Y. Guo, R. Wang, Q. Hu, X. Xiong, Chemical characterization and antitumor activities of polysaccharide extracted from *Ganoderma lucidum*, *Int. J. Mol. Sci.* 15 (2014) 9103–9116, <https://doi.org/10.3390/ijms15059103>.
- [109] I.B. Jeff, X. Yuan, L. Sun, R.M.R. Kassim, A.D. Foday, Y. Zhou, Purification and in vitro anti-proliferative effect of novel neutral polysaccharides from *Lentinus edodes*, *Int. J. Biol. Macromol.* 52 (2013) 99–106, <https://doi.org/10.1016/j.ijbiomac.2012.10.007>.
- [110] S. Zhang, S. Nie, D. Huang, W. Li, M. Xie, Immunomodulatory effect of *Ganoderma atrum* polysaccharide on CT26 tumor-bearing mice, *Food Chem.* 136 (2013) 1213–1219, <https://doi.org/10.1016/j.foodchem.2012.08.090>.
- [111] D. Cheng, X. Zhang, M. Meng, L. Han, C. Li, L. Hou, W. Qi, C. Wang, Inhibitory effect on HT-29 colon cancer cells of a water-soluble polysaccharide obtained from highland barley, *Int. J. Biol. Macromol.* 92 (2016) 88–95, <https://doi.org/10.1016/j.ijbiomac.2016.06.099>.
- [112] L. Ma, C. Qin, M. Wang, D. Gan, L. Cao, H. Ye, X. Zeng, Preparation, preliminary characterization and inhibitory effect on human colon cancer HT-29 cells of an acidic polysaccharide fraction from *Stachys floridana* Schuttll. ex Benth, *Food Chem. Toxicol.* 60 (2013) 269–276, <https://doi.org/10.1016/j.foct.2013.07.060>.
- [113] P. Shao, J. Liu, X. Chen, Z. Fang, P. Sun, Structural features and antitumor activity of a purified polysaccharide extracted from *Sargassum horneri*, *Int. J. Biol. Macromol.* 73 (2015) 124–130, <https://doi.org/10.1016/j.ijbiomac.2014.10.056>.
- [114] K.S. Lee, J.S. Shin, K.S. Nam, Inhibitory effect of starfish polysaccharides on metastasis in HT-29 human colorectal adenocarcinoma, *Biotechnol. Bioproc. Eng.* 17 (2012) 764–769, <https://doi.org/10.1007/s12257-012-0099-x>.
- [115] X. Ji, C. Hou, Y. Gao, Y. Xue, Y. Yan, X. Guo, Function Metagenomic analysis of gut microbiota modulatory effects of jujube (*Ziziphos jujuba* Mill) polysaccharides in a colorectal cancer mouse, 2020, pp. 163–173, <https://doi.org/10.1039/c9fo02171j>.
- [116] G. Song, Y. Lu, Z. Yu, L. Xu, J. Liu, K. Chen, P. Zhang, The inhibitory effect of polysaccharide from *Rhizopus nigricans* on colitis-associated colorectal cancer, *Biomed. Pharmacother.* 112 (2019), 108593, <https://doi.org/10.1016/j.biopha.2019.01.054>.
- [117] Y. Li, L. Liu, Y. Niu, J. Feng, Y. Sun, X. Kong, Y. Chen, X. Chen, H. Gan, S. Cao, Q. Mei, Modified apple polysaccharide prevents against tumorigenesis in a mouse model of colitis-associated colon cancer: role of galectin-3 and apoptosis in cancer

- prevention, *Eur. J. Nutr.* 51 (2012) 107–117, <https://doi.org/10.1007/s00394-011-0194-3>.
- [118] Q. Wang, Y. Huang, M. Jia, D. Lu, H. Zhang, D. Huang, M. Chen, Safflower Polysaccharide Inhibits AOM/DSS-Induced Mice Colorectal Cancer through the Regulation of Macrophage Polarization, vol. 12, 2021, pp. 1–13, <https://doi.org/10.3389/fphar.2021.761641>.
- [119] J. Liang, H. Li, J. Chen, L. He, X. Du, L. Zhou, Q. Xiong, X. Lai, Y. Yang, S. Huang, S. Hou, Dendrobium officinale polysaccharides alleviate colon tumorigenesis via restoring intestinal barrier function and enhancing anti-tumor immune response, *Pharmacol. Res.* 148 (2019), 104417, <https://doi.org/10.1016/j.phrs.2019.104417>.
- [120] S. Ohwada, T. Ogawa, F. Makita, Y. Tanahashi, T. Ohya, N. Tomizawa, Y. Satoh, I. Kobayashi, M. Izumi, I. Takeyoshi, K. Hamada, S. Minaguchi, Y. Togo, T. Toshihiko, T. Koyama, M. Kamio, Beneficial effects of protein-bound polysaccharide K plus tegafur/uracil in patients with stage II or III colorectal cancer: analysis of immunological parameters, *Oncol. Rep.* 15 (2006) 861–868, <https://doi.org/10.3892/or.15.4.861>.
- [121] W. Tan, W. Zhou, Y. Zhao, T. Fu, X. Huang, J. Lin, xiaohe Lan, R. Yu, C. Min, W. Qiu, C. Wang, Effect of Poria polysaccharide oral liquid on cancer-related fatigue in postoperative patients with colorectal cancer, *Tob Regul Sci* 7 (2021) 6519–6528, <https://doi.org/10.18001/trs.7.6.127>.
- [122] Combined Nutritional Therapies for the Treatment of Ulcerative Colitis, *Clinicaltrials.Net.* (n.d.). <https://clinicaltrials.gov/ct2/show/NCT03444311?term=Pectin&cond=Ulcerative+Colitis&draw=2&rank=1>.
- [123] Effects of pectin on flora intestinal colonization and maintenance after fecal transplantation, n.d. <https://clinicaltrials.gov/ct2/show/NCT02016469?term=Pectin&cond=Inflammatory+Bowel+Diseases&draw=2&rank=1>. (Accessed 3 December 2021). accessed
- [124] Effect of soluble dietary fiber on bacterial translocation in crohn's disease, n.d. <https://clinicaltrials.gov/ct2/show/NCT02164877?term=Pectin&cond=Inflammatory+Bowel+Diseases&draw=2&rank=2>. (Accessed 3 December 2021). accessed
- [125] Effects of Pectin Supplementation, Diarrhea-predominant Irritable Bowel Syndrome, 2014. <https://clinicaltrials.gov/ct2/show/NCT02270268?cond=pectin&draw=2&rank=8>. (Accessed 4 December 2021). accessed.
- [126] A real world study of bismuth colloidal pectin granules quadruple therapy for H. Pylori eradication, n.d. <https://clinicaltrials.gov/ct2/show/NCT04660123?cond=pectin&draw=2&rank=9>. (Accessed 4 December 2021). accessed
- [127] The effect of alginate on carbohydrate and fat digestion in a mixed meal, n.d. <https://clinicaltrials.gov/ct2/show/NCT03860337?cond=alginate&draw=2&rank=1>. (Accessed 4 December 2021).
- [128] Efficacy and safety of sodium alginate oral suspension to treat non-erosive gastro-esophageal reflux disease, n.d. <https://clinicaltrials.gov/ct2/show/NCT01338077?cond=alginate&draw=2&rank=2>. (Accessed 4 December 2021). accessed
- [129] Feasibility and safety of the calcium alginate hydrogel sealant for the treatment of cryptoglandular fistula-in-ano: phase I/IIa clinical tria, n.d. <https://clinicaltrials.gov/ct2/show/NCT04740086?cond=alginate&draw=2&rank=4>. (Accessed 4 December 2021). accessed
- [130] Effectiveness of partially hydrolyzed guar gum in improving fecal characteristics in long term care facility residents, n.d. <https://clinicaltrials.gov/ct2/show/NCT05037565?cond=Guar+gum&draw=2&rank=2>. (Accessed 4 December 2021). accessed
- [131] The role of partial hydrolyzed guar gum in high stoma output management among cancer patients with ileostomy, n.d. <https://clinicaltrials.gov/ct2/show/NCT04678349?cond=Guar+gum&draw=2&rank=3>. (Accessed 4 December 2021). accessed
- [132] The efficacy of hydrolyzed guar gum (PHGG) in the treatment of patients with irritable bowel syndrome (IBS), n.d. <https://clinicaltrials.gov/ct2/show/NCT01779765?cond=Guar+gum&draw=2&rank=5>. (Accessed 4 December 2021). accessed
- [133] Treating IBD with inulin (TII), n.d. <https://clinicaltrials.gov/ct2/show/NCT003653481?cond=Inulin&draw=2&rank=5>. (Accessed 4 December 2021). accessed
- [134] Effect of consumption of Orafti® inulin on bowel motor function in subjects with constipation, n.d. <https://clinicaltrials.gov/ct2/show/NCT02548247?cond=inulin&draw=2&rank=7>. (Accessed 4 December 2021). accessed
- [135] Atorvastatin calcium, oligofructose-enriched inulin, or sulindac in preventing cancer in patients at increased risk of developing colorectal neoplasia. <https://clinicaltrials.gov/ct2/show/NCT00335504?cond=inulin&draw=6&rank=41>. (Accessed 4 December 2021) accessed.
- [136] Beta-1,3/1,6-D-Glucan Ganoderma Lucidum on Ulcerative Colitis, (n.d.). <https://clinicaltrials.gov/ct2/show/NCT04029649?cond=ganoderma+lucidum&draw=2&rank=3> (accessed December 4, 2021).
- [137] Clinical trial on Ganoderma spore lipids combined with chemo in patients with G. I. Cancers, n.d. <https://clinicaltrials.gov/ct2/show/NCT02785523?cond=ganoderma+lucidum&draw=3&rank=15>. (Accessed 6 December 2021). accessed
- [138] Evaluation of Acacia gum on microbiome and bowel function in participants with chronic constipation, n.d. <https://clinicaltrials.gov/ct2/show/NCT04382456?cond=Acacia+Gum&draw=4&rank=1>. (Accessed 6 December 2021). accessed
- [139] Effect of agar administration on defecation and fecal condition in chronic constipated patients, n.d. <https://clinicaltrials.gov/ct2/show/NCT02012543?cond=Agar&draw=2&rank=1>. (Accessed 6 December 2021). accessed
- [140] To assess the safety and tolerance of infant formula with locust bean gum in infants with regurgitation (solar). <https://clinicaltrials.gov/ct2/show/NCT04042454?cond=locust+bean&draw=2&rank=1>. (Accessed 6 December 2021) accessed.
- [141] H. Jiang, J. Dong, S. Jiang, Q. Liang, Y. Zhang, Z. Liu, C. Ma, J. Wang, W. Kang, Effect of Durio zibethinus rind polysaccharide on functional constipation and intestinal microbiota in rats, *Food Res. Int.* 136 (2020), 109316, <https://doi.org/10.1016/j.foodres.2020.109316>.
- [142] M. Schultz, K. Munro, G.W. Tannock, I. Melchner, C. Go, H. Schwiertz, H.C. Rath, Effects of feeding a probiotic preparation (SIM) containing inulin on the severity of colitis and on the composition of the intestinal microflora in HLA-B27 transgenic, Rats 11 (2004) 581–587, <https://doi.org/10.1128/CDLI.11.3.581>.
- [143] R.K. le Leu, L.L. Brown, Y. Hu, A.R. Bird, M. Jackson, A. Esterman, G.P. Young, A symbiotic combination of resistant starch and Bifidobacterium lactis facilitates apoptotic deletion of carcinogen-damaged cells in rat colon, *J. Nutr.* 135 (2005) 996–1001, <https://doi.org/10.1093/jn/135.5.996>.
- [144] R. Zhang, J. Sun, X. Chen, C. Nie, J. Zhao, W. Guan, L. Lei, T. He, Y. Chen, L. J. Johnston, J. Zhao, X. Ma, Combination of Clostridium butyricum and corn bran optimized intestinal microbial fermentation using a weaned pig model, *Front. Microbiol.* 9 (2018) 1–10, <https://doi.org/10.3389/fmicb.2018.03091>.
- [145] G. Prudhviraj, Y. Vaidya, S.K. Singh, A.K. Yadav, P. Kaur, M. Gulati, K. Gowthamarajan, Effect of co-administration of probiotics with polysaccharide based colon targeted delivery systems to optimize site specific drug release, *Eur. J. Pharm. Biopharm.* 97 (2015) 164–172, <https://doi.org/10.1016/j.ejpb.2015.09.012>.
- [146] R. Kumar, A. Butreddy, N. Kommineni, P.G. Reddy, N. Bunekar, C. Sarkar, S. Dutt, V.K. Mishra, K.R. Aadil, Lignin : Drug/Gene Delivery and Tissue Engineering Applications, 2021, pp. 2419–2441.
- [147] J.K. Patra, G. Das, L.F. Fraceto, E.V.R. Campos, M.D.P. Rodriguez-Torres, L. S. Acosta-Torres, L.A. Diaz-Torres, R. Grillo, M.K. Swamy, S. Sharma, S. Habtemariam, H.S. Shin, Nano based drug delivery systems: recent developments and future prospects, *J. Nanobiotechnol.* 16 (2018) 1–33, <https://doi.org/10.1186/s12951-018-0392-8>.
- [148] M.K. Chourasia, S.K. Jain, Polysaccharides for colon targeted drug delivery, drug delivery, *J. Deliv. Target. Therapeut. Agents.* 11 (2004) 129–148, <https://doi.org/10.1080/10717540490280778>.
- [149] S. Hua, Advances in oral drug delivery for regional targeting in the gastrointestinal tract - influence of physiological, pathophysiological and pharmaceutical factors, *Front. Pharmacol.* 11 (2020) 1–22, <https://doi.org/10.3389/fphar.2020.00524>.
- [150] R. Song, M. Murphy, C. Li, K. Ting, C. Soo, Z. Zheng, Current development of biodegradable polymeric materials for biomedical applications, *Drug Des. Dev. Ther.* 12 (2018) 3117–3145, <https://doi.org/10.2147/DDDT.S165440>.
- [151] I. Neamtu, A.G. Rusu, A. Diaconu, L.E. Nita, A.P. Chiriac, Basic concepts and recent advances in nanogels as carriers for medical applications, *Drug Deliv.* 24 (2017) 539–557, <https://doi.org/10.1080/10717544.2016.1276232>.
- [152] M. Curcio, F. Puoci, F. Iemma, O.I. Parisi, G. Cirillo, U.G. Spizzirri, N. Picci, Covalent insertion of antioxidant molecules on chitosan by a free radical grafting procedure, *J. Agric. Food Chem.* 57 (2009) 5933–5938, <https://doi.org/10.1021/jf900778u>.
- [153] Y. de Anda-Flores, E. Carvajal-Millan, J. Lizardi-Mendoza, A. Rascon-Chu, A. L. Martínez-López, J. Marquez-Escalante, F. Brown-Bojorquez, J. Tanori-Cordova, Covalently cross-linked nanoparticles based on ferulated arabinoxylans recovered from a distiller's dried grains byproduct, *Processes* 8 (2020) 691, <https://doi.org/10.3390/PR8060691>.
- [154] Y.F. Ding, T. Sun, S. Li, Q. Huang, L. Yue, L. Zhu, R. Wang, Oral colon-targeted konjac glucomannan hydrogel constructed through noncovalent cross-linking by cucurbit[8]uril for ulcerative colitis therapy, *ACS Appl. Bio Mater.* 3 (2020) 10–19, <https://doi.org/10.1021/acsbam.9b00676>.
- [155] N. Bhattarai, J. Gunn, M. Zhang, Chitosan-based hydrogels for controlled, localized drug delivery, *Adv. Drug Deliv. Rev.* 62 (2010) 83–99, <https://doi.org/10.1016/j.addr.2009.07.019>.
- [156] J.H. Hamman, Chitosan based polyelectrolyte complexes as potential carrier materials in drug delivery systems, *Mar. Drugs* 8 (2010) 1305–1322, <https://doi.org/10.3390/md8041305>.
- [157] S.A.A. AhmadMiraNasreenMazumdar, Preparation, characterization, release and antianemic studies of guar gum functionalized iron complexes, *Int. J. Biol. Macromol.* 183 (2021) 1495–1504.
- [158] K. Mitsuhashi, P. Qi, A. Takahashi, S. Ohta, T. Ito, Prevention of postoperative peritoneal adhesions in rats with sidewall defect-bowel abrasions using metal ion-crosslinked N-succinyl chitosan hydrogels, *React. Funct. Polym.* 145 (2019), 104374, <https://doi.org/10.1016/j.reactfunctpolym.2019.104374>.
- [159] S. Lankalapalli, V.R.M. Kolapalli, Polyelectrolyte complexes: a review of their applicability in drug delivery technology, *Indian J. Pharmaceut. Sci.* 71 (2009) 481–487, <https://doi.org/10.4103/0250-474X.58165>.
- [160] J. Cao, J. Cheng, S. Xi, X. Qi, S. Shen, Y. Ge, Alginate/chitosan microcapsules for in-situ delivery of the protein, interleukin-1 receptor antagonist (IL-1Ra), for the treatment of dextran sulfate sodium (DSS)-induced colitis in a mouse model, *Eur. J. Pharm. Biopharm.* 137 (2019) 112–121, <https://doi.org/10.1016/j.ejpb.2019.02.011>.
- [161] S. Trombino, S. Serini, R. Cassano, G. Calviello, Xanthan gum-based materials for omega-3 PUFA delivery: preparation, characterization and anti-neoplastic activity evaluation, *Carbohydr. Polym.* 208 (2019) 431–440, <https://doi.org/10.1016/j.carbpol.2019.01.001>.
- [162] B.B. Breitenbach, I. Schmid, P.R. Wich, Amphiphilic polysaccharide block copolymers for pH-responsive micellar nanoparticles, *Biomacromolecules* 18 (2017) 2839–2848, <https://doi.org/10.1021/acs.biomac.7b00771>.
- [163] C. Chen, D.Y.W. Ng, T. Weil, Polymer bioconjugates: modern design concepts toward precision hybrid materials, *Prog. Polym. Sci.* 105 (2020), 101241, <https://doi.org/10.1016/j.progpolymsci.2020.101241>.

- [164] A. Kumar, Deepak, S. Sharma, A. Srivastava, R. Kumar, Synthesis of xanthan gum graft copolymer and its application for controlled release of highly water soluble Levofloxacin drug in aqueous medium, Carbohydr. Polym. 171 (2017) 211–219, <https://doi.org/10.1016/j.carbpol.2017.05.010>.
- [165] M. Veneranda, Q. Hu, T. Wang, Y. Luo, K. Castro, J.M. Madariaga, Formation and characterization of zein-caseinate-pectin complex nanoparticles for encapsulation of eugenol, LWT - Food Sci. Technol. (Lebensmittel-Wissenschaft -Technol.) 89 (2018) 596–603, <https://doi.org/10.1016/j.lwt.2017.11.040>.
- [166] H. He, Y. Lu, J. Qi, Q. Zhu, Z. Chen, W. Wu, Adapting liposomes for oral drug delivery, Acta Pharm. Sin. B 9 (2019) 36–48, <https://doi.org/10.1016/j.apsb.2018.06.005>.
- [167] J. Deng, Z. Zhang, C. Liu, L. Yin, J. Zhou, H. Lv, The studies of N-Octyl-N-Arginine-Chitosan coated liposome as an oral delivery system of Cyclosporine A, J. Pharm. Pharmacol. 67 (2015) 1363–1370, <https://doi.org/10.1111/jphp.12448>.
- [168] I. Vural, C. Sarisozen, S.S. Olmez, Chitosan coated furosemide liposomes for improved bioavailability, J. Biomed. Nanotechnol. 7 (2011) 426–430, <https://doi.org/10.1166/jbn.2011.1294>.
- [169] K.M. Hosny, O.A.A. Ahmed, R.T. Al-Abdali, Enteric-coated alendronate sodium nanoliposomes: a novel formula to overcome barriers for the treatment of osteoporosis, Expet Opin. Drug Deliv. 10 (2013) 741–746, <https://doi.org/10.1517/17425247.2013.799136>.
- [170] A. Catalan-Latorre, M. Ravaggi, M.L. Manca, C. Caddeo, F. Marongiu, G. Ennas, E. Escibano-Ferrer, J.E. Peris, O. Diez-Salles, A.M. Fadda, M. Manconi, Freeze-dried eudragit-hyaluronan multicompartment liposomes to improve the intestinal bioavailability of curcumin, Eur. J. Pharm. Biopharm. 107 (2016) 49–55, <https://doi.org/10.1016/j.ejpb.2016.06.016>.
- [171] M. Román-Aguirre, C. Leyva-Porras, P. Cruz-Alcantar, A. Aguilar-Elguézabal, M. Z. Saavedra-Leos, Comparison of polysaccharides as coatings for quercetin-loaded liposomes (QL) and their effect as antioxidants on radical scavenging activity, Polymers 12 (2020) 1–15, <https://doi.org/10.3390/polym12122793>.
- [172] N. Shah, T. Shah, A. Amin, Polysaccharides : a Targeting Strategy for Colonic Drug Delivery, 2011, pp. 779–796.
- [173] E. Harel, A. Rubinstein, A. Nissan, E. Khazanov, M. Milbauer, Y. Barenholz, B. Tirosh, Enhanced transferrin receptor expression by proinflammatory cytokines in enterocytes as a means for local delivery of drugs to inflamed gut mucosa, PLoS One 6 (2011), <https://doi.org/10.1371/journal.pone.0024202>.
- [174] J. Xian, X. Zhong, H. Gu, X. Wang, J. Li, J. Li, Y. Wu, C. Zhang, J. Zhang, Colonic delivery of celastrol-loaded layer-by-layer liposomes with pectin/trimethylated chitosan coating to enhance its anti-ulcerative colitis effects, Pharmaceutics 13 (2021), <https://doi.org/10.3390/pharmaceutics13122005>.
- [175] S. Moghassemi, E. Parnian, A. Hakamivala, M. Darzianiazzi, M.M. Vardanjani, S. Kashanian, B. Larijani, K. Omidfar, Uptake and transport of insulin across intestinal membrane model using trimethyl chitosan coated insulin niosomes, Mater. Sci. Eng. C 46 (2015) 333–340, <https://doi.org/10.1016/j.msec.2014.10.070>.
- [176] A.Z.M. Khalifa, B.K. Abdul Rasool, Optimized mucoadhesive coated niosomes as a sustained oral delivery system of famotidine, AAPS PharmSciTech 18 (2017) 3064–3075, <https://doi.org/10.1208/s12249-017-0780-7>.
- [177] R.Ku Sahoo, N. Biswas, A. Guha, N. Sahoo, K. Kuotsu, Development and in vitro/ in vivo evaluation of controlled release polymeric of a nateglinide-maltodextrin complex, Acta Pharm. Sin. B 4 (2014) 408–416, <https://doi.org/10.1016/j.apsb.2014.08.001>.
- [178] S.H. Moghadam, E. Saliq, S.D. Wettig, C. Dong, M. v Ivanova, J.T. Huzil, M. Foldvari, Effect of Chemical Permeation Enhancers on Stratum Corneum, pdf, 2013.
- [179] P. Martin, M. Giardiello, T.O. McDonald, S.P. Rannard, A. Owen, Mediation of in vitro cytochrome P450 activity by common pharmaceutical excipients, Mol. Pharm. 10 (2013) 2739–2748, <https://doi.org/10.1021/mp400175n>.
- [180] W. Zhang, Y. Li, P. Zou, M. Wu, Z. Zhang, T. Zhang, The effects of pharmaceutical excipients on gastrointestinal tract metabolic enzymes and transporters—an update, AAPS J. 18 (2016) 830–843, <https://doi.org/10.1208/s12248-016-9928-8>.
- [181] S. Ullah, M.R. Shah, M. Shoaib, M. Imran, A.M.A. Elhissi, F. Ahmad, I. Ali, S.W. A. Shah, Development of a biocompatible creatinine-based niosomal delivery system for enhanced oral bioavailability of clarithromycin, Drug Deliv. 23 (2016) 3480–3491, <https://doi.org/10.1080/10717544.2016.1196768>.
- [182] E. Toutitou, N. Dayan, L. Bergelson, B. Godin, M. Eliaz, Ethosomes - novel vesicular carriers for enhanced delivery: characterization and skin penetration properties, J. Contr. Release 65 (2000) 403–418, [https://doi.org/10.1016/S0168-3659\(99\)00222-9](https://doi.org/10.1016/S0168-3659(99)00222-9).
- [183] Y. Zhang, H. Zhang, K. Zhang, Z. Li, T. Guo, T. Wu, X. Hou, N. Feng, Co-hybridized composite nanovesicles for enhanced transdermal eugenol and cinnamaldehyde delivery and their potential efficacy in ulcerative colitis, Nanomedicine 28 (2020), 102212, <https://doi.org/10.1016/j.nano.2020.102212>.
- [184] N. Dragicevic-Curic, S. Gräfe, B. Gitter, A. Fahr, Efficacy of temoporfin-loaded invosomes in the photodynamic therapy in human epidermoid and colorectal tumour cell lines, J. Photochem. Photobiol., B 101 (2010) 238–250, <https://doi.org/10.1016/j.jphotobiol.2010.07.009>.
- [185] N.A.N. Hanafy, M. El-Kemary, S. Leporatti, Micelles structure development as a strategy to improve smart cancer therapy, Cancers 10 (2018) 1–14, <https://doi.org/10.3390/cancers10070238>.
- [186] H. Yuan, L.J. Lu, Y.Z. Du, F.Q. Hu, Stearic acid-g-chitosan polymeric micelle for oral drug delivery: in vitro transport and in vivo absorption, Mol. Pharm. 8 (2011) 225–238, <https://doi.org/10.1021/mp100289v>.
- [187] P. Zhang, Y. Xu, X. Zhu, Y. Huang, Goblet cell targeting nanoparticle containing drug-loaded micelle cores for oral delivery of insulin, Int. J. Pharm. 496 (2015) 993–1005, <https://doi.org/10.1016/j.ijpharm.2015.10.078>.
- [188] X. Wang, Y. Chen, F.Z. Dahmani, L. Yin, J. Zhou, J. Yao, Amphiphilic carboxymethyl chitosan-quercetin conjugate with P-gp inhibitory properties for oral delivery of paclitaxel, Biomaterials 35 (2014) 7654–7665, <https://doi.org/10.1016/j.biomaterials.2014.05.053>.
- [189] T. Yin, Y. Zhang, Y. Liu, Q. Chen, Y. Fu, J. Liang, J. Zhou, X. Tang, J. Liu, M. Huo, The efficiency and mechanism of N-octyl-O, N-carboxymethyl chitosan-based micelles to enhance the oral absorption of silybin, Int. J. Pharm. 536 (2018) 231–240, <https://doi.org/10.1016/j.ijpharm.2017.11.034>.
- [190] F.Q. Hu, L.N. Liu, Y.Z. Du, H. Yuan, Synthesis and antitumor activity of doxorubicin conjugated stearic acid-g-chitosan oligosaccharide polymeric micelles, Biomaterials 30 (2009) 6955–6963, <https://doi.org/10.1016/j.biomaterials.2009.09.008>.
- [191] Y. Wang, Y. Li, L. He, B. Mao, S. Chen, V. Martinez, X. Guo, X. Shen, B. Liu, C. Li, Commensal flora triggered target anti-inflammation of alginate-curcumin micelle for ulcerative colitis treatment, Colloids Surf. B Biointerfaces 203 (2021), 111756, <https://doi.org/10.1016/j.colsurfb.2021.111756>.
- [192] H. Yu, D. Xia, Q. Zhu, C. Zhu, D. Chen, Y. Gan, Supersaturated polymeric micelles for oral cyclosporine A delivery, Eur. J. Pharm. Biopharm. 85 (2013) 1325–1336, <https://doi.org/10.1016/j.ejpb.2013.08.003>.
- [193] J. Dou, H. Zhang, X. Liu, M. Zhang, G. Zhai, Preparation and evaluation in vitro and in vivo of docetaxel loaded mixed micelles for oral administration, Colloids Surf. B Biointerfaces 114 (2014) 20–27, <https://doi.org/10.1016/j.colsurfb.2013.09.010>.
- [194] X. Zhang, H. Wang, T. Zhang, X. Zhou, B. Wu, Exploring the potential of self-assembled mixed micelles in enhancing the stability and oral bioavailability of an acid-labile drug, Eur. J. Pharmaceut. Sci. 62 (2014) 301–308, <https://doi.org/10.1016/j.ejps.2014.06.008>.
- [195] M.R. Gigliobianco, C. Casadidio, R. Censi, P. di Martino, Nanocrystals of poorly soluble drugs: drug bioavailability and physicochemical stability, Pharmaceutics 10 (2018), <https://doi.org/10.3390/pharmaceutics10030134>.
- [196] A. Ahmadi Tehrani, M.M. Omranpoor, A. Vatnara, M. Seyedabadi, V. Ramezani, Formation of nanosuspensions in bottom-up approach: theories and optimization, DARU, J. Pharmaceut. Sci. 27 (2019) 451–473, <https://doi.org/10.1007/s40199-018-00235-2>.
- [197] A. Bhakay, M. Rahman, R.N. Dave, E. Bilgili, Bioavailability enhancement of poorly water-soluble drugs via nanocomposites: formulation-Processing aspects and challenges, Pharmaceutics 10 (2018), <https://doi.org/10.3390/pharmaceutics10030086>.
- [198] S. Jain, V.A. Reddy, S. Arora, K. Patel, Development of surface stabilized candesartan cilexetil nanocrystals with enhanced dissolution rate, permeation rate across CaCo-2, and oral bioavailability, Drug Deliv Transl Res 6 (2016) 498–510, <https://doi.org/10.1007/s13346-016-0297-8>.
- [199] A.N. Allam, S.I. Hamdallah, O.Y. Abdallah, Chitosan-coated diacerein nanosuspensions as a platform for enhancing bioavailability and lowering side effects: preparation, characterization, and ex vivo/in vivo evaluation, Int. J. Nanomed. 12 (2017) 4733–4745, <https://doi.org/10.2147/IJN.S139706>.
- [200] Q. Fu, J. Sun, D. Zhang, M. Li, Y. Wang, G. Ling, X. Liu, Y. Sun, X. Sui, C. Luo, L. Sun, X. Han, H. Lian, M. Zhu, S. Wang, Z. He, Nimodipine nanocrystals for oral bioavailability improvement: preparation, characterization and pharmacokinetic studies, Colloids Surf. B Biointerfaces 109 (2013) 161–166, <https://doi.org/10.1016/j.colsurfb.2013.01.066>.
- [201] K. Marri, M. Arif, Y. Ding, Z. Chi, C. Liu, Preparation of novel hard capsule using water-soluble polysaccharides and cellulose nanocrystals for drug delivery, J Pharm Innov (2022), <https://doi.org/10.1007/s12247-022-09671-9>.
- [202] P. Quan, K. Shi, H. Piao, H. Piao, N. Liang, D. Xia, F. Cui, A novel surface modified nifedipine nanocrystals with enhancement of bioavailability and stability, Int. J. Pharm. 430 (2012) 366–371, <https://doi.org/10.1016/j.ijpharm.2012.04.025>.
- [203] J.B. Aswathanarayan, R.R. Vittal, Nanoemulsions and their potential applications in food industry, Front. Sustain. Food Syst. 3 (2019) 1–21, <https://doi.org/10.3389/fsufs.2019.00095>.
- [204] I.J. Dinshaw, N. Ahmad, N. Salim, B.F. Leo, Nanoemulsions, A Review on the Conceptualization of Treatment for Psoriasis Using a 'green' Surfactant with Low-Energy Emulsification Method, 2021, <https://doi.org/10.3390/pharmaceutics13071024>.
- [205] N. Azrini, N. Azmi, A.A.M. Elgharabawy, S.R. Motlagh, N. Samsudin, Nanoemulsions: factory for food, pharmaceutical and cosmetics, Processes 7 (2019) 1–34.
- [206] L. Bai, S. Huan, J. Gu, D.J. McClements, Fabrication of oil-in-water nanoemulsions by dual-channel microfluidization using natural emulsifiers: saponins, phospholipids, proteins, and polysaccharides, Food Hydrocolloids 61 (2016) 703–711, <https://doi.org/10.1016/j.foodhyd.2016.06.035>.
- [207] S.I. Shofia, K. Jayakumar, A. Mukherjee, N. Chandrasekaran, Efficiency of brown seaweed (*Sargassum longifolium*) polysaccharides encapsulated in nanoemulsion and nanostructured lipid carrier against colon cancer cell lines HCT 116, RSC Adv. 8 (2018), 15973, <https://doi.org/10.1039/c8ra02616e>. –15984.
- [208] R. Richa, A. Roy Choudhury, Exploration of polysaccharide based nanoemulsions for stabilization and entrapment of curcumin, Int. J. Biol. Macromol. 156 (2020) 1287–1296, <https://doi.org/10.1016/j.ijbiomac.2019.11.167>.
- [209] L. Corrie, M. Gulati, S. Vishwas, B. Kapoor, S.K. Singh, A. Awasthi, R. Khurshheed, Combination therapy of curcumin and fecal microbiota transplant: potential treatment of polycystic ovarian syndrome, Med. Hypotheses 154 (2021), 110644, <https://doi.org/10.1016/j.mehy.2021.110644>.

- [210] L. Corrie, M. Gulati, A. Awasthi, S. Vishwas, J. Kaur, R. Khursheed, R. Kumar, A. Kumar, M. Imran, D.K. Chellappan, G. Gupta, T.D.J. Andreoli, A. Morris, Y. E. Choonara, J. Adams, K. Dua, S.K. Singh, Polysaccharide, fecal microbiota, and curcumin-based novel oral colon-targeted solid self-nanoemulsifying delivery system: formulation, characterization, and in-vitro anticancer evaluation, *Mater. Today Chem.* 26 (2022), 101165, <https://doi.org/10.1016/j.mtchem.2022.101165>.
- [211] J.Y. Ye, Z.Y. Chen, C.L. Huang, B. Huang, Y.R. Zheng, Y.F. Zhang, B.Y. Lu, L. He, C.S. Liu, X.Y. Long, A non-lipolysis nanoemulsion improved oral bioavailability by reducing the first-pass metabolism of raloxifene, and related absorption mechanisms being studied, *Int. J. Nanomed.* 15 (2020) 6503–6518, <https://doi.org/10.2147/IJN.S259993>.
- [212] Y. de Anda-Flores, E. Carvajal-Millan, A. Campa-Mada, J. Lizardi-Mendoza, A. Rascon-Chu, J. Tanori-Cordova, A.L. Martínez-López, Polysaccharide-based nanoparticles for colon-targeted drug delivery systems, *Polysaccharides* 2 (2021) 626–647, <https://doi.org/10.3390/polysaccharides2030038>.
- [213] B. Duan, M. Li, Y. Sun, S. Zou, X. Xu, Orally delivered antisense oligodeoxyribonucleotides of TNF- α via polysaccharide-based nanocomposites targeting intestinal inflammation, *Adv Healthc Mater* 8 (2019) 1–12, <https://doi.org/10.1002/adhm.201801389>.
- [214] R.K. Eid, D.S. Ashour, E.A. Essa, G.M. el Maghraby, M.F. Arafa, Chitosan coated nanostructured lipid carriers for enhanced in vivo efficacy of albandazole against *Trichinella spiralis*, *Carbohydr. Polym.* 232 (2020), 115826, <https://doi.org/10.1016/j.carbpol.2019.115826>.
- [215] T. Andreani, J.F. Fangueiro, P. Severino, A.L.R. de Souza, C. Martins-Gomes, P.M. V. Fernandes, A.C. Calpena, M.P. Gremião, E.B. Souto, A.M. Silva, The influence of polysaccharide coating on the physicochemical parameters and cytotoxicity of silica nanoparticles for hydrophilic biomolecules delivery, *Nanomaterials* 9 (2019), <https://doi.org/10.3390/nano9081081>.
- [216] A. Dogan Ergin, Z.S. Bayindir, A.T. Ozelcikay, N. Yuksel, A novel delivery system for enhancing bioavailability of S-adenosyl-L-methionine: pectin nanoparticles-in-microparticles and their in vitro - in vivo evaluation, *J. Drug Deliv. Sci. Technol.* 61 (2021), 102096, <https://doi.org/10.1016/j.jddst.2020.102096>.
- [217] M. Li, Z. Tang, D. Zhang, H. Sun, H. Liu, Y. Zhang, Y. Zhang, X. Chen, Doxorubicin-loaded polysaccharide nanoparticles suppress the growth of murine colorectal carcinoma and inhibit the metastasis of murine mammary carcinoma in rodent models, *Biomaterials* 51 (2015) 161–172, <https://doi.org/10.1016/j.biomaterials.2015.02.002>.
- [218] C. Zhu, S. Zhang, C. Song, Y. Zhang, Q. Ling, P.R. Hoffmann, J. Li, T. Chen, W. Zheng, Z. Huang, Selenium nanoparticles decorated with *Ulva lactuca* polysaccharide potentially attenuate colitis by inhibiting NF- κ B mediated hyper inflammation, *J. Nanobiotechnol.* 15 (2017) 1–15, <https://doi.org/10.1186/s12951-017-0252-y>.
- [219] E.A.K. Nivethaa, S. Dhanavel, V. Narayanan, C.A. Vasu, A. Stephen, An in vitro cytotoxicity study of 5-fluorouracil encapsulated chitosan/gold nanocomposites towards MCF-7 cells, *RSC Adv.* 5 (2015) 1024–1032, <https://doi.org/10.1039/c4ra11615a>.
- [220] K.W. Kang, M.K. Chun, O. Kim, R.K. Subedi, S.G. Ahn, J.H. Yoon, H.K. Choi, Doxorubicin-loaded solid lipid nanoparticles to overcome multidrug resistance in cancer therapy, *Nanomedicine* 6 (2010) 210–213, <https://doi.org/10.1016/j.nano.2009.12.006>.
- [221] J.P. Quiñones, H. Peniche, C. Peniche, Chitosan based self-assembled nanoparticles in drug delivery, *Polymers* 10 (2018) 1–32, <https://doi.org/10.3390/polym10030235>.
- [222] B. Xiao, E. Viennois, Q. Chen, L. Wang, M.K. Han, Y. Zhang, Z. Zhang, Y. Kang, Y. Wan, D. Merlin, Silencing of intestinal glycoprotein CD98 by orally targeted nanoparticles enhances chemosensitization of colon cancer, *ACS Nano* 12 (2018) 5253–5265, <https://doi.org/10.1021/acsnano.7b08499>.
- [223] B. Xiao, X. Sia, M.K. Han, E. Viennois, D.M. Mingzhen Zhang, Co-delivery of camptothecin and curcumin by cationic polymeric nanoparticles for synergistic colon cancer combination chemotherapy, *J. Mater. Chem. C* 3 (2015) 10715–10722, <https://doi.org/10.1039/b000000x>.
- [224] M.B. Subudhi, A. Jain, A. Jain, P. Hurkat, S. Shilpi, A. Gulbake, S.K. Jain, Eudragit S100 coated citrus pectin nanoparticles for colon targeting of 5-fluorouracil, *Materials* 8 (2015) 832–849, <https://doi.org/10.3390/ma8030832>.
- [225] M.R. Cheng, Q. Li, T. Wan, B. He, J. Han, H.X. Chen, F.X. Yang, W. Wang, H.Z. Xu, T. Ye, B.B. Zha, Galactosylated chitosan/5-fluorouracil nanoparticles inhibit mouse hepatic cancer growth and its side effects, *World J. Gastroenterol.* 18 (2012) 6076–6087, <https://doi.org/10.3748/wjg.v18.i42.6076>.
- [226] B.Y. Maddina, G.S. Asthana, A. Asthana, Formulation and development of polysaccharide based mesalamine nanoparticles, *Int. J. Pharmaceut. Chem. Res.* 8 (2016) 676–684.
- [227] P. Tang, Q. Sun, L. Zhao, H. Pu, H. Yang, S. Zhang, R. Gan, N. Gan, H. Li, Mesalazine/hydroxypropyl- β -cyclodextrin/chitosan nanoparticles with sustained release and enhanced anti-inflammation activity, *Carbohydr. Polym.* 198 (2018) 418–425, <https://doi.org/10.1016/j.carbpol.2018.06.106>.
- [228] Y. Li, H. Song, S. Xiong, T. Tian, T. Liu, Y. Sun, Chitosan-stabilized bovine serum albumin nanoparticles having ability to control the release of NELL-1 protein, *Int. J. Biol. Macromol.* 109 (2018) 672–680, <https://doi.org/10.1016/j.ijbiomac.2017.12.104>.
- [229] J. Zhang, C. Tang, C. Yin, Galactosylated trimethyl chitosan-cysteine nanoparticles loaded with Map4k4 siRNA for targeting activated macrophages, *Biomaterials* 34 (2013) 3667–3677, <https://doi.org/10.1016/j.biomaterials.2013.01.079>.
- [230] T.K.B. Kruti, S. Soni, Swapnil S. Desale, Nanogels: an overview of properties, biomedical applications and obstacles to clinical translation, *J. Contr. Release* 176 (2016) 139–148, <https://doi.org/10.1016/j.jconrel.2015.11.009>.
- [231] C. Feng, J. Li, M. Kong, Y. Liu, X.J. Cheng, Y. Li, H.J. Park, X.G. Chen, Surface charge effect on mucoadhesion of chitosan based nanogels for local anti-colorectal cancer drug delivery, *Colloids Surf. B Biointerfaces* 128 (2015) 439–447, <https://doi.org/10.1016/j.colsurfb.2015.02.042>.
- [232] T. Hosseinfar, S. Sheybani, M. Abdouss, S.A. Hassani Najafabadi, M. Shafiee Ardestani, Pressure responsive nanogel base on Alginate-Cyclodextrin with enhanced apoptosis mechanism for colon cancer delivery, *J. Biomed. Mater. Res.* 106 (2018) 349–359, <https://doi.org/10.1002/jbm.a.36242>.
- [233] M. Molinos, V. Carvalho, D.M. Silva, F.M. Gama, Development of a hybrid dextrin hydrogel encapsulating dextrin nanogel as protein delivery system, *Biomacromolecules* 13 (2012) 517–527, <https://doi.org/10.1021/bm2015834>.
- [234] M. Vicario-De-la-torre, J. Forcada, The potential of stimuli-responsive nanogels in drug and active molecule delivery for targeted therapy, *Gels* (2017) 3, <https://doi.org/10.3390/gels3020016>.
- [235] C. Bharti, U. Nagaich, J. Pandey, S. Jain, N. Jain, Development of nitazoxanide-loaded colon-targeted formulation for intestinal parasitic infections: centre composite design-based optimization and characterization, *Futur J Pharm Sci* 6 (2020) 1–17, <https://doi.org/10.1186/s43094-020-00130-1>.
- [236] L. Wang, C. Lai, D. Li, Z. Luo, L. Liu, Y. Jiang, L. Li, Lecithin-polysaccharide self-assembled microspheres for resveratrol delivery, *Antioxidants* 11 (2022) 1666, <https://doi.org/10.3390/antiox11091666>.
- [237] A. Paharia, A.K. Yadav, G. Rai, S.K. Jain, S.S. Pancholi, G.P. Agrawal, Eudragit-coated pectin microspheres of 5-fluorouracil for colon targeting, *AAPS PharmSciTech* 8 (2007) E87, <https://doi.org/10.1208/pt0801012> –E93.
- [238] A.K. Pandey, N. Choudhary, V.K. Rai, H. Dwivedi, K.M. Kymonil, S.A. Saraf, Fabrication and evaluation of tinidazole microbeads for colon targeting, *Asian Pac J Trop Dis* 2 (2012) S197, [https://doi.org/10.1016/S2222-1808\(12\)60151-0](https://doi.org/10.1016/S2222-1808(12)60151-0) –S201.
- [239] F. Maestrelli, P. Mura, M.L. González-Rodríguez, M.J. Cózar-Bernal, A. M. Rabasco, L. di Cesare Mannelli, C. Ghelardini, Calcium alginate microspheres containing metformin hydrochloride niosomes and chitosomes aimed for oral therapy of type 2 diabetes mellitus, *Int. J. Pharm.* 530 (2017) 430–439, <https://doi.org/10.1016/j.ijpharm.2017.07.083>.
- [240] A. Zeng, K. Dong, M. Wang, J. Sun, Y. Dong, K. Wang, C. Guo, Y. Yan, L. Zhang, X. Shi, J. Xing, Investigation of the colon-targeting, improvement on the side-effects and therapy on the experimental colitis in mouse of a resin microcapsule loading dexamethasone sodium phosphate, *Drug Deliv.* 23 (2016), <https://doi.org/10.3109/10717544.2015.1046569>, 1992–2002.
- [241] S.P. Simi, R. Saraswathi, C. Sankar, P.N. Krishnan, C. Dilip, K. Ameena, Formulation and evaluation of Albendazole microcapsules for colon delivery using chitosan, *Asian Pac J Trop Med* 3 (2010) 374–378, [https://doi.org/10.1016/S1995-7645\(10\)60091-0](https://doi.org/10.1016/S1995-7645(10)60091-0).
- [242] J. Varshosaz, F. Ahmadi, J. Emami, N. Tavakoli, M. Minaian, P. Mahzouni, F. Dorkoosh, Microencapsulation of budenoside with dextran by spray drying technique for colon-targeted delivery: an in vitro/in vivo evaluation in induced colitis in rat, *J. Microencapsul.* 28 (2011) 62–73, <https://doi.org/10.3109/02652048.2010.529947>.
- [243] M. Debnath, Y.I. Muzib, S.A. Kumar, Formulation and Development, Optimization and In Vitro Release Kinetic Study on Colon Targeted Tinidazole- Guar Gum Microcapsules, vol. 5, 2013, 0–7.
- [244] K.S. Seo, R. Bajracharya, S.H. Lee, H.K. Han, Pharmaceutical application of tablet film coating, *Pharmaceutics* 12 (2020) 1–20, <https://doi.org/10.3390/pharmaceutics12090853>.
- [245] M.H. Othman, G.M. Zayed, U.F. Ali, A.A.H. Abdellatif, Colon-specific tablets containing 5-fluorouracil microsponges for colon cancer targeting, *Drug Dev. Ind. Pharm.* 46 (2020), <https://doi.org/10.1080/03639045.2020.1844730>, 2081–2088.
- [246] A. Kumar, M. Gulati, S.K. Singh, K. Gowthamarajan, R. Prashar, D. Mankotia, J. P. Gupta, M. Banerjee, S. Sinha, A. Awasthi, L. Corrie, R. Kumar, P. Patni, B. Kumar, N.K. Pandey, M. Sadotra, P. Kumar, R. Kumar, S. Wadhwa, R. Khursheed, Effect of co-administration of probiotics with guar gum, pectin and eudragit S100 based colon targeted mini tablets containing 5-Fluorouracil for site specific release, *J. Drug Deliv. Sci. Technol.* 60 (2020), 102004, <https://doi.org/10.1016/j.jddst.2020.102004>.
- [247] S.K. Vemula, Formulation and pharmacokinetics of colon-specific double-compression coated mini-tablets: chronopharmaceutical delivery of ketorolac tromethamine, *Int. J. Pharm.* 491 (2015) 35–41, <https://doi.org/10.1016/j.ijpharm.2015.06.007>.
- [248] N. Sharma, P. Srivastava, A. Sharma, D.K. Nishad, R. Karwasra, K. Khanna, D. Kakkara, A. Bhatnagar, Potential applications of *Abelmoschus moschatus* polysaccharide as colon release tablets-Rheology and gamma scintigraphic study, *J. Drug Deliv. Sci. Technol.* 57 (2020), 101632, <https://doi.org/10.1016/j.jddst.2020.101632>.
- [249] N. Sharma, A. Sharma, D.K. Nishad, K. Khanna, B.G. Sharma, D. Kakkara, A. Bhatnagar, Development and gamma scintigraphy study of *Trigonella foenum-graecum* (fenugreek) polysaccharide-based colon tablet, *AAPS PharmSciTech* 19 (2018) 2564–2571, <https://doi.org/10.1208/s12249-018-1066-4>.
- [250] V.R. Sinha, B.R. Mittal, R. Kumria, In vivo evaluation of time and site of disintegration of polysaccharide tablet prepared for colon-specific drug delivery, *Int. J. Pharm.* 289 (2005) 79–85, <https://doi.org/10.1016/j.ijpharm.2004.10.019>.
- [251] L.A. Hodges, S.M. Connolly, J. Band, B. O'Mahony, T. Ugurlu, M. Turkoglu, C. G. Wilson, H.N.E. Stevens, Scintigraphic evaluation of colon targeting pectin-

- HPMC tablets in healthy volunteers, *Int. J. Pharm.* 370 (2009) 144–150, <https://doi.org/10.1016/j.ijpharm.2008.12.002>.
- [252] J. Liu, L. Zhang, W. Hu, R. Tian, Y. Teng, C. Wang, Preparation of konjac glucomannan-based pulsatile capsule for colonic drug delivery system and its evaluation in vitro and in vivo, *Carbohydr. Polym.* 87 (2012) 377–382, <https://doi.org/10.1016/j.carbpol.2011.07.062>.
- [253] Y. Zhang, Y. Bai, H. Chen, Y. Huang, P. Yuan, L. Zhang, Preparation of a colon-specific sustained-release capsule with curcumin-loaded SMEDDS alginate beads, *RSC Adv.* 7 (2017) 22280–22285, <https://doi.org/10.1039/c6ra27693h>.
- [254] J. Liu, L. Zhang, Y. Jia, W. Hu, J. Zhang, H. Jiang, Preparation and evaluation of pectin-based colon-specific pulsatile capsule in vitro and in vivo, *Arch Pharm. Res. (Seoul)* 35 (2012) 1927, <https://doi.org/10.1007/s12272-012-1109-4>.
- [255] S.A. Yehia, A.H. Elshafeey, I. Elsayed, Pulsatile systems for colon targeting of budesonide: in vitro and in vivo evaluation, *Drug Deliv.* 18 (2011) 620–630, <https://doi.org/10.3109/10717544.2011.621987>.
- [256] G. Gangwar, A. Kumar, K. Pathak, Utilizing guar gum for development of “Tabs in Cap” system of losartan potassium for chronotherapeutics, *Int. J. Biol. Macromol.* 72 (2015) 812–818, <https://doi.org/10.1016/j.ijbiomac.2014.09.027>.
- [257] M.Z.I. Khan, Z. Prebeg, N. Kurjaković, A pH-dependent colon targeted oral drug delivery system using methacrylic acid copolymers. I. Manipulation of drug release using Eudragit® L100-55 and Eudragit® S100 combinations, *J. Contr. Release* 58 (1999) 215–222, [https://doi.org/10.1016/S0168-3659\(98\)00151-5](https://doi.org/10.1016/S0168-3659(98)00151-5).
- [258] Y.S.R. Krishnaiah, P.R. Bhaskar Reddy, V. Satyanarayana, R.S. Karthikeyan, Studies on the development of oral colon targeted drug delivery systems for metronidazole in the treatment of amoebiasis, *Int. J. Pharm.* 236 (2002) 43–55, [https://doi.org/10.1016/S0378-5173\(02\)00006-6](https://doi.org/10.1016/S0378-5173(02)00006-6).
- [259] Y.S.R. Krishnaiah, V. Satyanarayana, B.D. Kumar, R.S. Karthikeyan, In vitro drug release studies on guar gum-based colon targeted oral drug delivery systems of 5-fluorouracil, *Eur. J. Pharmaceut. Sci.* 16 (2002) 185–192, <https://doi.org/10.1001/jama.2012.56914>.
- [260] Y.S.R. Krishnaiah, P. Veer Raju, B. Dinesh Kumar, V. Satyanarayana, R. S. Karthikeyan, P. Bhaskar, Pharmacokinetic evaluation of guar gum-based colon-targeted drug delivery systems of mebendazole in healthy volunteers, *J. Contr. Release* 88 (2003) 95–103, [https://doi.org/10.1016/S0168-3659\(02\)00483-2](https://doi.org/10.1016/S0168-3659(02)00483-2).
- [261] Y.S.R. Krishnaiah, V. Satyanarayana, B.D. Kumar, R.S. Karthikeyan, P. Bhaskar, In vivo pharmacokinetics in human volunteers: oral administered guar gum-based colon-targeted 5-fluorouracil tablets, *Eur. J. Pharmaceut. Sci.* 19 (2003) 355–362, [https://doi.org/10.1016/S0928-0987\(03\)00139-8](https://doi.org/10.1016/S0928-0987(03)00139-8).
- [262] V.R. Sinha, R. Kumria, Coating polymers for colon specific drug delivery: a comparative in vitro evaluation, *Acta Pharm.* 53 (2003) 41–47.
- [263] V.R. Sinha, B.R. Mittal, K.K. Bhutani, R. Kumria, Colonic drug delivery of 5-fluorouracil: an in vitro evaluation, *Int. J. Pharm.* 269 (2004) 101–108, <https://doi.org/10.1016/j.ijpharm.2003.09.036>.
- [264] L.F. Siew, S.M. Man, J.M. Newton, A.W. Basit, Amylose formulations for drug delivery to the colon: a comparison of two fermentation models to assess colonic targeting performance in vitro, *Int. J. Pharm.* 273 (2004) 129–134, <https://doi.org/10.1016/j.ijpharm.2003.12.015>.
- [265] G. Dupuis, O. Chambin, C. Génelot, D. Champion, Y. Pourcelot, Colonic drug delivery: influence of cross-linking agent on pectin beads properties and role of the shell capsule type, *Drug Dev. Ind. Pharm.* 32 (2006) 847–855, <https://doi.org/10.1080/03639040500536718>.
- [266] C. Ji, H. Xu, W. Wu, In vitro evaluation and pharmacokinetics in dogs of guar gum and Eudragit FS30D-coated colon-targeted pellets of indomethacin, *J. Drug Target.* 15 (2007) 123–131, <https://doi.org/10.1080/10611860601143727>.
- [267] T. Ugurlu, M. Turkoglu, U.S. Gurer, B.G. Akarsu, Colonic delivery of compression coated nisin tablets using pectin/HPMC polymer mixture, *Eur. J. Pharm. Biopharm.* 67 (2007) 202–210, <https://doi.org/10.1016/j.ejpb.2007.01.016>.
- [268] Y. Karrou, C. Neut, D. Wils, F. Siepmann, L. Deremaux, M.P. Flament, L. Dubreuil, P. Desreumaux, J. Siepmann, Novel polymeric film coatings for colon targeting: drug release from coated pellets, *Eur. J. Pharmaceut. Sci.* 37 (2009) 427–433, <https://doi.org/10.1016/j.ejps.2009.03.014>.
- [269] L.F.A. Asghar, C.B. Chure, S. Chandran, Colon specific delivery of indomethacin: effect of incorporating pH sensitive polymers in xanthan gum matrix bases, *AAPS PharmSciTech* 10 (2009) 418–429, <https://doi.org/10.1208/s12249-009-9223-4>.
- [270] F. Li-Fang, H. Wei, C. Yong-Zhen, X. Bai, D. Qing, W. Feng, Q. Min, C. De-Ying, Studies of chitosan/Kollocoat SR 30D film-coated tablets for colonic drug delivery, *Int. J. Pharm.* 375 (2009) 8–15, <https://doi.org/10.1016/j.ijpharm.2009.03.023>.
- [271] J. Nunthanid, M. Luangtana-anan, P. Sriamornsak, S. Limmatvapirat, K. Huanbutta, S. Puttipipatkachorn, Use of spray-dried chitosan acetate and ethylcellulose as compression coats for colonic drug delivery: effect of swelling on triggering in vitro drug release, *Eur. J. Pharm. Biopharm.* 71 (2009) 356–361, <https://doi.org/10.1016/j.ejpb.2008.08.002>.
- [272] Y. Huang, R. Tian, W. Hu, Y. Jia, J. Zhang, H. Jiang, L. Zhang, A novel plug-controlled colon-specific pulsatile capsule with tablet of curcumin-loaded SMEDDS, *Carbohydr. Polym.* 92 (2013) 2218–2223, <https://doi.org/10.1016/j.carbpol.2012.11.105>.
- [273] M.M. Patel, A.F. Amin, Development of a novel tablet-in-capsule formulation of mesalazine for inflammatory bowel disease, *Pharmaceut. Dev. Technol.* 18 (2013) 390–400, <https://doi.org/10.3109/10837450.2011.653819>.
- [274] P. Sharma, K. Pathak, Inulin-based tablet in capsule device for variable multipulse delivery of aceclofenac: optimization and in vivo roentgenography, *AAPS PharmSciTech* 14 (2013) 736–747, <https://doi.org/10.1208/s12249-013-9959-8>.
- [275] S.K. Vemula, R. Katkum, Formulation, development and pharmacokinetics of ketorolac tromethamine colon targeted guar gum compression coated tablets, *Anal. Chem. Lett.* 5 (2015) 149–161, <https://doi.org/10.1080/22297928.2015.1069755>.
- [276] Wai-Wa Tanga, Fangyuan Donga, K.-H. Wonga, Y. Wang, Preparation, characterization and in vitro release of zein-pectin capsules for target delivery Wai-Wa Tang, *Curr. Drug Deliv.* (2015) 1–11.
- [277] A. Gupta, G. Tiwari, R. Tiwari, R. Srivastava, Factorial designed 5-fluorouracil-loaded microsponges and calcium pectinate beads plugged in hydroxypropyl methylcellulose capsules for colorectal cancer, *Int J Pharm Investig* 5 (2015) 234, <https://doi.org/10.4103/2230-973x.167688>.
- [278] A. Celkan, F. Acartürk, F. Tuğcu-demiröz, N. Gökçora, B.E. Akkaş, L.A. Güner, Gamma scintigraphic studies on guar gum-based compressed coated tablets for colonic delivery of theophylline in healthy volunteers, *J. Drug Deliv. Sci. Technol.* (2016), <https://doi.org/10.1016/j.jddst.2016.01.009>.
- [279] S. Sharma, K. Jyoti, R. Sinha, A. Katyal, U.K. Jain, J. Madan, Protamine coated proliposomes of recombinant human insulin encased in Eudragit S100 coated capsule offered improved peptide delivery and permeation across Caco-2 cells, *Mater. Sci. Eng. C* 67 (2016) 378–385, <https://doi.org/10.1016/j.msec.2016.05.010>.
- [280] V.S. Kumar, R. John, M. Sabitha, Guar gum and eudragit coated curcumin liquisolid tablets for colon specific drug delivery, *Int. J. Biol. Macromol.* (2018), <https://doi.org/10.1016/j.ijbiomac.2018.01.082>.
- [281] R. Deshmukh, R.K. Harwansh, S. das Paul, R. Shukla, Controlled release of sulfasalazine loaded amidated pectin microparticles through Eudragit S 100 coated capsule for management of inflammatory bowel disease, *J. Drug Deliv. Sci. Technol.* 55 (2020), 101495, <https://doi.org/10.1016/j.jddst.2019.101495>.
- [282] L.S.L. Janardhanam, V.V. Indukuri, P. Verma, A.C. Dusan, V.V.K. Venuganti, Functionalized layer-by-layer assembled film with directional 5-fluorouracil release to target colon cancer, *Mater. Sci. Eng. C* 115 (2020), 111118, <https://doi.org/10.1016/j.msec.2020.111118>.
- [283] P. Wanasawas, A. Mitrevej, N. Sinchaipanid, Influence of in situ calcium pectinate coating on metoprolol tartrate pellets for controlled release and colon-specific drug delivery, *Pharmaceutics* 14 (2022) 1061, <https://doi.org/10.3390/pharmaceutics14051061>.
- [284] L. Shasha, Enema for Treating Ulcerative Colitis and Preparation Method Thereof, 2022. CN114668730A, <https://worldwide.espacenet.com/patent/search/family/082077634/publication/CN114668730A?q=ap:3DCN202210417355A>.
- [285] W.R.W.J.L.M.Y.H.S. Haisu, Sulfdryl Codonopsis Pilosula Polysaccharide and Application Thereof in Colon-Targeted Probiotic Microcapsule Preparation, 2021. CN114057904A, <https://patents.google.com/patent/CN114057904A/en?oq=CN114057904A>.
- [286] S.W.X.W.J.C.Y.D.M.H.J.W.S. Haofang, Oral Colon-specific Preparation for Preventing and Treating Ulcerative Colitis, 2021. CN113616619A, <https://patent.s.google.com/patent/CN113616619A/zh>.
- [287] D.L.X.Z.S.C.L.L.K.L.Z.L.Q.Z. Xuemei, Astragalus Polysaccharide Extract Powder and Application Thereof in Anti-aging and Bowel Relaxing of Rats with Senile Constipation, 2021. CN113372460A, <https://worldwide.espacenet.com/patent/search/family/077571885/publication/CN113372460A?q=pn:3DCN113372460A>.
- [288] L.Z.C.J.Q. Xuemei, Silver Nanoparticles against Colon Cancer and Preparation Method of Silver Nanoparticles, 2020. CN111097921A, <https://patents.google.com/patent/CN111097921A/en>.
- [289] C. Yu, Gastric Controlled-Release Capsule, 2019. CN110200948A, <https://agri.cckest.cn/patentdetails/74F397D6-265F-4DA3-A3A4-F7EF21DD15C6.html>.
- [290] T.N.H.K.T.A.T.H.K. Hiroyuki, Capsule for Treating Ulcerative Colitis, CN111867583A, 2019. <https://patents.google.com/patent/CN111867583A/zh>.
- [291] G.Z.L. Zhao, Quercetin Nano-Micelle Preparation and Preparation Method Thereof, 2018, CN101982168A. <https://patents.google.com/patent/CN101982168A/en>.
- [292] F.S.L.W.L.J. Zheng, Anthocyanidin Composite Tablet Able to Improve Immunotherapy Effects for Colon Cancer And/or Rectal Cancer, 2018, CN108853478A. <https://patents.google.com/patent/CN108853478A/en>.
- [293] Y.H.F. Yoshiki, pH-RESPONSIVE LIPOSOME, JP2019019059A, 2017. <https://patents.google.com/patent/JP6901127B2/en>.
- [294] Y.Z.C.W.W.Y.L. Jianhong, pH-triggering-to-release multilevel targeting polymer micelle in tumor cells and preparation method of multilevel targeting polymer micelle, CN106265510A, <https://patents.google.com/patent/CN106265510A/zh>, 2016.
- [295] Z. Xiaoyun, Pharmaceutical Composition for Treating Constipation in Children, 2016. CN106727681A, <https://patents.google.com/patent/CN106727681A/zh>.
- [296] Y.Q.Y.Z.H.W.Y.S.Y.C.J.R.F.L.L.L.Z. Shuxian, Nanometer Composite Polysaccharide Colon-Targeting Pellets and Manufacturing Method Thereof, 2014. CN104382925A, <https://patents.google.com/patent/CN104382925A/zh>.
- [297] C. Peidong, Scutellaria Baicalensis Decoction Granules for Treating Ulcerative Colitis and Preparation Method Thereof, 2014, CN104069204A. <https://patents.google.com/patent/CN104069204A/en>.
- [298] F.J.L.J.W.L.S.G. Sandy, Mucoadhesive Nanoparticle Delivery System, US2015320694A1, 2013. <https://patents.google.com/patent/US2015320694A1/en>.
- [299] G.F.C.J. du Jiang, Preparation Method and Application of periplaneta Americana Double-Layer Gastric Floating Tablet, 2013. CN104224848A, <https://patents.google.com/patent/CN104224848A/zh>.
- [300] X.C.Y.H.Y.L.X.Z.L. Minggao, Gambogic Acid Colon-specific Controlled Release Tablet and Preparation Method Thereof, 2012. CN102871983A, <https://patents.google.com/patent/CN102871983A/zh>.
- [301] Z. Jianqiang, Soft Capsule for Relaxing Bowel, 2012. CN103445044A, <https://patents.google.com/patent/CN103445044A/en>.

- [302] M.S.S.D.S.S.R.S.G. Mamta, Improved Oral Targetted Drug Delivery System, WO2012035561A2, 2011. <https://patents.google.com/patent/WO2012035561A2/en>.
- [303] Y. Jun, Polysaccharide Cancer Prevention Tablet, 2009, CN101999645A. <https://patents.google.com/patent/CN101999645A/en>.
- [304] P.B.R.H. le Bu, Oral Nano Raw Baizhu Colon Tablet and Preparation Method Thereof, 2008. CN101336950A, <https://patents.google.com/patent/CN101336950A/zh>.
- [305] V. Thierry, Composition for Selective Drug Release in the Colon, Comprising Capsule Containing Carboxylated Polysaccharide-Coated Active Agent and Polyvalent Cations, FR2830446A1, 2001. <https://patents.google.com/patent/FR2830446A1/en>.
- [306] G.K.D. Stephen, Method of Treating Ulcerative Colitis, 1994. US5444054A, <https://patents.google.com/patent/US5444054>.
- [307] R. Advanced, D. Delivery, S. Farah, D.G. Anderson, R. Langer, Physical and Mechanical Properties of PLA, and Their Functions in, 2016, 0–26.
- [308] Z. Ferdous, A. Nemmar, Health Impact of Silver Nanoparticles: A Review of the Biodistribution and Toxicity Following Various Routes of Exposure, 2020, <https://doi.org/10.3390/ijms21072375>.
- [309] B.J. Huffman, R.A. Shenvi, Natural products in the “marketplace”: interfacing synthesis and biology, *J. Am. Chem. Soc.* 141 (2019) 3332–3346, <https://doi.org/10.1021/jacs.8b11297>.
- [310] J. Wagener, K. Striegler, N. Wagener, A- and B-1,3-glucan synthesis and remodeling, *Curr. Top. Microbiol. Immunol.* 425 (2020) 53–82, https://doi.org/10.1007/82_2020_200.
- [311] C.M. Soerensen, O.L. Nielsen, A. Willis, P.M.H. Heegaard, U. Holmskov, Purification, characterization and immunolocalization of porcine surfactant protein D, *Immunology* 114 (2005) 72–82, <https://doi.org/10.1111/j.1365-2567.2004.01999.x>.
- [312] G. Ghiselli, Heparin binding proteins as therapeutic target: an historical account and current trends, *Medicine (Baltim.)* 6 (2019) 80, <https://doi.org/10.3390/medicines6030080>.
- [313] G. Fittolani, T. Tyrikos-Ergas, D. Vargová, M.A. Chaube, M. Delbianco, Progress and challenges in the synthesis of sequence controlled polysaccharides, *Beilstein J. Org. Chem.* 17 (2021), <https://doi.org/10.3762/bjoc.17.129>, 1981–2025.
- [314] D. Ebert, M.E. Greenberg, In situ preactivation strategies for the expeditious synthesis of oligosaccharides: a review, *Bone* 23 (2013) 237–337, <https://doi.org/10.1080/07328303.2014.931964>.

CHAPTER 5

An Overview of Preparation, Characterization, and Application of Aquasomes

SANUSHA SANTHOSH, NARENDRA KUMAR PANDEY,
SACHIN KUMAR SINGH, BIMLESH KUMAR, MONICA GULATI,
and HARDEEP

*School of Pharmaceutical Sciences, Lovely Professional University,
Phagwara – 144411, Punjab, India,
E-mail: herenarendra4u@gmail.com (N. K. Pandey)*

ABSTRACT

Ceramic nanoparticles (NPs) are nanosized carriers which are globule shaped. These comprise of a hydroxyapatite core, whose surface is non-covalently altered by oligosaccharide, onto which the drug of interest are further adsorbed on the surface. These ceramic NPs are also referred to as “aquasomes.” Aquasomes are triple-layered self-assembled nanoparticulate drug delivery systems, which are used for the successful delivery of drugs without compromising with their conformational integrity. They establish a non-covalent link with various molecules which further promote more stability as compared to liposomes and other NPs. In the present chapter, various aspects of aquasomes are discussed such as properties, method of preparation, characterization, and various application in drug delivery.

5.1 INTRODUCTION

The potential need of nanoparticle as a carrier for drug was first stated on 1974 by Dr. Gregory Gregoriadis. He suggested that liposomes can be used as a nanoparticulate drug delivery system. Drug can be adsorbed or encapsulated in a nanocarrier system. Nowadays, nanoparticle drug delivery is the ideal choice for targeting the drug directly to the site of action, which can

be then referred to targeted drug delivery. They have improved drug loading and produce very negligible adverse effects as compared to the conventional dosage form. They are also used for the poorly soluble drugs so as to improve its dissolution inside body. As very less amount of drug reaches the targeted site, toxicity produced because of large dose of drug is also reduced by this targeting method [1].

Aquasomes are the biocompatible and biodegradable nanocarrier which was invented by Nir Kossovsky in 1995 [15]. Aquasomes are defined as three-layered self-assembled nanoparticle carrier system which constitute of central solid nanocrystalline ceramic core which is further coated with polyhydroxyl oligomer. Over this coated core, bioactive molecules are adsorbed or diffused with or without modification as shown in Figure 5.1.

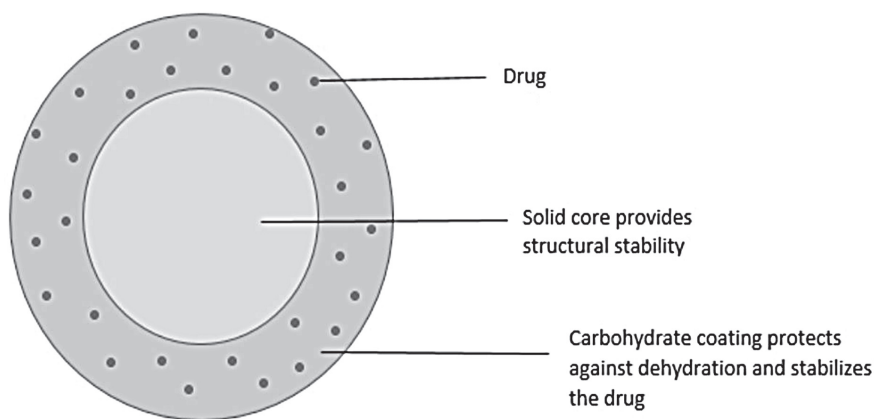
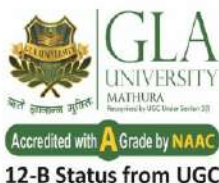


FIGURE 5.1 Structure of aquasome.

Hydroxyapatite and calcium phosphate are commonly used as ceramic core to prepare aquasomes. These aquasomes self-assemble themselves by means of ionic bonds, non-covalent bonds, or Van der Waals force [2]. Ceramic core which is coated with carbohydrate improve their cellular uptake. The main advantage of aquasomes is its non-interaction between the carrier system and the drug. It preserves the conformational integrity of the bioactive molecules which is adsorbed over the carbohydrate coated ceramic core. The structural stability is provided by the solid core while the oligomer coating helps the adsorbed bioactive molecule against dehydration and stabilizes them. It behaves like “water bodies.” The water-like properties of aquasomes protect the fragile therapeutically active molecules which further help in targeting of



Institute of Pharmaceutical Research GLA University, Mathura



Certificate

This is to certify that **Mr. Hardeep** from Lovely Professional University, Phagwara, Punjab, Presented Poster on **Methods of Development and Validation of Reverse Phase High Performance Liquid Chromatography for Simvastatin, Secured 1st Position** in 1st International Conference on “**Innovations in Chemical, Biological and Pharmaceutical Sciences (ICBPS-2021)**” held on November 26-27, 2021 through online mode.

Dr Ahsas Goyal
(Co-Convener)

Dr Yogesh Murti
(Co-Convener)

Dr Anuj Garg
(Convener)

Dr Prabhat K Upadhyay
(Convener)

Prof. Meenakshi Bajpai
(Chairperson)



ISFCO- 2021 Online International Conference on Recent Advances in Pharmaceutical Sciences: Vision **2030**

July 01 - 03, 2021.



In Collaboration with

Punjab State Council for Science & Technology, Chandigarh

Organized by

ISF COLLEGE OF PHARMACY, MOGA

(An Autonomous College)

Certificate of Participation

This is to certify that Prof./Dr./Mr./Ms.

HARDEEP

has participated as **Delegate** and received **"Best Poster Award"**

in

ISFCO- 2021 Online International Conference

Organizing Secretary
Dr. Vineet K. Rai

Organizing Secretary
Dr. Pooja Chawla

Finance Secretary
Prof. (Dr.) R. K. Narang

Convener
Prof. (Dr.) G. D. Gupta

Patron
Parveen Garg

Registration Number: ISFCO2021/.....
PHA065